AD_____

Award Number: DAMD17-01-1-0110

TITLE: Molecular Determinants of Radio Resistance in Prostate Cancer

PRINCIPAL INVESTIGATOR: Robert G. Bristow, M.D., Ph.D.
Lathar Lilge, Ph.D.
Jeremy Squire, Ph.D.
Michael Milosevic, M.D.
Padraig Warde

CONTRACTING ORGANIZATION: University Health Network
Toronto, Ontario M5G 2C4
Canada

REPORT DATE: August 2005

TYPE OF REPORT: Final

PREPARED FOR: U.S. Army Medical Research and Materiel Command
Fort Detrick, Maryland 21702-5012

REPORT DOCUMENTATION PAGE

Form Approved
OMB No. 0704-0188

1. REPORT DATE *(DD-MM-YYYY)*	2. REPORT TYPE	3. DATES COVERED *(From - To)*
01-08-2005	Final	1 Aug 2001 – 31 Jul 2005

4. TITLE AND SUBTITLE
Molecular Determinants of Radio Resistance in Prostate Cancer

5a. CONTRACT NUMBER

5b. GRANT NUMBER
DAMD17-01-1-0110

5c. PROGRAM ELEMENT NUMBER

6. AUTHOR(S)
Robert G. Bristow, M.D., Ph.D.; Lathar Lilge, Ph.D.; Jeremy Squire, Ph.D.;
Michael Milosevic, M.D.; Padraig Warde;

E-mail: Rob.Bristow@rmp.uhn.on.ca

5d. PROJECT NUMBER

5e. TASK NUMBER

5f. WORK UNIT NUMBER

7. PERFORMING ORGANIZATION NAME(S) AND ADDRESS(ES)
University Health Network
Toronto, Ontario M5G 2C4
Canada

8. PERFORMING ORGANIZATION REPORT NUMBER

9. SPONSORING / MONITORING AGENCY NAME(S) AND ADDRESS(ES)
U.S. Army Medical Research and Materiel Command
Fort Detrick, Maryland 21702-5012

10. SPONSOR/MONITOR'S ACRONYM(S)

11. SPONSOR/MONITOR'S REPORT NUMBER(S)

12. DISTRIBUTION / AVAILABILITY STATEMENT
Approved for Public Release; Distribution Unlimited

13. SUPPLEMENTARY NOTES

14. ABSTRACT

We are studying the radiation response of prostate tissues in relation to the sensing and repair of DNA breaks. Specific aims relate to determining the expression and interaction of DNA repair proteins in vitro using immunoflorescent confocal microscopy and biochemical DNA rejoining assays under both hypoxic and oxic conditions. An in vivo program of prostate xenograft radioresponse and patient biopsy studies will determine the level of DNA repair *in situ* using immunohistochemistry and immunoflorescent markers. Our studies show that DNA repair protein expression is abnormal in malignant versus normal prostate epithelial cultures, and that particularly the Rad51 protein is defective in localizing to the nucleus following DNA damage. We have accrued 13 patients onto a pre-operative radiotherapy trial and post-irradiation immunohistochemistry supports an induction of p53-pathway signaling following 25Gy in 5 fractions. Future experiments will be designed to determine whether DNA protein focal interactions using 2-photon microscopy can predict the radioresponse of prostate xenografts and human tumors, in vivo. Our studies support the use of novel molecular based therapies that target DNA repair for prostate cancer therapy.

15. SUBJECT TERMS
prostate cancer, DNA repair, xenografts, cell death

16. SECURITY CLASSIFICATION OF:			17. LIMITATION OF ABSTRACT	18. NUMBER OF PAGES	19a. NAME OF RESPONSIBLE PERSON
a. REPORT	b. ABSTRACT	c. THIS PAGE			USAMRMC
U	U	U	UU	89	19b. TELEPHONE NUMBER *(include area code)*

Table of Contents

Introduction:

The funding for the study entitled "Molecular mechanisms of radioresistance in prostate cancer", is now complete. This study investigated the role of DNA break repair in the radiation response of normal and malignant prostate epithelium.

The overall hypothesis of this project was that the radiation response of normal and cancerous prostate tissues can be correlated to the appropriate sensing and repair of DNA breaks by repair complexes following exposure to ionizing radiation.

Specific aims relate to determining the interaction of DNA repair proteins in vitro using immunoflorescent confocal microscopy and biochemical DNA rejoining assays under both hypoxic and oxic conditions (given in vivo tumour cell populations).

An in vivo program of prostate xenograft radioresponse is also being initiated to determine the level of DNA repair *in situ* using immunohistochemistry and immunoflorescent markers. These initial studies will determine the heterogeneity in fractionated response in a series of prostate xenografts as relates to DNA repair capacity, which may be translated to novel markers for radiation response in patients who receive prostate radiation therapy.

The relevance of this project is that this *in vitro* to *in vivo* pre-clinical approach may derive clinical biomarkers of radiation response which can predict which patients will most benefit from radiation therapy for prostate cancer. The project will also determine the molecular mechanisms behind radiation response, in general, in prostate epithelial tissues.

Body:

Task 1: Radiobiological and DNA-dsb Repair Studies in Normal and Malignant Prostate Epithelium

Initally, the first task was to primarily complete in vitro studies on PC-3; LNCaP, DU145 and normal prostate (PRSE and PREC) cells relating to senescent populations which was quantitated and found to be dose responsive and correlated to their clonogenic survival (using a novel fluorescent flow cytometric proliferation assay). This work has been published in ***Prostate Cancer and Prostate Diseases (see Appendix 1)***. THIS TASK WAS FULLY COMPLETED.

Task one projects were also completed for all 5 cell lines in determining the ability for the cells to repair double strand breaks, single strand breaks and DNA base damage (and oxidative damage) following ionizing radiation using the comet assay. We observed a series of novel observations which currently suggests that malignant prostate cancer cells have a DNA repair defect in the repair of DNA-dsbs, DNA-ssbs and DNA-base damage and oxidative damage in relation to the two normal prostate epithelial and stromal cell cultures. Primary prostatic cultures were initiated as prostatectomy specimen cultures available through Coriell Laboratories. We were successful in culturing both the prostate stromal and the prostate epithelial cell cultures in vitro to be utilized in a radiobiology and DNA repair experiments. DNA double stand break repair gene and protein expression was determined using RNA protection

analyses and Western Blotting techniques. DNA repair studies were completed using the Comet Assay and chromosomal repair assays.

The results showed that despite an increased expression of DNA-dsb repair complexes in malignant prostate cells, the repair of DNA-dsbs was compromised. This suggested that prostate cancer progression may be related to altered DNA repair and increased genetic instability. THIS TASK WAS FULLY COMPLETED. This work was published in ***Cancer Research (see Appendix II).***

We have therefore completed all endpoints for Task 1.

<u>Task 2:</u> Complete in vivo radiobiologic studies on human prostate xenografts (months 12-24).

We have determined that there are cell cycle phase specific changes in Rad51 or H2AX foci formation in relation to DNA-dsb rejoining, by irradiating cells under both asynchronous and G0-G1 synchronized conditions. Counterstaining with PCNA and CENP-F has determined that foci are specifically forming in a cell-cycle phase specific manner in malignant prostate cells.

Single dose (2 and 10Gy) and fractionated experiments (5 x 2 Gy) have been completed for the PC-3, 22RV1 and DU-145 xenografts. We have now hired a new technician (Ms. Helen Zhao) to continue to develop the prostate xenograft program and she has developed a new 22RV1 system in the lab. This moderately-differentiated prostate cancer xenograft maintains androgen sensitivity and WTp53 function, such that it makes a useful addition to our program when investigating p53-related reponses.

All current xenografts were removed and stained for immunohistochemical markers pertaining to p53, apoptosis related genes (BAX, BCL2 and TUNEL assay; as well as survivin) and DNA repair markers (RAD50, BRCA1, BRCA2, RAD50, $DNAPK_{cs,}$ KU70, KU80, ATM, P21, RB, MYC and RPA). The xenograft histology was also stained for proliferation markers such as MIB-1, KI-67 and PCNA.

Our results continue to suggest that RAD51, and H2AX, but not Ku70, increase in expression both in terms of the nuclear intensity of staining as well as a number of cells positively staining for protein following 10 Gy single dose or 5 x 2 Gy fractioned irradiation *in vivo* at 1-24 hours. The RAD51 data is consistent with cells moving into the G2 phase of the cell cycle during an irradiation-induced checkpoint. **This has not been reported in the literature before.** A manuscript is being prepared for these xenograft studies.

We have continued to collaborate with Dr. Peter Glazer's laboratory at Yale University to show that RAD51 expression is decreased under hypoxia conditions in vitro. We have confirmed these findings in vivo as RAD51 staining in hypoxic areas (as determined with EF-5 and CA-IX) is decreased, suggesting an inverse relationship between HR-related DNA repair proteins and hypoxia. This may explain in part hypoxia-mediated genetic instability.

We further investigated the expression of other DNA-dsb repair genes in terms of the homologous (HR) and non-homologous (NHEJ) recombination pathways of DNA-dsb repair and showed that other RAD51-related protein members of the HR pathway were also downregulated by hypoxia. The expression of homologous recombination (HR) and non-homologous recombination (NHEJ) genes following gas hypoxia (0_2%) or exposure to HIF1alpha-inducing agent, $CoCl_2$ (100uM), was determined

for normal diploid fibroblasts (GM05757) and the pre-malignant and malignant prostate cell lines, BPH-1, 22RV-1, DU145 and PC3. RNA and protein levels were determined using RT-PCR and Western blotting. Additionally, p53 genotype and function, the level of hypoxia-induced apoptosis, and cell cycle distribution, were determined to correlate to changes in DNA-dsb gene expression. Induction of hypoxia was confirmed using HIF1-alpha and VEGF expression in gas- and $CoCl_2$-treated cultures. Hypoxia (48-72 hours of 0.2% O_2) decreased RNA expression of a number of HR-related genes (e.g. *Rad51, Rad52, Rad54, BRCA1, BRCA2*) in both normal and malignant cultures. Similar decreases in RNA pertaining to the NHEJ-related genes (e.g. *Ku70, DNA-PKcs, DNA Ligase IV, Xrcc4*) were observed. In selected cases, hypoxia-mediated decreases in RNA expression led to decreased DNA-dsb protein expression. $CoCl_2$-treated cultures did not show decreased DNA-dsb protein expression. The ability of hypoxia to down-regulate *Rad51* and other HR-associated genes under hypoxia was not correlated to *c-Abl* or *c-Myc* gene expression, p53 genotype or function, propensity for hypoxia-mediated apoptosis, or specific changes in cell cycle distribution.

Hypoxia can therefore down-regulate expression of DNA-dsb repair genes in both normal and cancer cells. If associated with a functional decrease in DNA-dsb repair, this observation could provide a potential basis for the observed genetic instability within tumor cells exposed to hypoxia.
THIS SUB-TASK IS FULLY COMPLETED. Two manuscripts have been published in ***Molecular ad Cellular Biology*** and ***Radiotherapy and Oncology*** from this sub-task. ***These are appended as Appendices III and IV, respectively.***

Despite an initial contamination of our animals from our supplier with *Pseudomonas Aeruginos (when* our entire colony of mice (greater than 70 animals) bearing Rotterdam-xenografts had to be sacrificed before we could complete in vivo fractionation experiments in 2003-2004); we have hired a new technician (Helen Zhao; October 1, 2004) who will be re-growing the prostate xenograft facility to encompass fractionated and hypoxia experiments *in vivo*. These studies have shown that hypoxia exists within non-irradiated and irradiated xenografts using hypoxic markers EF5, CA-IX, HIF-1alpha. These results support the findings of induction fo these proteins by hypoxia in vitro as outlined in Appendix IV. **THIS SUB-TASK IS COMPLETE and a manuscript is in preparation. Data pertaining to this project are shown in Figures 1-3 in Appendix V.**

Task 3: (Months 18-36) Expression of DNA Repair Proteins in Clinical Specimens

We reviewed the need for biomarkers for prostate radiotherapy in a manuscript that was published in ***CANCER and is appended as Appendix VI.***

We therefore have completed a pre-operative radiotherapy study consisting of 12 patients who had paired pre-operative and post-operative biopsies available for the study of radiotherapy-induced gene expression. We have sequenced all patients for their p53 gene status for all 11 exons and all patients are wild-type for p53. Immunohistochemistry for p53, p21, TUNNEL, Bax, Bcl-2, BRCA1/2/Rad51/DNA-PKcs/KU70/KU80 and PCNA is completed. We have quantitated the staining pre and post-radiotherapy using the Image Pro Plus analysis program. During radiotherapy, one patient complained of mild dysuria (RTOG GU-1) and another complained of diarrhea (RTOG GI-2). Of the 15 patients entered on trial, 2 patients were lymph-node positive and their prostatectomy was aborted. Of the remaining 13 patients, median blood loss was 1000 cc. and only one patient had signs of intraoperative inflammation. None of the patients had post-operative infections or bleeding.

Gleason scores ranged from 6 to 10 in this cohort. Survivin was elevated in malignant disease prior to radiotherapy and did not alter its expression post-radiotherapy. The majority of irradiated prostate tumor tissues showed increased expression of p-ATM, p-p53 and p21WAF. The mean expression (ME) of P-ATM increased post-RT (p=0.293). p21WAF was negative pre-RT and positive in 7 post-RT cases. The ME of p21 increased from 0 to 50% (p=0.001). P53 expression increased in 7 cases post-RT. The ME of p53 increased from 41.1 to 51.8% (p=0.623). Ser15 p53 expression decreased in 6 cases post-RT. The ME of ser15 p53 decreased from 50.8 to 10% (p=0.025). Cell proliferation (Ki-67) was reduced with no evidence of apoptosis (TUNEL). MIB1 expression decreased in 11 cases post-RT. The ME of MIB1 decreased from 11.7 to 3.8% (p=0.001). ISEL decreased in 8 cases post-RT from a ME of 5.7 to 3.3% (p=0.334).

This is the first study to assess biomarkers of ATM and p53 radio-response in prostate cancer prior to and immediately following RT. Our observations of increased p21, decreased ser15 p53, and a decrease in MIB1 expression are consistent with decreased prostate cancer cell proliferation via p21-mediated cell cycle arrest at the G1/S checkpoint. Our results do not support apoptosis as a dominant mode of cell kill.
Clinically, intra-operative morbidity is low following short-course pre-operative conformal radiotherapy. A Phase II trial is planned to determine late toxicity and PSA responses. Additionally, a Phase I trial of intra-radiotherapy biopsies to measure expression of genes during radiotherapy relative to radiotherapy outcome has been approved by our REB.

THIS TASK IS COMPLETE and a manuscript is in preparation. Data relating to this project are shown in Figures 4-7 in Appendix V. We continue to optimize utilize 2-photon microscopy for better resolution of the innate foci with indirect immunofluorescence.

We also introduced a new tissue microarray to our program in the last 6 months of funding to track the expression of DNA-dsb repair proteins across normal, pre-malignant and malignant prostate epithelium to support our in vitro studies published as Appendix II. Preliminary data showing increased RAD51 expression in malignant versus normal or pre-malignant tissues was observed using this novel array which consists of tissues derived from 100 patients with either BPH, PIN or Gleason scores 6-10. Our data therefore do support the concept that aberrant DNA-dsb repair gene expression correlates with more aggressive prostate cancers. We therefore wrote a recent review (***see Appendix VII***) that explores the use of this information in a clinical setting with molecular targeted drugs

KEY RESEACH ACCOMPLISHMENTS FOR ENTIRE PERIOD OF STUDY:

1. The dominant mode of cell kill during prostate cancer radiotherapy is mitotic catastrophe and terminal growth arrest and NOT apoptosis during irradiation of normal and malignant prostate epithelial cultures in vitro..
2. DNA repair complexes can be visualized using confocal microscopy and the appearance and disappearance of these foci correlate to the kinetics of DNA biochemical rejoining assays (ie. Comet assay).
3. Malignant prostate epithelium may have an effect has an inherent DNA defect in terms of DNA double strand break repair, single strand break repair and base damage repair. This is correlated to

increased expression of proteins involved in each of these pathways (APE/REF1. RAD51, BRCA2, PARP, etc.). In the case of Rad51, altered expression is discordant from altered function and we believe that there is an intracellular trafficking defect in Rad51 related to post-translational modification.

4. Increased expression of DNA-dsb repair proteins in tissue microarrays (TMA) may be a novel biomarker of prostate cancer progression.

5. Completed accrual to the phase I pilot study of preoperative radiotherapy. Immunohistochemical markers for DNA repair and apoptosis related proteins has been completed. ATM/p53 activation occurs in vivo with fractionated treatments. Little evidence for apoptosis following radiotherapy in vivo during fractionated radiotherapy.

Reportable Outcomes for 2001-2005:

Manuscripts Directly Relating or Associated With Research In This Grant:

1. Bromfield G, Fan R, Meng A, Kumaravel Ts, **Bristow RG**. Cell death in irradiated prostate epithelial cells: role of apoptotic and clonogenic cell kill. Prostate Cancer and Prostate Diseases, 6(1):73-85, 2003. **(Senior Responsible Author)**

2. Ma B, **Bristow RG**, Kim J, Siu L. Combined-Modality Treatment of Solid Tumors Using Radiotherapy and Molecular Targeted Agents. Journal of Clinical Oncology, 21(14): 2760-2776, 2003. **(Collaborator)**

3. Coleman CN, Stone H, Alexander G, Barcellos-Hoff MH, Bedford J, **Bristow R**, Dynlacht J, Zvi Fuks, Gorelic L, Hill R, Joiner M, Liu FF, McBride W, McKenna G, Powell S, Robbins M, Rockwell S, Schiff P, Shaw E, Siemann D, Travis E, Wallner P, Wong R, Zeman E. Education and training for radiation scientists: Radiation Research Program and American Society of Therapeutic Radiology and Oncology Workshop, Bethesda, Maryland, May 12-14, 2003. Radiation Research, 160(6): 729-37, 2003. **(Collaborator)**

4. **Bristow R** on behalf of the CARO Task Force Members. "Recommendations for the future of translational radiobiology research: A Canadian perspective". Radiotherapy and Oncology, 70(2):159-164, 2004. **(Principal Author)**

5. Parker C, Milosevic M, Toi A, Sweet J, Panzarella T, **Bristow R**, Catton C, Catton P, Crook J, Gospodarowicz M, McLean M, Warde P, Hill R. Polarographic electrode study of tumor clinically localized prostate cancer. International Journal of Radiation Oncology, Biology, Physics, 58(3):750-757, 2004. **(Collaborator)**

6. Bindra R, Schaffer P, Meng A, Woo J, Maseide K, Roth ME, Lizardi P, Hedley D, **Bristow R**, Glazer P. Down-Regulation of Rad51 and Decreased Homologous Recombination in Hypoxic Cancer Cells. Molecular and Cellular Biology, 24(19):8504-18, 2004. **(Primary Collaborator)**

7. Fan R, Kumaravel TS, Jalali F, Bayani J, Squire J and **Bristow RG.** Defective DNA Strand Break Repair Following DNA Damage in Prostate Cancer Cells: Implications for Genetic Instability and Prostate Carcinogenesis. Cancer Research, 64(23):8526-33, 2004. **(Senior Responsible Author)**

8. West C, McKay M, Holscher T, Baumann M, Stratford I, **Bristow RG**, Iwakawa M, Imai T, Zingde S, Anscher M, Bourhis J, Begg A, Haustermans K, Bentzen S and Hendry J. Molecular Markers Predicting Radiotherapy Response: Report and Recommendations from an International Atomic Energy Agency Technical Meeting. International Journal of Radiation Oncology, Biology, Physics 62(5):1264-1273, July 2005. **(Collaborator)**

9. Nichol A, Lockwood G, Sweet J, Divanbeigi L, Rosewell T, Chung P, Bayley A, **Bristow R**, Crook J, Gospodarowicz M, McLean M, Milosevic M, Warde P, Catton C. A phase II study of localized prostate cancer treated to 75.6Gy with 3D conformal radiotherapy. Radiotherapy and Oncology 76:11-17, 2005. **(Collaborator)**

10. Horsburgh S, Matthew A, **Bristow RG**, Ritvo P, Squire J, Krahn M, Yue C, Jamnicky L, Trachtenberg J. Male BRCA1 and BRCA2 mutation carriers: A pilot study investigating medical characteristics of patients participating in a prostate cancer prevention clinic. The Prostate Journal, 65:124-129, 2005. **(Collaborator)**

11. Nichol A, Warde P, **and Bristow RG**. Intermediate Risk Prostate Cancer and Radical Radiotherapy: Clinical and Translational Issues. Cancer, 104:891-905, 2005. **(Senior Responsible Author)**

12. Meng A, Jalali F, Cuddihy A, Chan N, Bindra R, Glazer P and **Bristow RG**. Hypoxia Down-Regulators DNA Double Strand Break Repair Gene Expression in Prostate Cancer Cells. Radiotherapy and Oncology, 76:168-176, 2005 **(Senior Responsible Author)**

13. Choudhury A, Cuddihy A, **Bristow RG**. Radiation and Other New Molecular-Targeted Agents, Part I: Targeting ATM-ATR Checkpoints, DNA Repair and the Proteasome. Seminars in Radiation Oncology, *In Press,* 2005. **(Senior Responsible Author)**

Book Chapters:

1. **Bristow, RG**, Blussyen, H., de Klein, A. and van Gent, D. The PI3-Kinase family as Sensors and Signals for DNA Damage Responses. In: Trends in Molecular Biology; Chapter 6, (ed. MK Gospodarowicz), Wiley-Liss Inc., 71-94, USA, 2001. **(Principal Author)**

2. Gospodarowicz, MK, O'Sullivan and **Bristow RG**: Host and Tumor-related Prognostic Factors. In: UICC Handbook of Prognostic Factors: Chapter 6, (ed. MK Gospodarowicz) Wiley-Liss Inc., USA, 71-94, 2001. **(Collaborator)**

3. Catton C, Milosevic M, Warde P, Bayley A, Crook J, **Bristow RG**, Gospodarowicz M. Recurrent Prostate Cancer Following External Beam Radiotherapy: Follow-up Strategies and Management. In: The Urologic Clinics of North America (ed. D. Theodorescu), Vol 30 (4) pp. 751-763, 2003. **(Collaborator)**

4. **Bristow RG** and Harrington L. Genetic Instability and DNA Repair; Chapter 5. In: The Basic Science of Oncology, 4th Edition (eds. Tannock IF, Hill RP, Harrington L and Bristow RG); McGraw-Hill Ltd.; New York, pp. 77-99, 2005. **(Principal Author)**

5. **Bristow RG** and R.P. Hill. Molecular and Cellular Radiobiology; Chapter 14. In: The Basic Science of Oncology, 4th Edition (eds. Tannock IF, Hill RP, Harrington L and Bristow RG). McGraw-Hill Ltd.; New York, pp. 261-288, 2005. **(Principal Author)**

6. R.P. Hill and **Bristow RG**. The Scientific Basis of Clinical Radiotherapy; Chapter 15. IN: The Basic Science of Oncology, 4th Edition (eds. Tannock IF, Hill RP, Harrington L and Bristow RG). McGraw-Hill Ltd.; New York, 289-321, 2005. **(Principal Co-Author)**

7. Faulhaber O and **Bristow RG**. Basis of Cell Kill Following Clinical Radiotherapy. In: Application of Apoptosis to Cancer Treatment (ed. Mel Sluyser), Kluwer-Springer Press, New York, VII, 293-320, 2005. **(Senior Responsible Author)**

8. **Bristow R**. Targeting DNA-dsb Repair To Improve Radiotherapy Outcome. 7th Proceedings of International Conference on Dose, Time and Fractionation in Radiation Oncology Meeting, *In press* 2005. **(Principal Author)**

Manuscripts in preparation

1. Coleman A, Smith K, Trachtenberg J, Ozelich, Narod S and **Bristow RG.** BRCA2 mutations, DNA Repair and Prostate Cancer: Implications for Local and Systemic Management (Review). **(Senior Responsible Author)**

Published Abstracts and Presentations:

1. Milosevic M, Toi A, Sweet J, **Bristow R**, Warde P, McLean M, Crook J, Catton C, Catton P, Gospodarowicz M. "Trans-rectal oxygen measurements in prostate cancer". Presented at the14th Meeting of the Canadian Association of Radiation Oncologists (CARO). Clinical and Investigative Medicine, 23(Supp 4): S19; 2000. **(Collaborator)**

2. Bromfield, G P, **Bristow, R G**. "Relative Importance of Non-Apoptotic and Apoptotic Cell Death Pathways in Irradiated Prostate Cells". Presented at the 15th Meeting of the Canadian Association of Radiation Oncologists, Quebec City. Radiotherapy and Oncology, 23(Suppl): 2001. **(Senior Responsible Author)**

3. Parker CC, Milosevic M, Toi A, Sweet J, Panzarella T, Syed A, **Bristow R**, Catton C, Hill R, Warde P. "A polarographic electrode study of tumor oxygenation in localized prostate cancer." Presented at the 43rd Meeting of the American Society of Therapeutic Radiation Oncology (ASTRO), San Francisco. International Journal of Radiation Oncology, Biology, Physics, 51(Supp 3): 2001. **(Collaborator)**

4. **Bristow R. G.**, Bromfield G, Fan R, Meng A, Kumaravel TS. "Radiotherapy-induced death pathways in prostate cells: apoptosis versus permanent cell cycle arrest". Presented at the 57th Meeting of the Canadian Urological Association (CUA), St. John's, Newfoundland. The Canadian Journal of Urology, 10(Suppl 1): 2002. **(Principal Author)**

5. **Bristow RG**, Fan R, Kumaravel TS, Bromfield G, Jalali F, Meng A. "DNA Repair in normal and malignant prostate epithelial tissues: implications for genetic stability and radiotherapy". Presented at the 21st Meeting of the European Society for Therapeutic Radiation Oncology (ESTRO), Prague. Radiotherapy and Oncology, 65(Suppl 1): 2002. **(Principal Author)**

6. Dearnaley D, Parker C, Panzarella T, Catton C, **Bristow R**, Crook J, Gospodarowicz M, McLean M, Milosevic M, Warde P. "The effect of haemoglobin level on biochemical outcome following radiotherapy in in localised prostate cancer". Presented at the 21st Meeting of the European Society for Therapeutic Radiation Oncology (ESTRO), Prague. Radiotherapy and Oncology, 65(Suppl 1): S47, 2002. (Collaborator)

7. Parker C, Panzarella T, Catton C, **Bristow R**, Crook J, Gospodarowicz M, McLean M, Michael Milosevic M and Warde P "The Effect of Haemoglobin Level on Biochemical Outcome following Radiotherapy in Localised Prostate Cancer". Presented at the 16th Meeting of the Canadian Association of Radiation Oncologists (CARO), Toronto. Radiotherapy and Oncology, 65(Suppl 1): S47; 2002. **(Collaborator)**

8. Chung P, Haycocks T, Panzarella T, Warde P, Gospodarowicz M, Milosevic M, **Bristow R**, McLean M, Catton P, Crook J, Bayley A, Catton C. "Results of a phase II trial of escalated dose 3D-Conformal radiotherapy (3D-CRT) for localized prostate cancer". Presented at the 16th Meeting of the Canadian Association of Radiation Oncologists (CARO), Toronto. Radiotherapy and Oncology, 65(Suppl 1): S53, 2002. **(Collaborator)**

9. **Bristow RG**, Fan R, Kumaravel TS, Bromfield G, Jalali F, Meng A. "DNA Repair in normal and malignant prostate epithelial tissues: implications for genetic stability and radiotherapy", Presented at the 16th Meeting of the Canadian Association of Radiation Oncologists (CARO), Toronto. Radiotherapy and Oncology, 64:(Suppl), S361;2002. **(Principal Author)**

10. Catton CN, Chung P, Haycocks T, Warde P, Alasti H, Bayley AJ, **Bristow R**, Crook J, Gospodarowicz M, McLean M, Milosevic M. "Hypofractionated intensity modulated radiation therapy for prostate cancer". Presented at the 44th Meeting of the American Society of Therapeutic Radiation Oncology (ASTRO), Philadelphia. International Journal of Radiation Oncology Biology Physics, 54(Supp 2): 2002. **(Collaborator)**

11. **Bristow R**, Fan R, Kumaravel TS, Jalali F, Bromfield G. "Aberrant Rad51 Function in Prostate Cancer Cell Lines: Basis for Radiotherapy Prediction and Novel Therapy". Presented at the 2nd International Conference on Translational Research and Pre-Clinical Strategies in Clinical Radio-Oncology (ICTR), Lugano. Radiotherapy and Oncology, 66(Suppl); 2003. **(Principal Author)**

12. Catton C, Wallace K, Haycocks T, Alasti H, Bayley A, **Bristow R**, Gospodarowicz M, Milosevic M, Warde P, Crook J, McLean. "Hypofractionated Intensity Modulated Radiation Therapy (IMRT) for Localized Prostate Cancer". Presented at the 17th Meeting of the Canadian

Association of Radiation Oncologists (CARO), Montreal. Radiotherapy and Oncology, 69 (Suppl 1): S144; 2003. **(Collaborator)**

13. **Bristow R.** "The Homologous Recombination pathway of DNA repair as a novel target for prostate cancer radiotherapy". Presented at the 17th Meeting of the Canadian Association of Radiation Oncologists (CARO), Montreal. Radiotherapy and Oncology, 69 (Suppl 1): 2003. **(Principal Author)**

14. **Bristow R**, Fan R, Kumaravel T.S, Jalali F, Bromfield G. "The homologous recombination pathway of DNA repair as a novel target for prostate cancer radiotherapy". Presented at the 17th Meeting of the Canadian Association of Radiation Oncologists (CARO), Montreal. Radiotherapy and Oncology, 69: (Suppl 1), 118; 2003. **(Principal Author)**

15. Glazer PM, Bindar R, Schaffer P, **Bristow RG**, Hedley DW. Down-regulation of Rad51 and decreased homologous recombination in hypoxic cancer cells. International Journal of Radiation Oncology, Biology, Physics Suppl 1(60), S193, September 2004

16. Milosevic M, **Bristow R.** Chung P, Panzarella T, Toi A, Hill R. Prostate cancer hypoxia correlates with poor patient outcome following treatment with radiotherapy. International Journal of Radiation Oncology, Biology, Physics Suppl 1(60), S236-237, September 2004

17. Meng A, Cole H, Syed A, Billings S, Chung P, Sweet J, Milosevic M, Hedley D, Woo J, Maseide K, Hill RP, **Bristow RG.** "Hypoxia-Induces Gene Expression within Prostate Cancer: In Vitro and In Vivo Studies". Presented at the 18th Meeting of the Canadian Association of Radiation Oncologists (CARO), Halifax. Radiotherapy and Oncology, 72 (Suppl 1): S221; 2004. **(Senior Responsible Author)**

18. Coleman A, Jonkman J, **Bristow R.** "DNA-dsb Repair *In Situ* In Normal and Malignant Cells". Presented at the 18th Meeting of the Canadian Association of Radiation Oncologists(CARO), Halifax. Radiotherapy and Oncology, 72 (Suppl 1): S222; 2004. **(Senior Responsible Author)**

19. Faulhaber O, Blin N, **Bristow R.** "HDAC Inhibition and Demethylation as a Means for Radiosensitization in Prostate Cancer". Presented at the 18th Meeting of the Canadian Association of Radiation Oncologists(CARO), Halifax. Radiotherapy and Oncology, 72 (Suppl 1): S204; 2004. **(Senior Responsible Author)**

20. Milosevic M, Chung P, **Bristow R**, Toi A, Panzarella T, Hill R. "Prostate Cancer Hypoxia Adversely Influences Outcome Following Treatment with Radiotherapy". Presented at the 18th Meeting of the Canadian Association of Radiation Oncologists(CARO), Halifax. Radiotherapy and Oncology, 72 (Suppl 1): S25; 2004. **(Collaborator)**

21. Meng A, Jalali F, Hedley D, Nichol T, Sweet J, Milosevic M, Bindra R, Glazer P, **Bristow R.** "Expression of DNA-dsb Repair Proteins Is Altered Under Hypoxia in Prostate Cancer Cells" 9th

International Wolfsberg Meeting on Molecular Radiation Biology / Oncology. Proceeds Vol 6, SP111.2:2005. **(Senior Responsible Author)**

22. Hendry JH, **Bristow RG,** West CM, Begg A, McKay M, Baumann and IAEA Consultant Group. "Molecular Markers Predicting Radiotherapy Response": Recommendations from an IAEA Technical Meeting" International Wolfsberg Meeting on Molecular Radiation Biology / Oncology. Proceeds Vol 6, SPIV.38:2005.

23. Skala M, Catton C, Divanbeigi L, Bayley A, **Bristow R,** Catton P, Crook J, Gospodarowicz M, M. McLean, Milosevic M, Lockwood G, Rosewall T, Warde P. "Patient-reported late GI and GI toxicity following high-dose radiation therapy for prostate cancer, the PMH experience". Presented at the meeting of the Canadian Association of Radiation Oncologists(CARO), British Columbia. Radiotherapy and Oncology, 76 (Suppl 1): S23; 2005. **(Collaborator)**

24. **Bristow R,** Meng A, Jalali A, Hedley D, Nichol T, Sweet J, Milosevic M, Bindra R, Glazer P. "Expression of DNA-dsb Repair Proteins Is Altered Under Hypoxia in Prostate Cancer Cells". Presented at the meeting of the Canadian Association of Radiation Oncologists(CARO), British Columbia. Radiotherapy and Oncology, 76 (Suppl 1): S67; 2005. **(Principal Author)**

25. Nichol A, **Bristow R**, Warde P, Catton C. "A Prospective Study of Localised Prostate Cancer Treated to 75.6 Gy Using 3D Conformal Radiotherapy". Presented at the meeting of the Canadian Association of Radiation Oncologists(CARO), British Columbia. Radiotherapy and Oncology, 76 (Suppl 1): S10; 2005. **(Collaborator)**

Other reportable outcomes:

There is continued development of the tissue bank relating to irradiated prostate specimens as it relates to the phase I and phase III clinical trials; the latter has accumulated > 200 biopsies of patients having undergone radical radiotherapy at PMH-UHN. Our REBs has been re-approved for all human studies. Funding continues from a number of grants that were leveraged by initial monies from the US Army DOD Prostate Cancer Research Program:

(1) A Canadian Foundation of Innovation Award worth more than $ 300,000 in infrastructure relating to DNA repair studies
(2) An Ontario Cancer Research Network grant worth more than $ 300,000 for operating costs relating to novel DNA repair inhibitors to be used with radiotherapy in prostate cancer;
(3)Canadian Cancer Society Research Scientist Award to the PI (Bristow) worth more than $ 500,000 over 6 years is salary support;
(4)2) a new NCIC Operating grant on hypoxia and DNA repair worth > $ 500,000 over 5 years to PI(Bristow).

Conclusions:

We have gained excellent momentum regarding the importance of DNA-dsb repair as an important endpoint in the radiation response of prostate cancer and potentially, prostate carcinogenesis. A number

of manuscripts have been accepted or are in press. We have also leveraged the original US Army grant to more than 2.0 million Canadian dollars in external funding.

Out studies suggest that there are defects in DNA repair relating to intracellular trafficking or chaperoning of DNA repair factors to the nucleus. This is a novel concept and could give rise to new treatments targeting nuclear import and export of proteins in prostate cancer. Other DNA repair pathways amenable to study and targeting are the DNA-ddb and base excision repair (BER) pathways which also are abnormal in prostate cancer cells. Our data with human biopsies pre and post-clinical radiotherapy also supports the quantification of DNA damage signaling pathways and repair factors as potential determinants of radioresponse.

Radiotherapy and Oncology xx (2005) 1-9
www.elsevier.com/locate/radonline

Original article

Hypoxia down-regulates DNA double strand break repair gene expression in prostate cancer cells

Alice X. Meng[a], Farid Jalali[a], Andrew Cuddihy[a], Norman Chan[a], Ranjit S. Bindra[b], Peter M. Glazer[b], Robert G. Bristow[a,b,*]

[a]*Ontario Cancer Institute and Princess Margaret Hospital (University Health Network), Toronto, Ont., Canada,* [b]*Department of Therapeutic Radiology, Yale University School of Medicine, New Haven, CT, USA,* [c]*Departments of Medical Biophysics and Radiation Oncology, University of Toronto, Canada*

Abstract

***Background and purpose*: Intratumoral hypoxia has been correlated with poor clinical outcome in prostate cancer. Prostate cancer cells can be genetically unstable and have altered DNA repair. We, therefore, hypothesized that the expression of DNA double-strand break (DNA-dsb) repair genes in normal and malignant prostate cultures can be altered under hypoxic conditions.**

***Methods and materials*: The expression of homologous recombination (HR) and non-homologous recombination (NHEJ) genes following gas hypoxia (0.2%) or exposure to HIF1α-inducing agent, $CoCl_2$ (100 μM), was determined for normal diploid fibroblasts (GM05757) and the pre-malignant and malignant prostate cell lines, BPH-1, 22RV-1, DU145 and PC3. RNA and protein levels were determined using RT-PCR and Western blotting. Additionally, p53 genotype and function, the level of hypoxia-induced apoptosis, and cell cycle distribution, were determined to correlate to changes in DNA-dsb gene expression.**

***Results*: Induction of hypoxia was confirmed using HIF1α and VEGF expression in gas- and $CoCl_2$-treated cultures. Hypoxia (48-72 h of 0.2% O_2) decreased RNA expression of a number of HR-related genes (e.g. *Rad51*, *Rad52*, *Rad54*, *BRCA1*, *BRCA2*) in both normal and malignant cultures. Similar decreases in RNA pertaining to the NHEJ-related genes (e.g. *Ku70*, *DNA-PKcs*, *DNA Ligase IV*, *Xrcc4*) were observed. In selected cases, hypoxia-mediated decreases in RNA expression led to decreased DNA-dsb protein expression. $CoCl_2$-treated cultures did not show decreased DNA-dsb protein expression. The ability of hypoxia to down-regulate *Rad51* and other HR-associated genes under hypoxia was not correlated to *c-Abl* or *c-Myc* gene expression, p53 genotype or function, propensity for hypoxia-mediated apoptosis, or specific changes in cell cycle distribution.**

***Conclusions*: Hypoxia can down-regulate expression of DNA-dsb repair genes in both normal and cancer cells. If associated with a functional decrease in DNA-dsb repair, this observation could provide a potential basis for the observed genetic instability within tumor cells exposed to hypoxia.**

Keywords: Hypoxia; DNA repair; Rad51; Prostate cancer; Genetic instability

Despite improvements in physical targeting techniques, up to 40% of prostate cancer patients may fail radical radiotherapy [37]. This is likely due to genetic or micro-environmental factors that increase radioresistance or systemic spread [7]. Intratumoral hypoxia is an adverse clinical prognostic factor for prostate and other cancers and is associated with decreased disease-free survival. The hypoxic microenvironment may select for aggressive tumor cell variants [12,46,36,27], as hypoxic prostate cancer cells acquire increased cell proliferation, decreased sensitivity to apoptosis and increased angiogenesis [17,22]. Both experimental and spontaneous metastatic capacity can be increased when tumor cells are exposed to hypoxia or hypoxia followed by re-oxygenation [11].

Metastatic cells acquire autonomy from growth factors and normal apoptotic controls. Hypoxia-induced metastasis is associated with gene amplification, point mutation, hyper-mutagenesis and induction of DNA strand breaks [4]. Indeed, anoxia can induce a DNA replication arrest activating the ATR kinase, whereas re-oxygenation can lead to the formation of DNA breaks activating the ATM kinase [25]. These non-repaired DNA breaks could activate oncogenes or

0167-8140/$ - see front matter © 2005 Published by Elsevier Ireland Ltd. doi:10.1016/j.radonc.2005.06.025

inactivate tumor suppressor genes, giving rise to a *mutator* phenotype and the selection of tumor cell variants with increased growth potential [6].

The non-repair or mis-repair of DNA double-strand breaks (DNA-dsbs) is one of the most highly-carcinogenic processes leading to chromosomal deletions, translocations and rearrangements in the affected cell [3,4,24,39]. Human DNA-dsbs are repaired through two different pathways that can interact with each other across cell cycle transitions to complete DNA-dsb repair. These include homologous recombination (HR) and non-homologous recombination (i.e. end-joining or NHEJ) [20,41,49]. HR is an error-free pathway operational in S and G2 phases and involves RAD51, its paralogs RAD51B/C/D, XRCC2/3, and p53, RPA, BRCA2, BLM and MUS81 [3]. In contrast, NHEJ can occur without the use of homologous sequences and can be precise or imprecise, depending on the structure of the DNA end [48]. NHEJ can be utilized during all phases of the cell cycle and involves KU70/80, DNA-PKcs, Artemis, XRCC4, DNA Ligase IV and more recently, ATM, p53 and MDM2 [14,38,48]. Initial DNA-dsb sensing and nucleotide processing towards HR or NHEJ repair has been associated with the MRN (MRE11-RAD50-NBS1) complex [48]. Importantly, inhibition of HR or NHEJ activity has been linked to increased carcinogenesis and genetic instability [14,48]. However, little is known about the molecular expression and function of DNA-dsb repair proteins under conditions of hypoxia.

We have previously reported that hypoxia specifically down-regulates the expression and function of RAD51 protein, independent of cell cycle distribution and the expression of hypoxia-inducible factor, HIF1α [5]. In other work, we have suggested that DNA-dsb repair may be defective in prostate cancer cell lines when compared to normal prostate epithelium, despite malignant cells expressing high levels of DNA-dsb repair proteins [20]. In this study, we compare the expression of a number of HR- and NHEJ-related genes following gas hypoxia or $CoCl_2$ treatments in normal diploid fibroblasts and four prostate cancer cell lines. We show that many of the DNA-dsb-associated genes are down-regulated specifically by hypoxia and that this is not correlated to p53 status, propensity for hypoxia-mediated apoptosis or S-phase cell cycle arrests. Our findings support the concept that hypoxia may alter DNA repair to promote genetic instability during prostate carcinogenesis and tumor progression.

Materials and methods

Prostate cell cultures and hypoxic or $CoCl_2$ treatments

The human malignant prostate cell lines DU145 and PC3 were purchased from American Type Culture Collection (ATCC; Manassas, VA) and the 22RV-1 cell line was a kind gift of Dr Yoni Pinthus (PMH). These cell lines were supplemented with 10% fetal calf serum and 1% L-Glutamine in α-Modified Eagles Medium (MEM), Ham's F12K and RPMI1640, respectively. The normal diploid fibroblast strain GM05757 was purchased from Coriell Cell Repository (Camden, NJ). The SV40-immortalized, benign prostatic hyperplasia cell line, BPH-1, was a gift from Dr Simon Hayward (Vanderbilt University Medical Center). Both GM05757 and BPH-1 cells grow in α-Modified Eagles Medium with 15% fetal calf serum. Approximate doubling times for cell cultures under these conditions were as follows: DU-145 and BPH-1, 18 h; PC-3, 24 h; GM05757, 18 h; 22RV-1, 40 h [20].

For all experiments, $1\text{-}3\times10^5$ cells were plated in 10-cm dishes, such that cells were logarithmically growing at all time points tested. Cells were incubated in 5% CO_2 and air at 37 °C. To render cells low-oxygen hypoxic, dishes were placed in a modular incubator chamber (Billups-Rothenberg, Del Mar, CA). They were then flushed with 0.2% O_2 (hypoxia) or 21% O_2 (oxia) with 5% CO_2 and balanced with N_2 as previously described [52]. To test for HIF1-associated gene and protein responses, cells were treated with 100 μM $CoCl_2$ (Sigma-Aldrich, Inc. St Louis, MO) for 3-72 h.

p53 genomic DNA (gDNA) sequencing

Genomic DNA was isolated from the harvested cells using DNeasy™ Tissue Kit (QIAGEN Sciences, Inc. Germantown, MA). In order to have a high fidelity amplification of p53 gene, gDNA were amplified by PCR (Expand High Fidelity PCR System, Roche Applied Science, Indianapolis, IN) for exons 2-4, 5-9 and 10-11. Target PCR products were analyzed and extracted from a 1% agarose gel using a QIAquick Gel Purification Kit (QIAGEN Sciences, Inc. Germantown, MA). A Beckman Coulter capillary electrophoresis CEQ 2000XL DNA analysis instrument housed within the UHN DNA Sequencing Facility verified the sequences of the p53 PCR fragments [20].

Cell cycle and apoptosis assays

The level of cellular apoptosis was scored as previously described using a nuclear morphology endpoint [8,9]. Both floating and adherent cells from normoxic or hypoxic cultures were collected following treatment and stained with 10 μM Hoechst 33342 dye in 4% formalin-PBS for 30 min. Stained cells were visualized under a fluorescence microscope for evidence of distinct nuclear fragmentation and apoptotic bodies. The number of apoptotic cells per one hundred cells counted was quantified as the apoptotic index for each cell line. For each cell line, at least 2 independent experiments were performed.

The cell cycle distribution of cells grown under normoxia or hypoxia was quantitated using flow cytometry as previously described [8,9]. Briefly, treated cells were collected, washed and fixed in 70% ethanol. For flow cytometric analysis of cell cycle distribution, cells were washed with PBS without Mg^{2+}–Ca^{2+} prior to staining with 50 μM propidium iodide (Sigma-Aldrich, Inc., St Louis, MO) and 50 μg/ml Dnase-free RNase. Flow cytometry was performed using a FACSCalibre flow cytometer (BD Biosciences, San Jose, CA) and cell cycle distribution profiles were analysed using CellQuest software (BD Biosciences, San Jose, CA).

Western blot analyses for protein expression

Lysates for Western blotting were processed as previously described [20]. SDS-PAGE was performed using 8-10% bis-acrylamide gels at room temperature. Each well was loaded with 30 μg of total protein plus loading buffer (final

concentration 6% glycerol, 0.83% β-mercaptoethanol, 1.71% Tris-HCl (pH 6.8), and 0.002% bromphenol blue). Samples were resolved by electrophoresis at 80-110 V for 1.5-2.5 h and then transferred onto nitrocellulose (Schleicher & Schuell Bioscience, Keene, NH). Pre-hybridization staining with Ponceau solution confirmed optimal transfer between running lanes. After transfer, membranes were incubated in appropriate secondary antibodies and protein bands detected using ECL Detection Reagent (Amersham BioScience) prior to quantitation using Scion Image (Scicon Corporation, Frederick, MD).

Primary antibodies were used at dilutions ranging from 1:200 to 1:1000 as suggested by the supplier and included the following: HIF1α (BD Transduction Laboratories, Franklin Lakes, NJ), ACTIN (Sigma-Aldrich, Inc., St Louis, MO); $p21^{WAF}$, RAD51 (Oncogene Research Products, San Diego, CA); XRCC3, RAD51C, RAD51D, RAD50 (Novus Biologicals, Inc., Littletown, CO); KU70 (Santa Cruz Biotechnology, Santa Cruz, CA) and MRE11 (Genetex, San Antonio, TX). Results shown are representative of at least 2-6 independent experiments.

RNA extraction and reverse transcriptase-polymerase chain reaction (RT-PCR) for RNA expression

Total RNA was extracted using TRI reagent (Sigma-Aldrich, Inc., St Louis, MO) and digested initially with DNase I (Invitrogen, Carlsbad, CA). The digested products were then reverse-transcribed with random hexamer primers in a 20 μl volume (GeneAmp RNA PCR kit, Applied Biosystems, Foster City, CA). Three microlitre cDNA was amplified by PCR (Expand High Fidelity PCR System, Roche Applied Science, Indianapolis, IN) with the following primers specific for the hypoxia response gene, *VEGF*, and selected DNA repair genes:

VEGF (94 bp. Sense, 5′-CAGTTTTGGGAACACCGACAA-3′. Antisense, 5′-ATCCCGGAACCTGTGATTTG-3′),
Rad51 (473 bp. Sense, 5′-GCCTGCTGGAGAGAGGA-3′. Antisense, 5′-GGAAGCTGGCAGGTGAC-3′),
Rad51C (511 bp. Sense, 5′-AGTGGCAGGTGAAGCAGTTT-3′. Antisense, 5′-CTTTCGGTCCCAATGAAAGA-3′),
Rad51D (289 bp, 407 bp. Sense, 5′-CAGTGGTG-GACCTGGTTTCT-3′. Antisense, 5′-TTCTGCCTGTTCCTCCTCAT-3′),
Xrcc3 (600 bp. Sense, 5′-GTGCATCAACCAGGTGACAG -3′. Antisense, 5′-CCCAGGGAGTCACTGTAGG -3′),
BRCA1 (285 bp. Sense, 5′-TTGCGGGAGGAAAATGGG-TAGTTA-3′. Antisense, 5′-TGTGCCAAGGGTGAATGAT-GAAG-3′),
BRCA2 (248 bp. Sense, 5′-CCCATGAGGCAAAGCATAAT-3′. Antisense, 5′-CTGCATTTGACCCATTTCCT-3′),
Rad52 (597 bp. Sense, 5′-GACGCACAGCACTCCTGTAAC -3′. Antisense, 5′-CATCTGTCCAGAGCCTCTCC -3′),
c-Abl (201BP. SENSE, 5′-TTCAGCGGCCAGTAGCATCT-GACTT-3′. Antisense, 5′-TGTGATTATAGCCTAAGACCCG-GAG -3′),
Rad54 (278 bp. Sense, 5′-CATCATGGCTGATGAGATGG-3′. Antisense, 5′-TGAGGATGGGAGAAGACACC-3′),
Rad50 (322 bp. Sense, 5′-ACCCACCACCTTCTTCTCCT-3′. Antisense, 5′-TGGCATCTGAAGAGCAAATG-3′),
Mre11 (285 bp. Sense, 5′-CTTGTACGACTGCGAGTGGA-3′. Antisense, 5′-TTCACCCATCCCTCTTTCTG-3′),
Xrcc4 (499 bp. Sense, 5′-GGCAATGGAAAAAGGGAAAT-3′. Antisense, 5′-TCGGTCAGCAGTCATTTCAG-3′),
DNA Ligase IV (797 bp. Sense, 5′-GGCAACTGCAT-GATCCTTCT-3′. Antisense, 5′-GGGCTTCTCTGCTACTG-CAC-3′),
DNA-PKcs(236 bp. Sense, 5′-ACACCATGTCCCAAGAGGAG-3′. Antisense, 5′-AGCCTCAGGGCTTGTACTCA-3′)
Ku70 (981 bp. Sense, 5′-TATTTACGTCTTACAGGAGC-3′. Antisense, 5′-GCATCTTCCTTTTATCATCA-3′).

The β-*Actin* gene (226 bp. Sense, 5′-GACCCAGAT-CATGTTTGAGACC-3′; Antisense 5′-GGT GAG GAT CTT CAT GAG GTAG-3′) was amplified as an internal control. PCRs were performed in a PTC200 thermal cycler (MJ Research, Watertown, MA) at 95 °C for 2 min, and then subjected to 30 cycles of amplification at 94 °C for 1 min, 55 °C for 1 min and 72 °C for 1 min. The final elongation step was 72 °C for 5 min. Target PCR products were analyzed, extracted from a 1% agarose gel containing ethidium bromide and visualized by UV detection. Results shown are representative of at least 2-6 independent experiments.

Results

Initial experiments confirmed the gas hypoxic response (0.2 or 2.0% O_2 concentrations) in logarithmically-growing normal (normal diploid fibroblast strain, GM05757) and malignant (DU145 prostate cancer) cell cultures. Fig. 1 demonstrates up-regulation of *VEGF* RNA and increased expression of HIF1α protein at 48 and 72 h for both GM05757 and DU145 cells. Repeated experiments showed similar induction at times ranging from 24 to 72 h for all cultures tested at 0.2% and 2% oxygen gassing conditions (data not shown). Increased endogenous HIF1α expression following gassing with 21% oxygen in DU145 and PC3 cells was consistent with the reported increased basal expression and hyper-inducibility of HIF1α in malignant prostate cells [43].

Although the expression and function of *Rad51* can be down-regulated following hypoxia [5]. It was unknown whether *Rad51* expression following hypoxic exposure is differentially affected in normal cells relative to malignant cells. Fig. 2(a) and (b) shows the relative expression of RAD51 protein in DU145 and PC3 cells relative to GM05757 normal fibroblasts, in which RAD51 protein levels are uniformly decreased at 72 h following hypoxia in both normal and malignant cultures. We, therefore, chose this time-point to determine *Rad51* RNA and RAD51 protein levels amongst a group of immortalized and malignant prostate cell cultures (see Fig. 2(c) and (d)). In all cases, *Rad51* RNA and RAD51 protein were decreased, with final protein levels in the malignant cell lines approaching that of GM05757. However, there is discordance between RNA and protein levels amongst the cell lines following hypoxia: RNA expression can be ablated by hypoxia without the total ablation of RAD51 protein (c.f. RNA and protein expression of DU145 and PC3 cells). The latter observation may be due

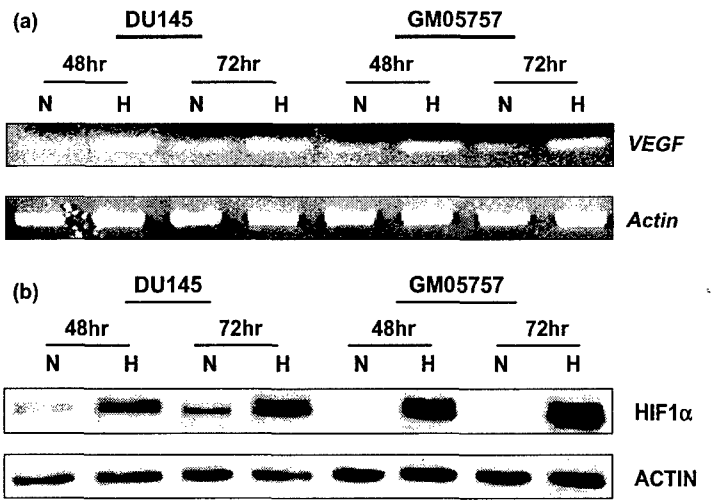

Fig. 1. Increased *VEGF* RNA and HIF1α protein in response to hypoxia. (a) RNA expression (based on RT-PCR) of the *VEGF* gene following 48 or 72 h of 0.2% O_2 in malignant DU145 prostate cells or normal GM05757 fibroblasts. The relative levels of *Actin* RNA are shown as a loading control. (b) Western blot for protein expression showing induction of the HIF1α protein following 48 or 72 h of 0.2% O_2 (hypoxia) in the same cell lines. ACTIN protein levels are shown as a loading control.

to the long-half life of the RAD51 protein in relation to the half-life of *Rad51* RNA [5].

In human cells, the majority of DNA-dsbs are repaired by either the HR and/or the NHEJ pathways in a cell cycle and cell-type specific manner [41,48]. We, therefore, compared the RNA and protein expression of selected genes within each of these pathways following hypoxic exposure (Fig. 3). At the RNA level, we observed that the *Rad51* paralogs (e.g. *Rad51C*, *Rad51D*, *Xrcc3*) and the HR-related genes, *BRCA1*, *BRCA2*, *Rad54*, *Rad52*, were all down-regulated in both normal and malignant hypoxic cultures, independent of *c-Abl* gene expression alterations (the latter reported to transcriptionally up-regulate *Rad51*; see Fig. 3(a)) [13,45].

Similar decreases in expression were also noted for *DNA-PKcs*, *Ku70* and *DNA-Ligase IV genes*, but not for the *Xrcc4* gene or the *Rad50* and *Mre11* genes (the latter involved in the MRN complex and DNA damage sensing; see Fig. 3(b)). Again, we observed discordance between RNA and final protein levels for some of these genes (c.f. Fig. 3(a) and (b) with (c)). For example, the RNA level for *Ku70* was decreased by hypoxia, yet there was not a resultant decrease at the protein level. Further biochemical studies will be required to determine whether hypoxia solely alters HR protein, rather than NHEJ, protein expression. However, we did not observe a similar down-regulation of RAD51-associated proteins following $CoCl_2$ treatment (100 μM for 3 or 72 h) when compared to gas hypoxia (for more detail see Appendix 1 in the online version of this article). This illustrates the potential for disparate results when using gas hypoxia or chemical inducers of HIF1α such as $CoCl_2$ or desferrioxamine (DFX).

Finally, the relative level of *Rad51* expression or function following hypoxic exposure could be biased by a number of molecular and cellular factors including p53 expression and function (e.g. ability to up-regulate $p21^{WAF}$), the capacity for hypoxia-mediated apoptosis, the level of *c-Myc* expression and relative cell cycle distribution [1,18,19,20,23,26,34,47,51,52]. Endogenous expression of HR-associated genes is increased within malignant prostate cell lines[20] and the expression or function of *Rad51* and other HR-associated genes can vary with differential p53 status and interact with $p21^{WAF}$-mediated G1 checkpoint control or be affected by cells undergoing apoptosis or cell cycle arrest during S-phase[19].

DU145 and PC3 cells lack p53 function and $p21^{WAF}$ up-regulation following DNA damage, due to mutant or null p53 expression, respectively [20]. Our sequencing experiments revealed there were no mutations within exons 2-11 of the p53 gene in GM05757, BPH-1 and 22RV-1 cells. Indeed, the latter three lines all up-regulated $p21^{WAF}$ following DNA damage, consistent with wild type p53 function (see Fig. 4(a)). Decreased *Rad51* expression following hypoxia is, therefore, not correlated to p53 expression nor function in our cell lines.

We next determined the cell cycle distribution of the five cell cultures pre-, and post-hypoxia, using flow cytometry (representative profiles in Fig. 4(b) and mean quantitative data in Fig. 4(c)). The S-phase fractions in the wild type p53-expressing cell lines varied minimally after 72 h of hypoxia, whereas the two cell lines which lack p53 function showed either decreased or increased S-phase fractions. This is supported by minimal changes in the expression of the *c-Myc* gene (Fig. 4(d)) which has been linked cell proliferation, apoptosis and HR [1,47]. All the cell lines showed a decrease in G2 phase cells and an increase or sustaining of the G1 fraction, consistent with the hypoxia-induced G1 arrest being p53-independent [26]. These slight cell cycle changes do not, however, account for the large RNA decreases observed for DNA-dsb repair genes within both the HR and NHEJ pathways.

Finally, we scored all cultures for apoptotic morphology (pre- and post-hypoxia) to rule out decreased *Rad51* expression as a consequence of hypoxia-induced apoptosis. We observed a large and significant increase in hypoxia-induced apoptosis solely in the wild-type p53-expressing 22RV-1 cells ($P<0.05$; Fig. 4(e)). Altogether, there is no

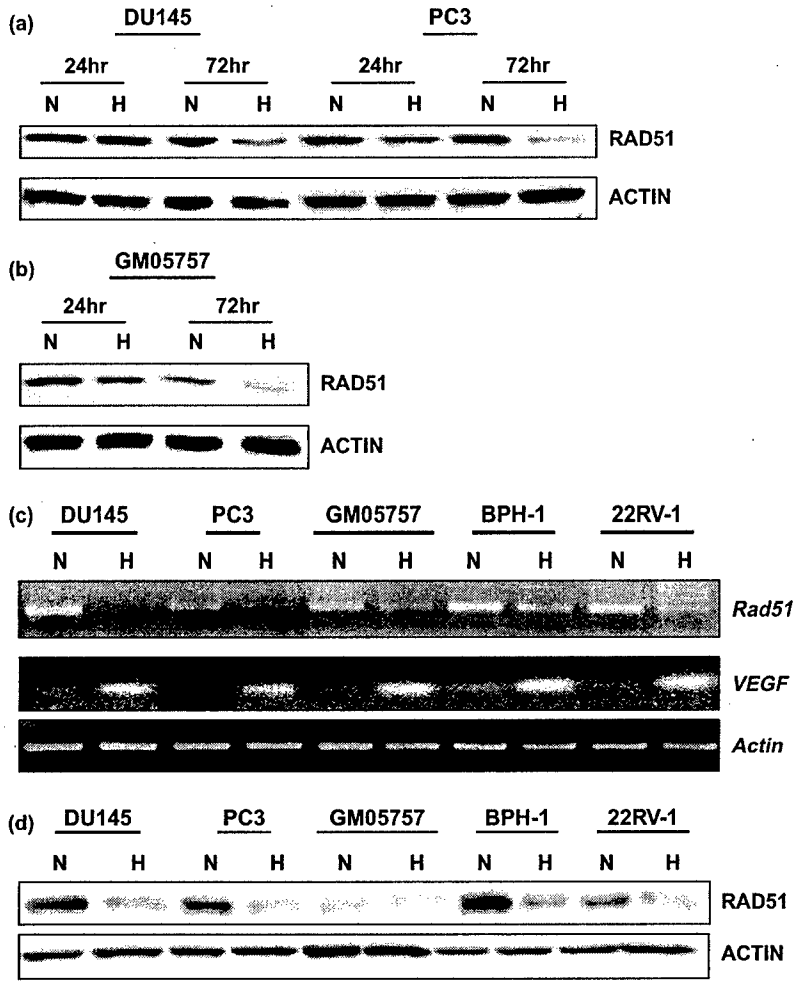

Fig. 2. Decreased Rad51 gene expression in normal and malignant cultures following hypoxia. (a) Western for protein expression showing decreased expression of the RAD51 protein following 24 or 72 h of 0.2% O_2 in malignant DU145 and PC3 prostate cells or normal GM05757 fibroblasts. The relative ACTIN protein levels are shown as a loading control. (b) Similar Western blot as in (a), but for normal GM05757 fibroblasts. (c) RNA expression of the *Rad51* and *VEGF* genes following 72 h of 0.2% O_2 in the prostate cell lines DU145, PC3, BPH-1 and 22RV-1 and normal GM05757 cells. The relative levels of *Actin* RNA are shown as a loading control. (d) Western blot for RAD51 protein expression following 72 h of 0.2% O_2 in malignant and normal cultures described in (c). The relative ACTIN protein levels are shown as a loading control.

correlation between decrease in HR-related gene expression and p53 status, apoptotic capacity or *c-Myc* levels or S-phase fraction following hypoxic exposure.

Discussion

To our knowledge, this is the first report that documents gene expression relating to members of the HR and NHEJ pathways following hypoxia in normal, immortalized and malignant cells. We observed decreases in HR-related DNA-dsb repair protein expression within several immortalized and malignant prostate cell lines following gas hypoxia, but not $CoCl_2$-treatment. In our study, the HIF1α-induced gene expression induced by $CoCl_2$ was insufficient to alter RAD51 protein expression. In a previous study using MCF-7 cells, DFX treatment led to a decrease in *Rad51* RNA and also in protein levels [4,5]. The differences between the two studies may relate to HIF1α-independent effects of DFX relative to $CoCl_2$ and reinforces the point that the use of DFX or $COCl_2$ may not directly mimic the gene expression or cell biology under low oxygen conditions.

Our observation that RNA expression was reduced for a number of DNA-dsb genes speaks to a mechanism by which hypoxia reduces HR-gene transcription through altered expression of transcriptional activators and/or repressors [4,10,50] such as has been described for RAD51 expression changes that are linked to E2F and growth state [28], or that hypoxia has a more general effect on RNA transcription. At the level of protein translation, it is known that hypoxia leads to a rapid and sustained inhibition of protein synthesis, mediated by eukaryotic initiation factor 2alpha (eIF2alpha) phosphorylation by the endoplasmic reticulum (ER) kinase, PERK; whether this pathway can alter RAD51 protein levels requires further study [33]. Future temporal studies of these and other modifications following hypoxia may help clarify the disparity between RNA and final protein levels amongst the DNA-dsb pathways tested.

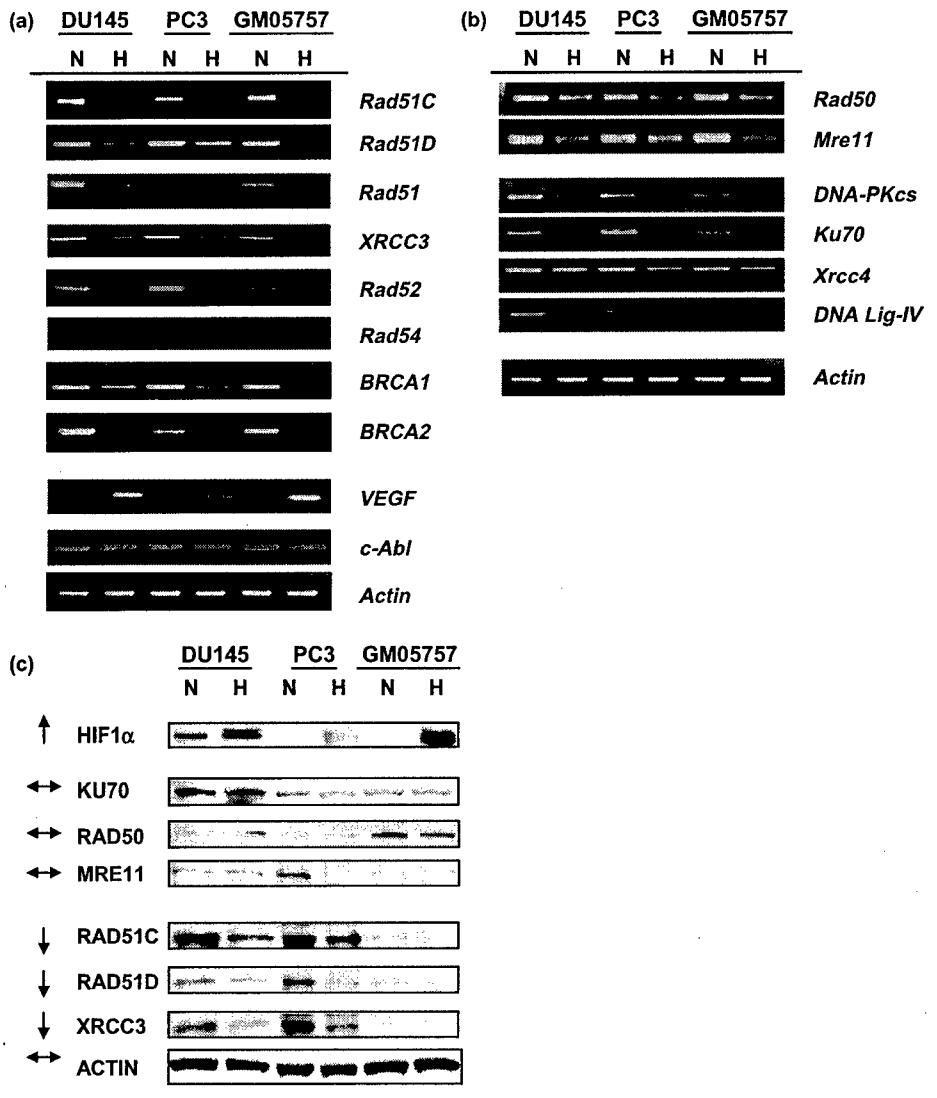

Fig. 3. Decreased HR- and NHEJ-related gene expression following hypoxia. (a) RNA expression of selected homologous recombination-related, *VEGF* and *c-Abl* genes following 72 h of 0.2% O_2 in the prostate cell lines DU145, PC3 and normal GM05757 fibroblasts. (b) RNA expression of selected non-homologous recombination and *Mre11*, *Rad50*, *VEGF* and *c-Abl* genes following 72 h of 0.2% O_2 in the prostate cell lines DU145, PC3 and normal GM05757 fibroblasts. The relative levels of *Actin* RNA are shown as a loading control for (a) and (b). (c) Western blot for selected homologous and non-homologous recombination protein expression following 72 h of 0.2% O_2 in malignant DU145, PC3 and normal GM05757 cultures. ACTIN protein levels are shown as a loading control.

When taken together with our previous studies [5], the present experiments suggest that a discordance between cell proliferation, induction of DNA breaks, and defective DNA repair, could drive genetic instability and emergence of aggressive cell clones within hypoxic sub-regions of tumors [4,20]. Other investigators have reported that the expression of genes relating to base excision repair (BER), DNA-single strand break (DNA-ssb) repair and mismatch repair (MMR) can also be modified under hypoxic conditions [15,29,31,32]. When placed in the context of hypoxia-induced genetic changes leading to hypoxic adaption and clonal selection, hypoxic tumor cells which have decreased expression of DNA repair genes may acquire increased DNA-dsbs, DNA-ssbs, oxidative damage and errors of replication to drive tumor progression with a mutator phenotype [20].

Functional assessments of the level and fidelity of DNA-dsb repair are still required to link altered expression with altered function. Hypoxia can reduce the initial number of DNA-dsbs by a factor of 2 to 3 [21,22,27,30]. However, the subsequent repair of these breaks by HR or NHEJ under hypoxic conditions and whether this is altered in malignant versus normal cells is not well-characterized. We are currently determining the relative ability of oxic and hypoxic cells to conduct HR using endpoints relating to intranuclear RAD51 repair foci in situ and gene conversion events using an intra-chromosomal, GFP-based plasmid reporter system [49]. These models will be helpful in determining whether repair-deficient clones are selected for by acute hypoxia and/or re-oxygenation or adaption to chronic hypoxia [50].

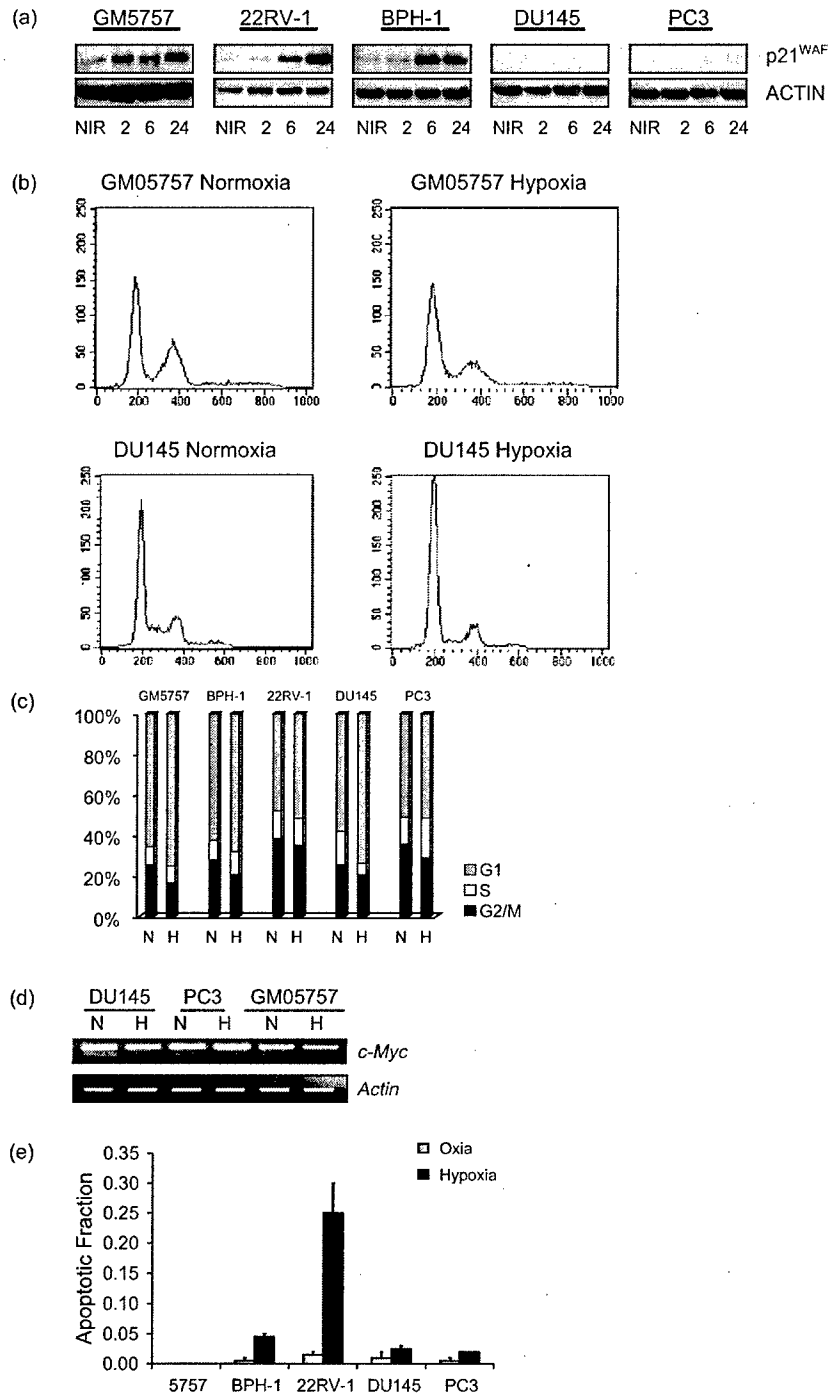

Fig. 4. DNA-dsb repair expression following hypoxia does not correlate directly with p53 status, hypoxia-induced apoptosis or cell cycle distribution. (a) Western blot for induction of the $p21^{WAF}$ protein at 0, 2, 6 and 24 h following a dose of 10 Gy in malignant prostate and normal diploid fibroblast cultures. ACTIN protein levels are shown as a loading control. (b) DNA histograms as flow cytometric profiles of GM05757 normal diploid fibroblasts and DU145 malignant prostate cancer cells cultured under normoxic conditions or under 0.2% O_2 for 72 h. Shown are the histograms used for quantitation of G1, S and G2/M fractions. (c) Mean fractions of cells in G1, S and G2/M when cultured under normoxic conditions or under 0.2% O_2 for 72 h. Data represents the mean values of each cell cycle phase based on two independent experiments. (d) RNA expression for the *c-Myc* gene following normoxia or 0.2% O2 for 72 h for the prostate cell lines DU145, PC3 and normal GM05757 fibroblasts. The relative levels of *Actin* RNA are shown as a loading control. (e) Relative fraction of cells with apoptotic morphology (based on Hoechst 33342 nuclear staining) for malignant and normal cells cultures exposed to normoxia (grey bars) or 0.2% O_2 (black bars) for 72 h. The data represents the mean, and standard errors of the mean, based on replicate experiments. The differences in apoptosis amongst the 4 positive cultures were significant ($P<0.05$). Less than 1% apoptosis was scored within the normal GM05757 fibroblasts following either treatment.

Hypoxic tumor cells remain an important target for oncology [10]. We have previously hypothesized that relative DNA-dsb repair expression and function amongst normal and malignant prostate cells, may be disparate under in vitro versus in vivo conditions due on microenvironmental factors [19]. The data in the current report support this hypothesis. As a result, the staining of DNA damage and response proteins within histologic sections of prostate, or other cancers, as biomarkers of carcinogenesis or genetic instability, will need co-staining with markers of intratumoral oxygen to avoid bias [2,16,20,42].

Intratumoral hypoxia can be modified by androgen deprivation [40,44] and is associated with the development of aggressive androgen-independent prostate cancer cells, which is a cause of mortality in prostate cancer patients. Our findings, therefore, support investigation of novel strategies that augment DNA repair as a means to prevent carcinogenesis and tumor progression. They also support the study of molecular-based strategies [35] which target hypoxia or abnormal DNA-dsb repair in prostate tumors as an adjunct to radiotherapy.

Acknowledgements

The authors would like to thank Drs D. Hedley, R.P. Hill and M. Milosevic for helpful discussions and encouragement. These studies are supported by operating grants to R.G.B. from the Terry Fox Foundation (Hypoxia Project Program Grant), Ontario Cancer Research Network PMH Foundation, US Army DOD Prostate Cancer Program and a grant to P.M.G. from the NIH (ES05775). R.S.B. was supported by NIH Medical Scientist Training Grant (GM07205). R.G.B. is a Canadian Cancer Society Research Scientist.

Supplementary Material

Supplementary data associated with this article can be found, in the online version at 10.1016/j.radonc.2005.06.025

* Corresponding author. Robert G. Bristow, Department of Radiation Oncology, Ontario Cancer Research Network, Princess Margaret Hospital, 610 University Avenue, Rm 5-923, Toronto, Ont., Canada M5G2M9. *E-mail address:* rob.bristow@rmp.uhn.on.ca

Received 10 May 2005; received in revised form 13 May 2005; accepted 19 June 2005

References

[1] Alarcon RM, Rupnow BA, et al. Modulation of c-Myc activity and apoptosis in vivo. Cancer Res 1996;56:4315-9.
[2] Bartkova J, Horejsi Z. DNA damage response as a candidate anti-cancer barrier in early human tumorigenesis. Nature 2005; 434:864-70.
[3] Bertrand P, Saintigny Y, et al. p53's double life: transactivation-independent repression of homologous recombination. Trends Genet 2004;20:235-43.
[4] Bindra RS, Glazer PM. Genetic instability and the tumor microenvironment: towards the concept of microenvironment-induced mutagenesis. Mutat Res 2005;569:75-85.
[5] Bindra RS, Schaffer PJ, et al. Down-regulation of Rad51 and decreased homologous recombination in hypoxic cancer cells. Mol Cell Biol 2004;24:8504-18.
[6] Bristow R, Harrington L. Genomic Stability and DNA Repair. In: Tannock HR, Harrington L, Bristow RG, editors. The basic science of oncology. 4th ed. New York: McGraw-Hill Ltd; 2005. p. 77-99.
[7] Bristow RG, Hill R. Molecular and Cellular Radiobiology. In: Tannock HR, Harrington L, Bristow RG, editors. The basic science of oncology. 4th ed. New York: McGraw-Hill Ltd; 2005. p. 261-88. Chapter 14.
[8] Bristow RG, Hu Q. Radioresistant MTp53-expressing rat embryo cell transformants exhibit increased DNA-dsb rejoining during exposure to ionizing radiation. Oncogene 1998;16:1789-802.
[9] Bromfield GP, Meng A, et al. Cell death in irradiated prostate epithelial cells: role of apoptotic and clonogenic cell kill. Prostate Cancer Prostat Dis; In Press.
[10] Brown JM, Wilson WR. Exploiting tumour hypoxia in cancer treatment. Nat Rev Cancer 2004;4:437-47.
[11] Cairns RA, Hill RP. Acute hypoxia enhances spontaneous lymph node metastasis in an orthotopic murine model of human cervical carcinoma. Cancer Res 2004;64:2054-61.
[12] Cairns RA, Khokha R, et al. Molecular mechanisms of tumor invasion and metastasis: an integrated view. Curr Mol Med 2003;3:659-71.
[13] Chen G, Yuan SS, et al. Radiation-induced assembly of Rad51 and Rad52 recombination complex requires ATM and c-Abl. J Biol Chem 1999;274:12748-52.
[14] Collis SJ, DeWeese TL, et al. The life and death of DNA-PK. Oncogene 2005;24:949-61.
[15] Coquelle A, Toledo F, et al. A new role for hypoxia in tumor progression: induction of fragile site triggering genomic rearrangements and formation of complex DMs and HSRs. Mol Cell 1998;2:259-65.
[16] Cuddihy AR, Bristow RG. The p53 protein family and radiation sensitivity: yes or no? Cancer Metastasis Rev 2004;23:237-57.
[17] Cvetkovic D, Movsas B, et al. Increased hypoxia correlates with increased expression of the angiogenesis marker vascular endothelial growth factor in human prostate cancer. Urology 2001;57:821-5.
[18] de Toledo SM, Azzam EI, et al. Regulation by ionizing radiation of CDC2, cyclin A, cyclin B, thymidine kinase, topoisomerase IIalpha, and RAD51 expression in normal human diploid fibroblasts is dependent on p53/p21Waf1. Cell Growth Differ 1998;9:887-96.
[19] Essers J, Hendriks RW, et al. Analysis of mouse Rad54 expression and its implications for homologous recombination. DNA Repair (Amst) 2002;1:779-93.
[20] Fan R, Kumaravel TS, et al. Defective DNA strand break repair after DNA damage in prostate cancer cells: implications for genetic instability and prostate cancer progression. Cancer Res 2004;64:8526-33.
[21] Frankenberg-Schwager M, Frankenberg D, et al. Different oxygen enhancement ratios for induced and unrejoined DNA double-strand breaks in eukaryotic cells. Radiat Res 1991;128: 243-50.
[22] Ghafar MA, Anastasiadis AG, et al. Acute hypoxia increases the aggressive characteristics and survival properties of prostate cancer cells. Prostate 2003;54:58-67.
[23] Graeber TG, Peterson JF, et al. Hypoxia induces accumulation of p53 protein, but activation of a G1-phase checkpoint by low-oxygen conditions is independent of p53 status. Mol Cell Biol 1994;14:6264-77.
[24] Guirouilh-Barbat J, Huck S, et al. Impact of the KU80 pathway on NHEJ-induced genome rearrangements in mammalian cells. Mol Cell 2004;14:611-23.

[25] Hammond EM, Dorie MJ, et al. Inhibition of ATR leads to increased sensitivity to hypoxia/reoxygenation. Cancer Res 2004;64:6556-62.
[26] Hammond EM, Giaccia AJ. The role of p53 in hypoxia-induced apoptosis. Biochem Biophys Res Commun 2005;331: 718-25.
[27] Hill R, Bristow RG. The scientific basis of clinical radiotherapy. In: Tannock HR, Harrington L, Bristow RG, editors. The basic science of oncology. 4th ed. New York: McGraw-Hill Ltd; 2005. p. 289-321. Chapter 15.
[28] Iwanaga R, Komori H, et al. Differential regulation of expression of the mammalian DNA repair genes by growth stimulation. Oncogene 2004;23:8581-90.
[29] Kelley MR, Cheng L, et al. Elevated and altered expression of the multifunctional DNA base excision repair and redox enzyme Ape1/ref-1 in prostate cancer. Clin Cancer Res 2001;7:824-30.
[30] Koch CJ, Painter RB. The effect of extreme hypoxia on the repair of DNA single-strand breaks in mammalian cells. Radiat Res 1975;64:256-69.
[31] Kondo A, Safaei R, et al. Hypoxia-induced enrichment and mutagenesis of cells that have lost DNA mismatch repair. Cancer Res 2001;61:7603-7.
[32] Koshiji M, To KK, et al. HIF-1alpha induces genetic instability by transcriptionally downregulating MutSalpha expression. Mol Cell 2005;17:793-803.
[33] Koumenis C, Naczki C. Regulation of protein synthesis by hypoxia via activation of the endoplasmic reticulum kinase PERK and phosphorylation of the translation initiation factor eIF2alpha. Mol Cell Biol 2002;22:7405-16.
[34] Kumari A, Schultz N, et al. p53 protects from replication-associated DNA double-strand breaks in mammalian cells. Oncogene 2004;23:2324-9.
[35] Ma BB, Bristow RG, et al. Combined-modality treatment of solid tumors using radiotherapy and molecular targeted agents. J Clin Oncol 2003;21:2760-76.
[36] Parker C, Milosevic M, et al. Polarographic electrode study of tumor oxygenation in clinically localized prostate cancer. Int J Radiat Oncol Biol Phys 2004;58:750-7.
[37] Pollack A, Hanlon A, et al. Radiation therapy dose escalation for prostate cancer: a rationale for IMRT. World J Urol 2003;21: 200-8.
[38] Riballo E, Kuhne M, et al. A pathway of double-strand break rejoining dependent upon ATM, Artemis, and proteins locating to gamma-H2AX foci. Mol Cell 2004;16:715-24.
[39] Richardson C, Stark JM, et al. Rad51 overexpression promotes alternative double-strand break repair pathways and genome instability. Oncogene 2004;23:546-53.
[40] Rothermund CA, Gopalakrishnan VK, et al. Casodex treatment induces hypoxia-related gene expression in the LNCaP prostate cancer progression model. BMC Urol 2005;5:5.
[41] Rothkamm K, Kruger I, et al. Pathways of DNA double-strand break repair during the mammalian cell cycle. Mol Cell Biol 2003;23:5706-15.
[42] Sak A, Stueben G, et al. Targeting of Rad51-dependent homologous recombination: implications for the radiation sensitivity of human lung cancer cell lines. Br J Cancer 2005; 92:1089-97.
[43] Salnikow K, Costa M, et al. Hyperinducibility of hypoxia-responsive genes without p53/p21-dependent checkpoint in aggressive prostate cancer. Cancer Res 2000;60:5630-4.
[44] Skov K, Adomat H, et al. Hypoxia in the androgen-dependent Shionogi model for prostate cancer at three stages. Radiat Res 2004;162:547-53.
[45] Slupianek A, Schmutte C, et al. BCR/ABL regulates mammalian RecA homologs, resulting in drug resistance. Mol Cell 2001;8: 795-806.
[46] Subarsky P, Hill RP. The hypoxic tumour microenvironment and metastatic progression. Clin Exp Metastasis 2003;20:237-50.
[47] Vafa O, Wade M, et al. c-Myc can induce DNA damage, increase reactive oxygen species, and mitigate p53 function: a mechanism for oncogene-induced genetic instability. Mol Cell 2002;9:1031-44.
[48] Weterings E, van Gent DC. The mechanism of non-homologous end-joining: a synopsis of synapsis. DNA Repair (Amst) 2004;3: 1425-35.
[49] Willers H, Dahm-Daphi J, et al. Repair of radiation damage to DNA. Br J Cancer 2004;90:1297-301.
[50] Wouters BG, van den Beucken T, et al. Targeting hypoxia tolerance in cancer. Drug Resist Updat 2004;7:25-40.
[51] Yun S, Lie ACC, et al. Discriminatory suppression of homologous recombination by p53. Nucleic Acids Res 2004;32:6479-89.
[52] Zhang L, Hill RP. Hypoxia enhances metastatic efficiency by up-regulating Mdm2 in KHT cells and increasing resistance to apoptosis. Cancer Res 2004;64:4180-9.

Optimal Treatment of Intermediate-Risk Prostate Carcinoma with Radiotherapy

Clinical and Translational Issues

Alan M. Nichol, M.D.
Padraig Warde, M.B.B.S.
Robert G. Bristow, M.D., Ph.D.

Department of Radiation Oncology, University of Toronto and the Princess Margaret Hospital-University Health Network, Toronto, Ontario, Canada.

The authors thank Dr. Charles Catton for critical reading of this review and the members of the Princess Margaret Hospital-University Health Network Genito-Urinary Oncology Group for stimulating discussions.

Robert G. Bristow is a Canadian Cancer Society Research Scientist.

Dr. Nichol's current address: Department of Radiation Oncology, British Columbia Cancer Agency, Vancouver, British Columbia, Canada.

Address for reprints: Robert G. Bristow, M.D., Ph.D., Department of Radiation Oncology, Princess Margaret Hospital-University Health Network, 610 University Avenue, Toronto, Ontario M5G 2M9, Canada; Fax: (416) 946-4586; E-mail: rob.bristow@rmp.uhn.on.ca

Received January 18, 2005; revision received March 29, 2005; accepted April 25, 2005.

The clinical heterogeneity of intermediate-risk prostate carcinoma presents a challenge to urologic oncology in terms of prognosis and management. There is controversy regarding whether patients with intermediate-risk prostate carcinoma should be treated with dose-escalated external beam radiotherapy (EBRT) (e.g., doses > 74 gray [Gy]), or conventional-dose EBRT (e.g., doses < 74 Gy) combined with androgen deprivation (AD). Data for this review were identified through searches for articles in MEDLINE and in conference proceedings, indexed from 1966 to 2004. Currently, the intermediate-risk prostate carcinoma grouping is defined on the basis of prostate-specific antigen (PSA), tumor classification (T classification), and Gleason score. Emerging evidence suggests that additional prognostic information may be derived from the percentage of positive core needle biopsies at the time of diagnosis and/or from the pretreatment PSA doubling time. Novel prognostic biomarkers include protein expression relating to cell cycle control, cell death, DNA repair, and intracellular signal transduction. Preclinical data support dose escalation or combined AD with radiation as a means to increase prostate carcinoma cell kill. There is Level I evidence that patients with intermediate-risk prostate carcinoma benefit from dose-escalated EBRT or AD plus conventional-dose EBRT. However, clinical evidence is lacking to support the uniform use of AD plus dose-escalated EBRT. Patients in the intermediate-risk group should be entered into well designed, randomized clinical trials of dose-escalated EBRT and AD with sufficient power to address biochemical failure and cause-specific survival endpoints. These studies should be stratified by novel prognostic markers and accompanied by strong translational endpoints to address clinical heterogeneity and to allow for individualized treatment. ***Cancer* 2005;104:891–905.**

KEYWORDS: prostate carcinoma, androgen ablation, radiotherapy, prognostic factors, genomics, cell death, molecular therapy, prostate-specific antigen, combined-modality treatment, dose escalation

In 2004, the American Cancer Society estimated that 230,110 men would be diagnosed with prostate carcinoma and that 29,900 would die of the disease (available from URL: http://www.cancer.org [accessed January 10, 2005]). Recent data from the Cancer of the Prostate Strategic Urological Research Endeavor (CaPSURE) registry indicate that there has been a stage migration of prostate carcinoma over the last 15 years, when prostate-specific antigen (PSA) screening became widely available in the U.S.[1] The CaPSURE data base uses the risk stratification for prostate carcinoma defined by D'Amico et al.[2] In their scheme, intermediate-risk prostate carcinoma is defined as clinical T1–T2 disease, Gleason score < 8, and PSA ≤ 20 ng/mL with at

DOI 10.1002/cncr.21257
Published online 8 July 2005 in Wiley InterScience (www.interscience.wiley.com).

TABLE 1
Risk Group Definitions for Clinically Staged Patients with Prostate Carcinoma

Study/definition	Low stage	Intermediate stage	High stage	Very high stage
Scherr et al., 2003[17] (NCCN; 2002 TNM classification)	T1–T2a, and GS ≤ 6, and PSA < 10	T2b–T2c,[a] or GS = 7, or PSA = 10–20	T3a,[a] or GS = 8–10, or PSA > 20	T3b–T4
Roach et al., 2003[15] (15–35% risk of positive pelvic lymph nodes)		PSA < 30 and GS = 7–10 or PSA ≥ 30 and GS ≤ 6		
Lukka et al., 2001[18] (Canadian Consensus: 1997 TNM classification)	T1a–T2a, and GS ≤ 6, and PSA < 10	T2b, or GS = 7, or PSA = 10–20	T3/T4, or GS = 8–10, or PSA > 20	
Roach et al., 2000[13] (RTOG trials)[b]	T1–T2 and GS ≤ 6	T1–T2 and GS = 7 or T3 and GS ≤ 6	T1–T2 and GS = 8–10 or T3 and GS = 7	T3 and GS = 8–10
Zelefsky et al., 1998[10]	T1–T2, and GS ≤ 6, and PSA < 10	One of the following: T3, or GS ≥ 7, or PSA > 10	Two of T3, or GS ≥ 7, or PSA > 10	
D'Amico et al., 1998[2] (1992 TNM classification)	T1c–T2a, and GS ≤ 6, and PSA < 10	T2b, or GS = 7, or PSA = 10–20	T2c, or GS = 8–10, or PSA > 20	

NCCN: National Comprehensive Cancer Network; GS: Gleason score (range, 2–10); PSA: prostate-specific antigen (ng/mL); 2002 TNM classification: T2a: half of 1 lobe of the prostate, T2b: 1 lobe of the prostate, and T2c: both lobes of the prostate; 1997 TNM classification: T2a: 1 lobe of the prostate, and T2b: both lobes of the prostate; RTOG: Radiation Therapy Oncology Group; 1992 TNM classification: T2a: half of 1 lobe of the prostate, T2b: 1 lobe of the prostate, and T2c: both lobes of the prostate.

[a] Patients with multiple adverse factors may have been shifted into the next highest risk group.

[b] Bulky T2 areas (> 5 cm^2 × 5 cm^2) were grouped as T3.

least 1 of the following adverse factors present: clinical T2b disease, PSA > 10 ng/mL, or Gleason score = 7. According to CaPSURE, between 1989 and 2002, the proportion of patients presenting with high-risk disease (clinical T3–T4 disease, or Gleason score = 8–10, or PSA > 20 ng/mL) decreased from 41% to 15%, and the proportion of patients presenting with low-risk disease (clinical T1c–T2a disease, Gleason score = 2–6, and PSA ≤ 10 ng/mL) increased from 31% to 47%.[3] Therefore, despite the introduction of PSA screening, nearly one-third of all new patients with prostate carcinoma continue to present with intermediate-risk disease.

Treatment approaches for low-risk prostate carcinoma include watchful waiting, hormone therapy (e.g., androgen deprivation [AD]), radical prostatectomy, brachytherapy, or external beam radiotherapy (EBRT), depending on tumor and patient characteristics. A number of nonrandomized, retrospective studies have shown equipoise between surgical, brachytherapy, and EBRT approaches for low-risk disease.[2,4] High-risk disease now is approached routinely with combined hormono-radiotherapy based on randomized studies that have shown improvements in overall survival.[5,6] Between 1990 and 2000, the use of neoadjuvant androgen deprivation (NAD) and EBRT rose from 4.9% to 73.5% in the intermediate-risk group, despite the absence of any randomized clinical trial (RCT) for this risk group.[7]

There is considerable controversy regarding the optimal treatment of patients with intermediate-risk prostatic carcinoma in relation to the role of dose-escalated EBRT (e.g., total dose > 74 gray [Gy]) versus conventional-dose EBRT (e.g., total dose < 74 Gy) and AD. To address this controversy, we have reviewed the categorization and prognostication of intermediate-risk prostate carcinoma. In this report, we also discuss new molecular and cellular biomarkers that may triage intermediate-risk patients further into subgroups for refined prognostication and treatment. Finally, we critically appraise the available pre-clinical and clinical evidence for dose-escalated EBRT alone or in combination with AD for this heterogeneous group of patients.

Defining Intermediate-Risk Prostate Carcinoma

Prognostic variables for PSA-based outcomes after treatment for localized prostate carcinoma can be defined in terms of biochemical freedom from survival (bFFS) or biochemical no evidence of disease (bNED) and have been studied within both univariate and multivariate models. Consequently, biochemical prognostic groupings are based on initial clinical tumor classification (T classification), pretreatment PSA level, and Gleason score[8–10] (see Table 1). The biochemical outcome of the intermediate-risk subgroup is highly dependent on the selected definition of biochemical failure. This currently is defined by the American Society for Therapeutic Radiology and Oncology (ASTRO) consensus definition as three consecutive rises in the PSA level after treatment.[11] Other biochemical failure definitions are being studied, but

none had supplanted the ASTRO definition at the time of this writing.[12]

Several authors and organizations have defined variably the interface between the intermediate and high-risk groupings (Table 1). For example, the initial risk groupings defined by Roach et al. were derived from a metaanalysis of the Radiation Therapy Oncology Group (RTOG) randomized trials that were conducted in the pre-PSA era.[13,14] An application of these risk groupings to a recent cohort of patients has validated them again in the modern PSA-era, in which a PSA value > 20 ng/mL confers a high risk of biochemical failure, lower progression-free survival, and lower overall survival.[15] Also in 2003, Roach et al. defined an intermediate-risk group (e.g., patients with a 15–35% risk of lymph node involvement, as determined by the following formula: percent risk = 2/3*PSA + 10*[Gleason score = 6]) based on the results of the RTOG 94-13 study.[16] Because this definition includes patients with clinical T3 disease and PSA values > 20 ng/mL, it would be classified otherwise as high-risk by a number of groups, including authors of the RTOG meta-analyses, the National Comprehensive Cancer Network (NCCN[17]), and the Canadian Consensus.[18] A recent report suggested that the use of a single-factor prognostic model (e.g., clinical T2b disease, or PSA > 10 ng/mL, or Gleason score = 7) to define intermediate-risk disease created prognostic groups with greater internal consistency than a 2-factor model (e.g., any 2 of clinical T2b disease, PSA > 10 ng/mL, or Gleason score = 7).[19] For the purpose of the current review, we have defined patients with intermediate-risk prostate carcinoma using the single-factor interpretation of the NCCN criteria,[17] which is the as the same Canadian Consensus definition.[18] We also have confined our discussion to the use of EBRT in intermediate-risk disease; however, it is recognized that some groups may utilize brachytherapy (another form of dose-escalation) as a component of therapy for patients with intermediate-risk disease.[4]

Prognostic Markers for Intermediate-Risk Prostate Carcinoma

Interrogating the relative slopes of EBRT dose-response curves (i.e., the PSA-based tumor control probability vs. the total radiotherapy dose) for prostate carcinoma leads to the conclusion that there is great heterogeneity within the intermediate-risk group.[20,21] Understanding this heterogeneity may allow for more effective triaging a priori of intermediate-risk patients into subgroups with varying probabilities of local control or development of distant metastases. This can be illustrated using prostate-specific nomograms, such as the Memorial Sloan-Kettering Prostogram (version 4.02; available from URL://www.nomograms.org [accessed May 27, 2004]). For example, 2 patients who receive 78 Gy (1 patient with T1c disease, Gleason score = 6, and PSA = 10.1 and the other patient with T2b disease, Gleason score = 7, and PSA = 19.9) would have 5-year PSA progression-free probabilities of 88% and 54%, respectively.[22,23] The well established prognostic factors of PSA, clinical T classification, and Gleason score determine < 50% of the variability of biochemical failure-free survival.[24] Indeed, the clinical stage, as determined by digital rectal examination, historically has been an important prognostic variable; however, as more and more patients are diagnosed with nonpalpable disease, it has become less useful.[25] Furthermore, the utility of computed tomography scanning and bone scans to address the heterogeneity within the intermediate-risk group is low.[26] Clearly, better prognostic and predictive factors are required for this heterogeneous group of patients. A strong predictor of tumor radiocurability, independent of known prognostic factors, could lead to novel treatment strategies combined with radiotherapy or to a decision to abort radiotherapy altogether in favor of a radical prostatectomy.

There are a number of promising methods for improving our ability to stratify and select the appropriate treatment for patients with intermediate-risk prostate carcinoma. For example, information obtained from systematic prostate biopsies can identify patients with a greater volume of disease and, thus, a greater risk of PSA failure, metastatic burden, and prostate carcinoma-specific mortality (PCSM).[27–29] The percentage of positive biopsies (i.e., ≥ 50% diagnostic cores involved with malignancy) is an independent prognostic variable that may triage patients within the intermediate-risk group into relatively favorable or unfavorable risk groups.[27,29] Results from more recent analyses suggest that the pretherapy PSA doubling time, or a high proliferative index (as measured by Ki-67 staining) can predict the risk for distant metastases and death in prostate carcinoma patients who are treated with radical intent.[30–32] Other approaches to the determination of pretreatment local or systemic tumor bulk include magnetic resonance spectroscopy of metabolically active tumor cells within the prostate[33] and the use of the polymerase chain reaction to detect potentially metastatic prostate carcinoma cells in the bloodstream. The latter assay, or one similar to it, could guide the use of systemic therapy in addition to radiotherapy.[34]

A number of intrinsic, pretreatment molecular biomarkers also may predict tumor cell radioresistance, extracapsular disease, and/or the presence of metas-

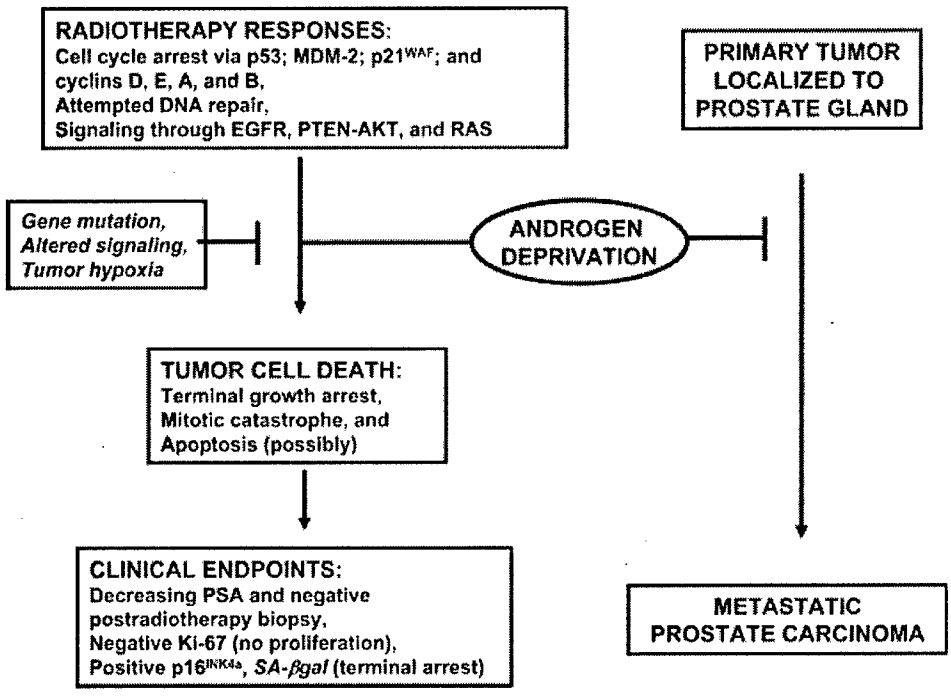

FIGURE 1. Radiotherapy induces damage within the DNA, the cytoplasm, and the outer plasma membrane of prostate carcinoma cells. This elicits a series of intracellular signal-transduction cascades leading to G_1, S-phase, and G_2 cell cycle arrests and attempted DNA repair. Initial sensing of cellular damage also activates the epidermal growth factor receptor (EGFR) pathway, including downstream RAS and phosphatase and tensin homolog (PTEN)-AKT signaling. Mutations in the genes involved in these pathways or increased levels of intratumoral hypoxia can lead to relative tumor cell resistance and decreased tumor cell kill. These radioresistance pathways are targets for a number of novel molecular agents that may be used in combination with radiotherapy. For prostate carcinoma cells that sustain lethal amounts of damage, tumor cell death occurs in a dose-responsive manner through terminal growth arrest, mitotic catastrophe, and possibly, apoptosis. Androgen deprivation likely increases radiation-induced cell death in vivo by augmenting terminal growth arrest. For patients with subclinical metastatic disease, androgen deprivation also may arrest the growth of systemic metastases terminally or transiently and alter rates of disease progression. To our knowledge, there is no assay currently available that directly determines the killing of prostate carcinoma clonogens in a quantitative manner. Instead, clinical surrogates for cell kill include postradiotherapy prostate-specific antigen (PSA) values and their nadir and/or the presence of active disease within prostate biopsies taken 2–3 years after radiotherapy and stained for biomarkers of cell proliferation. SA-βgal: senescence-associated β-galactosidase.

tases (see Fig. 1). These include markers of intratumoral hypoxia, genetic stability, cell proliferation, or cell death.[35,36] Intratumoral hypoxia is viewed as a negative prognostic factor capable of generating aggressive prostate tumor cell variants that have increased capacity for chemoresistance and radioresistance, androgen independence, and/or metastases.[37–41] Using a polarographic pO_2 electrode, groups at Princess Margaret Hospital and at the Fox Chase Cancer Center have shown that intermediate-risk patients are heterogeneous for intratumoral hypoxia.[42,43] Furthermore, the level of hypoxia may predict for intrinsic radioresistance after brachytherapy or EBRT.[43,44]

Gene or protein expression relating to tumor cell apoptosis also has been tested as a predictive assay for radiocurability. Pollack et al.[45] have altered expression of the antiapoptotic protein BCL-2 or the proapoptotic protein BAX as independent biomarkers predicting for bNED after radiotherapy alone. However, staining for p53, BAX, or BCL-2 as potential predictive factors of radiocurability remains controversial.[35,46] This may be due to small clinical sample sizes, differences in the quantitation or timing of immunohistochemical endpoints, and variable clinical treatment parameters. Alternate mechanisms of prostate cell death (e.g., mitotic catastrophe or terminal growth arrest) (see Fig. 1) also could confound analyses that are focused solely on apoptotic endpoints.[47,48]

Other potential prognostic biomarkers relate to cell proliferation (e.g., proliferating cell nuclear antigen and Ki-67[45,49]) or terminal cell growth arrest (e.g., p53, p21WAF, $p16^{INK4a}$, senescence-associated β-galactosidase).[35,48] The terminal arrest proteins are activated by lethal DNA damage during radiotherapy and can correlate to clonogenic cell kill.[48] Indeed, the loss of $p16^{INK4a}$ expression within pretreatment prostate biopsies predicted for an increased risk of local failure and distant metastatic disease in patients with locally

advanced prostate carcinoma who were treated within the RTOG 86-10 trial.[50]

Both gene expression profiling (e.g., DNA microarrays) and protein expression profiling (e.g., serum or tumor proteomics) soon may "fingerprint" those patients who harbor resistant disease on the basis of these genetic and/or microenvironmental factors. The recent use of DNA microarrays associated with robust bioinformatics has identified unique prognostic gene clusters and specific biomarkers that are independent of PSA, T classification, and Gleason score.[51,52] For example, the genes *hepsin*, *MUC1*, and *AZGP1* may be important new markers that can differentiate between the least aggressive and most aggressive prostate carcinomas.[53,54]

Other studies using comparative genomic hybridization have characterized unique molecular identifiers associated with Gleason score pattern 3 or 4.[55,56] This may be useful in discerning the relative prognosis for patients who have tumors with a Gleason score of 7 within the intermediate-risk category (e.g., Gleason score 3 + 4 vs. 4 + 3), because it has been considered traditionally that tumors with a higher component of the 4 pattern indicate a worse prognosis.[57,58] This information may help distinguish between truly aggressive tumors and the effect of "Gleason score shift" over the last decade. The latter shift or "creep" is the observed phenomenon of migration of Gleason scores upward associated with improved prognosis, most probably due to increased rates of PSA screening and altered pathologic scoring approaches.[59-62] Improved biologic prognostic factors, thus, are required to prevent aggressive treatment based on a small component of Gleason score = 4 (e.g., 3 + 4) that may not be associated with an adverse prognosis.

Clinical Radiotherapy and Intermediate-Risk Prostate Carcinoma

The success or failure of radical radiotherapy depends on the daily proportionate killing of tumor clonogens, which make up < 1% of the total population of cells within a tumor.[63] Both preclinical and clinical data support a dose-response relation for prostate carcinoma, in which increased killing of tumor clonogens leads to increased local control.[32,64-67] Currently, local control of prostate carcinoma after radical radiotherapy is inferred from postradiotherapy PSA kinetics and/or PSA nadir values or by the absence of active tumor within postradiotherapy biopsies.[30,48,68,69] We now review the use of these endpoints and others to appraise critically the use of dose-escalated EBRT or conventional EBRT in combination with AD as therapeutic options for patients with intermediate-risk prostate carcinoma.

Clinical Outcomes after Dose Escalation for Intermediate-Risk Prostate Carcinoma

Three comprehensive, systematic reviews of dose escalation for patients with localized prostate carcinoma have been completed.[70-72] These reviews summarize the results from cohort studies and describe multiple sources of bias inherent in the literature. Three important biases arise from the use of higher radiotherapy doses as technology improves over time. Regarding the first bias, many cohort studies report bFFS using the ASTRO consensus definition. This definition back-dates failure to the midpoint between the nadir PSA and the first of three consecutive PSA rises.[11] Because of this back-dating, the ASTRO consensus definition favors cohorts with shorter follow-up.[12,73,74] In addition, it has been shown on multivariate analysis that "treatment year" (a surrogate for stage migration) is a significant predictor of bFFS.[75] Because the radiation dose tends to track with treatment year, this stage migration represents another bias that favors the patients with shorter follow-up. The third bias relates to Gleason score shift migration (see above). Pollack and colleagues have shown, using a matched-pair analysis, that upgrading of Gleason scores occurred over the period 1992–1997 in an early and late cohort treated with conformal radiotherapy. Over this period, increasing numbers of tumors were upgraded to Gleason scores ≥ 6–8. This led to an apparent improvement in biochemical outcome for the most recent cohort across all Gleason score groups.[59] With these caveats, for the endpoint of bFFS, Vicini et al. identified improved outcomes in patients with intermediate-risk prostate carcinoma who were treated with dose-escalated EBRT.[70] Brundage et al., as part of the Ontario Practice Guidelines process, also found considerable evidence for the use of dose-escalated EBRT (e.g., doses > 74 Gy) in the intermediate-risk group.[71] Nilsson et al., using the principles adopted by the Swedish Council of Technology Assessment in Health Care, reached the same conclusion.[72]

Kuban et al. reported the bFFS of a multiinstitutional cohort of 4839 patients with T1 and T2 prostate carcinoma who were treated with EBRT alone and were followed for a minimum of 5 years.[76] Their cohort included 2190 patients with intermediate-risk disease. With a median follow-up of 6.3 years, the authors observed a significant improvement in PSA outcomes for patients who received doses > 72 Gy compared with patients who received lesser doses (e.g. 70% vs. 55% 5-year bFFS; $P < 0.0001$). Those authors verified that differences in neither the duration of follow-up nor the treatment year had an im-

pact on their finding that a higher total radiation dose improved biochemical outcome.

The only definitive method for testing the hypothesis of an EBRT dose-response relation in prostate carcinoma is through prospective RCTs. In the RCT of dose escalation reported by Pollack et al., the patients with intermediate-risk prostate carcinoma (defined as PSA > 10 ng/mL) who were treated with a dose of 78 Gy had improved 5-year bFFS outcomes compared with patients who were treated with a dose of 70 Gy (62% vs. 43% 5-year bFFS).[77] In the recently reported RCT by Zietman et al. comparing 70.2 Gy equivalent (GyE) (a combination of photons and protons) with 79.2 GyE in patients with low-risk and intermediate-risk disease, there was a significant benefit from dose escalation in the intermediate-risk group (78.7% vs. 60.5% bFFS; note that the majority of patients in the study had low-risk disease with Gleason scores ≤ 6 and PSA < 10 ng/mL).[67] Within the next few years, other RCT data will become available to elucidate the benefit of dose-escalation in EBRT for patients with intermediate-risk prostate carcinoma.[78,79]

Toxicity Associated with Dose-Escalated Radiotherapy

The normal tissue toxicity associated with dose-escalated EBRT also has been reviewed.[80] Significantly worse rectal and bladder toxicity was reported by both physicians and patients for the 78-Gy cohort arm compared with the 70-Gy arm in the RCT by Pollack et al.[77,81] However, this largely has historic interest, because these patients were treated with suboptimal radiation techniques compared with to today's standards. With appropriate attention to dose-volume constraints for the bladder and rectum, and with the use of intensity-modulated radiotherapy (IMRT), doses of > 80 Gy can be given safely to patients with prostate carcinoma. For example, at a median follow-up of 3 years, Zelefsky et al. found that RTOG Grade 3 rectal toxicity and bladder toxicity occurred in 0.8% and 0.6% of patients, respectively.[82,83] However, caution should be exercised in interpreting toxicity data with short follow-up. Late effects could continue to increase beyond the 5-year mark, and there is great interest in standardizing the approach to both the recording and analysis of late toxicity at periods > 5–10 years.[84,85] Indeed, analysis of late toxicity in the second decade after combined photon and proton prostate radiotherapy to 77.4 Gy suggests that, although severe gastrointestinal toxicity is rare, genitourinary morbidity continues to develop well into the second decade associated with high rates of posttreatment hematuria.[86]

Clinical Outcomes after Combined Hormonoradiotherapy for Intermediate-Risk Prostate Carcinoma.

An understanding of the interaction between AD and radiotherapy during prostate carcinoma cell kill may provide unique insights into the future role of AD as a modifier of tumor cell radiosensitivity. Initially, it was believed that the preclinical radiosensitization of prostate xenografts observed with AD and large, single radiation doses was secondary to increased radiation-induced apoptosis.[87] However, this was not confirmed when AD was combined with more clinically relevant fractionated irradiation protocols. Instead, the radiosensitization in vivo was correlated with increased tumor cell growth arrest.[35,48,88–90] In their preclinical studies of AD plus radiation, Kaminski et al.[91] suggested that AD may lead to delayed tumor regrowth through both increased clonogen cell kill (see Fig. 1) and/or a reduced growth rate of surviving clonogens.

These preclinical data support the clinical use of AD plus EBRT in patients who harbor micrometastatic disease at the time of diagnosis (in whom the metastatic cells may be arrested permanently or significantly by AD) or in patients with radioresistant tumors that may be sensitized by adjunctive or concurrent AD. A review of RCTs and subgroup analyses in which AD was given concurrent with EBRT versus AD given in an adjuvant setting suggests that concurrent AD-EBRT synergistically improves local control in the prostate and pelvis. This is consistent with a unique biologic effect different from that of adjuvant AD given post-EBRT, because the latter would impact solely on systemic disease and would affect overall survival and not local control.[16,92]

The RCT data presented in Table 2 show that improvement in local control and/or disease-free or overall survival can be achieved when AD is combined with conventional-dose EBRT.[5,6,29,93–96] The trials with the greatest numbers of patients did not address combined-modality therapy in the intermediate-risk group. However, D'Amico et al.[97] recently reported improved survival in 206 patients who were treated with 70 Gy plus 6 months of AD compared with patients who received 70 Gy alone (88% vs. 78%; $P < 0.04$). Approximately 80% of those patients could be classified with intermediate-risk disease. A number of concerns have been raised concerning the trial, however, including the fact that the difference in survival was based on only six prostate carcinoma-specific deaths in the control arm, compared with no prostate carcinoma-specific deaths in the experimental arm.[98,99] Nonetheless, another study[93] showed improved PSA-based outcomes using 64 Gy plus AD. In that RCT, 70% of patients could be classified with

TABLE 2
Trials of Radiotherapy Alone versus Combined Radiotherapy and Androgen Deprivation

Measure	Trial				
	D'Amico et al., 2004[97]	Laverdiere et al., 2004[93]	RTOG 8531 (Pilepich et al., 2003[6] and Lawton et al., 2004[94])	RTOG 8610 (Pilepich et al., 2001[95])	EORTC 22863 (Bolla et al., 2002 and Bolla et al., 1997[96])
No. of patients with intermediate-risk disease (definition)[a]	~ 163/206 (PSA = 10–20 or GS = 7)	~112/161 (T2 clinical stage)	0/977	0/456	0/415
Treatment arms	70 Gy vs. 70 Gy + 2 mos each NAD, CAD, and AAD	1) 64 Gy vs. 2) 64 Gy + 3 mo NAD vs. 3) 64 Gy + 3 mo NAD and 6 mo CAD and AAD	65–70 Gy vs. 65–70 Gy + IAD	65–70 Gy vs. 65–70 Gy + 4 mo NAD and CAD	70 Gy vs. 70 Gy + 3 yr CAD and AAD
Time of reported endpoints	5 yrs	7 yrs	10 yrs	8 yrs	5 yrs
Local control	N/A	N/A	61% vs. 77% $P < 0.0001$	58% vs. 70% $P < 0.02$	77% vs. 97% $P < 0.001$
Biochemical control (endpoint)	66% vs. 79% $P = 0.001$ (No AD for salvage)	1) 42% vs. 2) 66% $P = 0.009$; 1) 42% vs. 3) 69% $P = 0.003$ (PSA < 1.5)	9% vs. 30% $P < 0.0001$ (PSA < 1.5)	3% vs. 16% $P < 0.0001$ (PSA < 1.5)	45% vs. 76% $P < 0.0001$ (PSA < 1.5)
Disease-specific mortality	93% vs. 100% $P = 0.02$	N/A	17% vs. 22% $P = 0.005$	23% vs. 32% $P = 0.05$	6% vs. 21% $P = 0.0001$
Overall survival	88% vs. 78% $P = 0.04$	N/A	38% vs. 53% $P = 0.004$	44% vs. 53% $P < 0.1$	62% vs. 78% $P = 0.0002$

RTOG: Radiation Therapy Oncology Group; EORTC: European Organization for Research and Treatment of Cancer; GS: Gleason score; Gy: gray; NAD: neoadjuvant androgen deprivation; CAD: concurrent androgen deprivation; AAD: adjuvant androgen deprivation; IAD: indefinite androgen deprivation; N/A: not available in reference.
[a] PSA: prostate specific antigen (ng/ml).

intermediate-risk disease. More recently, Dearnaley et al.[100] reported a nonsignificant trend toward improved freedom from PSA failure in patients who were treated with 74 Gy, rather than 64 Gy, after 3–6 months of neoadjuvant AD. The vast majority of patients in both arms in that trial had World Health Organization Grade 2 pathology (68–77%; 5–15% of patients had Grade 3 pathology), and 74–83% of patients had T2 or T3 tumors and median baseline PSA values of 14–15 ng/mL. In that study, the 5-year actuarial control rates were 71% versus 59%, respectively ($P = 0.10$); no survival data were reported at the time of the current report.

Despite these recent data, two issues confound current decision making with regard to the role of AD in patients with intermediate-risk prostate carcinoma. The first issue is that the largest randomized trials that have shown a benefit to adjunctive AD (either neoadjuvant or adjuvant) combined with EBRT largely have been completed in patients with high-risk disease. Thus, the conclusions from those trials may not be applicable to all patients with intermediate-risk disease. The second issue is that many of these trials were completed in the era of conventional-dose EBRT (e.g., doses < 74 Gy), when long-term bFFS rates with EBRT at these lower doses alone were approximately 40% in patients with intermediate-risk disease.[101,102]

Nonrandomized, single-institution series have reported clinical outcome data regarding the role of AD in addition to dose-escalated EBRT for patients with intermediate-risk prostate carcinoma. Kupelian et al.[103] reported on the treatment outcomes in a cohort of 1041 consecutively treated patients with T1–T2 prostate carcinoma who were treated either with radical prostatectomy, EBRT, and brachytherapy (permanent seed implantation) or with combined brachytherapy and EBRT. Seven hundred eighty-five patients were treated with EBRT (484 patients received ≤ 72 Gy and 301 patients received > 72 Gy), and 143 of those patients were given neoadjuvant AD for ≤ 6 months. Although AD was found to be a significant predictor of biochemical outcome on univariate analysis for the entire patient cohort, when the group of patients who received ≤ 72 Gy was excluded, it was no longer significant ($P = 0.91$). Zelefsky et al. also reported in their cohort of 772 patients (89% with T1–T2 disease; treated with IMRT to a median dose of 81 Gy) that AD appeared to have no influence on bFFS (median fol-

low-up, 24 months).[82] Furthermore, a lack of benefit (and a possible detrimental effect) of short-course AD on 5-year metastasis-free survival or cause-specific survival was reported by Martinez et al. in a large retrospective review of 1260 patients who were treated with combined EBRT and brachytherapy.[104] Although these studies do not represent RCT data, their uniform findings suggest that the addition of AD to dose-escalated EBRT may not be required to optimize biochemical outcomes for patients intermediate-risk prostate carcinoma.

The recent RCT by D'Amico et al. is promising. Compared with the randomized trials of dose-escalation alone that had similar control arms of 64–70 Gy, only the study by D'Amico et al. showed a survival benefit; and their study also had a greater number of patients with intermediate-risk and high-risk disease.[29] Further data showing similar survival benefits will be required before uniformly recommending AD plus conventional-dose EBRT versus dose-escalated EBRT for the intermediate-risk group. However, it is conceivable that selected patients may benefit from short-term AD plus dose-escalated EBRT if their tumors have adverse features that reflect local radioresistance and/or increased systemic spread.

Toxicity of Adjunctive AD

Long-term AD is the treatment of choice for patients with high-risk prostate carcinoma on the basis of randomized trials, which show a survival advantage.[5,6,105] The physiological side effects of long-term AD are well known and include anemia, sarcopeniam and osteoporosis.[106–108] More relevant to the treatment of intermediate-risk prostate carcinoma is the toxicity of AD administration for a period of 3–6 months. Hot flashes occur in approximately 80% of men.[109] Decreased libido, erectile dysfunction, and fatigue also are experienced in the majority of treated men.[110,111] Reversible depression and cognitive impairment also have been linked to short-term use of hormones, but the correlation is not consistent across all studies.[104,106]

When patients were treated with a luteinizing hormone-releasing hormone agonist and an antiandrogen as complete AD (CAD) therapy, a decline in hemoglobin (Hgb) of > 1.0 g/dL was observed in 75% of patients after 2 months.[112] D'Amico et al. studied biochemical outcomes in a cohort of 110, mostly intermediate-risk patients (and some high-risk patients) treated with 6 months of CAD and radiotherapy.[113] Based on values taken prior to and 1 month after AD, it was found that patients who had a drop in Hgb > 1 g/dL had significantly poorer biochemical outcomes (median follow-up, 20 months).[113] This finding is somewhat unexpected, because patients with high-risk prostate carcinoma have improved biochemical outcomes with long-term AD (Table 2). However, the Hgb effect is similar to that observed during radical radiotherapy studies in patients with cervical carcinoma[114] and head and neck carcinoma.[115,116] It is possible that the AD, which improves survival by controlling metastatic disease in high-risk patients, impairs biochemical control by reducing local control in intermediate-risk patients. This awaits a formal subgroup analysis of the recent RCT of 6 months of CAD and EBRT versus EBRT alone.[29] In the meantime, these results suggest that caution is warranted when AD and EBRT are used for the treatment of patients with intermediate-risk prostate carcinoma outside of the context of a clinical trial.

The Future Relevant Clinical Endpoints for Future Clinical Trials

Although overall survival and PCSM remain the gold standards in determining the efficacy of new treatment approaches, the natural history of prostate carcinoma necessitates prolonged observation periods to identify these endpoints. PSA-based failure may not always be a reliable surrogate for PCSM; because, in some studies, up to 20% of patients who died after developing PSA failure died of nonprostate carcinoma-related causes.[117] The use of "time to second PSA failure" (or development of hormone-refractory disease) has been suggested as a potential surrogate endpoint for PCSM in localized disease, but this observation has yet to be validated in multiple data sets.[118]

Reports of outcomes from trials of AD and EBRT that use a biochemical endpoint face several challenges. With neoadjuvant AD, it is difficult to choose a start point for follow-up that does not favor one arm over the other in the short term. In addition, there is a period of recovery of testosterone after cessation of the AD that may lead to a rising PSA profile. This is particularly problematic for the ASTRO consensus definition of bFFS and may lead falsely to the conclusion that neoadjuvant-treated patients fail at a higher rate. More recently, the groups of D'Amico et al. and Albertson et al. suggested that the posttreatment PSA doubling time can be a useful surrogate for PCSM.[31,117,119] The rising testosterone profile seen in patients after treatment with AD likely would generate a falsely short PSA doubling time, rendering this measure difficult to interpret in AD-treated patients in the short term. Future definitions of biochemical failure that predict clinical failure better after radiotherapy may supercede the currently used ASTRO definition.[120,121] These include failure defined when the PSA is greater than a current nadir + 2 ng/mL or 3 ng/mL and dated at call (i.e., the failure date called when that

TABLE 3
Unreported Trials of Dose Escalation and/or Androgen Deprivation that Included Patients with Intermediate-Risk Prostate Carcinoma from the MetaRegister of Controlled Trials[a]

Study	Eligibility criteria[b]	Treatment arms	Sample size
RTOG 9408	T1b–T2b and PSA ≤ 20	75.6 Gy vs. 75.6 Gy with 4 mos of NAD and CAD	1980
EORTC 22991	T1b-c and either PSA = 10–50 or GS = 7; or T2a and PSA < 50	70–78 Gy vs. 70–78 Gy with 6 mos of CAD and AAD	800
PMH 9907	T1b–T2b, PSA = 4–20 and GS = 7–10; or T1b–T2b, PSA = 10–20 and GS ≤ 6	75.6–79.8 Gy vs. 75.6–79.8 Gy with 3 mos of NAA and 2 mos of CAA	378
RTOG 9910	T1b–T4, GS = 2–6 and PSA 10–100; or T1b–T4, GS = 7 and PSA < 20; or T1b–T1c, GS = 8–10 and PSA < 20	70.2 Gy with 2 mos of NAD and CAD vs. 70.2 Gy with 6 mos of NAD and 2 mos of CAD	1540
MSKCC	At least 2 of: PSA > 10, GS > 7, or T4	86.4 Gy vs. 75.6 Gy with 2 yrs of NAD, CAD, and AAD	400
RTOG P-0126	T1b–T2b, GS = 2–6 and PSA = 10–20; or T1b–T2b, GS = 7 and PSA < 15	70.2 Gy (39 fractions in 7.8 weeks) vs. 79.2 Gy (44 fractions in 8.8 weeks)	1520
MRC	T1b–T3a and PSA < 50	64 Gy vs. 74 Gy	800
FCCC	T1b–T3c and 1 of: PSA > 10, GS ≥ 7, or Stage ≥ T2b	76.0 Gy (36 fractions in 7.2 weeks) vs. 70.2 Gy (26 fractions in 5.2 weeks)	300

RTOG: Radiation Therapy Oncology Group; PSA: prostate-specific antigen; Gy: gray; NAD: neoadjuvant androgen deprivation; CAD: concurrent androgen deprivation; EORTC: European Organization for Research and Treatment of Cancer; GS: Gleason score; AAD: adjuvant androgen deprivation; PMH: Princess Margaret Hospital; NAA: neoadjuvant antiandrogen; CAA: concurrent antiandrogen; MSKCC: Memorial Sloan-Kettering Cancer Center; MRC: Medical Research Council; FCCC: Fox-Chase Cancer Center.

[a] Available from URL: http: www.controlled-trials.com [accessed August 15, 2004].

[b] PSA: prostate specific antigen (ng/ml).

criterion was met[12,122]) or 2 consecutive rises of at least 0.5 ng/mL beyond the nadir and back-dated.[123] Based on a recent, multiinstitutional, pooled analysis of 4839 patients, these latter definitions appear to have increased sensitivity and specificity relating to clinical and distant failure.[120]

Studies of neoadjuvant AD with surgery have shown significant reductions in the detection of positive surgical margins without a long-term improvement in bFFS. This observation supports the concept that AD alters the tissues and reduces the ability of pathologists to detect disease at the surgical margin without eliminating viable, unresected disease.[124] Similarly, AD and/or EBRT therapy effects on tissue histology can confound biopsy interpretation and its role in predicting local control.[49,125,126] Furthermore, patients are reluctant to undergo biopsies if their PSA profile is stable, and clinicians are reluctant to insist on biopsies due to perceived risks of infection, bleeding, or patient discomfort. This may introduce a substantial bias in the reporting of biopsy endpoints unless a large proportion of similarly treated patients agree to undergo posttreatment biopsies. Nonetheless, local control, as assessed by prostatic biopsies 2–3 years after radiotherapy, perhaps also stained for relevant biomarkers (e.g., $p21^{WAF}$, $p16^{INK4a}$, Ki-67), also may provide relevant early endpoints for future trials of AD plus dose-escalated EBRT.

Ongoing Trials in Intermediate-Risk Disease

A search of the MetaRegister of Controlled Trials (available from URL: www.controlled-trials.com [accessed August 15, 2004]) identified a number of ongoing studies that involve intermediate-risk patients (Table 3). The RTOG P-0126 and MRC trials are investigating dose-escalation using conventional fractionation schemes. The Princess Margaret Hospital PMH 99-07 and the EORTC 22991 studies may provide some answers regarding the usefulness of neoadjuvant hormone therapy in intermediate-risk patients treated with dose-escalated EBRT. Both the RTOG studies, 94-08 and 99-10, use conventional doses of EBRT and will not address the issue of the utility of AD in the setting of high-dose EBRT. The Memorial Sloan-Kettering Cancer Center study is comparing high-dose EBRT alone with the use of neoadjuvant AD and EBRT. In the latter study, if an equivalent PSA-based outcome is achieved in both arms, then the study may be extremely useful for the radiobiologic calculation of the radiation dose-equivalent cell kill achieved by the addition of AD.

The Fox Chase Cancer Center study is comparing moderate dose escalation with a hypofractionated regimen. Recent analyses of clinical results have suggested that the α/β ratio for prostate carcinoma is approximately 1.5 Gy (much lower than the typical value of 10 Gy for many other tumors) and, thus, is comparable to or lower than the ratio of the surround-

ing, late-responding rectal mucosa (i.e., an α/β ratio of approximately 3 Gy[127]). The lower α/β ratio for prostate carcinoma compared, with surrounding, late-responding, normal tissue, creates the potential for therapeutic gain. Indeed, recent reports of protocols that delivered 70 Gy with 2.5 Gy per fraction[128,129] or 50 Gy with 3.13 Gy per fraction[130] are consistent with bNED rates of 60–80% and were associated with favorable toxicity profiles. This may result in future combined-modality trials using hypofractioned EBRT with or without AD.

Molecular-Based Protocols for Intermediate-Risk Prostate Carcinoma

Information regarding the molecular signaling pathways that are activated after ionizing radiation has increased exponentially over the last decade.[131] A number of protein pathways have been associated with tumor radioresistance, including intratumoral hypoxia and the p53, RAS, epidermal growth factor receptor (EFGR), vascular endothelial growth factor receptor (VEGF), and phosphoinositide-3 kinase-phosphatase and tensin homolog (PTEN)/AKT pathways.[35,36,132]

The pretreatment assessment of biomarkers that represent these signaling pathways may lead to the appropriate choice of novel, molecular-targeted agents to use in combination with EBRT. For example, tumor cell kill as a result of terminal growth arrest explains the slow kinetics of decreasing PSA values and a final nadir occurring over a 12–16 month period after EBRT for prostate carcinoma.[30,48] In light of this finding, new treatment strategies that augment EBRT-induced terminal growth arrest in vivo may be possible clinically using histone deactylase inhibitors or retinoids.[133] These agents also may radioprotect normal tissues[134,135] and currently are being tested prospectively in Phase I/II trials.[136,137]

New molecular therapies that target *p53*, MDM2, BCL-2, BAX, PTEN/AKT, RAS, or clusterin pathways also hold promise for augmenting radiation-induced tumor cell kill and improving local control.[46,138–149] Improved outcomes also may be achieved with the use of hypoxia-targeted drugs in combination with EBRT. Preliminary data suggest that the neoadjuvant use of AD increases tumor oxygenation, which may be another mode of radiosensitization for this combination.[150] Clinical interventions designed to improve oxygenation through direct hypoxic cell targeting or altered angiogenesis are underway in other tumor sites using a variety of agents (e.g., *HIF1-α* gene therapy; tirapazamine; VEGF inhibitors, such as SU5416 or SU6668; and cyclooxygenase-2 inhibitors) and could be used in hypoxic subgroups of patients with intermediate-risk disease.[151–153] The recent success of the EGFR inhibitors (e.g., cetuximab) as radiosensitizers in head and neck carcinoma, leading to improved overall survival with minimal excess toxicity, serves as an excellent model for molecular-targeted EBRT approaches in future studies.[140,154]

Conclusions and Recommended Management of Intermediate-Risk Patients with Radiotherapy

The heterogeneity of intermediate-risk prostate carcinoma presents a challenge to genitourinary oncology in terms of prognosis and optimal management. Although there is reasonable evidence that these patients benefit from dose-escalated EBRT or adjunctive hormone therapy with conventional EBRT, to our knowledge there is little evidence to date that these patients uniformly benefit from adjunctive AD when the total dose is > 74 Gy.

Currently, patients in the intermediate-risk group should be entered into well designed, RCTs of combined dose-escalation and AD of sufficient power to answer the important questions raised by nonrandomized studies. These trials also should investigate the optimal duration of hormone therapy. In addition, they should be stratified by new prognostic markers and should be accompanied by strong, correlative, scientific endpoints that can address risk-group heterogeneity and potential predictive factors for local or systemic recurrence.

With the advent of molecular profiling and the use of tissue arrays that facilitate the simultaneous study of thousands of genes or proteins within large patient cohorts, clinicians soon will be able to acquire individual pharmacogenomic and prognostic profiles for use in the clinical management of patients. This likely will lead to individualized treatment for patients with intermediate-risk prostate carcinoma and will stimulate novel combined-modality protocols to decrease local and distant failure in this diverse clinical prostate carcinoma population.

REFERENCES

1. Cooperberg MR, Lubeck DP, Mehta SS, Carroll PR. Time trends in clinical risk stratification for prostate cancer: implications for outcomes (data from CaPSURE). *J Urol.* 2003; 170:S21–S25; discussion, S26–S27.
2. D'Amico AV, Whittington R, Malkowicz SB, et al. Biochemical outcome after radical prostatectomy, external beam radiation therapy, or interstitial radiation therapy for clinically localized prostate cancer. *JAMA.* 1998;280:969–974.
3. Cooperberg MR, Broering JM, Litwin MS, et al. The contemporary management of prostate cancer in the United States: lessons from the Cancer of the Prostate Strategic Urologic Research Endeavor (CapSURE), a national disease registry. *J Urol.* 2004;171:1393–1401.

4. Potters L, Klein EA, Kattan MW, et al. Monotherapy for Stage T1–T2 prostate cancer: radical prostatectomy, external beam radiotherapy, or permanent seed implantation. *Radiother Oncol.* 2004;71:29–33.
5. Bolla M, Collette L, Blank L, et al. Long-term results with immediate androgen suppression and external irradiation in patients with locally advanced prostate cancer (an EORTC study): a Phase III randomised trial. *Lancet.* 2002;360:103–106.
6. Pilepich MV, Winter K, Lawton C, et al. Androgen suppression adjuvant to radiotherapy in carcinoma of the prostate. long-term results of Phase III RTOG study 85-31. *Int J Radiat Oncol Biol Phys.* 2003;57:S172–S173.
7. Cooperberg MR, Grossfeld GD, Lubeck DP, Carroll PR. National practice patterns and time trends in androgen ablation for localized prostate cancer. *J Natl Cancer Inst.* 2003; 95:981–989.
8. Williams SG, Millar JL, Dally MJ, Sia S, Miles W, Duchesne GM. What defines intermediate-risk prostate cancer? Variability in published prognostic models. *Int J Radiat Oncol Biol Phys.* 2004;58:11–18.
9. Pisansky TM, Kahn MJ, Rasp GM, Cha SS, Haddock MG, Bostwick DG. A multiple prognostic index predictive of disease outcome after irradiation for clinically localized prostate carcinoma. *Cancer.* 1997;79:337–344.
10. Zelefsky MJ, Leibel SA, Gaudin PB, et al. Dose escalation with three-dimensional conformal radiation therapy affects the outcome in prostate cancer. *Int J Radiat Oncol Biol Phys.* 1998;41:491–500.
11. ASTRO Panel. Consensus statement: guidelines for PSA following radiation therapy. American Society for Therapeutic Radiology and Oncology Consensus Panel. *Int J Radiat Oncol Biol Phys.* 1997;37:1035–1041.
12. Thames H, Kuban D, Levy L, et al. Comparison of alternative biochemical failure definitions based on clinical outcome in 4839 prostate cancer patients treated by external beam radiotherapy between 1986 and 1995. *Int J Radiat Oncol Biol Phys.* 2003;57:929–943.
13. Roach M 3rd, Lu J, Pilepich MV, et al. Predicting long-term survival, and the need for hormonal therapy: a meta-analysis of RTOG prostate cancer trials. *Int J Radiat Oncol Biol Phys.* 2000;47:617–627.
14. Roach M, Lu J, Pilepich MV, et al. Four prognostic groups predict long-term survival from prostate cancer following radiotherapy alone on Radiation Therapy Oncology Group clinical trials. *Int J Radiat Oncol Biol Phys.* 2000;47:609–615.
15. Roach M 3rd, Weinberg V, McLaughlin PW, Grossfeld G, Sandler HM. Serum prostate-specific antigen and survival after external beam radiotherapy for carcinoma of the prostate. *Urology.* 2003;61:730–735.
16. Roach M 3rd, DeSilvio M, Lawton C, et al. Phase III trial comparing whole-pelvic versus prostate-only radiotherapy and neoadjuvant versus adjuvant combined androgen suppression: Radiation Therapy Oncology Group 9413. *J Clin Oncol.* 2003;21:1904–1911.
17. Scherr D, Swindle PW, Scardino PT. National Comprehensive Cancer Network guidelines for the management of prostate cancer. *Urology.* 2003;61:14–24.
18. Lukka H, Warde P, Pickles T, Morton G, Brundage M, Souhami L. Controversies in prostate cancer radiotherapy: consensus development. *Can J Urol.* 2001;8:1314–1322.
19. Chism DB, Hanlon AL, Horwitz EM, Feigenberg SJ, Pollack A. A comparison of the single and double factor high-risk models for risk assignment of prostate cancer treated with 3D conformal radiotherapy. *Int J Radiat Oncol Biol Phys.* 2004;59:380–385.
20. Hung AY, Levy L, Kuban DA. Stage T1c prostate cancer: a heterogeneous category with widely varying prognosis. *Cancer J.* 2002;8:440–444.
21. Levegrun S, Jackson A, Zelefsky MJ, et al. Risk group dependence of dose-response for biopsy outcome after three-dimensional conformal radiation therapy of prostate cancer. *Radiother Oncol.* 2002;63:11–26.
22. Diblasio CJ, Kattan MW. Use of nomograms to predict the risk of disease recurrence after definitive local therapy for prostate cancer. *Urology.* 2003;62(Suppl 1):9–18.
23. Kattan MW, Zelefsky MJ, Kupelian PA, et al. Pretreatment nomogram that predicts 5-year probability of metastasis following three-dimensional conformal radiation therapy for localized prostate cancer. *J Clin Oncol.* 2003;21:4568–4571.
24. D'Amico AV, Whittington R, Malkowicz SB, et al. Pretreatment nomogram for prostate-specific antigen recurrence after radical prostatectomy or external-beam radiation therapy for clinically localized prostate cancer. *J Clin Oncol.* 1999;17:168–172.
25. Ross JS, Jennings TA, Nazeer T, et al. Prognostic factors in prostate cancer. *Am J Clin Pathol.* 2003;120(Suppl):S85–S100.
26. Abuzallouf S, Dayes I, Lukka H. Baseline staging of newly diagnosed prostate cancer: a summary of the literature. *J Urol.* 2004;171:2122–2127.
27. D'Amico AV, Schultz D, Silver B, et al. The clinical utility of the percent of positive prostate biopsies in predicting biochemical outcome following external-beam radiation therapy for patients with clinically localized prostate cancer. *Int J Radiat Oncol Biol Phys.* 2001;49:679–684.
28. Kestin LL, Goldstein NS, Vicini FA, et al. Pathologic evidence of dose-response and dose-volume relationships for prostate cancer treated with combined external beam radiotherapy and high-dose-rate brachytherapy. *Int J Radiat Oncol Biol Phys.* 2002;54:107–118.
29. D'Amico AV, Renshaw AA, Cote K, et al. Impact of the percentage of positive prostate cores on prostate cancer-specific mortality for patients with low or favorable intermediate-risk disease. *J Clin Oncol.* 2004;22:3726–3732.
30. Cavanaugh SX, Kupelian PA, Fuller CD, et al. Early prostate-specific antigen (PSA) kinetics following prostate carcinoma radiotherapy: prognostic value of a time-and-PSA threshold model. *Cancer.* 2004;101:96–105.
31. D'Amico AV, Chen MH, Roehl KA, Catalona WJ. Preoperative PSA velocity and the risk of death from prostate cancer after radical prostatectomy. *N Engl J Med.* 2004;351:125–135.
32. Pollack A, Hanlon AL, Horwitz EM, Feigenberg SJ, Uzzo RG, Hanks GE. Prostate cancer radiotherapy dose response: an update of the fox chase experience. *J Urol* 2004;171:1132–1136.
33. Yuen JS, Thng CH, Tan PH, et al. Endorectal magnetic resonance imaging and spectroscopy for the detection of tumor foci in men with prior negative transrectal ultrasound prostate biopsy. *J Urol.* 2004;171:1482–1486.
34. Gewanter RM, Katz AE, Olsson CA, et al. RT-PCR for PSA as a prognostic factor for patients with clinically localized prostate cancer treated with radiotherapy. *Urology.* 2003;61:967–971.
35. Faulhaber O, Bristow RG. Basis of cell kill following clinical radiotherapy. In: Sluyser M, editor. Application of apoptosis to cancer treatment. –Dordrecht, the Netherlands: Springer Publishing, 2005:293–320.

36. Ma BB, Bristow RG, Kim J, Siu LL. Combined-modality treatment of solid tumors using radiotherapy and molecular targeted agents. *J Clin Oncol.* 2003;21:2760–2776.
37. Ghafar MA, Anastasiadis AG, Chen MW, et al. Acute hypoxia increases the aggressive characteristics and survival properties of prostate cancer cells. *Prostate.* 2003;54:58–67.
38. Anastasiadis AG, Bemis DL, Stisser BC, Salomon L, Ghafar MA, Buttyan R. Tumor cell hypoxia and the hypoxia-response signaling system as a target for prostate cancer therapy. *Curr Drug Targets.* 2003;4:191–196.
39. Zhao D, Constantinescu A, Chang CH, Hahn EW, Mason RP. Correlation of tumor oxygen dynamics with radiation response of the dunning prostate R3327-HI tumor. *Radiat Res.* 2003;159:621–631.
40. Vordermark D, Brown JM. Endogenous markers of tumor hypoxia predictors of clinical radiation resistance? *Strahlenther Onkol.* 2003;179:801–811.
41. Subarsky P, Hill RP. The hypoxic tumour microenvironment and metastatic progression. *Clin Exp Metastasis.* 2003;20: 237–250.
42. Parker C, Milosevic M, Toi A, et al. Polarographic electrode study of tumor oxygenation in clinically localized prostate cancer. *Int J Radiat Oncol Biol Phys.* 2004;58:750–757.
43. Movsas B, Chapman JD, Hanlon AL, et al. Hypoxic prostate/muscle pO_2 ratio predicts for biochemical failure in patients with prostate cancer: preliminary findings. *Urology.* 2002;60: 634–639.
44. Nahum AE, Movsas B, Horwitz EM, Stobbe CC, Chapman JD. Incorporating clinical measurements of hypoxia into tumor local control modeling of prostate cancer: implications for the alpha/beta ratio. *Int J Radiat Oncol Biol Phys.* 2003;57:391–401.
45. Pollack A, Cowen D, Troncoso P, et al. Molecular markers of outcome after radiotherapy in patients with prostate carcinoma: Ki-67, bcl-2, bax, and bcl-x. *Cancer.* 2003;97:1630–1638.
46. Cuddihy A, Bristow RG. The p53 protein family and radiosensitivity: yes or no? [review.] *Cancer Metastasis Rev.* 2004; 23(3–4);237–257.
47. Ritter MA, Gilchrist KW, Voytovich M, Chappell RJ, Verhoven BM. The role of p53 in radiation therapy outcomes for favorable-to-intermediate-risk prostate cancer. *Int J Radiat Oncol Biol Phys.* 2002;53:574–580.
48. Bromfield GP, Meng A, Warde P, Bristow RG. Cell death in irradiated prostate epithelial cells: role of apoptotic and clonogenic cell kill. *Prostate Cancer Prostatic Dis.* 2003;6:73–85.
49. Crook JM, Bahadur YA, Robertson SJ, Perry GA, Esche BA. Evaluation of radiation effect, tumor differentiation, and prostate specific antigen staining in sequential prostate biopsies after external beam radiotherapy for patients with prostate carcinoma. *Cancer.* 1997;79:81–89.
50. Chakravarti A, Heydon K, Wu CL, et al. Loss of p16 expression is of prognostic significance in locally advanced prostate cancer: an analysis from the Radiation Therapy Oncology Group protocol 86-10. *J Clin Oncol.* 2003;21:3328–3334.
51. Dhanasekaran SM, Barrette TR, Ghosh D, et al. Delineation of prognostic biomarkers in prostate cancer. *Nature.* 2001; 412:822–826.
52. Singh D, Febbo PG, Ross K, et al. Gene expression correlates of clinical prostate cancer behavior. *Cancer Cell.* 2002;1:203–209.
53. Lapointe J, Li C, Higgins JP, et al. Gene expression profiling identifies clinically relevant subtypes of prostate cancer. *Proc Natl Acad Sci USA.* 2004;101:811–816.
54. Stephan C, Yousef GM, Scorilas A, et al. Hepsin is highly over expressed in and a new candidate for a prognostic indicator in prostate cancer. *J Urol.* 2004;171:187–191.
55. van Dekken H, Paris PL, Albertson DG, et al. Evaluation of genetic patterns in different tumor areas of intermediate-grade prostatic adenocarcinomas by high-resolution genomic array analysis. *Genes Chromosomes Cancer.* 2004; 39:249–256.
56. Paris PL, Andaya A, Fridlyand J, et al. Whole genome scanning identifies genotypes associated with recurrence and metastasis in prostate tumors. *Hum Mol Genet.* 2004;13: 1303–1313.
57. Mosse CA, Magi-Galluzzi C, Tsuzuki T, Epstein JI. The prognostic significance of tertiary Gleason pattern 5 in radical prostatectomy specimens. *Am J Surg Pathol.* 2004;28:394–398.
58. Chan TY, Partin AW, Walsh PC, Epstein JI. Prognostic significance of Gleason score 3+4 versus Gleason score 4+3 tumor at radical prostatectomy. *Urology.* 2000;56:823–827.
59. Chism DB, Hanlon AL, Troncoso P, Al-Saleem T, Horwitz EM, Pollack A. The Gleason score shift: score four and seven years ago. *Int J Radiat Oncol Biol Phys.* 2003;56:1241–1247.
60. Humphrey PA. Gleason grading and prognostic factors in carcinoma of the prostate. *Mod Pathol.* 2004;17:292–306.
61. Smart CR. The results of prostate carcinoma screening in the U.S. as reflected in the Surveillance, Epidemiology, and End Results Program. *Cancer.* 1997;80:1835–1844.
62. Smith EB, Frierson HF Jr., Mills SE, Boyd JC, Theodorescu D. Gleason scores of prostate biopsy and radical prostatectomy specimens over the past 10 years: is there evidence for systematic upgrading? *Cancer.* 2002;94:2282–2287.
63. Hill RP, Bristow RG. The scientific basis of clinical radiotherapy. In: Tannock IF, Hill RP, Harrington L, Bristow RG, editors. Basic science of oncology, 4th edition. New York: McGraw-Hill Publishing, 2005;289–381.
64. Hill RP, Milas L. The proportion of stem cells in murine tumors. *Int J Radiat Oncol Biol Phys.* 1989;16:513–518.
65. Suit H. The Gray Lecture 2001: coming technical advances in radiation oncology. *Int J Radiat Oncol Biol Phys.* 2002;53: 798–809.
66. Suwinski R, Withers HR. Time factor and treatment strategies in subclinical disease. *Int J Radiat Biol.* 2003;79:495–502.
67. Zietman AL, DeSilvio M, Slater JD, et al. A randomized trial comparing conventional dose (70.2GyE) and high-dose (79.2GyE) conformal radiation in early stage adenocarcinoma of the prostate: results of an interim analysis of PROG 95-09. *Int J Radiat Oncol Biol Phys.* 2004;60:S131–S132.
68. Small EJ, Roach M 3rd. Prostate-specific antigen in prostate cancer: a case study in the development of a tumor marker to monitor recurrence and assess response. *Semin Oncol.* 2002;29:264–273.
69. Wiltshire K, Bristow RG, Warde P, Gospodarowicz M. Re: Vikram, B., the PSA conundrum. [*Radiother Oncol.* 2004;71): 1–2]. *Radiother Oncol.* 2004;73:252–254; author reply, 254–255.
70. Vicini FA, Abner A, Baglan KL, Kestin LL, Martinez AA. Defining a dose-response relationship with radiotherapy for prostate cancer: is more really better? *Int J Radiat Oncol Biol Phys.* 2001;51:1200–1208.
71. Brundage M, Lukka H, Crook J, et al. The use of conformal radiotherapy and the selection of radiation dose in T1 or T2 low or intermediate risk prostate cancer—a systematic review. *Radiother Oncol.* 2002;64:239–250.

72. Nilsson S, Norlen BJ, Widmark A. A systematic overview of radiation therapy effects in prostate cancer. *Acta Oncol.* 2004;43:316–381.
73. Vicini FA, Kestin LL, Martinez AA. The importance of adequate follow-up in defining treatment success after external beam irradiation for prostate cancer. *Int J Radiat Oncol Biol Phys.* 1999;45:553–561.
74. Lu J. Statistical aspects of evaluating treatment and prognostic factors for clinically localized prostate cancer. *Semin Urol Oncol.* 2000;18:83–92.
75. Kupelian PA, Buchsbaum JC, Elshaikh MA, Reddy CA, Klein EA. Improvement in relapse-free survival throughout the PSA era in patients with localized prostate cancer treated with definitive radiotherapy: year of treatment an independent predictor of outcome. *Int J Radiat Oncol Biol Phys.* 2003;57:629–634.
76. Kuban DA, Thames HD, Levy LB, et al. Long-term multiinstitutional analysis of Stage T1–T2 prostate cancer treated with radiotherapy in the PSA era. *Int J Radiat Oncol Biol Phys.* 2003;57:915–928.
77. Pollack A, Zagars GK, Starkschall G, et al. Prostate cancer radiation dose response: results of the M. D. Anderson Phase III randomized trial. *Int J Radiat Oncol Biol Phys.* 2002;53:1097–1105.
78. Lebesque JV, Koper PC, Slot A, et al. Acute and late GI and GU toxicity after prostate irradiation to doses of 68 Gy and 78 Gy: results of a randomized trial. Proceedings of the 45th Annual ASTRO Meeting, October 19–23, 2003, Salt Lake City, Utah [abstract 48]. *Int J Radiat Oncol Biol Phys.* 2003; 57(Suppl 2):S152.
79. Beckendorf V, Guerif S, Le Prise E. The French 70 Gy vs. 80 Gy dose escalation trial for localized prostate cancer: feasibility and toxicity. Proceedings of the 45th Annual ASTRO Meeting, October 19–23, 2003, Salt Lake City, Utah [abstract 47]. *Int J Radiat Oncol Biol Phys.* 2003;57(Suppl 2):S152.
80. Kuban D, Pollack A, Huang E, Levy L, Dong L, Starkschall G, Rosen I. Hazards of dose escalation in prostate cancer radiotherapy. *Int J Radiat Oncol Biol Phys.* 2003;57:1260–1268.
81. Little DJ, Kuban DA, Levy LB, Zagars GK, Pollack A. Quality-of-life questionnaire results 2 and 3 years after radiotherapy for prostate cancer in a randomized dose-escalation study. *Urology.* 2003;62:707–713.
82. Zelefsky MJ, Fuks Z, Hunt M, et al. High-dose intensity modulated radiation therapy for prostate cancer: early toxicity and biochemical outcome in 772 patients. *Int J Radiat Oncol Biol Phys.* 2002;53:1111–1116.
83. Leibel SA, Fuks Z, Zelefsky MJ, et al. Technological advances in external-beam radiation therapy for the treatment of localized prostate cancer. *Semin Oncol.* 2003;30:596–615.
84. Bentzen SM, Dorr W, Anscher MS, et al. Normal tissue effects: reporting and analysis. *Semin Radiat Oncol.* 2003;13:189–202.
85. Power DA. Late effects of radiotherapy: how to assess and improve outcomes. *Br J Radiol.* 2005;78:150–152.
86. Gardner BG, Zietman AL, Shipley WU, Skowronski UE, McManus P. Late normal tissue sequelae in the second decade after high dose radiation therapy with combined photons and conformal protons for locally advanced prostate cancer. *J Urol.* 2002;167:123–126.
87. Zietman AL, Shipley WU, Coen JJ. Radical prostatectomy and radical radiation therapy for clinical Stages T1 to 2 adenocarcinoma of the prostate: new insights into outcome from repeat biopsy and prostate specific antigen follow-up. *J Urol.* 1994;152:1806–1812.
88. Pollack A, Salem N, Ashoori F, et al. Lack of prostate cancer radiosensitization by androgen deprivation. *Int J Radiat Oncol Biol Phys.* 2001;51:1002–1007.
89. Pollack A, Zagars GK, Smith LG, et al. Preliminary results of a randomized radiotherapy dose-escalation study comparing 70 Gy with 78 Gy for prostate cancer. *J Clin Oncol.* 2000;18:3904–3911.
90. Hintz BL, Koo C, Murphy JF. Pattern of proliferative index (Ki-67) after anti-androgen manipulation reflects the ability of irradiation to control prostate cancer. *Am J Clin Oncol.* 2004;27:85–88.
91. Kaminski JM, Hanlon AL, Joon DL, Meistrich M, Hachem P, Pollack A. Effect of sequencing of androgen deprivation and radiotherapy on prostate cancer growth. *Int J Radiat Oncol Biol Phys.* 2003;57:24–28.
92. Gottschalk AR, Roach M. The use of hormonal therapy with radiotherapy for prostate cancer: analysis of prospective randomised trials. *Br J Cancer.* 2004;90:950–954.
93. Laverdiere J, Nabid A, De Bedoya LD, et al. The efficacy and sequencing of a short course of androgen suppression on freedom from biochemical failure when administered with radiation therapy for T2–T3 prostate cancer. *J Urol.* 2004; 171:1137–1140.
94. Lawton CA, Winter K, Murray K, et al. Updated results of the Phase III Radiation Therapy Oncology Group (RTOG) trial 85-31 evaluating the potential benefit of androgen suppression following standard radiation therapy for unfavorable prognosis carcinoma of the prostate. *Int J Radiat Oncol Biol Phys.* 2001;49:937–946.
95. Pilepich MV, Winter K, John MJ, et al. Phase III Radiation Therapy Oncology Group (RTOG) trial 86-10 of androgen deprivation adjuvant to definitive radiotherapy in locally advanced carcinoma of the prostate. *Int J Radiat Oncol Biol Phys.* 2001;50:1243–1252.
96. Bolla M, Gonzalez D, Warde P, et al. Improved survival in patients with locally advanced prostate cancer treated with radiotherapy and goserelin. *N Engl J Med.* 1997;337:295–300.
97. D'Amico AV, Manola J, Loffredo M, Renshaw AA, DellaCroce A, Kantoff PW. 6-month androgen suppression plus radiation therapy vs. radiation therapy alone for patients with clinically localized prostate cancer: a randomized controlled trial. *JAMA.* 2004;292:821–827.
98. DeWeese TL. Radiation therapy and androgen suppression as treatment for clinically localized prostate cancer: the new standard? *JAMA.* 2004;292:864–866.
99. Horwitz EM, Feigenberg SJ, Pollack A, Hanks GE, Uzzo RG. Androgen suppression plus radiation therapy for prostate cancer. *JAMA.* 2004;292:2084–2085; author reply, 2085.
100. Dearnaley DP, Hall E, Lawrence D, et al. Phase III pilot study of dose escalation using conformal radiotherapy in prostate cancer: PSA control and side effects. *Br J Cancer.* 2005;92:488–498.
101. Zietman AL, Chung CS, Coen JJ, Shipley WU. 10-year outcome for men with localized prostate cancer treated with external radiation therapy: results of a cohort study. *J Urol.* 2004;171:210–214.
102. Catton C, Gospodarowicz M, Mui J, et al. Clinical and biochemical outcome of conventional dose radiotherapy for localized prostate cancer. *Can J Urol.* 2002;9:1444–1452; discussion, 1453.
103. Kupelian PA, Potters L, Khuntia D, et al. Radical prostatectomy, external beam radiotherapy < 72 Gy, external beam radiotherapy > or = 72 Gy, permanent seed implantation, or combined seeds/external beam radiotherapy for Stage T1–T2 prostate cancer. *Int J Radiat Oncol Biol Phys.* 2004; 58:25–33.

104. Martinez A, Galalae R, Gonzalez J, Mitchell C, Gustafson G, Kovacs G. No apparent benefit at 5 years from a course of neoadjuvant/concurrent androgen deprivation for patients with prostate cancer treated with a high total radiation dose. *J Urol.* 2003;170:2296–2301.
105. Moul JW, Chodak G. Combination hormonal therapy: a reassessment within advanced prostate cancer. *Prostate Cancer Prostatic Dis.* 2004;7(Suppl 1):S2–S7.
106. Thompson CA, Shanafelt TD, Loprinzi CL. Andropause: symptom management for prostate cancer patients treated with hormonal ablation. *Oncologist.* 2003;8:474–487.
107. Smith MR, Goode M, Zietman AL, McGovern FJ, Lee H, Finkelstein JS. Bicalutamide monotherapy versus leuprolide monotherapy for prostate cancer: effects on bone mineral density and body composition. *J Clin Oncol.* 2004;22:2546–2553.
108. Diamond TH, Higano CS, Smith MR, Guise TA, Singer FR. Osteoporosis in men with prostate carcinoma receiving androgen-deprivation therapy: recommendations for diagnosis and therapies. *Cancer.* 2004;100:892–899.
109. Schow DA, Renfer LG, Rozanski TA, Thompson IM. Prevalence of hot flushes during and after neoadjuvant hormonal therapy for localized prostate cancer. *South Med J.* 1998;91:855–857.
110. Green HJ, Pakenham KI, Headley BC, Gardiner RA. Coping and health-related quality of life in men with prostate cancer randomly assigned to hormonal medication or close monitoring. *Psychooncology.* 2002;11:401–414.
111. Herr HW, O'Sullivan M. Quality of life of asymptomatic men with nonmetastatic prostate cancer on androgen deprivation therapy. *J Urol.* 2000;163:1743–1746.
112. Asbell SO, Leon SA, Tester WJ, Brereton HD, Ago CT, Rotman M. Development of anemia and recovery in prostate cancer patients treated with combined androgen blockade and radiotherapy. *Prostate.* 1996;29:243–248.
113. D'Amico AV, Saegaert T, Chen MH, Renshaw AA, George D, et al. Initial decline in hemoglobin during neoadjuvant hormonal therapy predicts for early prostate specific antigen failure following radiation and hormonal therapy for patients with intermediate and high-risk prostate cancer. *Cancer.* 2002;95:275–280.
114. Grogan M, Thomas GM, Melamed I, et al. The importance of hemoglobin levels during radiotherapy for carcinoma of the cervix. *Cancer.* 1999;86:1528–1536.
115. Warde P, O'Sullivan B, Bristow RG, et al. T1/T2 glottic cancer managed by external beam radiotherapy: the influence of pretreatment hemoglobin on local control. *Int J Radiat Oncol Biol Phys.* 1998;41:347–353.
116. Rudat V, Dietz A, Schramm O, et al. Prognostic impact of total tumor volume and hemoglobin concentration on the outcome of patients with advanced head and neck cancer after concomitant boost radiochemotherapy. *Radiother Oncol.* 1999;53:119–125.
117. D'Amico AV, Cote K, Loffredo M, Renshaw AA, Chen MH. Pretreatment predictors of time to cancer specific death after prostate specific antigen failure. *J Urol.* 2003;169:1320–1324.
118. Zietman AL, Dallow KC, McManus PA, Heney NM, Shipley WU. Time to second prostate-specific antigen failure is a surrogate endpoint for prostate cancer death in a prospective trial of therapy for localized disease. *Urology.* 1996;47:236–239.
119. Albertsen PC, Hanley JA, Penson DF, Fine J. Validation of increasing prostate specific antigen as a predictor of prostate cancer death after treatment of localized prostate cancer with surgery or radiation. *J Urol.* 2004;171:2221–2225.
120. Horwitz EM, Thames HD, Kuban DA, et al. Definitions of biochemical failure that best predict clinical failure in patients with prostate cancer treated with external beam radiation alone: a multi-institutional pooled analysis. *J Urol.* 2005;173:797–802.
121. Pickles T, Kim-Sing C, Morris WJ, Tyldesley S, Paltiel C. Evaluation of the Houston biochemical relapse definition in men treated with prolonged neoadjuvant and adjuvant androgen ablation and assessment of follow-up lead-time bias. *Int J Radiat Oncol Biol Phys.* 2003;57:11–18.
122. Vicini FA, Kestin LL, Martinez AA. The correlation of serial prostate specific antigen measurements with clinical outcome after external beam radiation therapy of patients for prostate carcinoma. *Cancer.* 2000;88:2305–2318.
123. Pickles T, Duncan GG, Kim-Sing C, McKenzie MR, Morris WJ. PSA relapse definitions—the Vancouver Rules show superior predictive power. *Int J Radiat Oncol Biol Phys.* 1999;43:699–700.
124. Gleave ME, Goldenberg SL, Chin JL, et al. Randomized comparative study of 3 versus 8-month neoadjuvant hormonal therapy before radical prostatectomy: biochemical and pathological effects. *J Urol.* 2001;166:500–506; discussion, 506–507.
125. Crook J, Malone S, Perry G, Bahadur Y, Robertson S, Abdolell M. Postradiotherapy prostate biopsies: what do they really mean? Results for 498 patients. *Int J Radiat Oncol Biol Phys.* 2000;48:355–367.
126. Crook JM, Perry GA, Robertson S, Esche BA. Routine prostate biopsies following radiotherapy for prostate cancer: results for 226 patients. *Urology.* 1995;45:624–631; discussion, 631–622.
127. Fowler JF, Ritter MA, Chappell RJ, Brenner DJ. What hypofractionated protocols should be tested for prostate cancer? *Int J Radiat Oncol Biol Phys.* 2003;56:1093–1104.
128. Kupelian PA, Willoughby TR. Short-course, intensity-modulated radiotherapy for localized prostate cancer. *Cancer J.* 2001;7:421–426.
129. Kitamura K, Shirato H, Shinohara N, et al. Reduction in acute morbidity using hypofractionated intensity-modulated radiation therapy assisted with a fluoroscopic real-time tumor-tracking system for prostate cancer: preliminary results of a Phase I/II study. *Cancer J.* 2003;9:268–276.
130. Livsey JE, Cowan RA, Wylie JP, et al. Hypofractionated conformal radiotherapy in carcinoma of the prostate: five-year outcome analysis. *Int J Radiat Oncol Biol Phys.* 2003;57:1254–1259.
131. Bristow RG, Hill RP. Molecular and cellular radiobiology. In: Tannock IF, Hill RP, Harrington L, Bristow RG, editors. Basic science of oncology, 4th edition. New York: McGraw-Hill Publishing, 2005:261–288.
132. McKenna WG, Muschel RJ. Targeting tumor cells by enhancing radiation sensitivity. *Genes Chromosomes Cancer.* 2003;38:330–338.
133. Shay JW, Roninson IB. Hallmarks of senescence in carcinogenesis and cancer therapy. *Oncogene.* 2004;23:2919–2933.
134. Paoluzzi L, Figg WD. Histone deacetylase inhibitors are potent radiation protectants. *Cancer Biol Ther.* 2004;3:612–613.
135. Chung YL, Wang AJ, Yao LF. Antitumor histone deacetylase inhibitors suppress cutaneous radiation syndrome: implications for increasing therapeutic gain in cancer radiotherapy. *Mol Cancer Ther.* 2004;3:317–325.

136. Somech R, Izraeli S, J Simon A. Histone deacetylase inhibitors—a new tool to treat cancer. *Cancer Treat Rev.* 2004;30: 461–472.
137. Vigushin DM, Coombes RC. Targeted histone deacetylase inhibition for cancer therapy. *Curr Cancer Drug Targets.* 2004;4:205–218.
138. Sasaki R, Shirakawa T, Zhang ZJ, et al. Additional gene therapy with Ad5CMV-p53 enhanced the efficacy of radiotherapy in human prostate cancer cells. *Int J Radiat Oncol Biol Phys.* 2001;51:1336–1345.
139. Carlsson J, Gedda L, Grönvik C, et al. Strategy for boron neutron capture therapy against tumor cells with over-expression of the epidermal growth factor-receptor. *Int J Radiat Oncol Biol Phys.* 1994;30:105–115.
140. Bonner JA, Giralt J, Harari PM, et al. Cetuximab prolongs survival in patients with locoregionally advanced squamous cell carcinoma of head and neck: a Phase III study of high dose radiation therapy with or without cetuximab [abstract 5507]. Presented at the 40th annual meeting of the American Society for Clinical Oncology, June 5–8, New Orleans, Louisiana.
141. Mu Z, Hachem P, Agrawal S, Pollack A. Antisense MDM2 sensitizes prostate cancer cells to androgen deprivation, radiation, and the combination. *Int J Radiat Oncol Biol Phys.* 2003;57:S256–S257.
142. Zellweger T, Kiyama S, Chi K, et al. Overexpression of the cytoprotective protein clusterin decreases radiosensitivity in the human LNCaP prostate tumour model. *BJU Int.* 2003; 92:463–469.
143. Sheikh MS. Radiosensitivity with Par-4 expression in prostate cancer. *Cancer Biol Ther.* 2002;1:161–162.
144. Honda T, Gjertsen BT, Spurgers KB, et al. Restoration of bax in prostate cancer suppresses tumor growth and augments therapeutic cell death induction. *Anticancer Res.* 2001;21: 3141–3146.
145. Trofimova I, Dimtchev A, Jung M, et al. Gene therapy for prostate cancer by targeting poly(ADP-ribose) polymerase. *Cancer Res.* 2002;62:6879–6883.
146. Butler J, Rangnekar VM. Par-4 for molecular therapy of prostate cancer. *Curr Drug Targets.* 2003;4:223–230.
147. Colletier PJ, Ashoori F, Cowen D, et al. Adenoviral-mediated p53 transgene expression sensitizes both wild-type and null p53 prostate cancer cells in vitro to radiation. *Int J Radiat Oncol Biol Phys.* 2000;48:1507–1512.
148. Rosser CJ, Tanaka M, Pisters LL, et al. Adenoviral-mediated PTEN transgene expression sensitizes Bcl-2-expressing prostate cancer cells to radiation. *Cancer Gene Ther.* 2004; 11:273–279.
149. Sah NK, Munshi A, Nishikawa T, Mukhopadhyay T, Roth JA, Meyn RE. Adenovirus-mediated wild-type p53 radiosensitizes human tumor cells by suppressing DNA repair capacity. *Mol Cancer Ther.* 2003;2:1223–1231.
150. Milosevic M, Bristow RG, Chung T, Panzarella T, Toi A, Hill RH. Prostate cancer hypoxia correlates with poor patient outcome following treatment with radiotherapy. *Int J Radiat Oncol Biol Phys.* 2004;60:S236–S237.
151. Abdollahi A, Lipson KE, Han X, et al. SU5416 and SU6668 attenuate the angiogenic effects of radiation-induced tumor cell growth factor production and amplify the direct anti-endothelial action of radiation in vitro. *Cancer Res.* 2003;63: 3755–3763.
152. Brown JM, Wilson WR. Exploiting tumour hypoxia in cancer treatment. *Nat Rev Cancer.* 2004;4:437–447.
153. Pruthi RS, Derksen JE, Moore D. A pilot study of use of the cyclooxygenase-2 inhibitor celecoxib in recurrent prostate cancer after definitive radiation therapy or radical prostatectomy. *BJU Int.* 2004;93:275–278.
154. Harari PM, Huang SM. Combining EGFR inhibitors with radiation or chemotherapy: will preclinical studies predict clinical results? *Int J Radiat Oncol Biol Phys.* 2004;58:976–983.

FIGURE 1

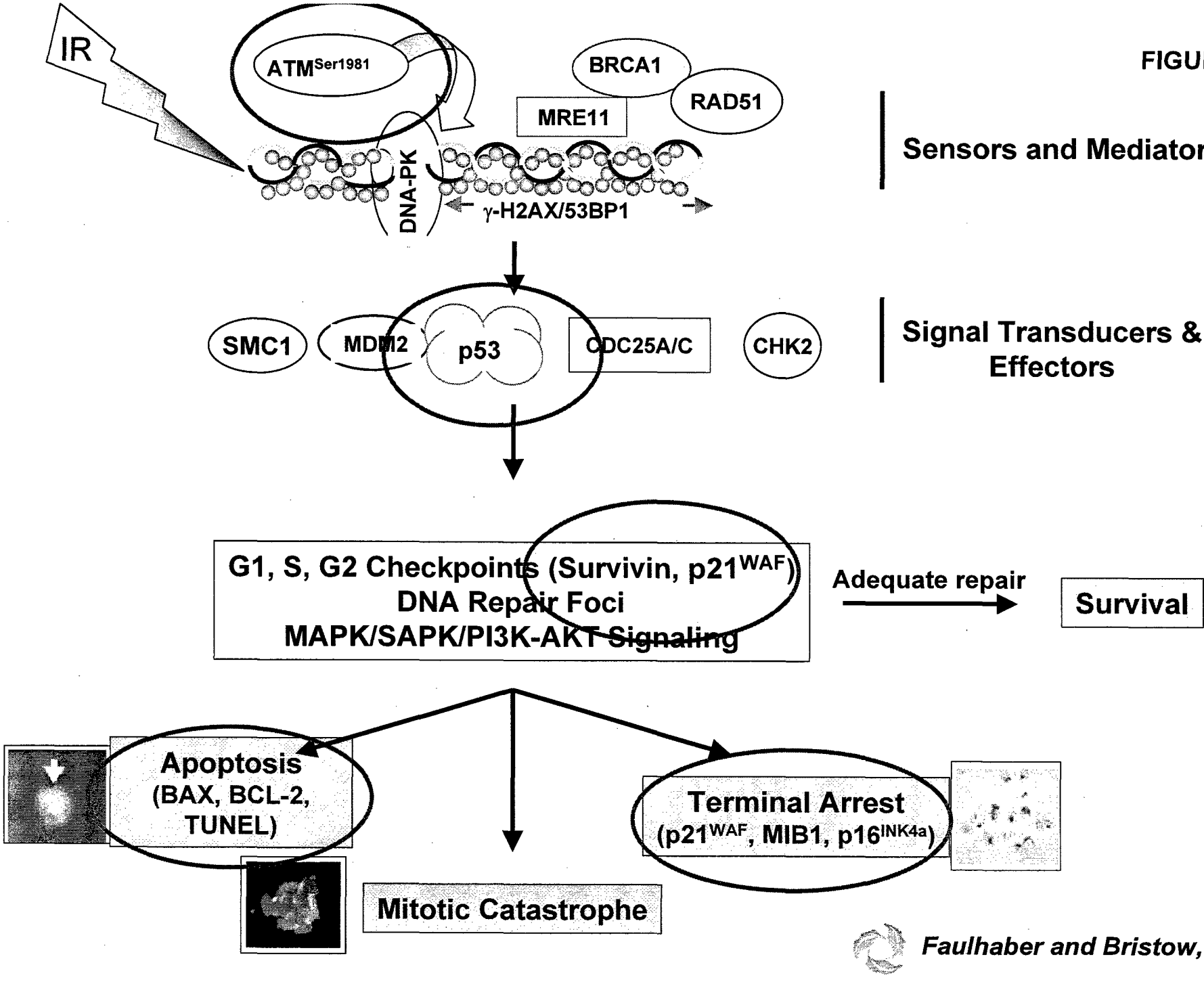

Faulhaber and Bristow, 2004

HYPOXIA & RAD51 Expression

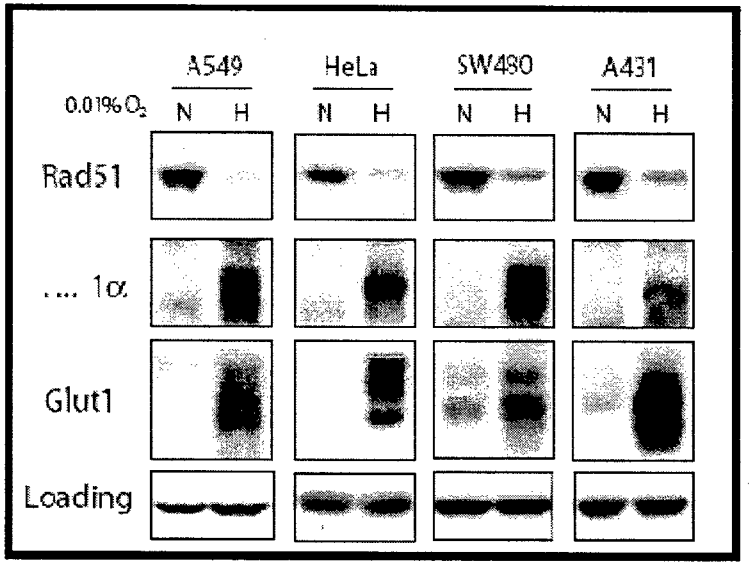

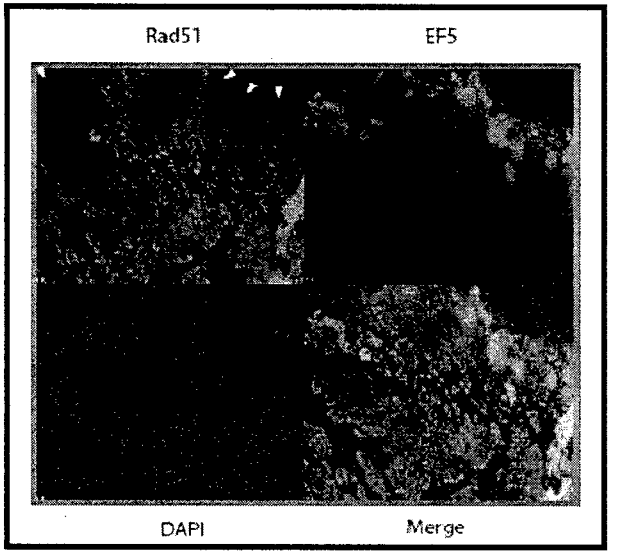

HYPOXIA → **Decreased RAD51-BRCA2 & Homologous Recombination In Cells Adapted to Low Oxygen** → **Increased Genetic Instability & Progression (Metastases)**

Bindra, Glazer, Bristow; 2004
Meng,Bristow; 2005

FIGURE 2

Measuring DNA-dsb Breaks In Vitro (22RV1 prostate cancer cells) And In Vivo (22RV1 Xenografts) Using gamma-H2AX

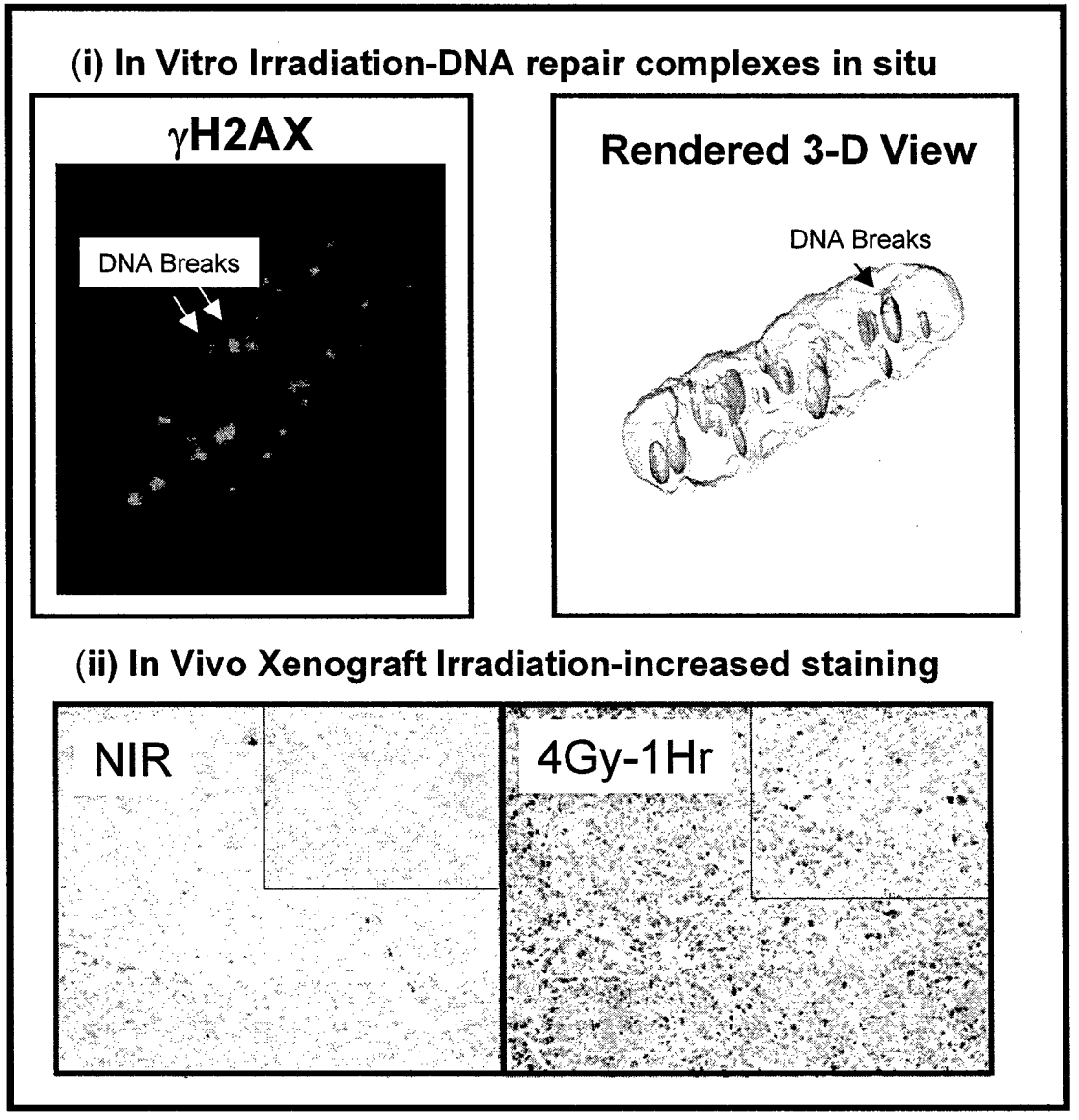

FIGURE 3

Pre-Operative Radiotherapy Study

- Between 2001 and 2004, 15 patients were entered on trial (PSAs: 7.5-39; Ages 55-68; Volumes 22-88 cc.).
  - Eligible patients included those with a high-risk of extra-prostatic disease: T1/T2N0M0 tumors plus (i) Gleason ≥7, PSA>10 ng/ml and <35 ng/ml, or (ii), PSA >15 ng/ml and less <35 ng/ml (any Gleason).

- Patients received 25 Gy in 5 fractions of conformal radiotherapy followed by radical prostatectomy within 1-2 weeks (usually within 4 days) . Trial endpoints included acute radiotherapy toxicity (RTOG scale) and intra-operative morbidity.

- Twelve(12) patients were studied for DNA damage signalling based on paired pre- and post-radiotherapy tissue samples; GS 7 (7/12); GS 6(4/12); GS 10(1/12) on pre-XRT biopsy

FIGURE 4

ATM-p53 Signaling In Patient Prostate Biopsies/ Post-Op Tissues (25Gy/5)

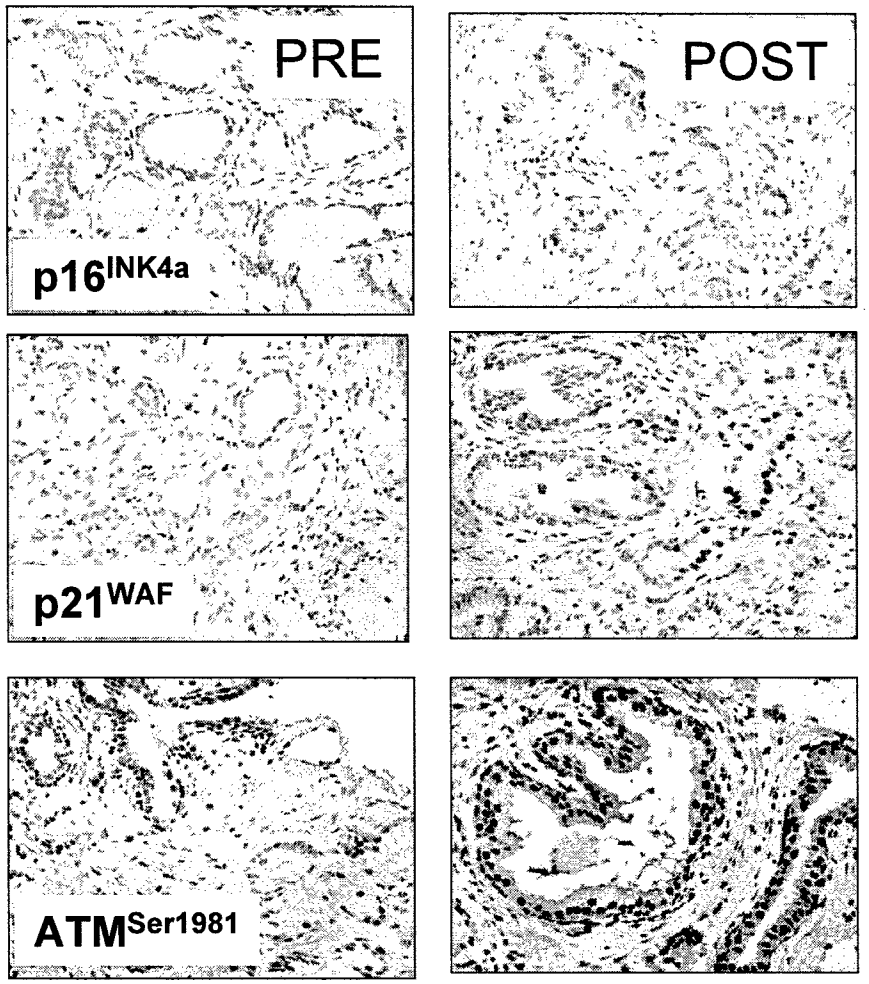

N=12; all WTp53 by direct DNA sequencing

- Majority of irradiated prostate tumor tissues showed increased expression of p-ATM p53 and $p21^{WAF}$
- Mean expression (ME) of p-ATM increased post-RT (p=0.293)
- ME of p21WAF increased from 0 to 50% (p=0.001)
- ME of p53 increased from 41.1 to 51.8% (p=0.623).

FIGURE 5

DNA Repair Proteins & TMAs

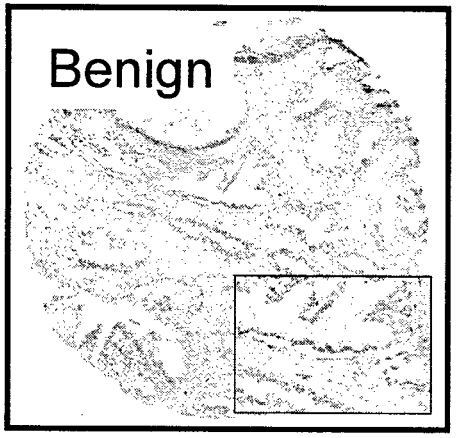

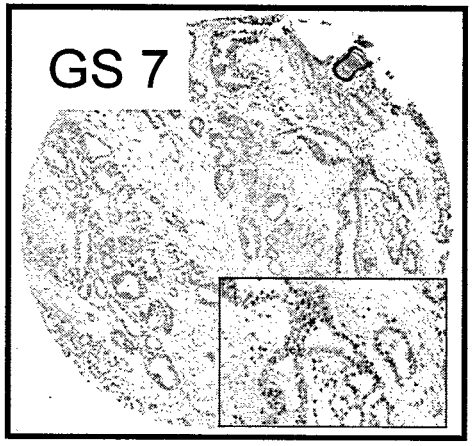

- No differences in DNA-PKcs, RAD51 or KU70 expression pre- and post-XRT
- However, may be a relationship between DNA repair protein (e.g. ATM and RAD51) expression and tumour progression based on recent TMA results
- Correlation with outcome ? Pending…

FIGURE 6

Conclusions: DNA Damage Biomarkers and Prostate Radiotherapy

- First study to show that the ATM-p53 axis is operational in human prostate tissues during radiotherapy
- Radiotherapy leads to a $p21^{WAF}$-induced arrest, rather than apoptosis
  - REB approval for intra-radiotherapy biopsies using 2 Gy per day (Fraction 3-5 of 39 fractions = 78 Gy total)
    - May be used to triage patients to XRT vs surgery
    - Implications for new drug design

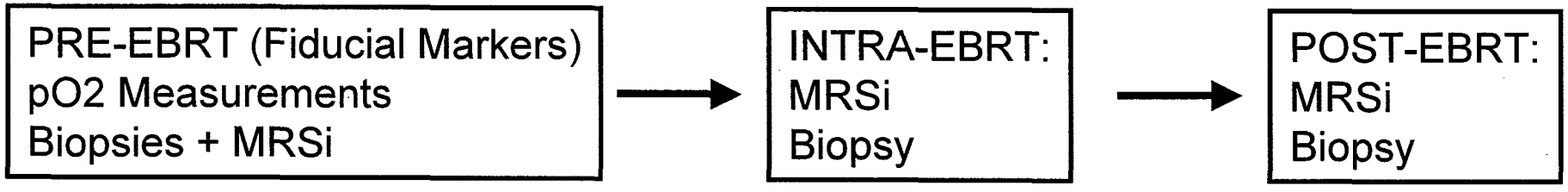

FIGURE 7

Prostate Cancer and Prostatic Diseases (2003) 6, 73–85
 1365-7852/03 $25.00
www.nature.com/pcan

Cell death in irradiated prostate epithelial cells: role of apoptotic and clonogenic cell kill

GP Bromfield[2], A Meng[2], P Warde[1] & RG Bristow[1,2]*

[1]*Department of Radiation Oncology, University of Toronto and the Ontario Cancer Institute/Princess Margaret Hospital, University Health Network, Toronto, Ontario, Canada; and* [2]*Department of Medical Biophysics, University of Toronto, Toronto, Ontario, Canada*

Dose-escalated conformal radiotherapy is increasingly being used to radically treat prostate cancer with encouraging results and minimal long-term toxicity, yet little is known regarding the response of normal or malignant prostate cells to ionizing radiation (IR). To clarify the basis for cell killing during prostate cancer radiotherapy, we determined the IR-induced expression of several apoptotic- (bax, bcl-2, survivin and PARP) and G1-cell cycle checkpoint- (p53 and $p21^{WAF1/Cip1}$) related proteins, in both normal (PrEC-epithelial and PrSC-stromal) and malignant (LNCaP, DU-145 and PC-3; all epithelial) prostate cells. For these experiments, we chose doses ranging from 2 to 10 Gy, to be representative of the 1.8–2 Gy daily clinical fractions given during curative radiotherapy and the 8–10 Gy single doses given in palliative radiotherapy. We observed that IR-induced bax and $p21^{WAF1/Cip1}$ protein expression were attenuated selectively in normal stromal and epithelial cell cultures, yet maintained their p53-dependency in malignant cell lines. For each cell culture, we also determined total apoptotic and overall radiation cell kill using a short-term nuclear morphologic assay and a long-term clonogenic survival assay, respectively. Clonogenic survival, as measured by the surviving fraction at 2 Gy (SF2), ranged from 0.05 (PrEC) to 0.55 (DU-145), suggesting that malignant prostate cells are more radioresistant than normal prostate cells, for this series. IR-induced apoptotic cell kill was minimal (less than 6% cell after a dose of 10 Gy at times of 24–96 h) and was not dose-dependent. Furthermore, apoptotic kill was not correlated with either molecular apoptotic response or clonogenic cell kill. Using a flow cytometric proliferation assay with the PrSC (stromal) and DU-145 (epithelial) representative cultures, we observed that a senescent-like phenotype (SLP) emerges within a sub-population of cells post-irradiation that is non-clonogenic. Terminal growth arrest was dose-responsive at 96 h following irradiation and associated with long-term expression of both $p21^{WAF1/Cip1}$ and $p16^{INK4a}$ genes. Future strategies for prostate radiotherapy prediction or novel treatments should additionally focus on terminal growth arrest as an important endpoint in prostate cancer therapy.
Prostate Cancer and Prostatic Diseases (2003) **6**, 73–85. doi:10.1038/sj.pcan.4500628

Keywords: prostate cancer; epithelium; senescence; apoptosis; radiosensitivity

Introduction

Dose-escalated (ie 76–80 Gy) radiotherapy is an important treatment option for men with intermediate-risk prostate cancer who present with T1 or T2 disease, a Gleason score greater than 6 out of 10 and serum prostatic specific antigen (PSA) values in the order of 10–20 μg/ml.[1] Successful radiotherapy results in a gradual decline of the serum PSA over 12–24 months following treatment where a PSA nadir of less than 1.0 μg/ml predicts for 5 year, long-term local control.[2] With three-dimensional conformal (3D-CRT) or intensity-modulated (IMRT) radiotherapy treatment protocols, 5 year PSA-free relapse rates are approximately 75–85% and associated with minimal late toxicity (less than 5%

*Correspondence to: RG Bristow, Department of Radiation Oncology, Princess Margaret Hospital (UHN), 610 University Avenue, Toronto, Ontario, Canada M5G 2M9.
E-mail: rob.bristow@rmp.uhn on.ca
Received 9 May 2002; revised 25 July 2002; accepted 7 August 2002

with Radiotherapy Oncology Group (RTOG) Grade 3–4 rectal or bladder damage).[2]

Yet these same data predict that 15–25% will not achieve local control following radical radiotherapy, thought in part to be due to the intrinsic radioresistance of prostate cancer cells secondary to genetic (eg apoptosis, cell-cycle or DNA-repair-related gene expression) or microenvironmental factors (eg hypoxia or altered growth factor expression).[3] The success of radiation therapy in prostate cancer treatment is therefore dependent on the eradication of all prostate tumor clonogens (ie tumor stem cells, estimated to be less than 1% of cells within a tumor), which are select tumor cells capable of unlimited proliferative potential. Failure to eradicate this particular population will result in the regrowth of the tumor following treatment.[4] Despite many advances towards understanding prostate carcinogenesis, little work has been published to date relating the mode of clonogenic cell kill following DNA damage in either normal and malignant prostate epithelial cell cultures. This information is important in defining new strategies to augment prostate cancer cell kill and understand the kinetics of cell kill following radiotherapy (in comparison to decreasing PSA value kinetics *in vivo*) and may allow optimal interpretation of post-radiotherapy biopsies as a secondary measure of local tumor control.

Apoptosis plays an important role in the death of both normal prostate and androgen-dependent malignant prostate tissue following androgen withdrawal, leading to a decrease in either glandular or tumor volume, respectively. This is supported by the observation of rapid apoptosis following castration in the rat prostate glands[5,6] (a response lacking in mice deficient in expression of the pro-apoptotic gene, bax[7]) and in patients treated with androgen-withdrawal therapy for locally advanced or metastatic prostate cancer.[8] The relationship between androgen ablation and apoptosis has led to a number of clinical studies that have attempted to determine whether local failure following radical radiotherapy is secondary to genetic factors that control radiation-induced apoptosis. However, taken together, clinicopathologic studies that have attempted to correlate altered expression of the p53, $p21^{WAF1/Cip1}$, bax, bcl-2 and caspase apoptosis-related genes and radiocurability have been inconclusive.[9,10] This may be due to small clinical sample size, differences in the quantitation or timing of immunohistochemical or gene expression endpoints,[11,12] variable clinical treatment parameters, or perhaps due to alternate mechanisms of prostate cell death that confound analyses focused solely on apoptotic endpoints.

Recent data has supported the hypothesis that apoptosis may not be the dominant mode of cell death following radio- and chemotherapy in stromal (ie fibroblast) and epithelial tissues.[13,14] Indeed, it has been suggested that in these and selected tumor models, apoptosis may actually occur in a non-clonogenic population following DNA damage.[15,16] Alternatively, a permanent cell-cycle arrest or senescence-like terminal growth arrest may also be a factor in determining prostate cell death following radiotherapy.[17] Markers of senescence, such as senescence-associated β-galactosidase (SA β-gal) activity and permanently elevated levels of $p21^{WAF1/Cip1}$ and $p16^{INK4a}$ are actively under investigation as biomarkers of terminal growth arrest in human tumors.[18] Chang and co-workers[19] observed that a number of DNA-damaging agents (including ionizing radiation) could induce a senescence-like phenotype (SLP) in 11/14 cell lines tested. Other laboratories[13] and reviews have outlined a number of considerations regarding radiation-induced cell-death, including cell-type dependency in defining the dominant mode(s) of death (ie apoptosis, mitotic-linked death and reproductive death (SLP)/necrosis).[20] An improved understanding of death processes has been afforded by novel flow cytometric methods to detect terminally-arrested tumor cells following drug treatment,[19,20] and ascertain their relative morphology and clonogenic potential.

The purpose of the current study was to examine the mode(s) of prostate cell death *in vitro* following exposure to ionizing radiation to possibly refine clinical biomarkers for prediction of radiotherapeutic response and suggest future treatment strategies. Apoptosis, proliferation and clonogenic survival were assessed in a panel of cell lines comprised of both normal (stromal-PrSC and epithelial-PREC) and malignant (LNCaP, DU-145, PC-3; all epithelial) cultures, to determine the overall cellular response. We demonstrate that apoptosis is not the dominant mode of cell kill in this panel of cell cultures post-IR. Instead, data on selected cell lines supports the concept that long-term proliferative arrest relates to clonogenic radiation cell killing *in vitro*.

Materials and methods

Cell culture

All cell cultures were incubated in vented tissue culture flasks under 5% CO_2 and 37°C culture conditions. LNCaP cells (a gift from L Chung, University of Virginia) were maintained in T-media (Gibco-BRL) and supplemented with 10% FCS. PC-3 and DU-145 cells were purchased from ATCC and maintained as suggested in Ham's F12K, and alpha-Modified Eagles Medium respectively, supplemented with 10% FCS and 2 mM L-glutamine. PrEC (normal prostate epithelial cells) and PrSC (normal prostate stromal cells) were purchased from Clonetics and maintained as per suggested protocol in PrEGM media and SCGM media, without testosterone supplementation, respectively. Both cell cultures have limited lifespan and proliferative potential in culture according to the supplier and we have consistently observed decreased growth rates following passage 5 *in vitro* for both cultures. Immortalized myc-infected Rat-1 HO15.19 fibroblast cells (a gift from Dr L Penn, OCI/PMH[21]) were maintained in Dulbecco's H21 media supplemented with 10% FBS. Cultures were maintained without testosterone supplementation to ensure that radiation survival studies were completed under similar conditions in normal and malignant prostate cultures and as previous experiments have determined that exogenous testosterone may not always alter apoptotic responses, clonogenic survival or IR-induced $p21^{WAF1/Cip1}$ expression and cell arrest in androgen-*sensitive* cells (J Tsihlias, personal communication[22,23]) Approximate doubling times for cell cultures under these conditions were as follows: PrEC, 36–48 h (highly variable); PrSC, 18 h; LNCaP, 36 h; PC-3, 24 h; DU-145, 18 h; Myc-expressing Rat-1HO15.19, 16 h.

SF2Gy and clonogenic radiation survival curves

Logarithmically growing cells were rinsed with PBS/HBSS, trypsinized for 5 min at 37°C, and then were seeded at appropriate densities for colony formation in six-well dishes (Nunc). Asynchronous cultures were irradiated 16–20 h post-plating to reduce the immediate effects of trypsinization and such that the multiplicity index was less than 1.1.[24] At least two dilutions of cells in triplicate were used for each dose point for any given individual experiment. At least three independent clonogenic radiation experiments were completed for each cell line. Plated cells were either mock irradiated or irradiated with 0–10 Gy under aerobic conditions using a ^{137}Cs irradiator at ~1 Gy/min at room temperature. Plates were then incubated at 37°C for 7–14 days depending on cell doubling time *in vitro* and re-fed every 4–5 days before fixation and staining (methylene blue/50% methanol) of resulting colonies (aggregates of greater than 50 cells were scored as a colony). Radiation survival was calculated as the plating efficiency of treated cells divided by the plating efficiency of untreated cells and plotted as a function of dose on a semi-logarithmic plot as previously described.[24] We were unable to derive colonies at doses greater than 2 Gy in the LNCaP and PrEC cell cultures due to poor plating efficiencies, and therefore only SF2 values are presented for these cultures. For a given cell culture, there was no correlation between the SF2 values and plating efficiency amongst individual experiments, although mean SF2 values were increased in cell lines which exhibited increased plating efficiency, as reported in the literature (ie DU-145 and PC-3).[3,21]

Western blotting

Logarithmically-growing cells were irradiated and lysed on ice for 20 min with E7 lysis buffer as previously described.[24] Protein quantification was performed determined using a commercial Pierce-BCA assay kit to derive a mean concentration value based on three assays per lysate. SDS–PAGE was performed using 7–12% bis–acrylamide (29:1) gels with a 4% stacking gel run in a Novex X-cell semi-dry Mini Cell western blotting apparatus at room temperature. Each well was loaded with 20 µg of total protein plus loading buffer (final concentration 1×–6% glycerol, 0.83% β-mercaptoethanol, 1.71% Tris-HCl pH 6.8, 0.002% Bromophenol Blue) after boiling for 3 min. Samples resolved by electrophoresis at 80–110 V for 1.5–2.5 h were transferred onto nitrocellulose overnight at 14 V/4°C or for 1.5 h at 24 V/room temperature in transfer buffer (75 mM glycine, 10 mM Tris, 20% methanol). For selected blots, pre-hybridization staining with Ponceau S confirmed equal loading and transfer between running lanes.

To detect protein, membranes were blocked in TBST/0–10% low fat milk and then exposed to the primary antibody 2–4 h at room temperature constant rotation. Membranes were then rinsed with TBST and exposed to the appropriate secondary antibody for 1 h under similar conditions, rinsed again with TBST, once with 10× TBS and finally incubated in Amersham ECL chemiluminescence solution for 1 min. Membranes were exposed to Hyperfilm ECL from AmershamPharmacia and analyzed by densitometry (Molecular Dynamics Computing Densitometer, ImageQuant Mac version 1.2). Primary antibodies used in these studies included: p53-mouse monoclonal (Santa Cruz Bp53-12, 1:3000); $p21^{WAF1}$-mouse monoclonal (Oncogene Ab-1, 1:3000); Bax-rabbit polyclonal (Santa Cruz N-20, 1:1000); Bcl-2-mouse monoclonal (Santa Cruz 509, 1:500); PARP-mouse monoclonal (BioMol SA-249, 1:1000), survivin-rabbit polyclonal (Alpha Diagnostics SURV11, 1:5000), and $p16^{INK4A}$ mouse monoclonal (Oncogene Ab-1, 1:1000).

Assays for apoptotic cell death

Radiation-induced apoptosis was quantified on the basis of distinct nuclear morphology and associated apoptotic bodies based on a previously standardized immunofluorescence protocol (Hoechst 33342 staining).[24] For the morphology assay, logarithmically growing cells were re-plated at appropriate densities in triplicate and mock/irradiated with 0, 2, 10 or 20 Gy. These were scored for apoptotic morphology (ie apoptotic bodies and nuclear condensation—see sample in Figure 2a) at periods of 24–96 h following irradiation. Total adherent and floating cells in each culture were fixed and stained in 4% formalin-PBS/10 µM Hoechst 33342 DNA-specific dye for 30 min at RT. Cell counts to evaluate any cell loss/lysis into culture media were also performed at each time point. All experiments utilized Rat-1 HO15.19 cell line as positive control for gamma-irradiation induced apoptosis (L Penn, personal communication and Lee *et al*[25]).

Radiation survival in proliferating and non-proliferating irradiated cultures: the CFDA-SE flow cytometry proliferation assay

To determine if permanent arrest is associated with decreased clonogenic survival, a modification of the protocol by Chang *et al*[19] utilized the CFDA-SE (CFSE) fluorescent dye.[20,26] The CFSE compound (Molecular Probes, C-1157) is distributed throughout the cellular membranes and is divided evenly amongst subsequent progeny based on division of equal volumes of membrane at cell division. Multiple rounds of cell division are therefore represented by a corresponding decrease in total membrane fluorescence within a proliferating population, which can be detected by flow cytometry. Analyzing cell populations for relative fluorescence (FL1 (CFSE) parameter; increased non-proliferating cultures) and increasing side-scatter (SSC parameter; due to increased granularity associated with senescent cells) allows for flow cytometric analysis of senescent-like populations post-treatment.

Sub-confluent flasks of cells were trypsinized, collected and centrifuged into a pellet and 5×10^6 cells were re-suspended in 1 ml serum-free media plus 1 µl of stock solution (5 M CFSE in DMSO) at 37°C for 10 min with occasional inversion. Ice-cold RPMI 1640 + 10% FBS was then added prior to a subsequent cell centrifugation, and finally the cells were re-suspended in PBS. The cells were further washed twice in PBS, re-plated at low density (approximately 10% confluence) into multiple, 175 cm^2

Falcon flasks for next-day irradiation (0–10 Gy). As a control, all cells (floating and adherent) from one untreated flask were harvested one day post-plating and analyzed with flow cytometry to find baseline fluorescence (FL1(CFSE)) intensity. Remaining cultures were followed until day 5 when all cells (floating and adherent) were harvested, analyzed and sorted by FACS into 'non-proliferating' ($FL1(CFSE)^{hi}SSC^{hi}$), and 'proliferating' (ie all cells other than $FL1(CFSE)^{hi}SSC^{hi}$) populations to determine clonogenic potential within each population. The 5 day time point was initially chosen as it represents the point at wbich surviving cells would begin to show their colony-forming ability.[3] Sorted populations of DU-145 and PrSC were used to derive colonies in each sub-group as examples of epithelial and stromal (ie fibroblast-like) models. Pre-sort samples were analyzed on a BDIS FACScan analyzer and samples sorted using either a Becton Dickonson Immunocytometry system FACStarPLUS or BDIS FACS Vantage system. BDIS CELLQuest Software version 3.3 was used for both sorting and analysis. Cell lysates from adherent and floating cells in parallel cultures treated similarly (stained, irradiated with 0, 2 and 10 Gy) were also harvested on days 5–9, and analyzed for expression of the $p16^{INK4a}$ and $p21^{WAF1}$ genes. Cultures were also stained for senescence-associated β-galactosidase (SA β-gal) using the method of Chang *et al*,[19] as a complementary biomarker of senescence-like death.

Results

Gene expression of apoptosis-related genes within irradiated prostate cell cultures

As different laboratories may contain variants of original cell stocks, we initially determined the p53 status of the malignant prostate epithelial cell lines using full-length DNA sequencing of exons 1–11 of the p53 gene. Consistent with previous reports, LNCaP cells were found to express two wild-type (WT) alleles, whereas the PC-3 cells were devoid of p53 protein expression due to chromosome 17p hemizygosity and a mutation in the remaining allele at codon 138 which results in a premature stop codon at position 169. The DU-145 cells express mutant (MT) p53 protein due to mutations at codons 223 and 274. We observed that the level of bax protein expression is p53-dependent following IR, given the increased expression in the WTp53-expressing LNCaP cells at 24 h following 10 Gy. This molecular response was attenuated, or absent, in the remaining PC-3 and DU-145 malignant epithelial cell lines, which have altered p53 protein expression. Of note, despite the western blots shown in Figure 1b, bax expression is detectable in DU-145 cells, albeit at a very low level. The response was also attenuated within the normal epithelial and stromal cultures (see Figure 1a, b and Table 1). Bcl-2 protein levels were low, yet detectable, using our antibody, and remained unchanged in all cell cultures following 10 Gy for periods up to 24 h following radiation (see Figure 1c, d). In other experiments in our laboratory, the relative levels of bax and bcl-2 protein have been confirmed at the mRNA level by RNA protection analyses (R Fan and RG Bristow, manuscript in preparation). The IAP-related protein, survivin, has been suggested to be a prognostic indicator in a variety of cancers, presumably due to its influence on cellular apoptosis and G2 phase cell cycle control[27] and reported differential upregulation in malignant tissues, relative to normal tissues.[28] *In vitro*, endogenous survivin levels were observed to be detectable in all of the cell cultures within our series (normal and malignant), and were invariant following irradiation (Table 1) except for a slight (1.6-fold) increase in PrSC. Subsequent experiments have revealed lower levels of survivin in PrEC cultures than in their stromal and malignant counterparts.

Terminal apoptotic transduction involves altered expression and cleavage of the caspase family of proteins and the PARP protein.[29,30] Other laboratories have reported that caspase 1 and 3 protein expression can be deficient in some of our malignant cell lines.[31] In our experiments, analysis for PARP cleavage revealed that, although we detected an increase in the characteristic 89 kD a apoptotic-related PARP protein fragment in our highly apoptotic Rat-1 HO15.19 cell line, there was no such change in any of the five prostate cell cultures at 24 h following a dose of 10 Gy (data not shown). Our results (summarized in Table 1) suggest that gene and protein expression related to terminal apoptosis-defining events following IR is not consistent with observations made for other cells (eg lymphocytes or thymocyctes), which are classically more susceptible to radiation-induced apoptosis; however we recognize that the molecular apoptotic and morphologic (see below) response of our cell panel may be variable, depending on type of cell stress and drug treatment.

Minimal evidence of apoptotic cell death in irradiated prostate cultures

We next determined the level of radiation-induced apoptosis following various doses (2–20 Gy) and time points (0–96 h post-IR) using a distinct nuclear morphology assay (see Figure 2a) as previously described.[24] A dose of 10 Gy has been shown to decrease clonogenic survival by 3 logs or more, in other malignant cell lines. The highly apoptotic adherent Rat-1 HO15.19 cell line formed a positive control for IR-induced apoptosis in these experiments and irradiated cultures were observed to contain decreasing numbers of cells over 24–96 h consistent with a rapid induction of cell death (data not shown). The level of apoptosis in Rat-1 HO15.19 control following 20 Gy became difficult to quantify at 24 h due to a large amount of cellular debris and may be underestimated, as presented in Figure 2b. The apoptotic response of our prostate cell panel at times of 24–96 h following 10 Gy as determined by morphology is presented in Figure 2b, and reveals that neither normal nor malignant prostate cells undergo high levels of apoptosis at any time point up to 96 h (a time at which the earliest colonies indicative of clonogenic survival can be detected). Additionally, careful total cell counts of adherent and floating cells within all the irradiated cultures suggested that there was no decrease at any time point up to 96 h in total cell number, which ruled out underestimating apoptotic responses (data not shown). Moreover, in contrast to the

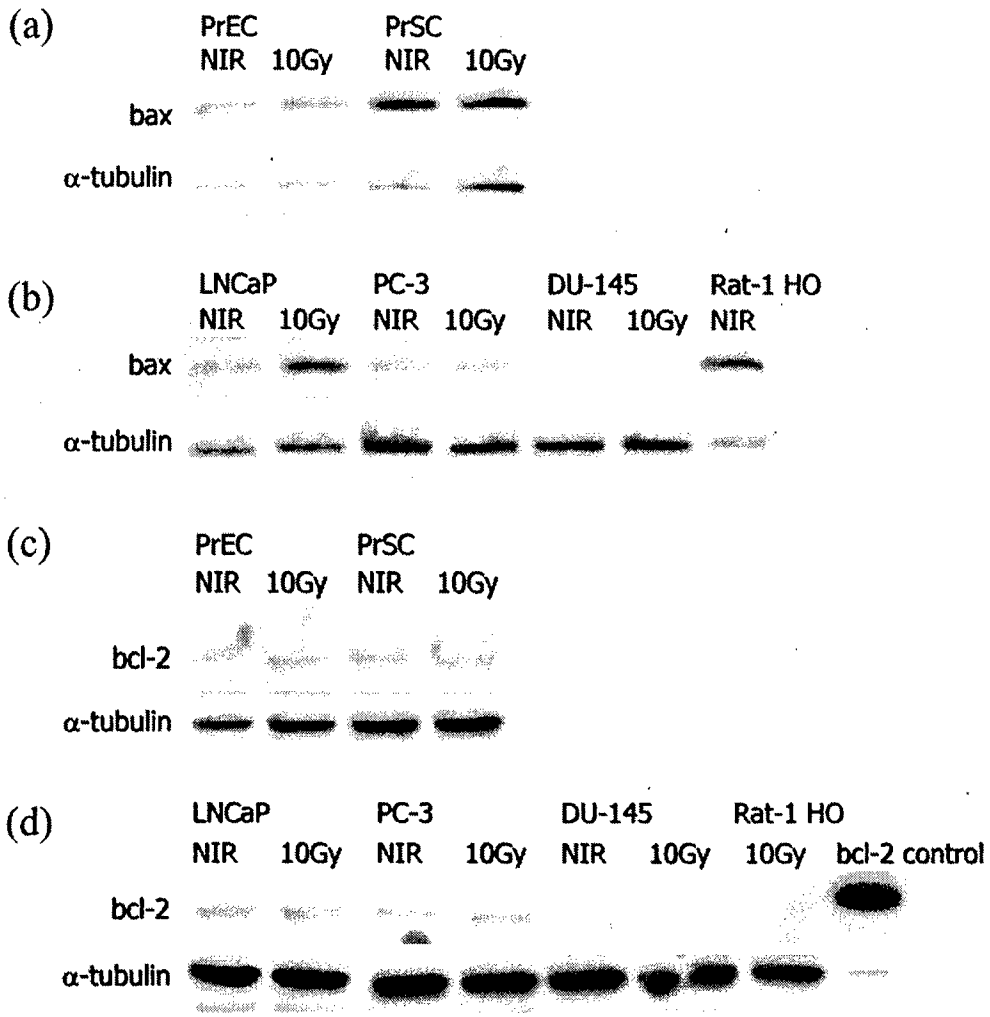

Figure 1 *Western blot analyses for apoptotic-related protein expression pre- and post-irradiation, in a panel of normal and malignant prostate cell cultures: (a) bax protein expression in normal prostate epithelial (PrEC) and stromal (PrSC) cell cultures; (b) bax protein expression in malignant prostate cell cultures (Rat-1 HO15.19 cell-lysate shown as positive control); (c) bcl-2 protein expression in normal prostate cell cultures; (d) bcl-2 protein expression in malignant prostate cell cultures (human bcl-2 transfected Rat-1 fibroblast lysate shown as positive control).*

Table 1 Apoptosis- and cell cycle-related gene expression in prostate cell cultures 24 h post-10 Gy irradiation, as compared to mock-irradiated controls

	p53	p21	bax	bcl-2	survivin
Normal					
PrEc	↑↑	↑	↔	↔	↔
PrSc	↑↑	↑↑	↔	↔	↔
Malignant					
LNCaP	↑↑	↑↑	↑↑	↔	↔
PC-3	n.d.*	Low[a]	↔	↔	↔
DU-145	↔	n.d.	n.d.	n.d.	↔

*n.d., non-detectable. [a]Low, barely detectable, no change post-XRT; ↔ less than 2-fold change; ↑ greater than 2-fold increase; ↑↑ greater than 4-fold increase (quantified using relative densitometry).

Rat-1 HO15.19 Myc-expressing control, there was no evidence for a dose-dependent increase in apoptosis in our panel of cultures (2 Gy range = 0–1%, 10 Gy range = 0–6%, 20 Gy range = 0–3%; see Figure 2c).

We observed a trend towards increased levels of apoptosis among the malignant cell lines as compared with the normal cell cultures, although these relative differences were not consistent. The data presented using the *in vitro* morphology assay was also supported by the absence of an apoptotic sub-G1[29] peak within DNA histograms of irradiated PC-3, DU-145 and LNCaP cells using flow cytometry, the lack of apoptotic morphology post-IR of the same cells as analyzed by the COMET DNA-damage assay,[32] and minimal TUNEL staining of the PC-3 cell line either *in vitro* or *in vivo* (growing as a xenograft i.m., in a nude mouse host) following irradiation (data not shown). These results suggest that cellular apoptosis is not a major mechanism of IR-induced prostate cell death under the culture and treatment conditions used in this study.

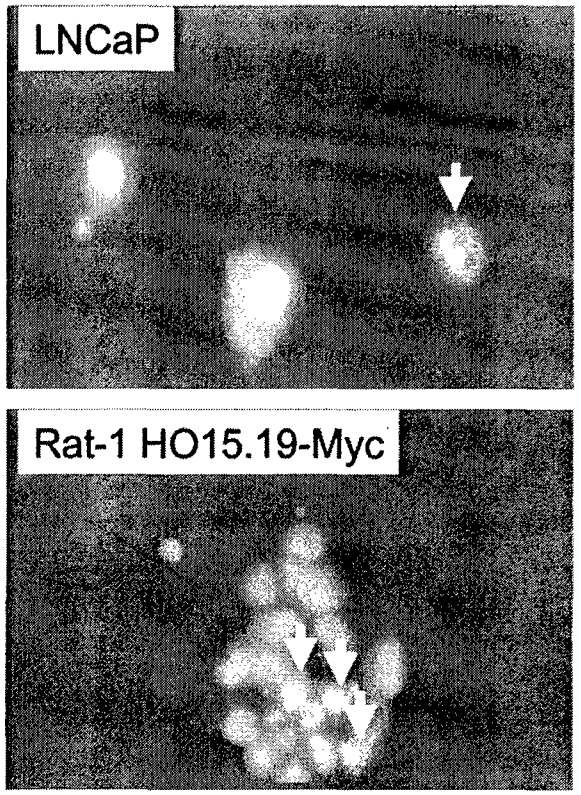

(a)

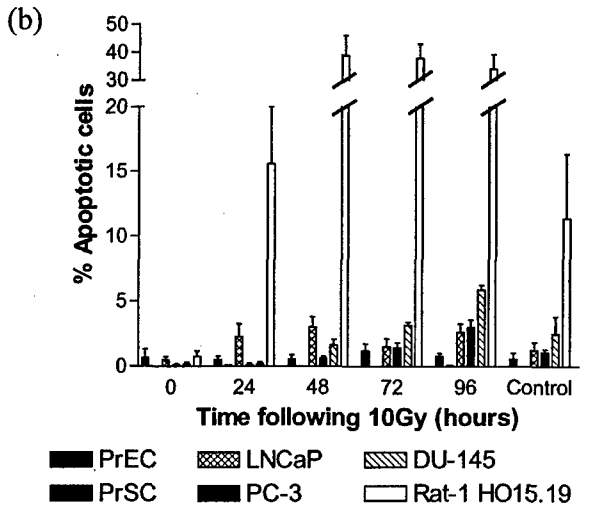

Figure 2 *IR-induced apoptosis in normal and malignant cell lines: (a) nuclear morphology of selected cell populations stained with Hoechst 33342 at 48 h following 10 Gy showing evidence of apoptotic bodies and chromatin condensation in cells denoted with white arrows: left panel, irradiated LNCaP cells; right panel, irradiated RAT-1 HO15.19 positive control cells (magnification 1000×); (b) time course of IR-induced apoptosis following a dose of 10 Gy (each bar represents the mean and s.e.m.); (c) dose-dependence of IR-induced apoptosis assayed at 48 h (error bars omitted for clarity in three-dimensional plot).*

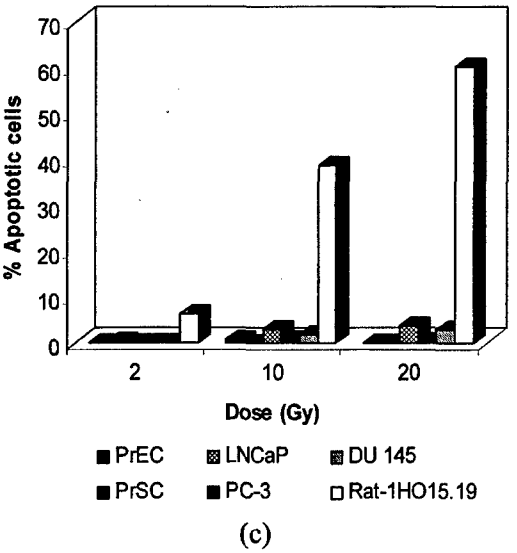

(c)

Figure 2 *(Continued).*

Molecular analysis of checkpoint control in prostate cells

The p53 status in normal and malignant cells can be functionally related to either apoptosis or a G1 and G2 cell cycle arrest or checkpoint, and dependent on cell type, level of DNA damage or cell stressor.[33,34] We therefore confirmed the presence or absence of a molecular p53-dependent G1 checkpoint in the normal and malignant prostate cells by determining the IR-induced upregulation of the cdk-inhibitory protein, $p21^{WAF1/Cip1}$. Following IR-induced DNA damage, the p53 protein is stabilized post-transcriptionally, by alternate phosphorylation of its amino terminus at serine residues 15 and 20 through both direct and indirect actions of the ATM protein. Stabilized p53 protein can then lead to a transcriptional upregulation of the $p21^{WAF1/Cip1}$ protein, which inhibits the G1 cyclin-cdk kinase complexes, and results in a G1 arrest secondary to hypo-phosphorylation of the pRB (retinoblastoma) protein. An increased level of p53 protein was observed following irradiation in all WTp53-expressing prostate cells and peaked at 2–6 h following IR-treatment (Figure 3). As expected, we observed a lack of p53 protein expression in irradiated null-p53 PC-3 cells and elevated endogenous levels of p53 protein in the MTp53-expressing DU-145 cells (consistent with a longer half-life for the MTp53 protein; Figure 3b), which were invariant post-IR. The PrEC and PrSC normal cultures both showed similar stabilization of the p53 protein relative to α-tubulin levels following irradiation. However, in the PrSC cells, the $p21^{WAF1/Cip1}$ levels were upregulated and sustained at 24 h; in the PrEC cells, the response was relatively attenuated in level and was duration reaching almost pre-irradiation levels at 24 h (Figure 3a). We failed to observe an increase in $p21^{WAF1/Cip1}$ expression in the MTp53-expressing and null-p53 cell lines (DU-145 and PC-3 respectively),[35] however the WTp53-expressing LNCaP cell line did show a strong IR-induced upregulation of $p21^{WAF1/Cip1}$.

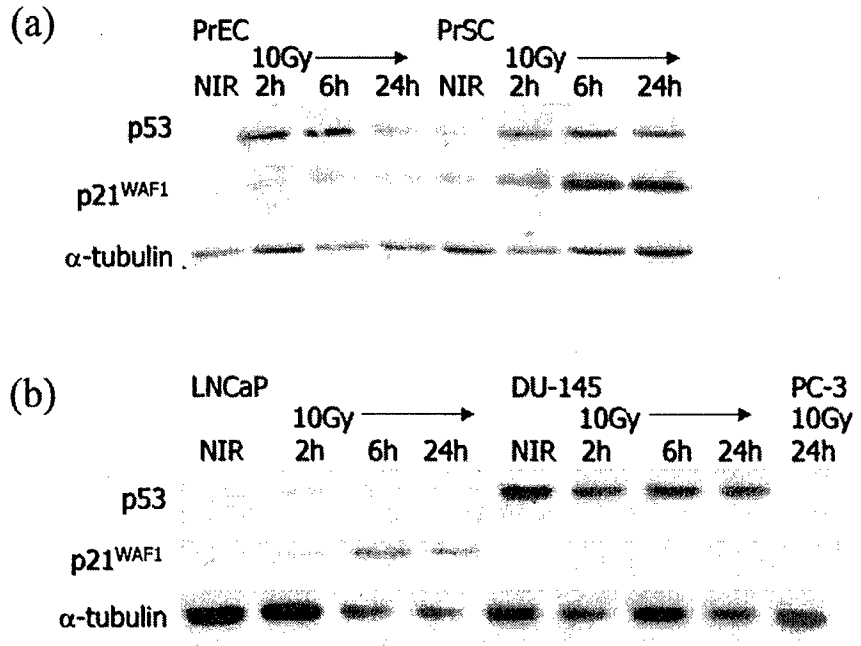

Figure 3 *Western blot analysis of p53 and p21$^{WAF1/Cip1}$ protein expression in (a) normal, and (b) malignant prostate cultures following 10 Gy irradiation.*

The p53 and p21$^{WAF1/Cip1}$ protein expression results were correlated to relative mRNA levels under similar culture conditions using RNA protection analyses in separate experiments (R Fan and RG Bristow, manuscript in preparation). These data support the idea that p53 can induce a molecular G1 checkpoint in both normal and malignant prostate epithelium, but highlights previous observations that, in certain normal epithelial cultures, p21$^{WAF1/Cip1}$ expression may be attenuated relative to stromal cultures[36] in a tissue-specific manner. This may relate to relative control of cell-cycle related checkpoint and carcinogenesis in these two tissues.[37]

SF2Gy and clonogenic survival for normal and malignant prostate cultures

Colony-formation after DNA damage measures the long-term survival of cells that are capable of unlimited proliferation and summarizes all types of IR-induced modes of cell death including apoptosis, mitotic-linked death (death after two or three aborted divisions followed by apoptosis or necrosis) and permanent growth arrest leading to necrosis.[33] Consistent with selected reports,[38,39] full clonogenic survival curves could not be generated for our LNCaP cell line, due to poor plating efficiencies, which made determination of colony-formation at doses greater than 2 Gy difficult. We encountered similar difficulties with PrEC normal epithelial cultures, which also had a poor plating efficiency (0.1–1%). Nonetheless, for all cell lines we were able to generate radiation survival data after a low, clinically relevant dose of 2 Gy (SF2), which approximates the daily fraction of radiation within curative radiation protocols. Full clonogenic survival curves following doses up to 10 Gy (a dose approximating a single-fraction palliative treatment) were derived for the PC-3, DU-145, PrSC and Rat-1 HO15.19 cell cultures and the results are plotted in Figure 4a. The SF2 values for all cell cultures are shown in Figure 4b. The normal stromal and epithelial cultures were the most radiosensitive based on SF2 values, even though they had the lowest levels of IR-induced apoptosis at similar doses. Furthermore, the apoptotic kill response in the DU-145 and Rat-1 HO Myc cell lines was quite disparate, despite similar clonogenic survival (see Figure 2b,c). We observed that the DU-145 and PC-3 cell lines with altered p53 status were more radioresistant than the WTp53-expressing LNCaP cell line. However, defined experiments with prostate cell lines that are isogenic save for p53 status are required before concluding that p53 status correlates with radiosensitivity in prostate cancer cells. In summary, we have observed that the overall level of apoptosis was not correlated to the overall level of clonogenic cell survival in our panel of cell lines. Plotting the relative cell kill following 2 and 10 Gy based on the two endpoints in Figure 4c illustrates the discrepancy between the results of two assays.

Permanent arrest in irradiated prostate cells

Given that apoptosis was not a dominant mechanism for clonogenic cell kill, we next investigated the contribution of terminal growth arrest associated with senescence-associated markers to clonogenic survival using both a representative stromal culture (PrSC cells), and a representative epithelial culture (DU-145 cells). The choice of these two cultures was predicated on the need for cell lines which would readily form colonies following flow cytometric sorting procedures at 2 and 10 Gy and to

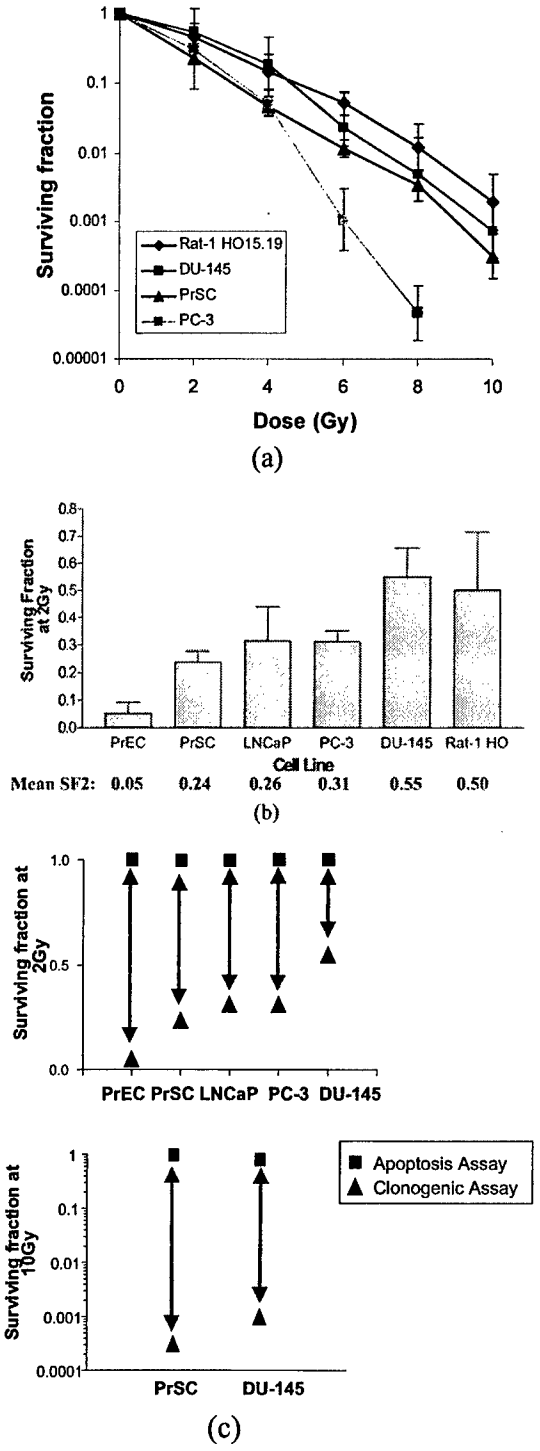

Figure 4 *Clonogenic survival data for normal and malignant prostate cultures: (a) full clonogenic radiation survival curves for PrSC, DU-145 and PC-3 and highly-apoptotic Rat-1 HO15.19 cell cultures (each point represents a geometric mean of three to five independent experiments plotted with associated geometric s.e.m.). (b) Surviving fraction following 2 Gy (SF2 values) with associated s.e.m. of normal and malignant prostate cell cultures. (c) Direct comparison of mean quantitative data for apoptotic and clonogenic kill following either 2 Gy (upper panel) or 10 Gy (lower panel).*

maximize the tissue-specific and genetic differences relating to propensity for senescence, clonogenic cell kill and G1 checkpoint control.

Using a flow cytometric assay that simultaneously determines relative levels of FL1-CFSE fluorescence (ie proliferation) and SSC-parameter (cell granularity), we determined that up to 87% of the PrSC population was non-proliferating with an associated increased granularity ($FL1(CFSE)^{hi}SSC^{hi}$) at 5 days, following a dose 10 Gy of radiation. In similarly plated cultures, only 14 and 8% showed the same cytometric profile in 2 Gy-treated or control cultures; these relative proportions being consistent over two or three representative experiments (Figure 5a, c). By comparison, only 32% of DU-145 cells had a senescent-like cytometric profile, although upon closer inspection the data suggest that the vast majority (ie greater than 70%) of DU-145 cells were actually non-proliferating, but that these cells were inconsistently associated with increased granularity when compared with stromal PrSC cells (compare CFSE-fluorescence axis in both cell lines following 10 Gy in Figure 5). The $FL1(CFSE)^{hi}SSC^{hi}$ cytometric profile was determined for 5% of DU-145 cells following 2 Gy and 3% in the untreated DU-145 population (Figure 5a, b; note that cells not growth-arrested following 2 Gy or in non-irradiated cultures may have undergone multiple rounds of division by this point differentially increasing the total 'proliferating' population). We then sorted and plated cells from the senescent-like, non-proliferating population relative to the remaining cells and observed that relative colony forming ability (plating efficiency) was decreased in the $FL1(CFSE)^{hi}SSC^{hi}$ ('non-proliferating'), SLP population in a dose-responsive manner (see Table 2).

In normal fibroblasts (ie stromal cells), cells undergo decreasing proliferative potential with increasing passage *in vitro*, until finally undergoing senescence associated with increased granularity, positive SA β-gal staining and upregulation of the $p21^{WAF1/Cip1}$ and $p16^{INK4a}$ proteins. Similar changes occur in normal fibroblast cultures when exposed to IR and has been referred to as a 'premature IR-induced senescence'.[40–42] Although we observed greater SA β-gal staining intensity in an increased number of PrSC stromal cells following a dose of 10 Gy (see Figure 6a), we found the endpoint to be highly variable across all cell lines and difficult to quantitate in epithelial cells (further data not shown; noted by others[43]). Whether upregulation of one or both genes is absolutely required for senescence and whether the process is p53-dependent in all cell types remains controversial.

In order to determine whether similar gene expression changes occurred in PrSC and DU-145 cells, we performed western blot analyses of cell populations obtained in parallel with flow cytometric experiments at day 5. These analyses showed high, IR-invariant levels of $p16^{INK4a}$ protein in both PrSC and DU-145 cultures and a dose-dependent increase in $p21^{WAF1/Cip1}$ levels in PrSC cells only (Figure 6b; confirmed using densitometry). We also analyzed $p16^{INK4a}$ expression in all of the cell cultures at 24 h following 10 Gy. In this case, levels of $p16^{INK4a}$ were either invariant (PrEC, LNCaP, DU-145) or undetectable (PrSC, PC-3) as confirmed by relative densitometry (data not shown). Long-term (up to 9 days) analysis of $p16^{INK4a}$ expression post-10 Gy irradiation DU-145 and PrSC demonstrated increasing

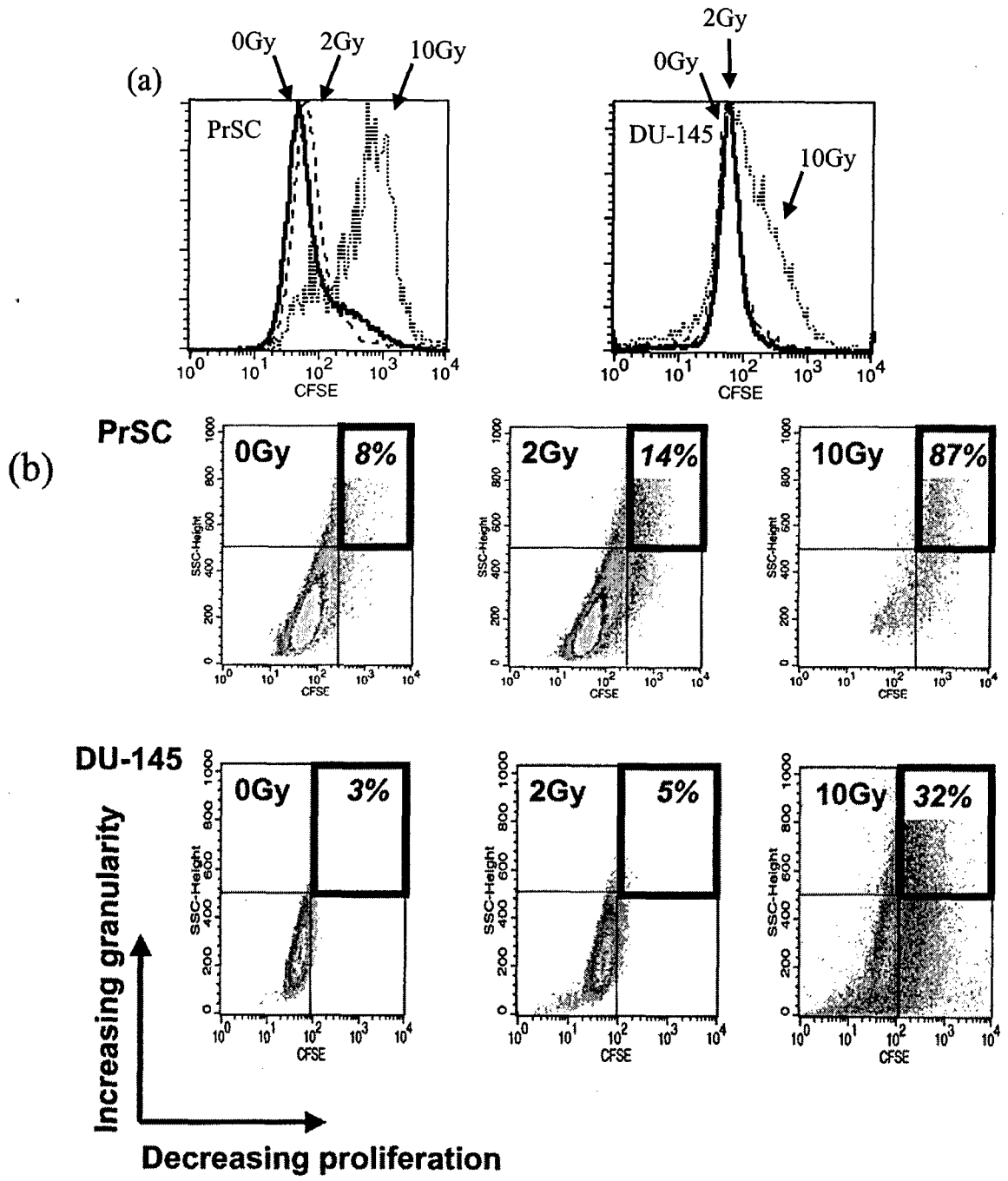

Figure 5 *Frequency histogram of FL1 fluorescence parameter (ie CFSE vital dye fluorescence) for (a) PrSC (left) and DU-145 (right) at 5 days post-irradiation following doses of 0 (control, mock-irradiated), 2 and 10 Gy. Shown is a representative experiment with total cell population analyzed for each dose. (b) Two-dimensional plots of FL1(CFSE) fluorescence intensity vs SSC (side scatter-granularity) for total cell numbers in mock irradiated and irradiated flasks of cells (see text for details) for PrSC (top) and DU-145 (bottom). Note increasing FL1(CFSE)^{hi} SSC^{hi} fractional sub-population (representing a senescent-like phenotype) with increasing dose; similar cytometric data was observed in all replicate experiments. These populations as shown were sorted using flow cytometry to determine relative colony forming ability as tabulated in Table 2.*

expression with time (data not shown), suggesting a time-dependent, though not dose-dependent, expression of p16^{INK4a}. We conclude that cells within a terminally arrested population that have increased cellular granularity (SLP) are incapable of forming colonies and that the sub-population of proliferating cells without associated increased granularity defines the colony-forming potential of the entire irradiated culture.

Table 2 Relative colony forming ability within FL1(CFSE)^{hi}SSC^{hi} (non-proliferating) and proliferating populations, as sorted by flow cytometry at day 5 post-irradiation

Cell type	Dose (Gy)	Number of cells plated	Plating efficiency (proliferating)	Plating efficiency (non-proliferating)
PrSC	0	100	0.33 ± 0.34[a]	0.03 ± 0.02
	2	1000	0.06 ± 0.03	0.01 ± 0.01
	10	1000	0.00 ± 0.00	0.00 ± 0.00
DU-145	0	100	0.41 ± 0.35	0.15 ± 0.14
	2	1000	0.22 ± 0.17	0.01 ± 0.01
	10	1000	0.01 ± 0.00	0.00 ± 0.00

[a]Mean values and associated s.e.m.

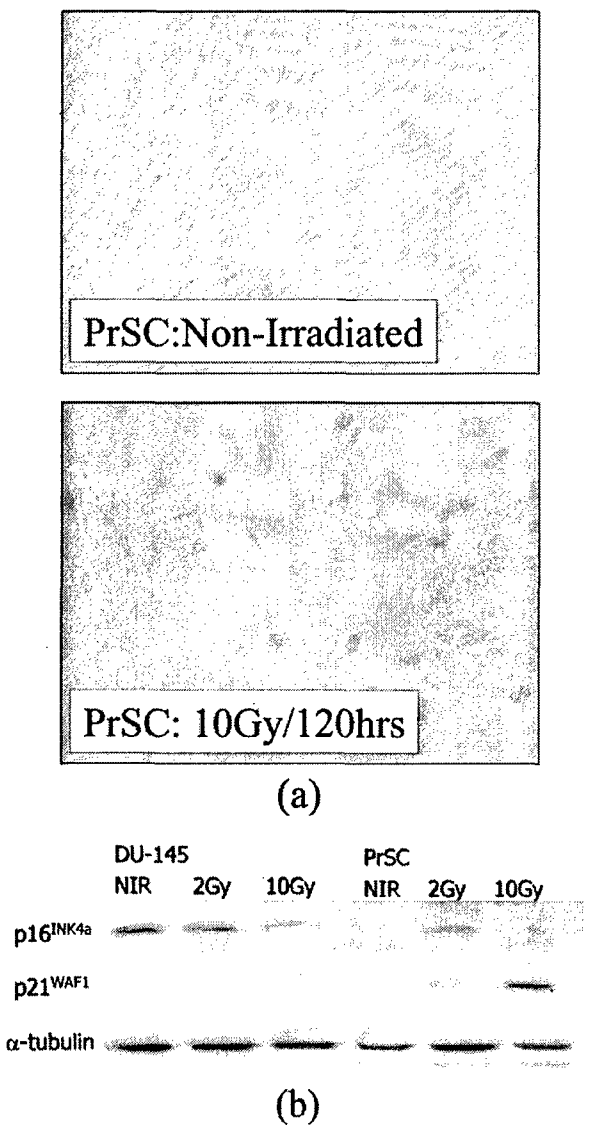

Figure 6 *Senescent biomarkers in prostate cell populations: (a) example of negative (left) and positive (right) SA β-gal staining in non-irradiated and irradiated PrSC cultures respectively, at 120 h following a dose of 10 Gy; (b) western blot analysis of p16^{INK4a} and p21$^{WAF1/Cip1}$ protein expression in entire PrSC and DU-145 cultures at day 5 following irradiation.*

Discussion

This is the first report, to our knowledge, documenting the relative role of apoptosis and terminal growth arrest as factors in determining overall clonogenic radiation cell survival for a panel of normal and malignant prostate cell cultures within the same laboratory setting. Using clinically relevant radiation doses, we observed a strong molecular apoptotic response in certain cell lines (bax and p53 upregulation in LNCaP cells, post-IR), yet this response did not correlate with quantitative determinations of apoptosis using morphology endpoints. The apoptotic response was not dose-responsive and did not correlate with final clonogenic cell kill. Further support for our data are the observations that manipulation of the ceramide-sphingomyelin and bcl-2-associated apoptotic pathways, or androgen ablation, can increase the apoptotic responses of prostate cells without altering final clonogenic radiation survival (K Shim and RG Bristow, unpublished observation[22,23,44]). Many groups have indicated that apoptosis may be the primary mode of death following gamma-irradiation only in specific cell types such as hematopoetic or lymphocytic cells, but not in stromal- or epithelial-derived tissues.[16,44–47] Furthermore, many attempts to alter apoptotic indices in epithelial- and stromal-derived tissues have failed to affect clonogenic survival. This suggests that, although the apoptotic pathway is intact in malignant prostate cells, other death mechanisms may override this response following irradiation.

It has been suggested that epithelial cell G1 checkpoint may be abrogated or less efficient than that of its stromal counterpart, despite wild-type p53 status. Girinski *et al*[36] found an abrogated p21$^{WAF1/Cip1}$ induction and G1 checkpoint in a panel of normal prostate epithelial cells as compared to a panel of normal prostate stromal cells following ionizing radiation. Meyer *et al*[48] reported similar findings for mammary epithelial *vs* stromal tissues. Within the same group, Romonov *et al*[49] observed an abrogated response to replicative crisis in the mammary epithelial cells suggesting a global defect in epithelial response to stress in comparison to its stromal counterpart. Our own experiments illustrated that, even for similar levels of p53 induction/stabilization, the p21$^{WAF1/Cip1}$ response in PrEC is greatly attenuated in comparison to its stromal counterpart. While the p53/p21$^{WAF1/Cip1}$ responses for our panel of malignant cell lines were as previously reported, the LNCaP cell line's

strong $p21^{WAF1/Cip1}$ induction is still surprising in light of its epithelial nature. Girinski *et al*[36] suggested that epithelial cell response might be partially dependant on interactions with surrounding stromal tissues.[37,50,51] LNCaP cells may have altered characteristics such that it does not require this interaction for a strong $p21^{WAF1/Cip1}$ induction following irradiation. Furthermore, studying G1 arrest alone may not be sufficient, since cells lacking a functional G1 checkpoint can exhibit a G2 delay that may be linked to DNA repair[52] and cellular survival following radiation.[53] Indeed, although our results suggest increased survival for cells which lack the G1 checkpoint, defined studies in isogenic tissue culture or solid tumor models which differ in p53 status and specific G1, S and G2 checkpoint control experiments are required to prove this hypothesis, and are part of a current research program.[11]

The success or failure of radical radiotherapy depends on the daily proportionate killing of tumor clonogens, which make up less than 1% of the total population of cells within a tumor. For example, it has been estimated that each gram of tumor contains approximately 1×10^9 tumor cells, with approximately less than 1×10^7 cells having clonogenic capacity. To date, no formal test or data exists for the pre-treatment determination of the number of clonogens existing prior to prostate radiotherapy. One can estimate that for a radiotherapy protocol using 35–40 fractions of 2 Gy, the clonogenic SF2 value should be less than 0.60 (ie death after 35 treatments $= 0.6^{35} = 1.7 \times 10^{-8}$) to cure a 1 g tumor, assuming equal killing per radiotherapy fraction.[4] Our data suggests that the SF2 *in vitro* is less than 0.6 for the cell lines tested. However, the effective SF2 may be higher *in vivo*, due to cell–cell interactions, hypoxia, altered gene expression or cell cycle phase during irradiation[3] and the relative importance of these factors remains to be determined in radiotherapy cohorts. Our observed *in vitro* radiosensitivity of normal epithelial and stromal cultures *in vitro* may explain the observation of glandular atrophy, fibrosis and decreased glandular function observed in prostate glands following irradiation. Exquisite sensitivity of normal epithelial cells may also explain why final post-therapy nadir PSA values in patients who achieve local control are lower than the PSA values in men without a diagnosis of prostate cancer, reflecting residual normal gland function after IR-induced cell kill.[54]

In our experiments, relative clonogenic cell kill was approximated by quantitative endpoints of a dose-responsive terminal growth arrest, in which certain cells acquired a senescent-like phenotype. Terminal growth arrest, rather than apoptosis, may begin to explain the slow kinetics of decreasing PSA values following radiotherapy over 12–16 months following treatment.[2] Recent experiments by Pollack and colleagues[23,55] are consistent with our data, as the supra-additive radioresponses observed in LNCaP and Dunning rat R3327-G tumor models following combined androgen withdrawal and fractionated radiation (mimicking clinical stage T3-T4 prostate cancer treatment protocols which increase overall patient survival).[56] were secondary to factors which determined post-treatment cellular growth arrest rather than apoptosis.

If a surrogate measure of radiation sensitivity was developed to use prior to, or early during, the course of radiotherapy, specific measures could be used to increase radiocurability or abort radiotherapy altogether in favor of radical prostatectomy (if medically feasible). Crook *et al*[57] found that markers of proliferation (PCNA, MIB-1) in post-radiotherapy biopsies from 498 men were an independent indicator of treatment failure, but indeterminate biopsies do occur which complicate interpretation as to whether viable clonogenic cells remain 2–2.5 y following radical radiotherapy. Our data suggests that other surrogate predictive factors might include molecular or cellular senescence or cell cycle arrest factors, such as the cdk inhibitors, $p21^{WAF}$ or $p16^{INK4a}$ that are activated by DNA damage and lead to altered proliferation and terminal growth arrest.

At present, no predictive test can determine which cells in the tumor are prostate clonogens rather than non-clonogens, however we believe that terminal growth arrest should be further investigated as a major mechanism of cell death in addition to apoptosis, in protocols that utilize radiotherapy. If proven to be important in prostate cancer, the former mechanism of cell death might be augmented *in vivo* using radiotherapy in conjunction with inhibitors of prostate cancer cell proliferation such as retinoic acid, antisense to cdk inhibitors, inhibitors of telomerase, or inhibitors of histone deactylase (HDAC).[58,59] Indeed these agents are currently being prospectively tested as single agents or in combination with chemotherapy in phase I/II trials; our results suggest further studies of the efficacy of these agents in combination with radiation as a novel prostate treatment strategy are necessary.

Acknowledgements

The authors would like to thank Dr L Chung for donating our LNCaP cell line, and Dr L Penn and E Soucie for the Rat-1 HO15.19 cell line. Special thanks to S Al Rashid, C Cantin, and F Jalali for help in selected assays and guidance. These studies were supported by the National Cancer Institute of Canada, the Princess Margaret Hospital Foundation and the US Army DOD Prostate Research Program.

References

1 Lukka H *et al*. Controversies in prostate cancer radiotherapy: consensus development. *Can J Urol* 2001; **8**: 1314–1322.
2 Dearnaley DP. Radiotherapy and combined modality approaches in localised prostate cancer. *Eur J Cancer* 2001; **37**: S137–145.
3 Bristow RG, Hill P. Molecular and cellular basis of radiotherapy In: Tannock IF and Hill RP (eds). *The Basic Science of Oncology*. McGraw-Hill: Toronto, 1998, pp 295–321.
4 Wong CS, Hill RP. Experimental Radiotherapy In: Tannock IF and Hill RP (eds). *The Basic Science of Oncology*, 3rd edn. McGraw-Hill: Toronto, 1998, pp 322–349.
5 Sandford NL, Searle JW, Kerr JF. Successive waves of apoptosis in the rat prostate alter repeated withdrawal of testosterone stimulation. *Pathology* 1984; **16**: 400–410.
6 Kyprianou N, Issacs JT. Expression of transforming growth factor-beta in rat ventral prostate during castration-induced programmed cell death. *Mol Endocrinol* 1989; **3**: 1515–1522.
7 Bruckheimer EM *et al*. The impact of bcl-2 expression and bax deficiency on prostate homeostasis *in vivo*. *Oncogene* 2000; **19**: 2404–2412.
8 Westin P, Stattin P, Damber JE, Bergh A. Castration therapy rapidly induces apoptosis in a minority and decreases cell proliferation in a majority of human prostatic tumors. *Am J Pathol* 1995; **146**: 1368–1375.

9 Rakozy C *et al.* Expression of bcl-2, p53, and p21 in benign and malignant prostatic tissue before and after radiation therapy. *Mod Pathol* 1998; **11**: 892–899.
10 Grossfeld GD *et al.* Locally recurrent prostate tumors following either radiation therapy or radical prostatectomy have changes in Ki-67 labeling index, p53 and bcl-2 immunoreactivity. *J Urol* 1998; **159**: 1437–1443.
11 Bristow RG, Benchimol S, Hill RP. The p53 gene as a modifier of intrinsic radiosensitivity: implications for radiotherapy. *Radiother Oncol* 1996; **40**: 197–223.
12 Bristow RG, Benchimol S, Hill R. p53 protein expression or protein function? *Int J Radiat Oncol Biol Phys* 1996; **35**: 1123–1125.
13 Dewey WC, Ling CC, Meyn RE. Radiation-induced apoptosis: relevance to radiotherapy. *Int J Radiat Oncol Biol Phys* 1995; **33**: 781–796.
14 Olive PL, Vikse CM, Vanderbyl S. Increase in the fraction of necrotic, not apoptotic, cells in SiHa xenograft tumours shortly after irradiation. *Radiother Oncol* 1999; **50**: 113–119.
15 Stephens LC *et al.* Development of apoptosis in irradiated murine tumors as a function of time and dose. *Radiat Res* 1993; **135**: 75–80.
16 Tannock IF, Lee C. Evidence against apoptosis as a major mechanism for reproductive cell death following treatment of cell lines with anti-cancer drugs. *Br J Cancer* 2001; **84**: 100–105.
17 Schwarze SR *et al.* Role of cyclin-dependent kinase inhibitors in the growth arrest at senescence in human prostate epithelial and uroepithelial cells. *Oncogene* 2001; **20**: 8184–8192.
18 Stein GH, Drullinger LF, Soulard A, Dulic V. Differential roles for cyclin-dependent kinase inhibitors p21 and p16 in the mechanisms of senescence and differentiation in human fibroblasts. *Mol Cell Biol* 1999; **19**: 2109–2117.
19 Chang BD *et al.* A senescence-like phenotype distinguishes tumor cells that undergo terminal proliferation arrest after exposure to anticancer agents. *Cancer Res* 1999; **59**: 3761–3767.
20 Lyons AB, Hasbold J, Hodgkin PD. Flow cytometric analysis of cell division history using dilution of carboxyfluorescein diacetate succinimidyl ester, a stably integrated fluorescent probe. *Meth Cell Biol* 2001; **63**: 375–398.
21 Soucie EL *et al.* Myc protentiates apoptosis by stimulating Bax activity at the mitochondria. *Mol Cell Biol* 2001; **21**: 4725–4736.
22 Garzotto M *et al.* Reversal of radiation resistance in LNCaP cells by targeting apoptosis through ceramide synthase. *Cancer Res* 1999; **59**: 5194–5201.
23 Pollack A *et al.* Lack of prostate cancer radiosensitization by androgen deprivation. *Int J Radiat Oncol Biol Phys* 2001; **51**: 1002–1007.
24 Bristow RG *et al.* Radioresistant MTp53-expressing rat embryo cell transformants exhibit increased DNA-dsb rejoining during exposure to ionizing radiation. *Oncogene* 1998; **16**: 1789–1802.
25 Lee ST *et al.* Bcl-2 targeted to the endoplasmic reticulum can inhibit apoptosis induced by Myc but not etoposide in Rat-1 fibroblasts. *Oncogene* 1999; **18**: 3520–3528.
26 Kurts C *et al.* Class I-restricted cross-presentation of exogenous self-antigens leads to deletion of autoreactive CD8(+) T cells. *J Exp Med* 1997; **186**: 239–245.
27 Altieri DC. The molecular basis and potential role of survivin in cancer diagnosis and therapy. *Trends Mol Med* 2001; **7**: 542–547.
28 Ambrosini G, Adida C, Altieri DC. A novel anti-apoptosis gene, survivin, expressed in cancer and lymphoma. *Nat Med* 1997; **3**: 917–921.
29 Slingerland JM, Tannock IF. Cell proliferation and cell death In: Tannock IF, Hill RP. (eds). *The Basic Science of Oncology*, 3rd ed. McGraw-Hill: Toronto, 1998, pp 134–165.
30 Kaufmann SH *et al.* Specific proteolytic cleavage of poly(ADP-ribose) polymerase: an early marker of chemotherapy-induced apoptosis. *Cancer Res* 1993; **53**: 3976–3985.
31 Winter RN, Kramer A, Borkowski A, Kyprianou N. Loss of caspase-1 and caspase-3 protein expression in human prostate cancer. *Cancer Res* 2001; **61**: 1227–1232.
32 Olive PL. DNA damage and repair in individual cells: applications of the comet assay in radiobiology. *Int J Radiat Biol* 1999; **75**: 395–405.
33 Wahl GM, Carr AM. The evolution of diverse biological responses to DNA damage: insights from yeast and p53. *Nat Cell Biol* 2001; **3**: E277–286.
34 Giaccia AJ, Kastan MB. The complexity of p53 modulation: emerging patterns from divergent signals. *Genes Dev* 1998; **12**: 2973–2983.
35 Carroll AG, Voeller HJ, Sugars L, Gelmann EP. p53 oncogene mutations in three human prostate cancer cell lines. *Prostate* 1993; **23**: 123–134.
36 Girinsky T *et al.* Attenuated response of p53 and p21 in primary cultures of human prostatic epithelial cells exposed to DNA-damaging agents. *Cancer Res* 1995; **55**: 3726–3731.
37 Krtolica A *et al.* Senescent fibroblasts promote epithelial cell growth and tumorigenesis: a link between cancer and aging. *Proc Natl Acad Sci USA* 2001; **98**: 12072–12077.
38 Leith JT. *In vitro* radiation sensitivity of the LNCaP prostatic tumor cell line. *Prostate* 1994; **24**: 119–124.
39 DeWeese TL, Shipman JM, Dillehay LE, Nelson WG. Sensitivity of human prostatic carcinoma cell lines to low dose rate radiation exposure. *J Urol* 1998; **159**: 591–598.
40 Suzuki K *et al.* Radiation-induced senescence-like growth arrest requires TP53 function but not telomere shortening. *Radiat Res* 2001; **155**: 248–253.
41 Rave-Frank M *et al. In vitro* response of human dermal fibroblasts to X-irradiation: relationship between radiation-induced clonogenic cell death, chromosome aberrations and markers of proliferative senescence or differentiation. *Int J Radiat Biol* 2001; **77**: 1163–1174.
42 Kamijo T *et al.* Loss of the ARF tumor suppressor reverses premature replicative arrest but not radiation hypersensitivity arising from disabled atm function. *Cancer Res* 1999; **59**: 2464–2469.
43 Chang BD *et al.* Molecular determinants of terminal growth arrest induced in tumor cells by a chemotherapeutic agent. *Proc Natl Acad Sci USA* 2002; **99**: 389–394.
44 Kyprianou N, King ED, Bradbury D, Rhee JG. bcl-2 overexpression delays radiation-induced apoptosis without affecting the clonogenic survival of human prostate cancer cells. *Int J Cancer* 1997; **70**: 341–348.
45 Sheridan MT, West CM. Ability to undergo apoptosis does not correlate with the intrinsic radiosensitivity (SF2) of human cervix tumor cell lines. *Int J Radiat Oncol Biol Phys* 2001; **50**: 503–509.
46 Lock RB, Stribinskiene L. Dual modes of death induced by etoposide in human epithelial tumor cells allow Bc1-2 to inhibit apoptosis without affecting clonogenic survival. *Cancer Res* 1996; **56**: 4006–4012.
47 Aldridge DR, Arends MJ, Radford IR. Increasing the susceptibility of the rat 208F fibroblast cell line to radiation-induced apoptosis does not alter its clonogenic survival dose-response. *Br J Cancer* 1995; **71**: 571–577.
48 Meyer KM, Hess SM, Tlsty TD, Leadon SA. Human mammary epithelial cells exhibit a differential p53-mediated response following exposure to ionizing radiation or UV light. *Oncogene* 1999; **18**: 5795–5805.
49 Romanov SR *et al.* Normal human mammary epithelial cells spontaneously escape senescence and acquire genomic changes. *Nature* 2001; **409**: 633–637.
50 Kabalin JN, Peehl DM, Stamey TA. Clonal growth of human prostatic epithelial cells is stimulated by fibroblasts. *Prostate* 1989; **14**: 251–263.
51 Camps JL *et al.* Fibroblast-mediated acceleration of human epithelial tumor growth *in vivo*. *Proc Natl Acad Sci USA* 1990; **87**: 75–79.
52 Kao GD, McKenna WG, Yen TJ. Detection of repair activity during the DNA damage-induced G2 delay in human cancer cells. *Oncogene* 2001; **20**: 3486–3496.
53 Hwang A, Muschel RJ. Radiation and the G2 phase of the cell cycle. *Radiat Res* 1998; **150**: S52–59.
54 Gaudin PB *et al.* Histopathologic effects of three-dimensional conformal external beam radiation therapy on benign and malignant prostate tissues. *Am J Surg Pathol* 1999; **23**: 1021–1031.
55 Pollack A *et al.* The early supra-additive apoptotic response of R3327-G prostate tumors to androgen ablation and radiation is not sustained with multiple fractions. *Int J Radiat Oncol Biol Phys* 2000; **46**: 153–158.

56 Bolla, M *et al*. Improved survival in patients with locally advanced prostate cancer treated with radiotherapy and goserelin. *New Engl J Med* 1997; **337**: 295–300.
57 Crook J *et al*. Postradiotherapy prostate biopsies: what do they really mean? Results for 498 patients. *Int J Radiat Oncol Biol Phys* 2000; **48**: 355–367.
58 Suenaga M *et al*. Histone deacetylase inhibitors suppress telomerase reverse transcriptase mRNA expression in prostate cancer cells. *Int J Cancer* 2002; **97**: 621–625.
59 Marks PA, Rifkind RA, Richon VM, Breslow R. Inhibitors of histone deacetylase are potentially effective anticancer agents. *Clin Cancer Res* 2001; **7**: 759–760.

[CANCER RESEARCH 64, 8526–8533, December 1, 2004]

Defective DNA Strand Break Repair after DNA Damage in Prostate Cancer Cells: Implications for Genetic Instability and Prostate Cancer Progression

Rong Fan,[1] Tirukalikundram S. Kumaravel,[1] Farid Jalali,[1] Paula Marrano,[1] Jeremy A. Squire,[1,3,4] and Robert G. Bristow[1,2,4]

[1]Ontario Cancer Institute/Princess Margaret Hospital, University Health Network; and Departments of [2]Radiation Oncology, [3]Pathology, and [4]Medical Biophysics, University of Toronto, Toronto, Ontario, Canada

ABSTRACT

Together with cell cycle checkpoint control, DNA repair plays a pivotal role in protecting the genome from endogenous and exogenous DNA damage. Although increased genetic instability has been associated with prostate cancer progression, the relative role of DNA double-strand break repair in malignant *versus* normal prostate epithelial cells is not known. In this study, we determined the RNA and protein expression of a series of DNA double-strand break repair genes in both normal (PrEC-epithelial and PrSC-stromal) and malignant (LNCaP, DU-145, and PC-3) prostate cultures. Expression of genes downstream of *ATM* after ionizing radiation-induced DNA damage reflected the p53 status of the cell lines. In the malignant prostate cell lines, mRNA and protein levels of the *Rad51, Xrcc3, Rad52,* and *Rad54* genes involved in homologous recombination were elevated ~2- to 5-fold in comparison to normal PrEC cells. The XRCC1, DNA polymerase-β and -δ proteins were also elevated. There were no consistent differences in gene expression relating to the nonhomologous end-joining pathway. Despite increased expression of DNA repair genes, malignant prostate cancer cells had defective repair of DNA breaks, alkali-labile sites, and oxidative base damage. Furthermore, after ionizing radiation and mitomycin C treatment, chromosomal aberration assays confirmed that malignant prostate cells had defective DNA repair. This discordance between expression and function of DNA repair genes in malignant prostate cancer cells supports the hypothesis that prostate tumor progression may reflect aberrant DNA repair. Our findings support the development of novel treatment strategies designed to reinstate normal DNA repair in prostate cancer cells.

INTRODUCTION

The genetic determinants of prostate tumor progression are still poorly understood (1). However, numerous models of prostate carcinogenesis suggest that increasing chromosomal instability with the acquisition of mutations and chromosomal aberrations drives progression from preneoplasia to neoplasia (2). Furthermore, increased levels of chromosomal aberrations can be associated with decreased telomere length in high-grade prostatic intraepithelial neoplasia, and acquired centrosome dysfunction is associated with prostate cancer progression and dissemination (3, 4). Human cells have therefore evolved complex signaling responses to both endogenous and exogenous DNA damage to preserve genomic integrity. Tumor progression in a number of epithelial malignancies has been associated with the sequential loss of function of genes that normally protect against DNA damage. For example, in response to DNA double-strand breaks, the ATM (ataxia telangiectasia mutated) protein is activated and stabilizes the p53 tumor suppressor protein. This leads to the up-regulation of *p53*-dependent genes (*e.g., p21WAF, Bax,* and *Gadd45*) and post-translational modifications of the CHK2, BRCA1, and NBS1 proteins. These act together to induce G_1, S, and G_2 cell cycle arrest; DNA repair; and/or activation of cell death pathways (e.g., apoptosis, mitotic catastrophe, or terminal growth arrest) depending on the cellular context (5–7).

Defective DNA repair as a determinant of prostate cancer progression has not been extensively studied. Several groups have observed defective mismatch-repair in prostate cancer cell lines (8, 9). Other data support DNA polymorphisms in the *Xrcc1, Ogg1,* and DNA polymerase-β genes (involved in base excision repair or DNA single-strand break repair) as risk factors for prostate cancer (8, 10, 11). However, data are lacking concerning the homologous recombination and nonhomologous recombination (*i.e.,* end-joining) pathways, which are involved in the repair of DNA double-strand breaks.

Nonhomologous end-joining repair requires little or no homology on the ends of the strands being joined and involves two main discrete repair protein complexes (1): the DNA-PK/XRCC4/LigIV complex and (2) the MRE11/RAD50 complex (12). In homologous recombination, extensive homology is required between the region of the DNA double-strand break and the sister chromatid or homologous chromosome from which repair is directed. Homologous recombination involves the BRCA2, RAD51, RAD52, RAD54, RAD55–57, and RPA proteins and the RAD51 paralogs, XRCC2/3 and RAD51B/C/D. The homologous recombination pathway predominates in the late S/G_2 phases of the cell cycle and provides relatively error-free repair. In contrast, the nonhomologous end-joining pathway predominates in the G_1 phase of the cell cycle (13). Recent data suggest an interplay between the two pathways dependent on cell type and initial *versus* late times after induction of DNA double-strand breaks (11). Cells defective for either homologous recombination or nonhomologous end-joining show increased rates of mutagenesis and chromosomal instability, which could relate to the propensity for acquired genetic instability during prostate carcinogenesis and tumor progression. Consistent with a possible role for DNA double-strand break repair in prostate cancer progression, *BRCA1* and *BRCA2* mutations are associated with an increased risk of prostate cancer and development of an aggressive disease course (2, 13–15).

Our laboratory has shown previously that normal and malignant prostate cells preferentially respond to DNA damage by undergoing terminal growth arrest rather than apoptosis (16). This may allow for attempted DNA repair during cell cycle arrests as a response to DNA damage. However, in malignant cells with aberrant cell cycle checkpoint control, defective DNA double-strand break repair could increase genetic instability as part of a "mutator" phenotype (17). We hypothesized that one of the critical steps in prostate tumor progression may be the loss of the normal repair response to DNA damage and that specific defects in DNA double-strand break repair would be associated with prostate malignancy.

Herein, we show that malignant prostate cancer cells have increased

Received 5/10/04; revised 8/17/04; accepted 9/28/04.

Grant support: United States Army Department of Defense Prostate Program [DAMD17-01-1-0110 (A-10308)], Canadian Foundation for Innovation, and the G.H. Woods and PMH Foundations (R. G. Bristow).

The costs of publication of this article were defrayed in part by the payment of page charges. This article must therefore be hereby marked *advertisement* in accordance with 18 U.S.C. Section 1734 solely to indicate this fact.

Note: R. Fan and T. S. Kumaravel contributed equally to this work; T. S. Kumaravel is currently at the Genetic and Molecular Toxicology, Covance Labs Limited, Otley Road, Harrogate HG3 2XQ, United Kingdom. Supplementary data for this article can be found at Cancer Research Online (http://cancerres.aacrjournals.org).

Requests for reprints: Robert G. Bristow, Radiation Medicine Program, Princess Margaret Hospital (UHN), 610 University Avenue, Room 5-923, Toronto, Ontario, Canada M5G2M9. Phone: 416-946-2129; Fax: 416-946-4586; E-mail: rob.bristow@rmp.uhn.on.ca.

expression of homologous recombination-related and base excision repair-related genes independent of *p53* status, G_1 cell cycle checkpoint control, and relative cell proliferation. However, despite expressing high levels of DNA repair proteins, malignant cells have a decreased capacity for DNA double-strand break, DNA single-strand break, and base excision repair and acquire discrete chromosomal aberrations after exposure to DNA-damaging agents. Our findings support inappropriate DNA repair as a potential determinant of prostate cancer progression.

MATERIALS AND METHODS

Prostate Cell Cultures and DNA-Damaging Treatments. All of the cell cultures were incubated in vented tissue culture flasks under 5% CO_2 and 37°C culture conditions as described previously (16). LNCaP cells were maintained in T-media (Life Technologies, Inc., Gaithersburg, MD) and supplemented with 10% fetal calf serum. PC-3 and DU-145 cells were purchased from American Type Culture collection (Manassas, VA) and supplemented with 10% fetal calf serum in Ham's F12K or α-Modified Eagles Medium, respectively. PrEC (normal prostate epithelial cells) and PrSC (normal prostate stromal cells) were purchased from Clonetics Corporation (San Diego, CA) and maintained using suggested PrEGM and SCGM medium, respectively. The latter cell cultures have limited proliferative potential in culture and decrease in proliferation after passages 5 to 8 from frozen stock. Approximate doubling times for cell cultures under these conditions were as follows: PrEC, 48 to 72 hours; PrSC, 18 hours; LNCaP, 36 hours; PC-3, 24 hours; and DU-145, 18 hours (16).

Asynchronous cultures were irradiated, or treated with mitomycin C, at 16 to 20 hours after plating to reduce the immediate effects of trypsinization. Cells were either mock irradiated or irradiated with 0 to 10 Gy under aerobic conditions using a ^{137}Cs irradiator at ~1 Gy/min at room temperature (16). Mitomycin C was prepared as a stock solution of 0.5 mg/mL in distilled water before each use.

Quantification of Gene Expression by RNase Protection Assays. Asynchronously growing cells were harvested at 70% to 80% growth confluence from either nonirradiated cultures or at 0 to 24 hours after irradiation. RNase protection assays were carried out as per the manufacturer's instructions (BD Sciences-PharMingen, San Diego, CA). Total RNA was first extracted using Trizol reagent (Life Technologies, Inc.). Antisense riboprobes (*Rad50, Mre11, Rad52, Rad54, Rad51, Xrcc2, Xrcc3, Rad51B, Rad51C, Rad51D, L32 and Gapdh* from *DBSR1* set; *Atm, Nbs1, Xrcc2, Xrcc3, Xrcc9, Ligase IV, Xrcc4, Ku70, DNA-PK$_{cs}$, Ku86, L32,* and *Gapdh* from DBSR2 set; and *Bcl-x, p53, Gadd45, c-fos, p21^{WAF}, Bax, Bcl-2, Mcl-1, L32,* and *Gapdh* from HSTRESS set) were synthesized with multiprobe template sets and purified by MAXIscript (Ambion Inc., Houston, TX). Five micrograms of sample RNA were hybridized with 2,000 counts per minute of the synthesized multiriboprobe in a single tube with 10 mL hybridization buffer and digested with RNase centrifuged before acrylamide electrophoresis at 1200 to 1500V for 1 to 2 hours. The gel was then dried at 80C° for 1 hour, and the counts per minute values of the individual bands on the gel were counted using a Storm 840 PhosphorImager (Amersham Biosciences, Piscataway, NJ). The statement level of the *Gapdh* gene was used as an internal control for relative statement levels of other individual genes calculated as a ratio (*i.e.*, the observed total volume for the target gene divided by the volume of *Gapdh*). Three different RNA extracts were analyzed in triplicate for each cell line. The results of three independent experiments are expressed as the mean value ±1 SEM. Statistical differences in gene expression were determined using nonparametric Mann-Whitney analyses.

Western Blot Analyses for Relative Expression of Homologous Recombination, Nonhomologous End-Joining, and Base Excision Repair Proteins. Logarithmically growing cells were either mock-irradiated or irradiated and subsequently lysed on ice for 20 minutes with E7 lysis buffer (PBS, 0.1% SDS, and containing protease inhibitors; Roche Molecular Biochemicals, Indianapolis, IN) for Western blotting as described previously (16). SDS-PAGE was performed using 7% to 12% bis-acrylamide gels at room temperature. Each well was loaded with 20 μg of total protein plus loading buffer (final concentration 6% glycerol, 0.83% β-mercaptoethanol, 1.71% Tris-HCl (pH 6.8), and 0.002% bromphenol blue). Samples were resolved by electrophoresis at 80 to 110 volts for 1.5 to 2.5 hours and then transferred onto nitrocellulose (Schleicher & Schuell Bioscience, Keene, NH). Prehybridization staining with Ponceau solution confirmed equal loading and transfer between running lanes. After transfer, membranes were rinsed with Tris-buffered saline Tween-20, incubated in appropriate secondary antibodies, and protein bands were detected using ECL Detection Reagent (Amersham BioScience) before film exposure. Relative expression was determined by densitometry (Molecular Dynamics Computing ImageQuant, Amersham Sciences) and standardized by α-tubulin levels. Primary antibodies were used at dilutions ranging from 1:200 to 1:1,000 as suggested by the supplier and included the following: $p21^{WAF}$, RAD51, RNase protection assay, and α–tubulin (Oncogene Research Products, San Diego, CA); RAD50, NBS1 (p95), XRCC3, RAD51C, and RAD51D (Novus Biologicals, Inc., Littetown, CO), KU70, RAD52, RAD54, KU86, DNA polymerase-β, and APE/REF1 (Santa Cruz Biotechnology, Santa Cruz, CA); XRCC1 (Abcam, Cambridge, United Kingdom); PARP (Biomol, Plymouth Meeting, PA); DNA polymerase-δ (BD Biosciences, San Diego, CA); MRE11 (Genetex, San Antonio, TX); and phospho-H3 (Upstate Technologies, Waltham, MA). Relative protein expression among PrSC, LNCaP, DU-145, and PC-3 cells was normalized to PrEC expression (*e.g.*, arbitrary relative value of one). The Western blots shown are representative of at least two independent experiments.

Single-Cell Gel Electrophoresis (Comet Assay) to Detect DNA Strand Breaks and Base Damage. Repair of DNA double-strand breaks, DNA-single-strand breaks, DNA base damage, and repair of formamidopyrimidine-DNA glycosylase-sensitive sites was quantitated using the Comet assay as previously described (18, 19; www.cometassay.com). For the neutral comet assay, 10 and 25 Gy doses were used; for the alkaline comet and formamidopyrimidine-DNA glycosylase-comet assays, a dose of 6 Gy was used. For the determination of DNA double-strand breaks by the neutral comet assay, ~10^5 cells were admixed with 100 μL of 0.7% of low melting-point agarose (Sigma-Aldrich, St. Louis, MI) at 45°C and spread on regular glass microscope slides precoated with 1% normal melting agarose. Slides were then treated overnight with lysis solution [2.5 mol/L NaCl, 100 mmol/L EDTA, 10 mmol/L Trizma base, 10% DMSO, and 1% Triton X-100 (pH 9.0)] at pH 9.0. The slides were then placed in 1× Tris-buffer boric acid-EDTA and electrophoresed for 15 minutes at 32V (current ~25mA). After electrophoresis, the slides were dried and stored until scoring. The slides were finally stained with ethidium bromide (2 ng/mL) and the comets scored under a Zeiss fluorescence microscope coupled to KOMET 5.0 software (Kinetic Imaging, Durham, NC). The alkaline comet assay detects alkali-labile sites in the DNA, which are a global assessment of DNA single-strand breaks, DNA double-strand breaks, and DNA base damage. In brief, cells were suspended in 0.5% low melting-point agarose and spread on glass microscope slides precoated with 1% normal agarose. After immersion in lysis solution (2.5 mol/L NaCl, 100 mmol/L EDTA, 10 mmol/L Trizma base, 10% DMSO, and 1% Triton X-100) at 4°C for 1 hour to remove cellular proteins, the slides were immersed in electrophoresis buffer [300 mmol/L NaOH, 1 mmol/L EDTA (pH >13)] for unwinding DNA. Finally, single cells were subjected to electrophoresis (25 V; 300 mA) for a total of 20 minutes. Neutralized and dehydrated slides were finally stained with ethidium bromide (2 ng/mL; Sigma-Aldrich) before scoring.

Repair of DNA base damage was scored by treating the DNA with a lesion-specific glycosylase (formamidopyrimidine-DNA glycosylase). This enzyme recognizes oxidative damage as specific DNA base modifications including 8-oxo-7,8-dihydro-2′-deoxyguanosine, 7-methyl-guanine, 5-OH-cytosine, and 5-OH-uracil. Cells were suspended in 0.5% low-melting point agarose and spread on glass microscope slides precoated with 1% normal agarose. Slides were immersed in lysis solution (2.5 mol/L NaCl, 100 mmol/L EDTA, 10 mmol/L Trizma base, 10% DMSO, and 1% Triton X-100) at 4°C for a minimum period of 1 hour and then equilibrated with enzyme reaction buffer (HEPES 9.5g, KCl 7.5 g, and EDTA 0.5 mmol/L). Bovine serum albumin fraction V was then added [0.2 per mL (pH 8.0)] for 10 minutes on ice. The slides were finally treated with formamidopyrimidine-DNA glycosylase enzyme (obtained from Dr. Karel Angelis, Institute of Experimental Botany, Praha, Czech Republic; 1:100 dilution in enzyme reaction buffer) at 37°C for 30 minutes in a moist box. The enzyme treatment was terminated by dipping the slides in denaturing solution [0.3 mol/L NaOH and 5 mmol/L EDTA (pH 12.1)] for 20 minutes, followed by neutralization in 1× Tris-buffer-boric acid-EDTA for 5 minutes and, finally, electrophoresis. The ratio of DNA migration between the enzyme treated and buffer control slides gives an

estimate of the formamidopyrimidine-DNA glycosylase sensitive sites in the sample.

For all of the comet assays, the comet parameter, "Olive Tail Moment" (*i.e.*, % DNA × distance of center of gravity of DNA) was used as the indicator of DNA damage (19). One hundred consecutive cells were scored at random from the middle of each slide for two to three independent experiments and the final result expressed as the (mean of the median Olive Tail Moment values) ± SEM of the medians. For graphical purposes in the formamidopyrimidine-DNA glycosylase assay, the difference between the Olive Tail Moment for formamidopyrimidine-DNA glycosylase-treated slides *versus* the Olive Tail Moment of same population treated with buffer alone were plotted as the final end point of formamidopyrimidine-DNA glycosylase-sensitive sites. Statistical differences in Olive Tail Moment values were determined using nonparametric Mann-Whitney analyses.

Chromosomal Aberration Assays. The frequency of spontaneous, ionizing radiation-induced (4 Gy) or mitomycin C-induced (40 ng/mL for 24 hours) chromosomal aberrations were determined in exponentially growing cell cultures of PrSC, LNCaP, DU-145, and PC-3. The cells were harvested by trypsinization 24 hours after treatment and incubation with 1 μg of Colcemid/mL for 2 hours to collect metaphase spreads for analysis. The cells were fixed, after treatment with hypotonic solution (0.6% sodium citrate), in EtOH-glacial acetic acid (3:1). Air-dried preparations were made and slides were stained 4′, 6-diamidino-2-phenylindole/Vectashield antifade mixture (Vector-Laboratories, Burlingame, CA). For chromosomal aberrations, 25 mitotic cells were analyzed for each treatment per cell line.

Immunohistochemistry of Prostate Xenografts. For xenograft studies, 1×10^6 of PC-3 or DU-145 cells were injected i.m. into the gastronemius muscle (calf of hind leg) of Balb/c-*nu* mice. Tumors were mock-irradiated or irradiated at a weight of 0.5 g with 20 Gy using a 250KvP X-ray unit without anesthesia. For irradiation, the mouse was lightly restrained in a lucite holder box with lead shielding, such that only the tumor-bearing hind leg was within the irradiation volume. Tumors were then excised and placed immediately in formalin for subsequent fixation and immunostaining using primary RAD51 antibodies (Ab-1, Oncogene Research Products, San Diego, CA) and secondary horseradish peroxidase antibodies for immunodetection. All of the studies were in ethical compliance with the PMH-UHN Animal Care Committee.

RESULTS

Gene Expression Relating to *Atm-p53* DNA Damage Pathways in Prostate Cell Cultures. To initially test the utility of RNase protection assays in quantifying gene expression in our panel of two normal (PrEC-epithelial and PrSC-stromal) and three malignant (LNCaP, PC-3, and DU-145) prostate cell lines, we first quantitated ionizing radiation induction of genes associated with the *Atm-p53* DNA damage signaling cascade. We have reported previously the apoptotic and G_1-checkpoint responses in these cell cultures (16). All five of the cell cultures undergo minimal and nondifferential apoptosis (<5%) after doses of up to 20 Gy (measured 12–96 hours after ionizing radiation); yet the three malignant cell lines have the highest clonogenic survival (*i.e.*, mean SF2Gy values ranging from 0.40 to 0.55 relative to the values for PrSC and PrEC at 0.25 and 0.10, respectively).

PrSC, PrEC, and LNCaP cells express two wild-type *p53* alleles and have an intact G_1 cell cycle arrest checkpoint with increased $p21^{WAF}$ protein expression after irradiation. PC-3 cells are devoid of p53 protein expression due to chromosome 17p hemizygosity and a mutation in the remaining allele at codon 138 that results in a premature stop codon at position 169. DU-145 cells express high levels of *trans*-dominant, mutant (MT) p53 proteins due to missense mutations at codons 223 and 274. Both latter cell lines lack a G_1 checkpoint and do not show increased $p21^{WAF}$ protein expression after DNA damage (15). Using the RNase protection assay analyses at 4 hours after 10 Gy, we observed increased expression of *$p21^{WAF}$*, *Gadd45*, *Bax*, and *Bcl-2* genes in the WT*p53*-expressing cells (*i.e.*, PrSC, PrEC, and LNCaP), whereas similar increases in gene expression were not observed for the null-*p53* and MT*p53*-expressing, PC-3 and DU-145 cells (see Fig. 1*A* and *B*).

The RNase protection assay also confirmed a previous observation that the relative up-regulation of *$p21^{WAF}$* in PrEC epithelial cells was attenuated in comparison to PrSC stromal cells (16). Neither *Atm* nor *p53* RNA was increased after irradiation, consistent with post-translational modification as the basis for activation of these proteins (6). Furthermore, the level of *p53* RNA in PC-3 (null for *p53*) was at background. These results confirmed previous *$p21^{WAF}$* expression data from our laboratory for the same cell lines (16). We also confirmed a dose- and time-dependent (*i.e.*, maximal induction at 4–6 hours after ionizing radiation) induction of both RNA and protein relating to *$p21^{WAF}$* in the LNCaP cell line (Fig. 1*B inset* and data not shown). We conclude that the RNase protection assay is a sensitive indicator of gene expression under the conditions of DNA damage and repair within our panel of prostate cell cultures.

Expression and Functional Assessment of DNA Double-Strand Break and DNA Single-Strand Break Repair Proteins in Prostate Cultures. The initial data relating to the *Atm/p53* stress response provided confidence in the use of RNase protection assay for quantification of gene expression relating to the nonhomologous (nonhomolo-gous end-joining) and homologous recombination pathways of DNA double-strand break repair. We observed a significant and differential increase (approximately 2–3 fold) in homologous recombination associated genes (*i.e.*, *Rad51*, *Rad54*, *Xrcc3*, and *Rad52*) in malignant prostate cell cultures at both the RNA and protein levels when compared with PrEC cells (see Fig. 2). Gene expression relating to the MRN complex (*Mre11/Rad50/Nbs1-p95*) was not differentially expressed. We also found little evidence for increased basal mRNA or protein expression of the nonhomologous end-joining-related *Ku70*, *Ku80*, *DNA-PKcs*, *XRCC4*, or *Ligase IV* genes (see Fig. 3*A* and data not shown). We observed elevated levels of the DNA single-strand break repair protein XRCC1 in malignant cultures (Fig. 3*A*). In contrast to a previous report (20), homologous recombination and nonhomologous end-joining gene expression at both the RNA and protein levels was invariant after irradiation (Fig. 2*A* and data not shown). We conclude that the endogenous expression of the homologous recombination-related *Rad51*, *Rad52*, *Rad54*, *Xrcc3*, and *Xrcc1* genes are increased at RNA and/or protein levels in malignant prostate cell lines.

We next compared the panel of cell cultures for their relative ability to repair DNA double-strand breaks, DNA single-strand breaks, and alkali-labile sites using the Comet assay under neutral or alkaline lysis conditions (Fig. 3*B* and *C*). Despite similar amounts of initial DNA damage, the malignant cultures had significantly decreased capacity in repairing ionizing radiation-induced DNA damage. These data suggest that despite high levels of homologous recombination-related and XRCC1 proteins, malignant prostate cells are defective in the rejoining of DNA double-strand breaks and alkali-labile sites (the latter reflecting DNA single-strand breaks and DNA base damage).

Base Excision Repair in Malignant Prostate Cultures. As the alkaline Comet assay also scores abasic sites, we used the formamidopyrimidine-DNA glycosylase Comet assay to directly determine whether the malignant cultures had relatively increased spontaneous and ionizing radiation-induced levels of oxidative damage. Treating DNA with formamidopyrimidine-DNA glycosylase unmasks nonrepaired oxidative damage as 8-oxo-7,8-dihydro-2′-deoxyguanosine, 7-methyl-guanine, 5-OH-cytosine, or 5-OH-uracil DNA lesions (19). The results shown in Fig. 4*A* are consistent with a decreased capacity for base excision repair of these lesions in the malignant cultures. This defect was not related to decreased levels of the base excision repair-related p53, APE/REF1, or OGG1 proteins. In fact, the malignant

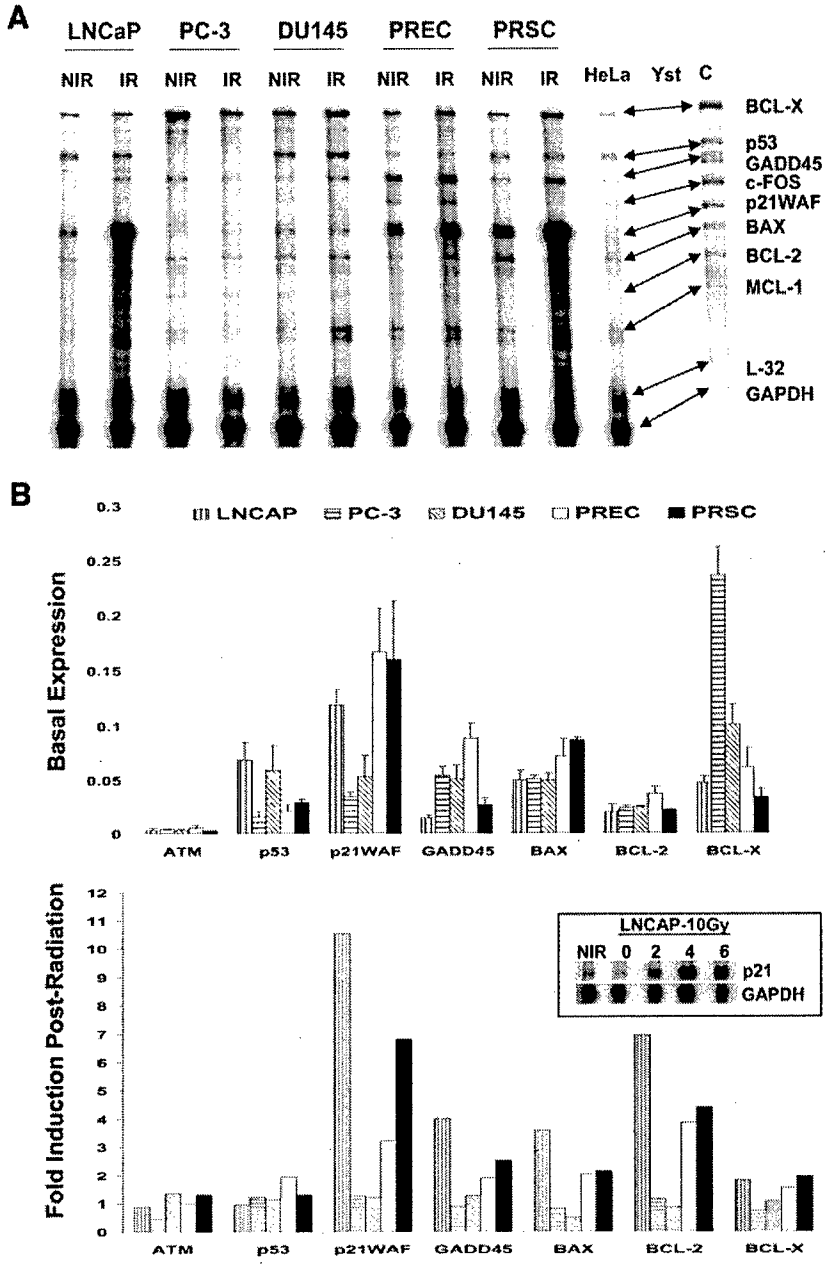

Fig. 1. Gene expression relating to *Atm-p53* signaling in malignant and normal prostate cultures using RNase protection assay analyses. *A*, representative example of RNase protection assay blot whereby ^{32}P-labeled multiriboprobes were hybridized to the total mRNA derived from mock-irradiated (*NIR*) or irradiated (*IR*: 10 Gy-4 hours) asynchronously growing prostate cultures. Specific multiprobes used in this analysis are indicated in the *far left margin* of the blot aside the corresponding gene band of interest. Also shown are lanes containing probed sequences within HeLa cells (positive control), Yeast (*Yst*; negative control), and the RNA probes themselves (*far right*). *Gapdh* was a housekeeping gene that served as internal control for densitometric quantitation of results. Note IR-induced $p21^{WAF}$ signal in WT-*p53* expressing PrSC, PrEC, and LNcaP cell lines consistent with wild-type *p53* status and an intact G_1-checkpoint in these cells. *B*, quantitation of *Atm/p53*-dependent stress response based on RNase protection assay analyses of mRNA in normal and malignant prostate cells. *Top figure* shows basal (*i.e.*, nonirradiated) levels of mRNA expression. Shown are mean gene expression values based on at least three independent experiments; *bars*, ±1 SEM. *Bottom panel* shows mean values of expression of same genes relative to basal levels at 4 hours after 10 Gy. Significantly increased expression was observed for the $p21^{WAF}$ gene in WTp53-expressing cells (PrSC, PrEC, and LNCaP), which is both time-dependent [see insert for $p21^{WAF}$ protein expression over 6 hours post-10 Gy in LNCaP cells) and dose dependent from 2 to 10 Gy (data not shown; Mann-Whitney test; $P < 0.05$)]. *Bax*, *Bcl-2*, and *Gadd45* mRNA in these cell lines was also significantly increased after irradiation (Mann-Whitney test; $P < 0.05$).

cells lines had increased levels of DNA-polymerase-β and -δ, two key enzymes involved in short-patch and long-patch base excision repair (ref. 21; Fig. 4*B* and *C*). We also assessed whether increased expression of homologous recombination-related or base excision repair-related proteins could be secondary to cell cycle bias given that these proteins are optimally expressed in S and G_2 phases of the cell cycle (13). In comparing the cell culture doubling times *in vitro* with mitotic and S-phase biomarkers (phosphorylated-histone 3 and RNase protection assay proteins, respectively), we did not observe any correlation between increased DNA repair protein expression and cell proliferation indices among the five cultures (Fig. 4*B*).

Chromosomal Repair and Heterogeneity of RAD51 Protein Expression *In vivo*. Homologous recombination and nonhomologous end-joining events can be scored using integrated genetic substrates (22) or characterization of distinct types of chromosomal aberrations after cellular exposure to mitomycin C or ionizing radiation (known to induce DNA cross-links or predominantly DNA strand breaks, respectively). We used the chromosomal damage assay, as it directly compares the capacity for homologous recombination and nonhomologous end-joining in both malignant and normal cells. Normal PrSc and PrEC cells are difficult to transfect with DNA repair plasmid reporter substrates (22). The metaphase spreads in Fig. 5*A* show representative structural cytogenetic aberrations, which are quantified in Table 1 for four of the five cultures. The protracted doubling time of PrEC cells precluded their assessment in this assay. All three malignant cell lines show an increased incidence of a variety of aberrations associated with aberrant homologous recombination occurring in the S and G_2 phases of the cell cycle phases including: chromatid breaks; double minutes; tri-, quad-, and complex-radial chromosomes; abnormal telomeric associations; and centromere fissions. Furthermore, nonhomologous end-joining–associated defects occurring within the G_1 cell cycle phase were also observed as increased chromosomal breaks and di- or tricentric chromosomes in malignant cultures. These data support our hypothesis that defects in DNA double-strand break repair

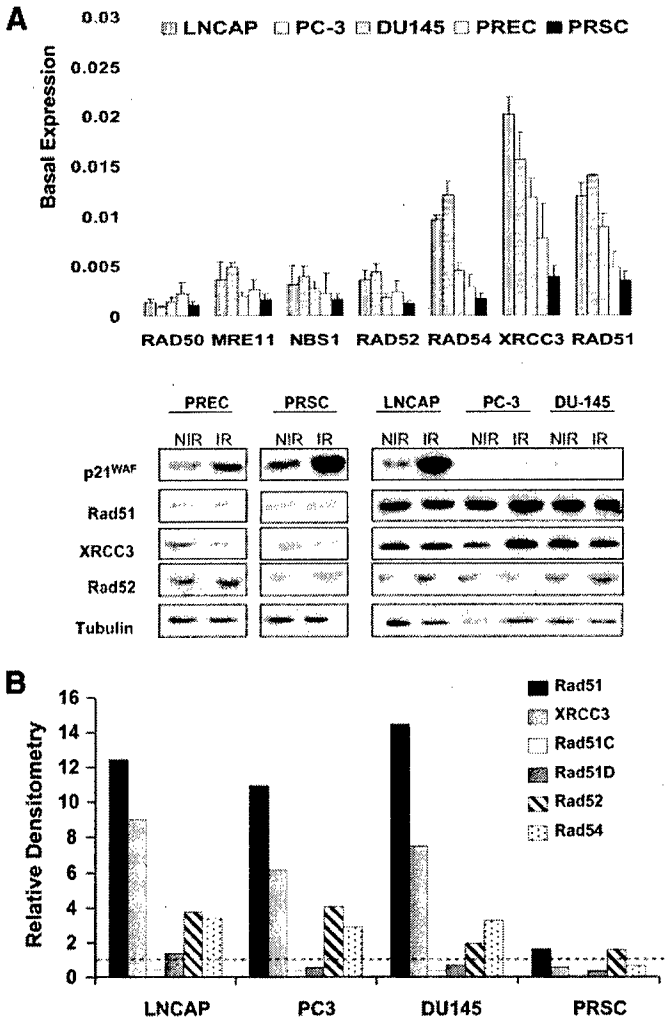

Fig. 2. Increased expression of the homologous recombination genes, *Rad51, Xrcc3, Rad52,* and *Rad54*, in malignant prostate cancer cell lines. *A. Top panel* shows relative basal homologous recombination gene expression based on RNase protection assay analyses in normal and malignant prostate cells. Significant increased mRNA expression of *Rad51, Rad54, Rad52,* and *XrccC3* is noted in the malignant prostate cultures in comparison with normal cell cultures (Mann-Whitney test. $P < 0.05$). Irradiated (*IR*) induction of the *Rad51, Rad54, Rad52,* and *Xrcc3* genes was observed solely in the PrSC stromal cell line (Mann-Whitney test, $P < 0.05$), but not the other epithelial cell lines (data not shown; Supplementary Fig. 1*A*). *Bottom panel* shows Western blots of selected homologous recombination proteins in which protein expression is invariant before (mock-irradiated, *NIR*) or at 4 hours after 10 Gy (IR). α-Tubulin is shown as the protein loading control. Increased $p21^{WAF}$ protein expression served as an irradiation control whereby $p21^{WAF}$ protein was elevated in cell lines with wild-type *p53* gene status. *B*, confirmation of increased basal RAD51, RAD52, RAD54, and XRCC3 protein expression in malignant prostate cells relative to PrEC cells using quantitative densitometry of Western blot analyses (see example blot in Supplementary Fig. 1*B*). Similar results were obtained among two independent experiments. The *dotted line* represents the relative expression compared with the PrEC cell line. Homologous recombination-related protein expression was not additionally increased at 4 hours after a 10 Gy (data not shown); *bars*, ± SEM.

can be observed in malignant cultures and augment our findings using the Comet assay.

Given the observed increase in homologous recombination-related protein expression *in vitro*, we also compared the expression of similar proteins *in vivo* within xenografts derived from the same malignant cell lines (*e.g.*, PC-3 and DU-145). Therefore, we immunostained for the RAD51 protein in histologic sections derived from xenografts before and after 20Gy irradiation *in vivo* (see Fig. 5*B*). Similar to a previous report in pancreatic cancer (23), we observed intratumoral heterogeneity with respect to endogenous RAD51 expression. Both cytoplasmic and nuclear RAD51 expression was observed in PC-3 and DU-145 xenograft histologic sections. However, in contrast to our data in which RAD51 expression *in vitro* was invariant after DNA damage, nuclear RAD51 expression increased in the PC-3 or DU-145 xenografts irradiated under *in vivo* conditions. Taken together, our data suggest that RAD51 expression *in vivo* can be additionally modified by intratumoral biology and physiology with the three-dimensional tumor architecture.

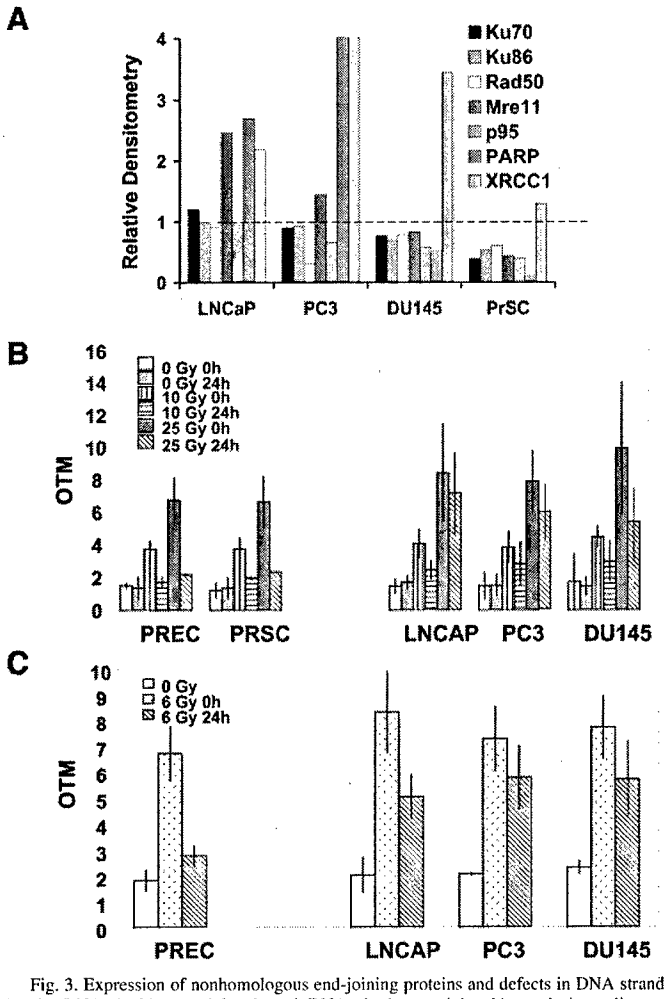

Fig. 3. Expression of nonhomologous end-joining proteins and defects in DNA strand break (DNA double-strand break and DNA single-strand break) repair in malignant prostate cell cultures. *A*, quantitation of nonhomologous end-joining and DNA single-strand break repair protein expression in malignant prostate cells relative to PrEC cells using quantitative densitometry of Western blot analyses (see example blot in Supplementary Fig. 1*C*). Similar results were obtained for two independent experiments. The *dotted line* represents the relative expression compared with the PrEC cell line. The level of XRCC1 protein expression was consistently elevated in all three of the malignant cell lines. Neither nonhomologous end-joining– nor DNA single-strand break-related protein expression was additionally induced at 4 hours after a 10 Gy dose (data not shown). *B*, neutral Comet assay of malignant and normal prostate cells before and after 10 or 25 Gy of ionizing radiation. Plotted is the Olive Tail Moment (*OTM, i.e.*, % DNA × distance of center of gravity of DNA) on the *Y* axis as the indicator of the presence of DNA double-strand breaks for a given time and radiation dose. No significant differences exist between the five cell lines for OTM values at baseline or immediately after irradiation (*i.e.*, time = 0). However, the residual number of DNA double-strand breaks at 24 hours after 25 Gy is greater in the three malignant cultures in comparison with the normal cultures (Mann-Whitney test, $P < 0.05$). *C*, alkaline (pH >13.0) Comet assay of malignant and normal prostate cells before and after 6 Gy of ionizing radiation. Similar to *B* above, the OTM on the *Y* axis as the indicator of the presence of alkali-labile sites, DNA-double-strand breaks, DNA single-strand breaks, and DNA base damage after irradiation. The residual damage at 24 hours after irradiation in the three malignant cultures is greater than that of the control PrEC cultures (Mann-Whitney test, $P < 0.05$). For both *B* and *C*, 100 consecutive cells were scored at random from the middle of each slide for two to three independent experiments and the final result expressed as the (mean of the OTM median values); *bars*, ± SEM.

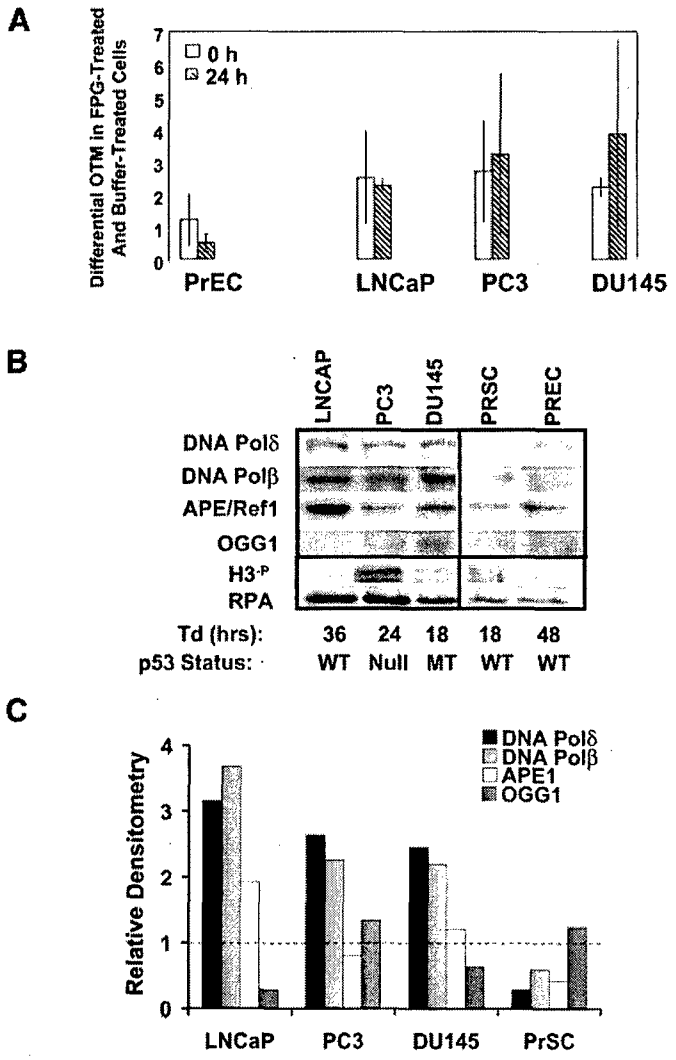

Fig. 4. Defective excision of oxidative damage in malignant prostate cancer cultures. *A*, Comet assay of formamidopyrimidine-DNA glycosylase-sensitive sites representing extent of oxidative base damage before and after 6 Gy irradiation in malignant prostate cell cultures relative to normal control (PrEC) epithelial culture. The final result expressed as the [mean of the Olive Tail Moment (*OTM*) median values] ± 1 SEM. A trend toward increased endogenous oxidative damage is observed (*i.e.*, at time = 0 of formamidopyrimidine-DNA glycosylase-treatment) in the malignant cells, although only the baseline levels of DU-145 are statistically increased when compared with levels of PrEC cultures (Mann-Whitney test, $P < 0.05$). However, at 24 hours after 6 Gy, the number of remaining oxidative lesions is statistically higher in all three of the malignant cultures (Mann-Whitney, $P < 0.05$). *B*, Western blot analyses and (*C*) relative densitometry of basal levels of base excision repair- and cell cycle-associated proteins in normal and malignant cell cultures. Elevated levels of DNA polymerase-β and -δ were consistently observed in a *p53*-independent manner in malignant cell cultures. Similar observations were made between two independent experiments. There is no correlation among phosphorylated-H3 (*H3-P*; a marker of mitosis), *RPA* (a marker of S phase), or cell doubling time *in vitro* (*Td*; hours) and DNA polymerase or homologous recombination-associated protein expression in Fig. 2. This confirms that the elevated expression of the homologous recombination-related proteins is not solely due to increased fraction of cells within the S and G_2 phases of cell cycle.

DISCUSSION

This is the first study to report defective DNA double-strand break, DNA single-strand break, and base damage repair in malignant prostate cancer cells and associate these defects with increased chromosomal aberrations and genetic instability. Our data are consistent with homologous recombination-related and base excision repair-related protein dysfunction in malignant cells as a biomarker of a "mutator" phenotype driving genomic instability after cytotoxic insult. These findings are supported by previous data in which LNCaP cells had a decreased ability to repair restriction-enzyme mediated DNA double-strand breaks based on a fluorescence-based plasmid reconstitution assay (24). Additionally, during the preparation of this article, Trzeciak *et al.* (25) reported that PC-3 and DU-145 cells have defective excision of oxidative lesions with altered levels of superoxide dismutase and glutathione peroxidase supporting our observation of decreased base excision repair in these cell lines. Other reports in the literature within panels of cell lines with varying histopathologic type have reported heterogeneity in DNA polymerase-β activity and elevated PARP expression (26–28).

There have been previous reports of elevated levels of *Rad51* mRNA or RAD51 protein expression within human tumor cell lines (29, 30). However, to our knowledge, this is the first direct comparison of DNA double-strand break gene expression within normal and malignant cells from the same histopathologic type linked to a functional assessment of DNA double-strand break repair. Altered stoichiometry of repair proteins or a disconnect between cell cycle checkpoint control and DNA repair may be the basis for the observed discordance between repair protein expression and function (13, 31). Altered homologous recombination-related protein expression might indirectly lead to altered nonhomologous end-joining activity given the interplay between the two pathways during DNA double-strand break repair (32, 33). Maintenance of survival in malignant cells, despite high levels of DNA double-strand breaks and chromosomal aberrations after DNA damage, is probably secondary to loss of potentially deleterious accentric fragments or other chromosomal abnormalities within micronuclei at 48 to 72 hours after irradiation (34, 35).

In isogenic systems, the relationship among RAD51 expression, homologous recombination, and induction of chromosomal aberrations remains controversial (29, 36–38). This may relate to variability in genetic background or the plasmid homologous recombination reporter substrates used for study (22). Transfection studies with forced overexpression of RAD51 have led to observations of both increased and decreased frequencies of homologous recombination, arguing for RAD51 acting as either a promoter or repressor of genetic instability and tumor progression (37, 39). Other transfection studies suggested that RAD51, XRCC3, and XRCC1 protein overexpression leads to increased $p21^{WAF}$ expression and a decreased apoptotic response with resulting radioresistance (23, 40, 41). However, our data do not support such a direct correlation. Our malignant cultures, which overexpress homologous recombination-related proteins have varying G_1 checkpoint control and p21WAF expression, and all five of the cultures are resistant to apoptosis (16). The increased DNA repair protein expression observed in the malignant cell lines was independent of *p53* status, G_1-checkpoint control, androgen responsiveness, clonogenic radiation cell survival, cell proliferation, and susceptibility for radiation-induced apoptosis (16, 20, 42).

It had also been hypothesized that RAD51 overexpression might abrogate RAD51-p53 interactions and override the G_1 checkpoint leading to aneuploidy and high levels of homologous recombination (37, 43). The decreased levels of MMS- and ionizing radiation-induced homologous recombination-related chromosomal aberrations in the G_1 checkpoint-proficient LNCaP cultures, relative to the G_1 checkpoint-deficient DU-145 and PC-3 cultures, would support this hypothesis. Additionally, our observed overexpression of the *Rad51*, *Xrcc3*, *Rad52*, and *Rad54* genes at both the RNA and protein level suggests that loss of control of homologous recombination expression in malignant cells is operational at the transcriptional level and may be secondary to altered activity of transcription factors in cancer cells. *Rad51* gene overexpression can be mediated by *Bcr/Abl* and *STAT5*-dependent transcription in addition to inhibition of caspase-3-dependent RAD51 protein

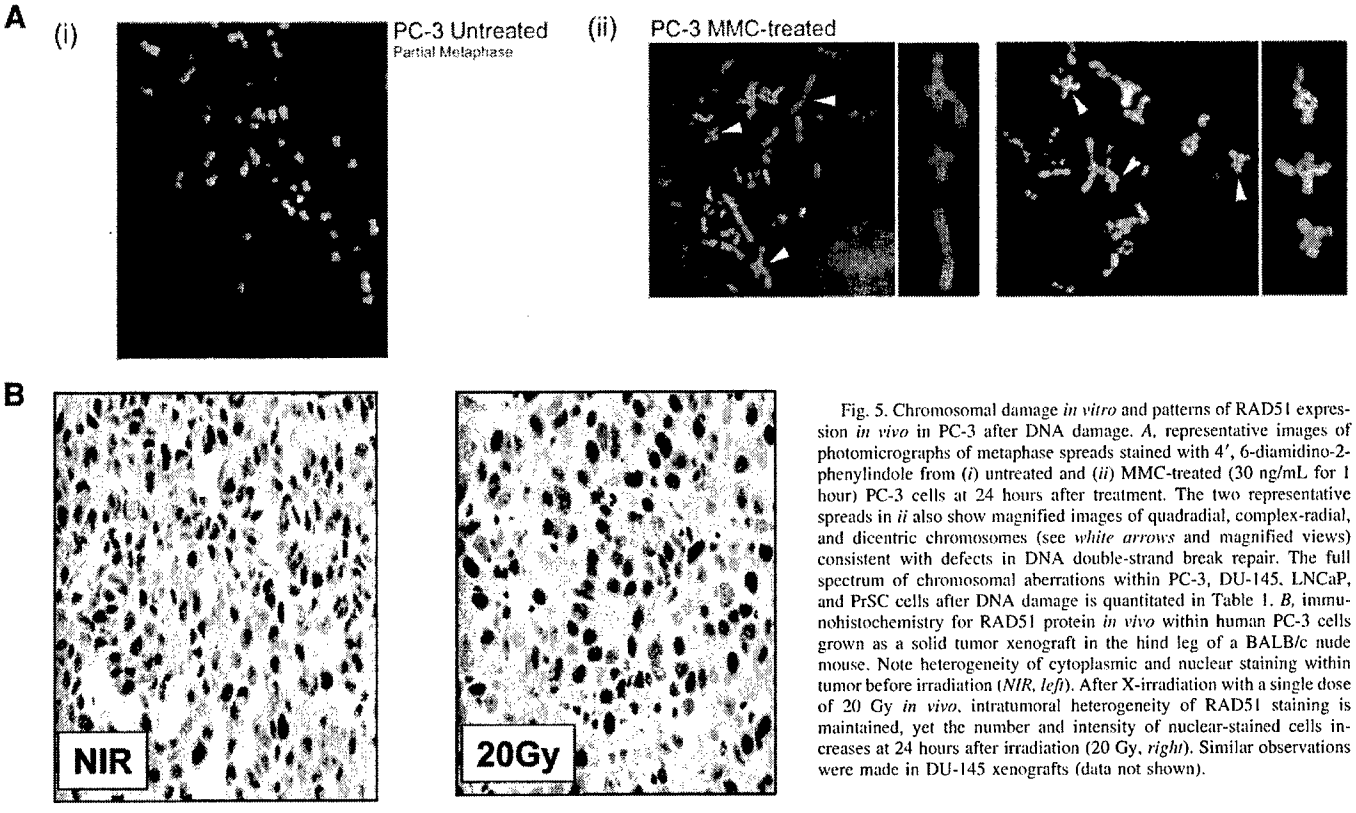

Fig. 5. Chromosomal damage *in vitro* and patterns of RAD51 expression *in vivo* in PC-3 after DNA damage. *A*, representative images of photomicrographs of metaphase spreads stained with 4′, 6-diamidino-2-phenylindole from (*i*) untreated and (*ii*) MMC-treated (30 ng/mL for 1 hour) PC-3 cells at 24 hours after treatment. The two representative spreads in *ii* also show magnified images of quadradial, complex-radial, and dicentric chromosomes (see *white arrows* and magnified views) consistent with defects in DNA double-strand break repair. The full spectrum of chromosomal aberrations within PC-3, DU-145, LNCaP, and PrSC cells after DNA damage is quantitated in Table 1. *B*, immunohistochemistry for RAD51 protein *in vivo* within human PC-3 cells grown as a solid tumor xenograft in the hind leg of a BALB/c nude mouse. Note heterogeneity of cytoplasmic and nuclear staining within tumor before irradiation (*NIR, left*). After X-irradiation with a single dose of 20 Gy *in vivo*, intratumoral heterogeneity of RAD51 staining is maintained, yet the number and intensity of nuclear-stained cells increases at 24 hours after irradiation (20 Gy, *right*). Similar observations were made in DU-145 xenografts (data not shown).

Table 1 *Chromosomal abberrations in prostate cell cultures in response to DNA damage*

	PRSC			LNCAP			DU145			PC-3		
Aberration	Control	MMC	IR	Control	MMC	IR	Control	MMC	IR	Control	MMC	IR
Chromosome break	0	3	0	0	0	1	0	0	2	1	3	1
Chromatid break	0	0	0	1	0	1	0	4	0	0	6	1
Tri-, quad-, or complex radial	0	1	0	3	2	8	0	2	1	0	8	9
Di- or tricentric	0	0	1	0	1	6	0	7	14	2	20	22
Ring chromosomes	0	0	0	0	0	0	0	0	0	0	1	3
Double minutes	0	0	0	0	0	3	0	2	14	2	4	6
Accentric fragments	0	0	1	1	0	18	3	4	15	12	10	15
Telomeric association of 2 acrocentric chromosomes	0	0	1	0	3	4	3	4	0	2	5	1
Centromere fission	0	1	0	0	2	0	4	0	0	0	0	1
Total	1	5	3	5	8	41	10	23	46	19	57	58

NOTE. For each cell culture, the frequency of spontaneous (control), IR-induced (4 Gy), or MMC-induced (40 ng/ml for 24 hours) chromosomal aberrations were determined in exponentially growing cell cultures of PRSC, LNCAP, DU145, and PC-3. The extremely slow doubling time of PrEC cells (>48 hours) precluded a similar analysis in this cell type. The cells were harvested by trypsinization 24 hours after treatment and then incubated with 1 μg of Colcemid/mL for 2 hours to collect metaphase spreads for analysis. Twenty-five metaphases were scored for each culture. Both increased chromosome and chromatid types of aberrations are observed in the malignant cells relative to PrSC cells after IR or MMC treatment, consistent with defects in homologous recombination and non-homologous end-joining repair.

Abbreviations: MMC, mitomycin-c; IR, ionizing radiation.

cleavage (44, 45). Similar mechanisms may exist for other homologous recombination-related genes in prostate cancer. Indeed, preliminary data in our laboratory suggests that endogenous BRCA1 and BRCA2 protein expression are also elevated in the three malignant cell lines.[5]

Our results implicate DNA repair, and particularly DNA double-strand break repair and homologous recombination, as a potential factor in prostate tumor progression. Importantly, our data may have implications for both prostate cancer diagnosis and therapy. Profiling of DNA repair protein expression may be useful to discover new biomarkers of genetic instability, malignant progression, and aggressive tumor phenotypes (46, 47). We would also hypothesize that prostate intraepithelial neoplasia (PIN) may have altered frequencies of homologous recombination and defective DNA double-strand break repair when compared with nonmalignant epithelium. Unfortunately, the paucity of cell lines for the study of prostatic intraepithelial neoplasia or early stage prostate cancer prevents us from making this direct link *in vitro* (48).

Prostate tissue arrays will be useful to confirm that our *in vitro* findings are operational *in vivo* and that loss of checkpoint control and DNA repair activity is correlated to tumor progression similar to that reported for breast cancer (49). However, the data presented in Fig. 5*B* suggest that interpretation of tissue arrays may be difficult without added information pertaining to cell cycle phase, oxygenation, nutritional status, or clonal variation, which may affect the intratumoral heterogeneity of protein expression. For example, the relative increase in RAD51 expression after irradiation *in vivo* may be secondary to the arrest of cells in the G_2 phase of the cell cycle, which has higher levels of RAD51 expression (50), or due to microenvironmental factors. Indeed, in a separate study, we have observed that RAD51 expression

[5] R. Fan, F. Jalali, and R. G. Bristow, unpublished observations.

can be altered under conditions of intratumoral hypoxia (51). Additional experiments with defined doses and time points after irradiation *in vivo* using prostate xenografts may clarify these issues and glean more information regarding RAD51 function within solid tumors.

We speculate that the use of agents that either augment DNA repair in premalignant prostate epithelium or inhibit the hyper-recombinogenic phenotype of malignant cells may be valuable in prostate cancer treatment. For example, the antioxidant selenium has been implicated as a chemoprotective agent for high-risk prostate cancer and has been shown recently to increase DNA repair and chemoprotect normal cells in response to DNA damaging agents (52). Additionally, molecular-targeted agents, which decrease aberrant *Rad51* or other DNA repair gene expression, such as STI571-Gleevec (45, 53) or small interfering RNA approaches (54), may be potentially novel strategies to sensitize prostate cancer cells to radiotherapy or chemotherapy (55, 56).

REFERENCES

1. Karayi MK, Markham AF. Molecular biology of prostate cancer. Prostate Cancer Prostatic Dis 2004;7:6–20.
2. Elliott B, Jasin M. Double-strand breaks and translocations in cancer. Cell Mol Life Sci 2002;59:373–85.
3. Pihan GA, Purohit A, Wallace J, Malhotra R, Liotta L, Doxsey SJ. Centrosome defects can account for cellular and genetic changes that characterize prostate cancer progression. Cancer Res 2001;61:2212–9.
4. Vukovic B, Park PC, Al-Maghrabi J, et al. Evidence of multifocality of telomere erosion in high-grade prostatic intraepithelial neoplasia (HPIN) and concurrent carcinoma. Oncogene 2003;22:1978–87.
5. Gangopadhyay S, Jalali F, Reda D, Peacock J, Bristow RG, Benchimol S. Expression of different mutant p53 transgenes in neuroblastoma cells leads to different cellular responses to genotoxic agents. Exp Cell Res 2002;275:122–31.
6. Kastan MB, Lim DS, Kim ST, Yang D. ATM–a key determinant of multiple cellular responses to irradiation. Acta Oncol 2001;40:686–8.
7. Roninson IB, Broude EV, Chang BD. If not apoptosis, then what? Treatment-induced senescence and mitotic catastrophe in tumor cells. Drug Resist Updat 2001;4:303–13.
8. Chen L, Elahi A, Pow-Sang J, Lazarus P, Park J. Association between polymorphism of human oxoguanine glycosylase 1 and risk of prostate cancer. J Urol 2003;170:2471–4.
9. Yeh CC, Lee C, Dahiya R. DNA mismatch repair enzyme activity and gene expression in prostate cancer. Biochem Biophys Res Commun 2001;285:409–13.
10. Rybicki BA, Conti DV, Moreira A, Cicek M, Casey G, Witte JS. DNA repair gene XRCC1 and XPD polymorphisms and risk of prostate cancer. Cancer Epidemiol Biomark Prev 2004;13:23–9.
11. Xu J, Zheng SL, Turner A, et al. Associations between hOGG1 sequence variants and prostate cancer susceptibility. Cancer Res 2002;62:2253–7.
12. Valerie K, Povirk LF. Regulation and mechanisms of mammalian double-strand break repair. Oncogene 2003;22:5792–812.
13. West SC. Molecular views of recombination proteins and their control. Nat Rev Mol Cell Biol 2003;4:435–45.
14. Takata M, Sasaki MS, Tachiiri S, et al. Chromosome instability and defective recombinational repair in knockout mutants of the five Rad51 paralogs. Mol Cell Biol 2001;21:2858–66.
15. Liede A, Karlan BY, Narod SA. Cancer risks for male carriers of germline mutations in BRCA1 or BRCA2: a review of the literature. J Clin Oncol 2004;22:735–42.
16. Bromfield GP, Meng A, Warde P, Bristow RG. Cell death in irradiated prostate epithelial cells: role of apoptotic and clonogenic cell kill. Prostate Cancer Prostatic Dis 2003;6:73–85.
17. Loeb LA, Loeb KR, Anderson JP. Multiple mutations and cancer. Proc Natl Acad Sci USA 2003;100:776–81.
18. Bristow RG, Hu Q, Jang A, et al. Radioresistant MTp53-expressing rat embryo cell transformants exhibit increased DNA-dsb rejoining during exposure to ionizing radiation. Oncogene 1998;16:1789–802.
19. Olive PL. The comet assay. An overview of techniques. Methods Mol Biol 2002; 203:179–94.
20. Yuan R, Fan S, Wang JA, et al. Coordinate alterations in the expression of BRCA1, BRCA2, p300, and Rad51 in response to genotoxic and other stresses in human prostate cancer cells. Prostate 1999;40:37–49.
21. Dianov GL, Sleeth KM, Dianova II, Allinson SL. Repair of abasic sites in DNA. Mutat Res 2003;531:157–63.
22. Willers H, Xia F, Powell SN. Recombinational DNA repair in cancer and normal cells: the challenge of functional analysis. J Biomed Biotechnol 2002;2:86–93.
23. Henning W, Sturzbecher HW. Homologous recombination and cell cycle checkpoints: Rad51 in tumour progression and therapy resistance. Toxicology 2003;193:91–109.
24. Collis SJ, Sangar VK, Tighe A, et al. Development of a novel rapid assay to assess the fidelity of DNA double-strand-break repair in human tumour cells. Nucleic Acids Res 2002;30:E1.
25. Trzeciak AR, Nyaga SG, Jaruga P, Lohani A, Dizdaroglu M, Evans MK. Cellular repair of oxidatively induced DNA base lesions is defective in prostate cancer cell lines, PC-3 and DU-145. Carcinogenesis. In press 2004.
26. Bhattacharyya N, Chen HC, Wang L, Banerjee S. Heterogeneity in expression of DNA polymerase beta and DNA repair activity in human tumor cell lines. Gene Expr 2002;10:115–23.
27. Dobashi Y, Shuin T, Tsuruga H, Uemura H, Torigoe S, Kubota Y. DNA polymerase beta gene mutation in human prostate cancer. Cancer Res 1994;54:2827–9.
28. McNealy T, Frey M, Trojon L, Knoll T, Alken P, Michel MS. Intrinsic presence of poly (ADP-ribose) is significantly increased in malignant prostate compared to benign prostate cell lines. Anticancer Res 2003;23:1473–8.
29. Lambert S, Lopez BS. Inactivation of the RAD51 recombination pathway stimulates UV-induced mutagenesis in mammalian cells. Oncogene 2002;21:4065–9.
30. Raderschall E, Stout K, Freier S, Suckow V, Schweiger S, Haaf T. Elevated levels of Rad51 recombination protein in tumor cells. Cancer Res 2002;62:219–25.
31. Venkitaraman AR. Cancer susceptibility and the functions of BRCA1 and BRCA2. Cell 2002;108:171–82.
32. Allen C, Halbrook J, Nickoloff JA. Interactive competition between homologous recombination and non-homologous end joining. Mol Cancer Res 2003;1:913–20.
33. Richardson C, Jasin M. Coupled homologous and nonhomologous repair of a double-strand break preserves genomic integrity in mammalian cells. Mol Cell Biol 2000; 20:9068–75.
34. Bishay K, Ory K, Lebeau J, Levalois C, Olivier MF, Chevillard S. DNA damage-related gene expression as biomarkers to assess cellular response after gamma irradiation of a human lymphoblastoid cell line. Oncogene 2000;19:916–23.
35. Muller WU, Nusse M, Miller BM, Slavotinek A, Viaggi S, Streffer C. Micronuclei: a biological indicator of radiation damage. Mutat Res 1996;366:163–9.
36. Kim PM, Allen C, Wagener BM, Shen Z, Nickoloff JA. Overexpression of human RAD51 and RAD52 reduces double-strand break-induced homologous recombination in mammalian cells. Nucleic Acids Res 2001;29:4352–60.
37. Richardson C, Stark JM, Ommundsen M, Jasin M. Rad51 overexpression promotes alternative double-strand break repair pathways and genome instability. Oncogene 2004;23:546–53.
38. Vispe S, Cazaux C, Lesca C, Defais M. Overexpression of Rad51 protein stimulates homologous recombination and increases resistance of mammalian cells to ionizing radiation. Nucleic Acids Res 1998;26:2859–64.
39. Bertrand P, Lambert S, Joubert C, Lopez BS. Overexpression of mammalian Rad51 does not stimulate tumorigenesis while a dominant-negative Rad51 affects centrosome fragmentation, ploidy and stimulates tumorigenesis, in p53-defective CHO cells. Oncogene 2003;22:7587–92.
40. Raderschall E, Bazarov A, Cao J, et al. Formation of higher-order nuclear Rad51 structures is functionally linked to p21 expression and protection from DNA damage-induced apoptosis. J Cell Sci 2002;115:153–64.
41. Yanagisawa T, Urade M, Yamamoto Y, Furuyama J. Increased expression of human DNA repair genes, XRCC1, XRCC3 and RAD51, in radioresistant human KB carcinoma cell line N10. Oral Oncol 1998;34:524–8.
42. Carlomagno F, Burnet NG, Turesson I, et al. Comparison of DNA repair protein expression and activities between human fibroblast cell lines with different radiosensitivities. Int J Cancer 2000;85:845–9.
43. Kumari A, Schultz N, Helleday T. p53 protects from replication-associated DNA double-strand breaks in mammalian cells. Oncogene 2004;23:2324–9.
44. Slupianek A, Schmutte C, Tombline G, et al. BCR/ABL regulates mammalian RecA homologs, resulting in drug resistance. Mol Cell 2001;8:795–806.
45. Skorski T. BCR/ABL regulates response to DNA damage: the role in resistance to genotoxic treatment and in genomic instability. Oncogene 2002;21:8591–604.
46. Bishay K, Ory K, Olivier MF, Lebeau J, Levalois C, Chevillard S. DNA damage-related RNA expression to assess individual sensitivity to ionizing radiation. Carcinogenesis 2001;22:1179–83.
47. Goode EL, Ulrich CM, Potter JD. Polymorphisms in DNA repair genes and associations with cancer risk. Cancer Epidemiol Biomark Prev 2002;11:1513–30.
48. Rhim JS. Research into molecular and genetic mechanisms underlying prostate carcinogenesis would be greatly advanced by in vitro prostate cell models. Drugs Today (Barc) 2003;39:837–47.
49. Gonzalez R, Silva JM, Dominguez G, et al. Detection of loss of heterozygosity at RAD51, RAD52, RAD54 and BRCA1 and BRCA2 loci in breast cancer: pathological correlations. Br J Cancer 1999;81:503–9.
50. Essers J, Hendriks RW, Wesoly J, et al. Analysis of mouse Rad54 expression and its implications for homologous recombination. DNA Repair (Amst) 2002;1:779–93.
51. Bindra RS, Schaffer PJ, Meng A, et al. Down-regulation of Rad51 and decreased homologous recombination in hypoxic cancer cells. Mol Cell Biol 2004; 24:8504–18.
52. Klein EA. Selenium: epidemiology and basic science. J Urol 2004;171:S50–53; discussion S53.
53. Russell JS, Brady K, Burgan WE, et al. Gleevec-mediated inhibition of Rad51 expression and enhancement of tumor cell radiosensitivity. Cancer Res 2003;63:7377–83.
54. Collis SJ, Tighe A, Scott SD, Roberts SA, Hendry JH, Margison GP. Ribozyme minigene-mediated RAD51 down-regulation increases radiosensitivity of human prostate cancer cells. Nucleic Acids Res 2001;29:1534–8.
55. Collis S, Swartz M, DeWeese T. siRNA-silencing of DNA repair factors results in enhanced radiation and chemotherapy-mediated killing of human cancer cells. Int J Radiat Oncol Biol Phys 2003;57:S144.
56. Taki T, Ohnishi T, Yamamoto A, et al. Antisense inhibition of the RAD51 enhances radiosensitivity. Biochem Biophys Res Commun 1996;223:434–8.

ELSEVIER

Seminars in
RADIATION
ONCOLOGY

Radiation and New Molecular Agents Part I: Targeting ATM-ATR Checkpoints, DNA Repair, and the Proteasome

Ananya Choudhury, MA, MRCP, FRCR, Andrew Cuddihy, PhD, and Robert G. Bristow, MD, PhD, FRCPC

In response to DNA breaks, human cells delay their progression through the G1, S, and G2 phases of the cell cycle. This response requires the coordinated effort of the ATM-CHK2-p53 and ATR-CHK1 DNA damage-sensing pathways and DNA repair (eg, DNA-PK and RAD51 complexes). The turnover of many of these DNA damage-associated proteins is controlled by the 26S proteasome. In this article, we review molecular strategies that target each of these pathways using silencing RNA (siRNA), antisense, or small-molecule inhibition. Although these agents can radiosensitize tumor cells, little data are available regarding potential effects on normal tissues to determine the potential therapeutic ratio of these strategies after fractionated radiotherapy. Clinical trials using such agents will require novel correlative science endpoints to track DNA repair and cell-cycle arrest and will need careful assessment of normal tissue toxicity and stability.
Semin Radiat Oncol 16:51-58

In modern radiotherapy, biological targeting requires an understanding of malignant and nonmalignant tissue responses pertaining to relative cell proliferation, DNA repair, and cell death (eg, tissue-specific apoptosis, mitotic catastrophe, and tumor cell senescence).[1,2] In this article, we review new molecular radiosensitizers that target cell-cycle checkpoint control and intracellular DNA damage responses. With increasing available information regarding the molecular pathways of radioresponse, we are learning that combined-modality chemoradiation protocols take advantage of disparate molecular DNA repair and cell-cycle transitions that can exist among malignant and normal cells.[3,4] This characteristic feature supports further exploitation of these pathways to improve local control. Improving the therapeutic ratio is paramount to the success of these new agents and underlies the need for simultaneous study of normal tissue toxicity, as outlined later.

Departments of Radiation Oncology and Medical Biophysics, University of Toronto and Princess Margaret Hospital-University Health Network, Toronto, Ontario, Canada;
Supported by operating grants from the Terry Fox Foundation, National Cancer Institute of Canada, Ontario Cancer Research Network, the Prostate Cancer Research Foundation of Canada, and the US Army DOD Prostate Cancer Research Program. RGB is a Canadian Cancer Society Research Scientist. The first two authors contributed equally to this manuscript.
Address reprint requests to Robert G. Bristow, MD, PhD, FRCPC, Department of Radiation Oncology, Princess Margaret Hospital, Room 5-923 610 University Avenue Toronto, Ontario, Canada.E-mail: rob.bristow@rmp.uhn.on.ca

Targeting the ATM-p53 and ATR-CHK1 Cell-Cycle Checkpoints

Molecular Basis for Cell-Cycle Checkpoints After DNA Damage

In response to DNA breaks, human cells delay their progression through the G1, S, and G2 phases of the cell cycle, potentially allowing for the repair of DNA damage (Fig 1). Central to the activation of the ionizing radiation checkpoints is the initial sensing of DNA breaks by the telomeric protein TRF2 and the MRE11-RAD50-NBS1 (MRN) complex with subsequent activation of the ATM kinase.[5,6] ATM is a member of the phosphatidylinositol 3-kinase-like family of serine/threonine protein kinases (PIKKs). Other members of this family include the ATM- and Rad3-related (ATR) kinase that responds to single-stranded DNA, stalled or collapsed DNA replication forks, and the DNA-dependent protein kinase catalytic subunit (DNA-PKcs), which is a DNA-dsb repair protein.[5] ATM, together with DNA-PKcs, phosphorylates the histone H2AX (called γ-H2AX when phosphorylated on serine residue

1053-4296/06/$-see front matter
doi:10.1016/j.semradonc.2005.08.007

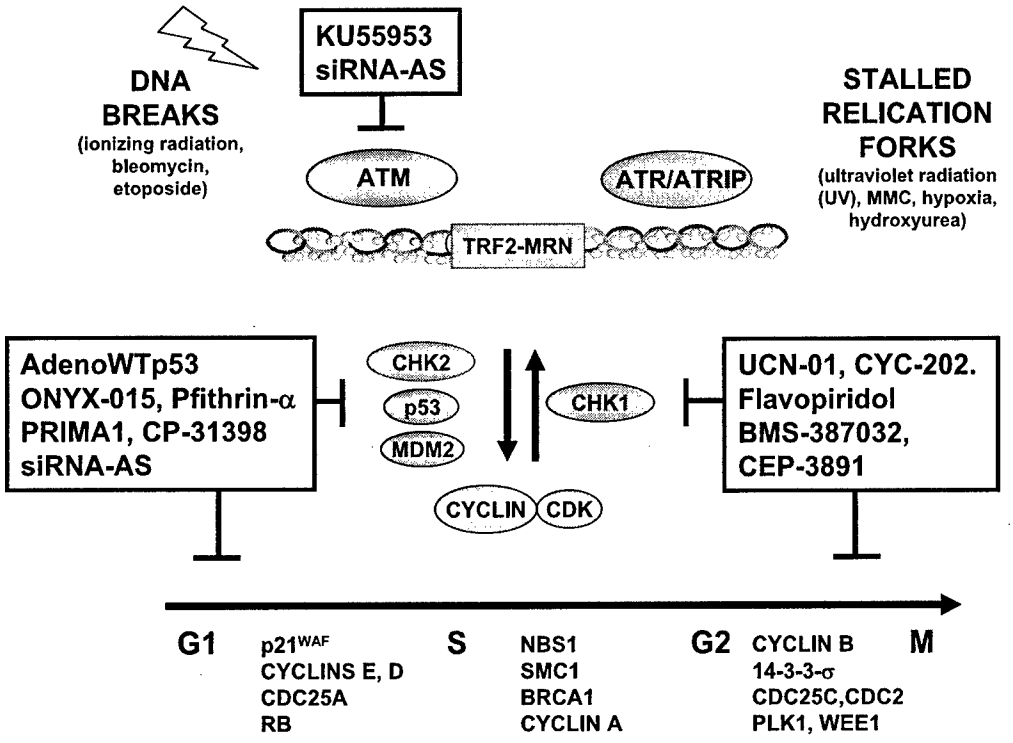

Figure 1 Radiosensitization by inhibiting cell-cycle checkpoints. Initial DNA-dsbs are recognized by the TRF2-MRN complex within 2 seconds after DNA damage. This is followed by recruitment of the ATM and ATR kinases that phosphorylate target proteins to enact the G1, S, and G2 checkpoints. These target proteins include the histone H2AX and the p53, 53BP1, CHK2, MDC1, NBS1, BRCA1, and SMC1 proteins. Distally, the G1, S, and G2 arrests are engaged by the cyclin D-CDK4, cyclin E-CDK2, RB-E2F, and cyclin B-CDC2 complexes. RNA antisense (AS) or siRNA strategies can inhibit ATM, ATR and MRN function, leading to radiosensitization. Reconstitution of normal wild-type p53 function in tumors can be achieved through gene therapy (eg, adenoviralWTp53 or ONXY-015) or novel pharmaceuticals (eg, CP-31398, PRIMA1). Finally, there are a number of ATM (eg, KU55953), CDK (eg, CYC-202 (roscovitine), BMS-387032), and CHK1 (eg, UCN-01) inhibitors that prevent cells from repairing DNA-dsbs before entry into mitosis and promote mitotic catastrophe and radiation cell kill. (Color version of figure is available online.)

139) along megabase-length tracks surrounding a DNA break. The MRN complex acts as an initial damage "beacon" for DNA-dsb repair proteins or proteins involved in signal transduction of the damage including BRCA1, MDC1, p53, MDM2, 53BP1, CHK2, and CHK1, which engage G1, S, and G2 cell-cycle arrests (Fig 1).[2,5]

The ATM-dependent G1 checkpoint is mediated by the p53 tumor suppressor protein and the CHK2 kinase. Their concerted actions through $p21^{WAF}$ and CDC25A alter the activity of cyclin E-CDK and retinoblastoma protein complexes at the G1-S interface and initiation of DNA replication. The ATM-dependent intra—S-phase checkpoint is controlled by both ATM-CHK2-CDC25A signaling and alternate phosphorylation of BRCA1, NBS1, FANCD2, and SMC1 proteins. The p53, 53BP-1, CHK1, and CHK2 proteins act as downstream mediators of ATM and ATR in the G2 checkpoint mediated by cyclin B-CDC2. After DNA damage, CHK2 and CHK1 phosphorylate CDC25C to inhibit its activity toward cyclin B-CDC2 and the cell arrests in G2/M. p53 also upregulates 14-3-3-σ, which subsequently sequesters CDC25C into the cytoplasm also culminating in an inactive cyclin B-CDC2 complex. Together the ATM and ATR pathways and their associated checkpoints represent exciting targets for therapy if tumor-specificity can be achieved. For further details, the reader is referred to specific reviews of these pathways.[5,7,8]

Targeting ATM-p53

Strategies designed to exploit the ATM-p53 pathway are based on the assumption that ATM signaling or p53 function is inactive within tumor cells because of gene mutation or protein degradation (eg, p53 degraded by the oncoproteins HPV-E6 or MDM2).[7] Although not universal, human tumors coexpressing mutant p53 and other oncogenes can show decreased rates of local control after radiotherapy.[7] In more recent studies, a single-nucleotide polymorphism (SNP) at p53 codon 72 has been correlated with sensitization of tumor cells to radiotherapy and chemotherapy in vitro and in vivo through increased levels of apoptosis.[9] Therefore, SNP and/or mutation analyses within normal and tumor tissues may soon drive the rational design of ATM-p53 pathway–specific therapies.

The nonspecific PIKK inhibitors wortmannin and caffeine have been used preclinically to sensitize tumor cells through inhibition of ATM; however, both agents are too toxic in vivo for clinical use.[10] ATM has been targeted in prostate cancer cells using specific antisense or siRNA; however, there was

only a moderate decrease in ATM expression and resultant radiosensitization (eg, dose-reduction factor of 1.4).[11] More recently, Hickson and colleagues[12] have reported the discovery of a specific ATM inhibitor, KU55933, by screening of a small molecular-compound library. With an inhibitory ICD50 value of 13 nmol/L, KU55933 decreased ATM phosphorylation of p53, NBS1, γH2AX, SMC1 and inhibited ATM-medicated checkpoints. Radiosensitization and chemosensitization to etoposide, doxorubicin, and camptothecin in HeLa cells using KU55933 produced sensitizer enhancement ratios ranging from 2.6 to 36.5.[12] At the present time, data are not available for differential radiosensitization of tumor over normal tissues.

Small-molecule inhibitors or peptides have been developed to bind to mutant forms of p53 (MTp53) and revert them to wild-type (WTp53) conformation. Two examples of these compounds are CP-31398 and PRIMA-1.[7] Both induce cell-cycle arrest and/or apoptosis in vitro; however, no preclinical data yet exist for these agents as radiosensitizers. In addition, the use of small molecules to mimic downstream $p21^{WAF}$, MDM2, or BAX activity can reactivate G1 and G2 checkpoints or apoptotic cascades and engage WTp53-mediated radiosensitization.[7]

WTp53 function in tumor cells can also be reconstituted through intratumoral or systemic (liposomal) delivery of adenoviral WTp53 (Ad-WTp53).[7] In both preclinical studies and phase I-III clinical trials, this has led to stimulation of cell-cycle arrests and apoptosis and also suppressed DNA-dsb repair.[13] Complete or partial responses have been achieved in lung cancer patients using this agent in combination with radiotherapy.[13] ONYX-015 is an adenovirus that lacks the E1B-55K gene product for p53 degradation and therefore was designed to selectively replicate within, and kill, p53-defective tumor cells. Although p53-dependent responses have not been universally shown, this agent has been used in more than 250 patients in 15 clinical trials using a variety of delivery strategies. It has elicited partial and complete responses when combined with chemotherapy or radiotherapy in sarcoma, head and neck, lung, and brain tumors.[14] Problems with intratumoral delivery, viral immune-mediated clearance, and lack of viral replication when given with chemotherapy, have slowed this agent's widespread clinical use.

Increases in the therapeutic ratio could also stem from a radioprotection of normal tissues. Pifithrin-α is a chemical inhibitor of p53 that was found to radioprotect mice from the gastrointestinal radiation syndrome.[15] However, a theoretical concern is that this agent will also reduce the anticarcinogenic effect of WTp53, resulting in radiation-induced carcinogenesis. This could be clinically relevant for intensity-modulated radiotherapy protocols in which multiple beams lead to large volumes of normal tissues receiving small daily radiation doses.[7]

Targeting ATR, CHK1, and the G2 Checkpoint

If the G2/M checkpoint is inhibited, this results in the catastrophic segregation of damaged, partially repaired chromosomes and mitotic cell death.[10] Targeting ATR, CHK1, and other G2 checkpoint-associated proteins in tumor cells, in combination with chemo- or radiotherapy such that they enter mitosis inappropriately, is an attractive therapeutic concept (Fig 1). Tumor cells usually lack a normal G1 checkpoint and rely more on the S and G2 checkpoints for survival when compared with normal cells.[16] This led to promising initial studies using caffeine, pentoxifylline, and staurosporine as G2-checkpoint inhibitors and radiosensitizers of tumor cells in vitro, but some proved too toxic for use in vivo.[10]

Other G2-inhibitors include nonspecific protein kinase inhibitors, such as UCN-01, and more selective cyclin-dependent kinase (CDK) antagonists, such as flavopiridol (see Table 1). These agents are in various stages of clinical trials. Single-agent and combined-modality phase I-II trials of UCN-01 and flavopiridol have shown dose-limiting toxicity that includes arrhythmias, syncope, nausea/vomiting, hypoxemia, and insulin-resistant hyperglycemia.[16] Several newer compounds have been identified that inhibit CHK1 with varying degrees of specificity.[10,16,17] For example, high-throughput screening of novel compound libraries have identified CDK inhibitors that target CDK1, 2, or 5 and decrease DNA-dsb repair as the basis for radiosensitization. These agents (eg, CYC-202-roscovitine and BMS-387032) are currently being tested in phase I/II lung and breast cancer trials.[16]

The use of UCN-01, or the expression of siRNA or dominant negative alleles against CHK1, abrogates the S and G_2 checkpoints and can sensitize MTp53-expressing cells to radiation.[10,16,18,19] A recent report shows that concomitant siRNA knockdown of both ATM and CHK1 (ie, targeting ATM signaling and the G2 checkpoints) radiosensitized prostate cancer cells in a p53-dependent manner. This result suggested a potential therapeutic ratio for irradiating tumors with nonfunctional p53 protein relative to WTp53-expressing normal tissues[20]; however, p53-independent radiosensitization has also been reported with CHK1-inhibition.[16]

Increased tumor cell kill in vivo with the use of these CHK1/CDK agents, in combination with radiotherapy, is predicted by preclinical studies showing synergistic radiosensitization by UCN-01 with fractionated radiotherapy.[21] A caveat to all these studies is a recent report showing that CHK1 is required during normal S-phase progression to avoid aberrantly increased initiation of DNA replication, thereby guarding against generation of potentially harmful DNA lesions.[19] If normal tissues are also sensitized to DNA breaks and/or genetic instability by CHK1-inhibition, the therapeutic ratio could be lost.

Targeting DNA Repair Pathways

One of the central radiobiological tenets is that DNA is an important target for the biological effects of ionizing radiation. Human DNA-dsbs are repaired mainly through 2 pathways that can both interact and compete with each other across cell-cycle transitions. These include homologous recombination (HR) and nonhomologous recombination (ie, end-joining or NHEJ) (Fig 2 and Table 1).[2] Strategies that target DNA repair pathways preferentially in tumor cells (eg, using chemoradiation or DNA repair inhibitors) may augment clinical radiotherapy response

Table 1 Evidence for Radiosensitization Using Chemical Inhibitors of Cell-Cycle Checkpoint Control, DNA Repair, and the Proteasome

Agent	Target/Action	Evidence for Radiosensitization
Checkpoint inhibitors		
UCN-01	CHK1; inhibits G2 checkpoint	In vitro: sensitizes colon, breast, lymphoma, cervix, lung cancer cell lines In vivo: synergistic growth delay in murine fibrosarcoma following fractionated radiotherapy in vivo; clinical trials ongoing
Flavopiridol	Non-specific for CDK; inhibits G2 checkpoint and DNA-dsb repair	In vitro: sensitizes esophageal and colon cancer cell lines In vivo: increased growth delay in murine tumors and colon cancer xenografts; clinical trials ongoing
Roscovitine(CYC-202)	CDK1/CDK2/CDK5; inhibits DNA-dsb repair	In vitro: sensitizes breast cancer cell lines In vivo: increased growth delay in breast cancer xenografts; clinical trials ongoing
CEP-3891	CHK1; inhibits S and G2 checkpoint	In vitro: sensitized osteosarcoma cells
KU55953	ATM; inhibits G1 and G2 checkpoints and DNA-dsb repair	In vitro: sensitized HeLa cells
AdenoWTp53	p53; inhibits cell cycle arrests and DNA-dsb repair and induces apoptosis	In vitro: sensitizes brain, lung, prostate, and head and neck cancer cell lines In vivo: complete and partial clinical responses in lung cancer; clinical trials ongoing
ONYX-015	p53; targets MTp53-expressing tumors through cell cycle arrest and apoptosis	In vitro: sensitizes colon and thyroid cancer cell lines In vivo: sensitized glioma xenografts in vivo; clinical trials ongoing
DNA repair inhibitors		
Vanillin, SU1172, IC886, NU7163, NU7026	DNA-PKcs and NHEJ; inhibits DNA-dsb repair	In vitro: sensitizes ovarian, HeLa, glioma, CHO, and fibroblast cells
Imatinib	c-ABL; inhibits RAD51/HR and DNA-dsb repair	In vitro: sensitizes leukemic and glioma cells
3-AB, ISQ, NU1025, KU0058684 or AG14361	PARP; inhibits DNA-ssb repair and homologous recombination	In vitro: sensitizes prostate, lung, and lymphoma cancer cell lines In vivo: AG14361 sensitized colon cancer xenografts
Proteasome inhibitors		
PS-341 (bortezomib)	26S proteasome; altered apoptosis, cell cycle arrest and signal tranduction	In vitro: sensitizes melanoma, lymphoma, colon cancer cell lines In vivo: sensitized colon cancer xenografts; clinical trials ongoing
Ritonavir, saquinavir	26 proteasome; HIV protease	In vitro: sensitizes glioma and prostate cancer cell lines

Abbreviations: NHEJ, nonhomologous end-joining; HR, homologous recombination; PARP, poly(ADP-ribose) polymerase-1; HIV, human immunodeficiency virus; DNA-dsb, DNA double-strand break; MTp53, mutant p53. Data from the following references.[1,2,7,8,10,11,13,14,16,18,28,31,32,37,41,44,48]

given correlations between DNA repair gene expression and radiosensitivity.[2,22,23] Indeed, cisplatin and gemcitabine are among the most effective clinical radiosensitizers, and recent reports suggest these drugs can act in part by inhibiting HR and NHEJ.[3,4] These observations support the concept that the predetermination of the repair capacity of tumor cells may help select appropriate agents for use in combination with radiotherapy.[2,24,25]

Targeting HR: RAD51, BRCA1/2, and PARP

HR is an error-free pathway operational in S and G2 phase and involves RAD51, its paralogs RAD51B/C/D and

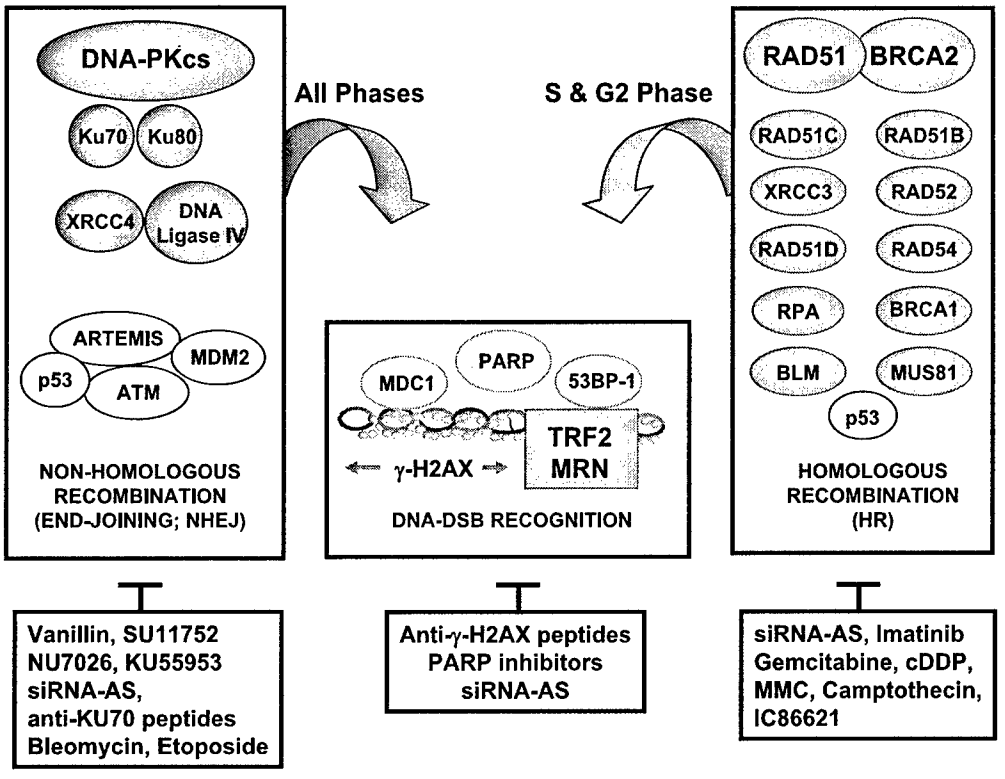

Figure 2 Radiosensitization by inhibiting DNA repair. The DNA-dsb is the most cytotoxic DNA lesion produced by ionizing radiation. Initially, DNA break sensing by TRF2-MRN leads to the recruitment of 53BP-1, MDC1, BRCA1, and specific DNA-dsb repair proteins within γ-H2AX–positive chromatin. Human DNA-dsbs are repaired mainly HR or nonhomologous recombination (ie, end-joining or NHEJ) in a cell-cycle specific manner. Radio- or chemosensitization can be achieved by the use of siRNA, antisense, or small-molecule inhibitors that block DNA-PK, ATM, or RAD51-BRCA2 function. The repair of DNA-ssbs and DNA base damage is mediated by the base excision repair pathway, including the PARP protein. PARP can be inhibited by 3-AB, ISQ, NU1025, KU0058684, or AG14361, and in the context of cells that are BRCA1 or BRCA2-deficient, these inhibitors lead to cell death because of the persistence of DNA lesions normally repaired by homologous recombination. (Color version of figure is available online.)

XRCC2/3, and p53, RPA, BRCA2, BLM, and MUS81.[26] The relative capacity for HR among various cell lines can be determined using plasmid repair and sister-chromatid exchange assays and the relative sensitivity to cross-linking and alkylating agents such as mitomycin C, cisplatin (cDDP), camptothecin, hydroxyurea and gemcitabine.[2,4,26] The overexpression of RAD51 has been linked to cellular resistance to chlorambucil, nitrogen mustard, caffeine, methylmethane sulfonate (MMS), gemcitabine, cisplatin, mitomycin C (MMC), and variably to ionizing radiation.[2,24,26,27] The BRCA1 and BRCA2 cancer-susceptibility proteins are also novel HR targets. BRCA1/2-defective cells have reduced RAD51 activity and foci formation and increased sensitivity to ionizing radiation and mitomycin C in vitro.[2,26,28]

Investigators have observed increased radiosensitization in vitro and in vivo by treating lung, glioma, and prostate tumor cells with siRNA or antisense to RAD51.[2,24,29] Targeting HR in this manner could exploit the therapeutic ratio because many normal tissues have a relatively slow cell turnover with an increased fraction of cells in the G1 phase (ie, NHEJ responsive). In contrast, malignant cells that have increased cells in the S and G2 phases may be more amenable to HR targeting (this may also increase siRNA uptake). RAD51 expression can also be inhibited by imatinib mesylate, an inhibitor of the c-ABL, c-KIT, and platelet-derived growth factor (PDGF) pathways. DNA damage leads to a c-ABL–dependent upregulation and phosphorylation of RAD51 allowing for foci formation at sites of DNA damage within a complex containing RAD52 and ATM. Treating leukemic cancer , prostate cancer, or glioma cells with imatinib sensitizes them to cross-linking agents and ionizing radiation in vitro.[30,31] This agent is already in clinical use for chronic myelogenous leukemia and selected solid tumors, yet clinical trials of radiosensitization have not yet been reported.

Poly (ADP-ribose) polymerase (PARP) facilitates base excision repair and binds DNA single-strand breaks (DNA-ssbs). PARP inhibitors such as 3-AB, ISQ, NU1025, KU0058684, or AG14361 can act as radiosensitizers in vitro and in vivo and trigger γ-H2AX and RAD51 foci formation.[32] Recently, it has been observed that BRCA1 or BRCA2 deficiency profoundly sensitizes cells to the inhibition of PARP enzymatic activity. The resulting chromosomal instability, cell-cycle arrest, and subsequent apoptosis is a result of persisting DNA lesions that would normally be repaired through homologous recombination.[33] This novel result could be clinically exploited to selectively kill BRCA2-

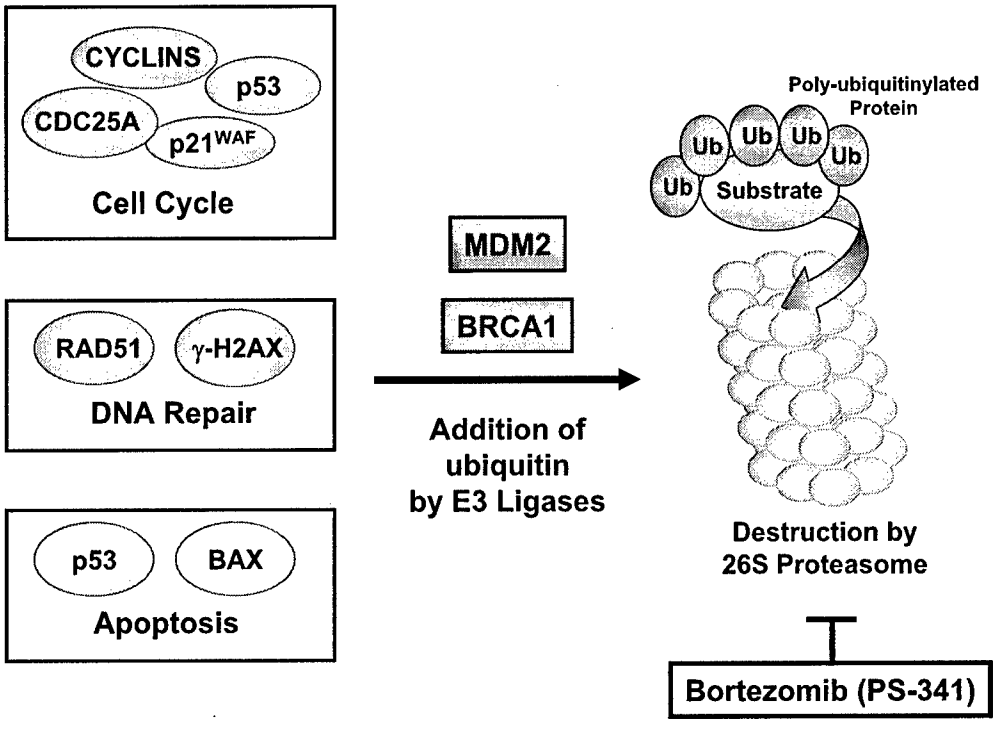

Figure 3 Radiosensitization by inhibiting the proteasome.

Ubiquitin-mediated degradation of regulatory proteins by the 26S proteasome plays an important role after irradiation by targeting proteins involved in cell-cycle progression, DNA repair, signal transduction, and transcriptional regulation (eg, cyclins, p53 and $p21^{WAF}$, RAD51, BAX). Proteins that are targeted for destruction become polyubiquitinylated by E3 ligases that include the BRCA1-BARD1 repair complex and the MDM2 protein (involved in p53 turnover). The peptide boronic acid compound, PS-341, inhibits proteasome activity and is currently in clinical trials. (Color version of figure is available online.)

deficient tumors by using PARP inhibition, in combination with chemotherapy or radiotherapy.

Targeting NHEJ: DNA-PK and γ-H2AX

NHEJ requires little homology at the DNA ends and can be operational during any phase of the cell cycle but is probably preferential to G1. NHEJ involves the proteins KU70/80, DNA-PKcs, Artemis, XRCC4, DNA ligase IV, and more recently, ATM, p53, and MDM2.[34,35] DNA-PK (consisting of DNA-PKcs and the Ku70/80 heterodimer) has emerged as a possible genetic target for molecular radiotherapeutics using siRNA, antisense, and novel inhibitory small molecules (Fig 2 and Table 1). Inhibition of DNA-PK has led to increased radiosensitization in vitro and in vivo in lung, colon, prostate, and brain cancer models but, unfortunately, also in normal human fibroblasts.[2,11,36] This latter observation may have important implications for normal tissue toxicity and an unfavorable therapeutic ratio. Reducing the level of DNA-PKcs may also affect the levels of other PIKKs, including ATM, which may augment radiosensitization.[36] Novel small-molecule inhibitors of DNA-PKcs have been tested both in vitro and in vivo (eg IC86621, NU7441 and NU7026, the vanillins, and SU11752). Some of these agents have greater than 100-fold or greater selectivity when compared with the activity of wortmannin.[37-39]

Within minutes of irradiation, γ-H2AX foci form in a dose-dependent manner at the site of DNA breaks.[2] The number and resolution of these foci over time is an indicator of global DNA-dsb repair and correlates to tumor cell radiosensitivity under oxic and hypoxic conditions.[2,40] Interfering with γ-H2AX signaling could alter the radiosensitivity of cells. For example, peptide mimics of the H2AX carboxy-terminus (where the Ser139 residue is phosphorylated during DNA damage) or H2AX gene knockdown can radiosensitize murine and human tumor cells in vitro and in vivo.[25] At present, the clinical utility of anti-DNA-PK or anti-H2AX strategies has not been realized.

Inhibiting the Proteasome

The proteasome is a multisubunit protease complex that is involved in the turnover of cellular proteins via degradation and recycling (Fig 3 and Table 1). In this ubiquitin (Ub)/proteasome pathway, proteins are targeted for degradation by conjugation to polymers of the 8-kDa polypeptide (ATP) ubiquitin and are degraded via an adenosine triphosphate–dependent process.[41] Over 80% of all cellular polyubiquitinylated proteins are recycled through the proteasome. The activation and conjugation of ubiquitin is, in part, mediated by E3 protein ligases, which include the BRCA1-BARD1 complex and the MDM2 protein. These ligases target the RAD51 and p53 proteins for proteasomal degradation, respectively.[41]

Ubiquitin-mediated degradation of regulatory proteins may play an important role in the radioresponse of tumor and normal cells because they target proteins involved in cell-cycle progression, signal transduction, transcriptional regulation, DNA repair, and cell death including histones: BAX, $p21^{WAF}$, $p27^{KIP}$, p53, RAD51, cyclins (D,E,B), PARP, and nuclear-factor kappa β (NF-kappaβ).[41,42] NF-kappaβ binds to its target sites (ie, kappaβ sites in the DNA) to initiate transcription after irradiation and along with antiapoptotic proteins may be a critical target for chemical inhibitors of proteasome inhibition.[41,43]

Bortezomib (PS-341) is a dipeptide boronic acid that inhibits tumor-cell or xenograft proliferation. PS-341 can ra-

diosensitize a variety of tumor cell types in vitro and in vivo potentially by inhibiting NF-kappaβor BCL-2.[41,44] Other proteasome inhibitors that can radiosensitize tumor cells include the HIV-protease inhibitors saquinavir and ritonavir.[41,45] Although a promising approach to clinical radiosensitization, Phase I or II trials using radiotherapy combined with proteasomal inhibitors have not yet been reported.

Conclusions and Outstanding Questions

Although exciting in concept, clinical trial data for many of these agents in combination with radiotherapy is still lacking. The relative sensitization in vitro may not predict the sensitization achieved in vivo because of microenvironmental factors or altered pharmacodynamics.[24] However, biomarker analyses may help. The temporal tracking of intranuclear focal complexes in situ using specific antibodies to activated checkpoint or DNA repair proteins (eg, tracking RAD51-BRCA2, DNA-PKcs, γ-H2AX, or ATM-Ser1981), in relation to hypoxia biomarkers, could provide a quantitative measure of DNA repair or genetic stability on a tissue-specific basis. Quantitation of these foci in vivo may therefore be useful in determining the efficacy of DNA repair inhibitors in combination with radiotherapy.[2,24,46,47]

The success of these agents is also dependent inhibiting DNA damage and repair responses in tumor cells, but not normal cells.[48] They must also not increase genetic instability within irradiated tissues.[19] We currently know little about the relative molecular repair responses among the different types of normal tissues after fractionated irradiation. This information will be required for the judicious choice of repair-based agents in combination with radiotherapy.

References

1. Faulhaber O, Bristow RG: Basis of cell kill following clinical radiotherapy, in Sluyser, Mels (eds): Application of Apoptosis to Cancer Treatment.Dordrecht, The Netherlands, Springer Publishing, 2005
2. Bristow RG, Harrington L: Genetic instability and DNA repair, in Tannock IFHR, Harrington L, Bristow RG (eds): The Basic Science of Oncology.4th ed.New York, McGraw-Hill Ltd, 2005, p 77-99
3. Diggle CP, Bentley J, Knowles MA, et al: Inhibition of double-strand break non-homologous end-joining by cisplatin adducts in human cell extracts. Nucleic Acids Res 33:2531-2539, 2005
4. Wachters FM, van Putten JW, Maring JG, et al: Selective targeting of homologous DNA recombination repair by gemcitabine. Int J Radiat Oncol Biol Phys 57:553-562, 2003
5. Lukas J, Lukas C, Bartek J: Mammalian cell cycle checkpoints: signalling pathways and their organization in space and time. DNA Repair (Amst) 3:997-1007, 2004
6. Bradshaw PS, Stavropoulos DJ, Meyn MS: Human telomeric protein TRF2 associates with genomic double-strand breaks as an early response to DNA damage. Nat Genet 37:193-197, 2005
7. Cuddihy AR, Bristow RG: The p53 protein family and radiation sensitivity: Yes or no? Cancer Metastasis Rev 23:237-257, 2004
8. Wilson GD: Radiation and the cell cycle, revisited. Cancer Metastasis Rev 23:209-225, 2004
9. Sullivan A, Syed N, Gasco M, et al: Polymorphism in wild-type p53 modulates response to chemotherapy in vitro and in vivo. Oncogene 23:3328-3337, 2004
10. Eastman A: Cell cycle checkpoints and their impact on anticancer therapeutic strategies. J Cell Biochem 91:223-231, 2004
11. Collis SJ, Swartz MJ, Nelson WG, et al: Enhanced radiation and chemotherapy-mediated cell killing of human cancer cells by small inhibitory RNA silencing of DNA repair factors. Cancer Res 63:1550-1554, 2003
12. Hickson I, Zhao Y, Richardson CJ, et al: Identification and characterization of a novel and specific inhibitor of the ataxia-telangiectasia mutated kinase ATM. Cancer Res 64:9152-9159, 2004
13. Swisher SG, Roth JA, Komaki R, et al: Induction of p53-regulated genes and tumor regression in lung cancer patients after intratumoral delivery of adenoviral p53 (INGN 201) and radiation therapy. Clin Cancer Res 9:93-101, 2003
14. Wildner O: Clinical trials: The sensitizing side of Onyx-015. Gene Ther 12:386-387, 2005
15. Komarov PG, Komarova EA, Kondratov RV, et al: A chemical inhibitor of p53 that protects mice from the side effects of cancer therapy. Science 285:1733-1737, 1999
16. Kawabe T: G2 checkpoint abrogators as anticancer drugs. Mol Cancer Ther 3:513-519, 2004
17. Noble ME, Endicott JA, Johnson LN: Protein kinase inhibitors: Insights into drug design from structure. Science 303:1800-1805, 2004
18. Xiao HH, Makeyev Y, Butler J, et al: 7-Hydroxystaurosporine (UCN-01) preferentially sensitizes cells with a disrupted TP53 to gamma radiation in lung cancer cell lines. Radiat Res 158:84-93, 2002
19. Syljuasen RG, Sorensen CS, Hansen LT, et al: Inhibition of human Chk1 causes increased initiation of DNA replication, phosphorylation of ATR targets, and DNA breakage. Mol Cell Biol 25:3553-3562, 2005
20. Mukhopadhyay UK, Senderowicz AM, Ferbeyre G: RNA silencing of checkpoint regulators sensitizes p53-defective prostate cancer cells to chemotherapy while sparing normal cells. Cancer Res 65:2872-2881, 2005
21. Tsuchida E, Urano M: The effect of UCN-01 (7-hydroxystaurosporine), a potent inhibitor of protein kinase C, on fractionated radiotherapy or daily chemotherapy of a murine fibrosarcoma. Int J Radiat Oncol Biol Phys 39:1153-1161, 1997
22. Bishay K, Ory K, Olivier MF, et al: DNA damage-related RNA expression to assess individual sensitivity to ionizing radiation. Carcinogenesis 22:1179-1183, 2001
23. Djuzenova C, Muhl B, Schakowski R, et al: Normal expression of DNA repair proteins, hMre11, Rad50 and Rad51 but protracted formation of Rad50 containing foci in X-irradiated skin fibroblasts from radiosensitive cancer patients. Br J Cancer 90:2356-2363, 2004
24. Fan R, Kumaravel TS, Jalali F, et al: Defective DNA strand break repair after DNA damage in prostate cancer cells: implications for genetic instability and prostate cancer progression. Cancer Res 64:8526-8533, 2004
25. Taneja N, Davis M, Choy JS, et al: Histone H2AX phosphorylation as a predictor of radiosensitivity and target for radiotherapy. J Biol Chem 279:2273-2280, 2004
26. Wyman C, Ristic D, Kanaar R: Homologous recombination-mediated double-strand break repair. DNA Repair (Amst) 3:827-833, 2004
27. Raderschall E, Stout K, Freier S, et al: Elevated levels of Rad51 recombination protein in tumor cells. Cancer Res 62:219-225, 2002
28. Farmer H, McCabe N, Lord CJ, et al: Targeting the DNA repair defect in BRCA mutant cells as a therapeutic strategy. Nature 434:917-921, 2005
29. Collis SJ, Tighe A, Scott SD, et al: Ribozyme minigene-mediated RAD51 down-regulation increases radiosensitivity of human prostate cancer cells. Nucleic Acids Res 29:1534-1538, 2001.
30. Russell JS, Brady K, Burgan WE, et al: Gleevec-mediated inhibition of Rad51 expression and enhancement of tumor cell radiosensitivity. Cancer Res 63:7377-7383, 2003
31. Slupianek A, Schmutte C, Tombline G, et al: BCR/ABL regulates mammalian RecA homologs, resulting in drug resistance. Mol Cell 8:795-806, 2001
32. Soldatenkov VA, Potaman VN: DNA-binding properties of poly(ADP-ribose) polymerase: a target for anticancer therapy. Curr Drug Targets 5:357-365, 2004
33. Bryant HE, Schultz N, Thomas HD, et al: Specific killing of BRCA2-

deficient tumours with inhibitors of poly(ADP-ribose) polymerase. Nature 434:913-917, 2005
34. Weterings E, van Gent DC: The mechanism of non-homologous end-joining: A synopsis of synapsis. DNA Repair 3:1425-1435, 2004
35. Riballo E, Kuhne M, Rief N, et al: A pathway of double-strand break rejoining dependent upon ATM, Artemis, and proteins locating to gamma-H2AX foci. Mol Cell 16:715-724, 2004
36. Peng Y, Woods RG, Beamish H, et al: Deficiency in the catalytic subunit of DNA-dependent protein kinase causes down-regulation of ATM. Cancer Res 65:1670-1677, 2005
37. Durant S, Karran P: Vanillins—A novel family of DNA-PK inhibitors. Nucleic Acids Res 31:5501-5512, 2003
38. Willmore E, de Caux S, Sunter NJ, et al: A novel DNA-dependent protein kinase inhibitor, NU7026, potentiates the cytotoxicity of topoisomerase II poisons used in the treatment of leukemia. Blood 103: 4659–4565, 2004
39. Veuger SJ, Curtin NJ, Richardson CJ, et al: Radiosensitization and DNA repair inhibition by the combined use of novel inhibitors of DNA-dependent protein kinase and poly(ADP-ribose) polymerase-1. Cancer Res 63:6008-6115, 2003
40. Banath JP, Macphail SH, Olive PL: Radiation sensitivity, H2AX phosphorylation, and kinetics of repair of DNA strand breaks in irradiated cervical cancer cell lines. Cancer Res 64:7144-7149, 2004
41. McBride WH, Iwamoto KS, Syljuasen R, et al: The role of the ubiquitin/proteasome system in cellular responses to radiation. Oncogene 22: 5755-5773, 2003
42. Krogan NJ, Lam MH, Fillingham J, et al: Proteasome involvement in the repair of DNA double-strand breaks. Mol Cell 16:1027-1034, 2004
43. Kurland JF, Meyn RE: Protease inhibitors restore radiation-induced apoptosis to Bcl-2-expressing lymphoma cells. Int J Cancer 96:327-333, 2001
44. Teicher BA, Ara G, Herbst R, et al: The proteasome inhibitor PS-341 in cancer therapy. Clin Cancer Res 5:2638-2645, 1999
45. Pajonk F, Himmelsbach J, Riess K, et al: The human immunodeficiency virus (HIV)-1 protease inhibitor saquinavir inhibits proteasome function and causes apoptosis and radiosensitization in non-HIV-associated human cancer cells. Cancer Res 62:5230-5235, 2002
46. Bartkova J, Horejsi Z, Koed K, et al: DNA damage response as a candidate anti-cancer barrier in early human tumorigenesis. Nature 434: 864-870, 2005
47. Qvarnstrom OF, Simonsson M, Johansson KA, et al: DNA double strand break quantification in skin biopsies. Radiother Oncol 72:311-317, 2004
48. Ma BB, Bristow RG, Kim J, et al: Combined-modality treatment of solid tumors using radiotherapy and molecular targeted agents. J Clin Oncol 21:2760-2776, 2003

MOLECULAR AND CELLULAR BIOLOGY, Oct. 2004, p. 8504–8518 Vol. 24, No. 19
0270-7306/04/$08.00+0 DOI: 10.1128/MCB.24.19.8504–8518.2004

Down-Regulation of Rad51 and Decreased Homologous Recombination in Hypoxic Cancer Cells

Ranjit S. Bindra,[1,2] Paul J. Schaffer,[3] Alice Meng,[4] Jennifer Woo,[4] Kårstein Måseide,[4] Matt E. Roth,[3] Paul Lizardi,[2,3] David W. Hedley,[4] Robert G. Bristow,[4] and Peter M. Glazer[1,5]*

Department of Therapeutic Radiology,[1] Department of Experimental Pathology,[2] and Department of Genetics,[5] Yale University School of Medicine, and Agilix Corporation,[3] New Haven, Connecticut, and Ontario Cancer Institute/Princess Margaret Hospital (University Health Network) and Department of Medical Biophysics, University of Toronto, Toronto, Ontario, Canada[4]

Received 16 April 2004/Returned for modification 24 May 2004/Accepted 6 July 2004

There is an emerging concept that acquired genetic instability in cancer cells can arise from the dysregulation of critical DNA repair pathways due to cell stresses such as inflammation and hypoxia. Here we report that hypoxia specifically down-regulates the expression of *RAD51*, a key mediator of homologous recombination in mammalian cells. Decreased levels of Rad51 were observed in multiple cancer cell types during hypoxic exposure and were not associated with the cell cycle profile or with expression of hypoxia-inducible factor. Analyses of *RAD51* gene promoter activity, as well as mRNA and protein stability, indicate that the hypoxia-mediated regulation of this gene occurs via transcriptional repression. Decreased expression of Rad51 was also observed to persist in posthypoxic cells for as long as 48 h following reoxygenation. Correspondingly, we found reduced levels of homologous recombination in both hypoxic and posthypoxic cells, suggesting that the hypoxia-associated reduction in Rad51 expression has functional consequences for DNA repair. In addition, hypoxia-mediated down-regulation of Rad51 was confirmed in vivo via immunofluorescent image analysis of experimental tumors in mice. Based on these findings, we propose a novel mechanism of genetic instability in the tumor microenvironment mediated by hypoxia-induced suppression of the homologous recombination pathway in cancer cells. The aberrant regulation of Rad51 expression may also create heterogeneity in the DNA damage response among cells within tumors, with implications for the response to cancer therapies.

Solid tumors constitute a unique tissue type, characterized by hypoxia, low pH, and nutrient deprivation (45). Although decreased oxygen tension is potentially toxic to normal human cells, cancer cells acquire genetic and adaptive changes allowing them to survive and proliferate in a hypoxic microenvironment. Intratumoral hypoxia induces profound alterations in numerous physiological processes, including altered glucose metabolism, up-regulated angiogenesis, increased invasive capacity, and dysregulation of apoptotic programs (37).

From a clinical standpoint, many studies have established hypoxia as an independent and adverse prognostic variable in patients with head and neck, cervical, or soft tissue (sarcoma) tumors (3, 26). With regard to the extent of hypoxia observed in tumors, it has been proposed that cells within hypoxic regions of solid tumors often derive almost all metabolic energy requirements from up-regulated glycolytic pathways. This phenomenon has been referred to as the Pasteur effect (34) and provides a partial physiologic explanation for the viability of tumor cells exposed to severe hypoxia within the tumor microenvironment. Polarographic needle electrode studies used to measure oxygen tension directly in cancer patients have revealed that a significant proportion of breast carcinomas (up to 40%) contain regions of severely decreased oxygen tension (0 to 2.5 mm Hg, compared to the normal tissue range of 24 to 66 mm Hg) while still supporting viable tumor cells (40). In addition, hypoxic cells are more resistant to radiotherapy and chemotherapy; this resistance represents a significant challenge in achieving maximal treatment efficacy (32). Collectively, these studies underscore the importance of elucidating the effects of hypoxia at the molecular level and the mechanisms by which such conditions can lead to a more aggressive phenotype and tumor progression.

Tumor progression has been specifically correlated with genetic instability (27). Furthermore, it has long been argued that the large number of mutations found in malignant cells cannot be accounted for by the low rate of mutation observed in somatic cells, leading to the suggestion that cancer cells assume a mutator phenotype during tumorigenesis (23). We and others have proposed that the tumor microenvironment contributes to such genetic instability (31). Indeed, several studies using both reporter genes and endogenous loci have demonstrated increased mutation rates in cells grown in tumors relative to those in identical cells grown in culture (22, 29, 31). Hypoxia appears to be a key microenvironmental factor involved in the development of genetic instability. Studies have suggested that it is associated with increased DNA damage, enhanced mutagenesis, and functional impairment in DNA repair pathways. With regard to DNA damage, hypoxia and subsequent reoxygenation induce DNA strand breaks and oxidative base damage such as 8-oxoguanine and thymine glycols (47). Exposure of cells in culture to hypoxic conditions yields increased frequencies of point mutations at reporter gene loci (31). Hypoxia-reoxygenation cycles are also associated with other genetic aberrations, including gene amplification and DNA overreplication, although the mechanism by which they

* Corresponding author. Mailing address: Department of Therapeutic Radiology, Yale University School of Medicine, P.O. Box 208040, New Haven, CT 06520-8040. Phone: (203) 737-2788. Fax: (203) 737-2630. E-mail: peter.glazer@yale.edu.

occur has not been fully elucidated (7, 46). Studies in our laboratory have also established that hypoxia induces functional decreases in the nucleotide excision repair (NER) pathway (48). Additionally, it has been reported previously that severe hypoxia (0.01% O_2) specifically down-regulates the expression of the DNA mismatch repair gene *MLH1*, contributing to increased mutation rates (25). Collectively, these phenomena constitute a source of genetic instability induced by hypoxia, thus potentially accelerating the multistep process of tumor progression.

Given the dynamic and complex gene expression changes that have been observed under hypoxia, we have been investigating whether alterations in the expression of other DNA repair genes could also occur in response to hypoxia and thereby play a role in hypoxia-induced genetic instability. In the present study, we utilized transcriptome profiling to identify DNA repair pathways which may be regulated by hypoxia. We report that the expression of *RAD51*, a critical mediator of homologous recombination (HR) in mammalian cells, is specifically down-regulated by hypoxia at the mRNA level, resulting in marked decreases in the protein expression of this gene. Decreased Rad51 protein expression under hypoxia was observed in numerous cell lines from a wide range of tissues, and importantly, these decreases persisted even during the posthypoxic phase following reoxygenation. This finding is especially relevant to solid tumors that typically experience fluctuating vascular perfusion, resulting in oxygen tensions that vary spatially and temporally. Analyses of protein stability, mRNA stability, and promoter activity indicate that hypoxia regulates this gene via a mechanism involving repression of the *RAD51* gene promoter. Rad51 down-regulation also appears to be independent of both the cell cycle and hypoxia-inducible factor (HIF), since no correlations were found between Rad51 expression and either the cell cycle profile or HIF induction. We also detected significantly decreased HR in both hypoxic and posthypoxic cells, indicating that hypoxia-mediated reductions in *RAD51* gene expression have functional consequences. Hypoxia-mediated Rad51 down-regulation was also confirmed in vivo within the tumor microenvironment: we observed a consistent inverse association between staining with a hypoxia marker (EF5) and Rad51 protein expression in vivo by use of immunofluorescent image analysis of cervical and prostate cancer xenografts. We propose the existence of a hypoxic and posthypoxic phenotype in solid tumors characterized by decreased expression of critical DNA repair genes, representing a novel mechanism of acquired genetic instability within the tumor microenvironment.

MATERIALS AND METHODS

Cells. MCF-7 (HTB-22), A549, RKO, SW-480, HeLa (CCL-2), ME180, SiHa, PC3, DU145, and A431 cells were obtained from the American Type Culture Collection (Manassas, Va.) and were grown according to supplier instructions and as previously described (4). 786-0 cell lines were a gift from W. G. Kaelin and were cultured as described previously (24).

Plasmids and transfections. The HIF-1α expression vector pCEP4-HIF-1α was a generous gift from G. Semenza and has been described previously (12). The 5X-HRE luciferase reporter plasmid was a gift from Zhong Yun and has been described previously (35). Transfections were performed by using the Fugene 6 reagent (Roche Diagnostics Corporation, Indianapolis, Ind.) according to the manufacturer's recommendations.

Hypoxia exposure. Cells were exposed to hypoxia in vitro as described previously (6). Briefly, for 0.2 to 0.5% oxygen experiments, a NAPCO incubator (Precision Scientific, Winchester, Va.) was equipped with a PROOX 710 sensor (BioSpherix, Redfield, N.Y.) to regulate the flow of 100% N_2 at low pressure (<25 lb/in^2) in order to achieve a constant oxygen concentration within the entire incubator for the indicated times. The CO_2 level was maintained at 5% by using a regulated internal CO_2 regulation system. Severe hypoxia (0.01% O_2) was established as described previously (31) by using a continuous flow of a humidified mixture of 95% N_2 and 5% CO_2 gas certified to contain less than 10 ppm O_2 (Airgas Northeast, Cheshire, Conn.). Desferrioxamine mesylate (DFX) (Sigma, St. Louis, Mo.) treatment was carried out by supplementation of the culture medium at a concentration of 250 μM under normoxic conditions for 24 h.

Transcriptome profiling. Microarray analysis was performed with the GenCompass universal microarray system (Agilix Corporation, New Haven, Conn.). The specific details of this technology have been described recently (33). The data reference the UniGene database Build 161 (National Center for Biotechnology Information, Bethesda, Md.). Gene regulation was calculated by averaging the ratios of the signal intensities of the tags of each hypoxia-exposed condition to the signal intensities of the tags from the control (normoxic) cells.

Western blot analysis. Radioimmunoprecipitation assay protein lysates were prepared, and Western blot analyses were performed, as described previously (4, 25). The following antibodies were used for analysis: anti-VHL (clone IG32) and anti-Rad51 (BD Pharmingen, Franklin Lakes, N.J.), anti-tubulin (clone B-512; Sigma), anti-β-actin (Research Diagnostics, Flanders, N.J.), anti-HIF-1α (clone 54; BD Transduction Laboratories, Franklin Lakes, N.J.), and anti-Glut1 (Alpha Diagnostic International, San Antonio, Tex.). Bands were quantified by using NIH Image (version 1.63; National Institutes of Health [NIH], Bethesda, Md.). Protein bands were visualized with horseradish peroxidase-conjugated anti-mouse or anti-rabbit immunoglobulin G and an enhanced chemiluminescence detection system (Amersham Biosciences, Little Chalfont, Buckinghamshire, England).

Semiquantitative RT-PCR and qPCR analysis. Semiquantitative reverse transcriptase PCR (RT-PCR) analyses were performed using the SuperScript One-Step RT-PCR kit (Life Technologies, Carlsbad, Calif.). Primer sequences for each gene used in all analyses are listed in the next section. Linear amplification ranges were determined for each gene by using 100-ng samples of normoxic and hypoxic RNA previously analyzed by Northern blotting. RT-PCR amplification was performed according to the manufacturer's recommendations. Additional information regarding the optimized RT-PCR protocol is available upon request. Bands were quantified by using NIH Image (version 1.63) analysis of SYBR Gold (Molecular Probes, Eugene, Oreg.)- or ethidium bromide (Sigma)-stained gels. For quantitative real-time PCRs (qPCRs), primers and probes were designed with Beacon Designer 2.06 (Premier Biosoft International, Palo Alto, Calif.), and analyses were performed using the MX400 Multiplex Quantitative PCR system (Stratagene, La Jolla, Calif.) as previously described (33). Primers and probes for all analyses are available upon request.

Northern blot analysis. Total RNA was isolated by using the TRIzol RNA isolation system (Life Technologies) followed by phenol-chloroform extraction. Northern blot analyses were performed as described previously (25). The following primer pairs were used to construct the probes: for *RAD51*, 5′-TGGCC CACAACCCATTTCAC-3′ (sense) and 5′-TCAATGTACATGGCCTTTCCTT CAC-3′ (antisense); for the vascular endothelial growth factor gene (*VEGF*), 5′-CTTCACTGGATGTATTTGACTGCTGTGG-3′ (sense) and 5′-GCTAGT GACTGTCACCGATCAGGGAG-3′ (antisense). β-*Actin* primers were obtained from Ambion. Blots were visualized by autoradiography and quantified either by phosphorimager analysis or by use of NIH Image software.

Protein and mRNA stability analyses. Cells were plated in 10-cm-diameter dishes and allowed to attach for 24 h, followed by a 24-h incubation in the presence or absence of DFX (250 μm). Cycloheximide (CHX) (10 μg/ml; Sigma), as an inhibitor of protein synthesis, or actinomycin D (ActD) (5 μg/ml; Sigma), as an inhibitor of transcription, was then added to the cell cultures. Cells were harvested at the indicated times after the addition of inhibitor, and Rad51 protein and mRNA expression levels were determined by Western and Northern blotting, respectively. *RAD51* mRNA half-lives were deduced from the regression line based on mRNA degradation plots.

Luciferase reporter gene assays. For luciferase reporter gene analyses, a 1.8-kb fragment from the 5′-flanking region of the *RAD51* gene was identified by using the UCSC genome browser (University of California—Santa Cruz), isolated by genomic PCR, and subsequently subcloned into the pGL3-basic vector (Promega, Madison, Wis.). Primers are available upon request. The subcloned fragment contains the core promoter region(s) described in the Eukaryotic Promoter Database (30) and that identified by in silico analysis using the Genomatix promoter identification algorithm PromoterInspector (44). For transfection, 5×10^5 RKO cells were seeded in duplicate into 6-well culture plates and

transfected with 1 μg of each reporter construct by using the Fugene 6 reagent (Roche Diagnostics Corporation). Firefly and *Renilla* luciferase activities were measured by using the Dual-Luciferase Reporter Assay System kit (Promega) according to the manufacturer's instructions. *Renilla* luciferase activity from a cotransfected pRL-SV40 control vector (5 ng/well) was used for normalization.

Cell cycle and fluorescence-activated cell sorter (FACS) analysis. Cell cycle analyses were performed as described previously (2). Stained cells were analyzed on a Becton Dickinson FACS-Calibur flow cytometer. Data capture, density plots, and histogram construction were performed by using BD CellQuest Pro software (Becton Dickinson), and cell cycle distribution profiles were determined by using ModFit LT software (Verity House Software, Topsham, Maine).

For FACS experiments, normoxic and hypoxic cells were incubated with 10 μg of Hoechst 33342 (Molecular Probes)/ml for 1 h at 37°C in the dark. Verapamil (100 mM; Sigma) was also added to the culture medium to inhibit dye efflux during the incubation. Cells were then trypsinized and resuspended in the culture medium supplemented with 0.1% fetal bovine serum, 10 μg of Hoechst 33342 dye/ml, and 100 mM verapamil to further enhance dye uptake. Equal numbers of specific G_1- and S-phase cell populations were sorted on the basis of DNA content by using a BD FACSvantage flow cytometer fitted with a UV laser, and cells were collected in 0.5 ml of culture medium supplemented with 10% fetal bovine serum. RNA was then extracted from the isolated cells by using a modified TRIzol protocol. This technique has recently been reported to facilitate the recovery of intact mRNA from viable cells in distinct phases of the cell cycle (20).

HR assay. The shuttle vector plasmid pSupFG1/G144C, containing a *supFG1* gene with an inactivating G:C-to-C:G point mutation at position 144, has been described previously (5). For all shuttle assays, 5 μg of pSupFG1/G144C plasmid DNA was mixed with 10 μg of a PCR-generated, 1-kb homologous donor fragment containing the wild-type *supFG1* gene in 50 mM Tris (pH 6.8). After transfection of the plasmid-donor mixture into cells for the indicated times, plasmid DNA was recovered by using a modified Hirt lysate procedure, as described previously (5). The purified plasmid was then used to transform *Escherichia coli* SY302 cells by electroporation, followed by growth of the cells on indicator plates for genetic analysis of *supFG1* gene function as described previously (5).

Hypoxia immunostaining within human xenografts. For each cell line, tumor cell suspensions (50 μl) containing 5×10^5 cells were injected into the gastrocnemius muscle of SCID mice. When a tumor diameter of 4 to 5 mm was reached, the nitroimidazole hypoxic marker EF5 (Ben Venue Laboratories, Bedford, Ohio) was injected (200 μl of a 10 mM stock solution) intravenously, and tumors were excised 3 h later, placed in Tissue-TekOCT compound (Sakura Finetek, Torrance, Calif.), and snap-frozen in liquid nitrogen. Immunofluorescence analyses were performed as described previously (42). Frozen sections were incubated overnight at 4°C with a monoclonal anti-Rad51 antibody (Affinity Bioreagents, Inc., Golden, Colo.) before incubation with a donkey anti-mouse Cy3-conjugated secondary antibody (diluted 1:400; Jackson ImmunoResearch Laboratories, West Grove, Pa.). Tissue-bound EF5 was labeled by using a 1:30 dilution of the monoclonal antibody ELK3-51 (provided by Cameron Koch, University of Pennsylvania, Philadelphia) directly labeled with Cy5. Sections were then imaged by using a cooled charge-coupled device camera (Quantix, Photometrics, Tucson, Ariz.) mounted on an epifluorescence microscope (Olympus, Melville, N.Y.) fitted with a computer-controlled motorized stage (Ludl Electronic Products, Hawthorne, N.Y.).

RESULTS

Transcriptome response to hypoxia. Several reports have been published with the primary goal of assessing gene expression patterns under hypoxic conditions (37). Most of these studies have focused on induced expression patterns during brief periods of exposure to mild or moderate hypoxia. In this work, we sought to further characterize gene expression patterns under more prolonged exposure to hypoxia (24 h at 0.5% O_2) by using a transcriptome profiling-based approach to screen for both known and novel genes which are regulated by hypoxia.

Analysis of hypoxia/normoxia (H/N) expression ratios for approximately 48,000 transcripts (16,000 unique transcripts in three biological replicates) detected in human MCF-7 breast cancer cells by transcriptome profiling revealed that the expression levels of the great majority of genes (~85%) are not altered by a 24-h exposure to hypoxia (0.5% O_2) (Fig. 1A); at a threshold of ≥2-fold regulation, approximately 5% of the genes detected demonstrated up-regulation, while 10% were down-regulated, by hypoxia. These findings were derived from pooled RNA samples analyzed in triplicate and obtained in two independent hypoxia-normoxia experiments. Interestingly, when the threshold for analysis is increased to a ≥6-fold change, more genes appear to be up-regulated than down-regulated by hypoxia (0.3 versus 0.1%, respectively). These results show that specific patterns of both up- and down-regulation occur in response to hypoxia, and they suggest that decreased expression of certain genes may be as important as increased expression in determining the phenotype of hypoxic cells.

As expected, hypoxic exposure led to increased expression of several known HIF target genes (Fig. 1B), such as glucose transporter 1 (*SLCA21*, or *Glut1*) and *VEGF* (17). Glycolysis-associated genes previously shown to be up-regulated by hypoxia, such as phosphoglycerate kinase I (*PGK1*) and aldolase C (*ALDOC*), were also significantly up-regulated. In addition, several other genes recently reported to be hypoxia inducible, such as DEC1 (*BHLHB2*) and hypoxia-inducible gene 2 (*HIG2*), displayed marked elevation, with 9.1- and 9.3-fold changes in H/N ratios, respectively. The H/N fold changes for the genes shown in Fig. 1B were verified by qPCR (data not shown).

Expression of DNA repair genes under hypoxia. Given that a comprehensive analysis of DNA repair gene expression under prolonged hypoxia had not been performed previously, we sought to determine whether there are specific genes in this category that exhibit novel regulation by hypoxia. The microarray detected the expression of more than 50 transcripts from genes that directly play a role in DNA repair, and representative genes from several repair pathways are shown in Fig. 1C. The expression levels of the majority of DNA repair genes detected were not substantially altered by hypoxia, including genes in pathways such as NER and base excision repair, consistent with previous work in our laboratory examining expression patterns of factors in these pathways by Western blot analyses (48). A more comprehensive list of DNA repair genes from these pathways, including qPCR expression validation for several of these genes, is available upon request. We did detect a moderate decrease in the level of *MLH1* expression under hypoxia (1.3-fold [data not shown]). It had been demonstrated previously that *MLH1* expression is down-regulated by hypoxia, especially after prolonged periods (>24 h) of severe hypoxia (<0.1% O_2), and thus the finding that *MLH1* mRNA is only slightly decreased at 24 h of moderate hypoxia (0.5% O_2) is consistent with previous data (25).

Intriguingly, we detected substantial decreases in the expression of *RAD51* under hypoxia (4.3-fold). This decrease was verified by qPCR and was specific to the *RAD51* gene; we did not detect hypoxia-induced decreases in the expression of other HR genes in the *RAD52* epistasis group (38), including *RAD51B*, *RAD54B*, *RAD52*, and *RAD50* (data not shown). Consequently, we reasoned that such decreases in a critical HR-associated gene could compromise recombinational repair in cells exposed to hypoxia.

A

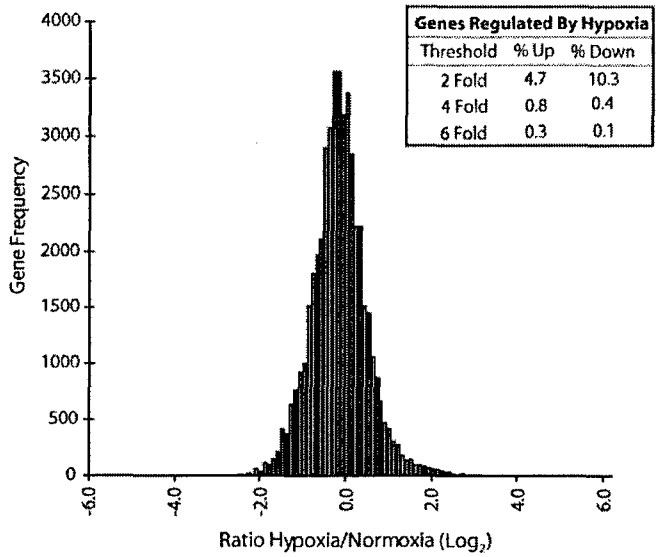

B

Known Genes Regulated by Hypoxia

Gene	Accession #	Fold H/N
SLC2A1	NM_006516	3.7
VEGF	NM_003376	3.2
PGK1	NM_000291	5.6
ALDOC	NM_005165	4.0
NDRG1	NM_006096	13.8
BHLHB2	NM_003670	9.1
HIG2	NM_013332	9.3

C

Expression of DNA Repair Genes in Hypoxia

Pathway	Gene	Accession #	Ratio H/N
NER	*ERCC1*	NM_001983	1.3
BER	*APEX2*	NM_014481	1.0
MMR	*PMS2*	NM_000535	1.3
HR	*RAD51*	NM_002875	-4.3

FIG. 1. Transcriptome response to hypoxia after 24-h exposure of MCF-7 cells to 0.5% O_2. (A) Histogram analysis of the approximately 48,000 transcripts (16,000 unique transcripts for each of three biological replicates) detected by the GenCompass microarray, based on H/N expression ratios (log_2). (Inset) Percentages of genes up-regulated and down-regulated at two-, four-, and sixfold thresholds. (B) Selection of genes previously identified as regulated by hypoxia which were detected by the GenCompass microarray. Accession numbers are given for reference. H/N ratios are averaged from three independent experiments. *NDRG1*, *N-myc* downstream-regulated gene 1. (C) GenCompass H/N expression ratios of selected DNA repair genes, with the respective pathways listed. H/N ratios are averaged from two experiments. BER, base excision repair; MMR, mismatch repair. *ERCC1*, excision repair cross-complementing group 1; *APEX2*, apurinic/apyrimidinic endonuclease/redox factor 2; *PMS2*, postmeiotic segregation increased 2; *RAD51*, RAD51 homolog.

Decreased expression of Rad51 protein in response to hypoxia or the Fe^{2+} chelator DFX. We sought to determine whether the changes observed in the microarray and qPCR experiments were also manifested at the protein level. In order to account for the effects of protein stability, we examined Rad51 protein expression levels not only at the 24-h time point used in the microarray experiments but also after 48 h of hypoxia. As shown in Fig. 2A, Western blot analysis revealed that Rad51 protein levels were substantially decreased after 48 h of hypoxia (approximately threefold) (lane 4), with minimal decreases observed after 24 h of hypoxia (lane 2). The expression of HIF-1α and its downstream target Glut1 (which appears as multiple isoforms between 37 and 75 kDa) is shown for comparison, to confirm physiologically relevant levels of hypoxia. In addition, levels of tubulin were unchanged and served as standards to confirm equal loading of cellular protein samples.

As discussed earlier, we had previously reported the specific down-regulation of the *MLH1* gene after prolonged exposure to more severe hypoxia. Based on this finding and on the relevance of such conditions to chronically hypoxic regions in tumors, we subjected MCF-7 cells to more severe hypoxia (0.01% O_2) for prolonged periods in order to determine whether there might be even greater reductions in Rad51 protein expression. As shown, a 48-h exposure to 0.01% O_2 resulted in a larger decrease (approximately sixfold) in Rad51 protein expression (Fig. 2A, lane 8). As expected, decreases were also observed in Mlh1 protein expression, but no reductions were observed in the expression of several other DNA repair proteins, including Msh2 and Msh6 (data not shown). Thus, both moderate hypoxia and severe hypoxia are associated with profound and specific decreases in the expression of the *RAD51* gene in MCF-7 cells.

The hypoxic state can be mimicked in cell culture by using the iron chelator DFX, which has been proposed to disrupt normal oxygen-sensing pathways in mammalian cells by inhibiting heme-Fe^{2+} interactions (43). As shown in Fig. 2A, a 24-h exposure of MCF-7 cells to DFX also resulted in decreased Rad51 protein expression (lane 10). In addition, HIF-1α and Glut1 levels were increased in DFX-treated MCF7 cells, confirming that this chemical treatment mimicked aspects of gas-induced hypoxia. These results show that Rad51 protein expression is reduced not only in truly hypoxic cells but also in cells in which hypoxia is simulated by interference with normal cellular oxygen sensing.

Given that such profound decreases in Rad51 protein ex-

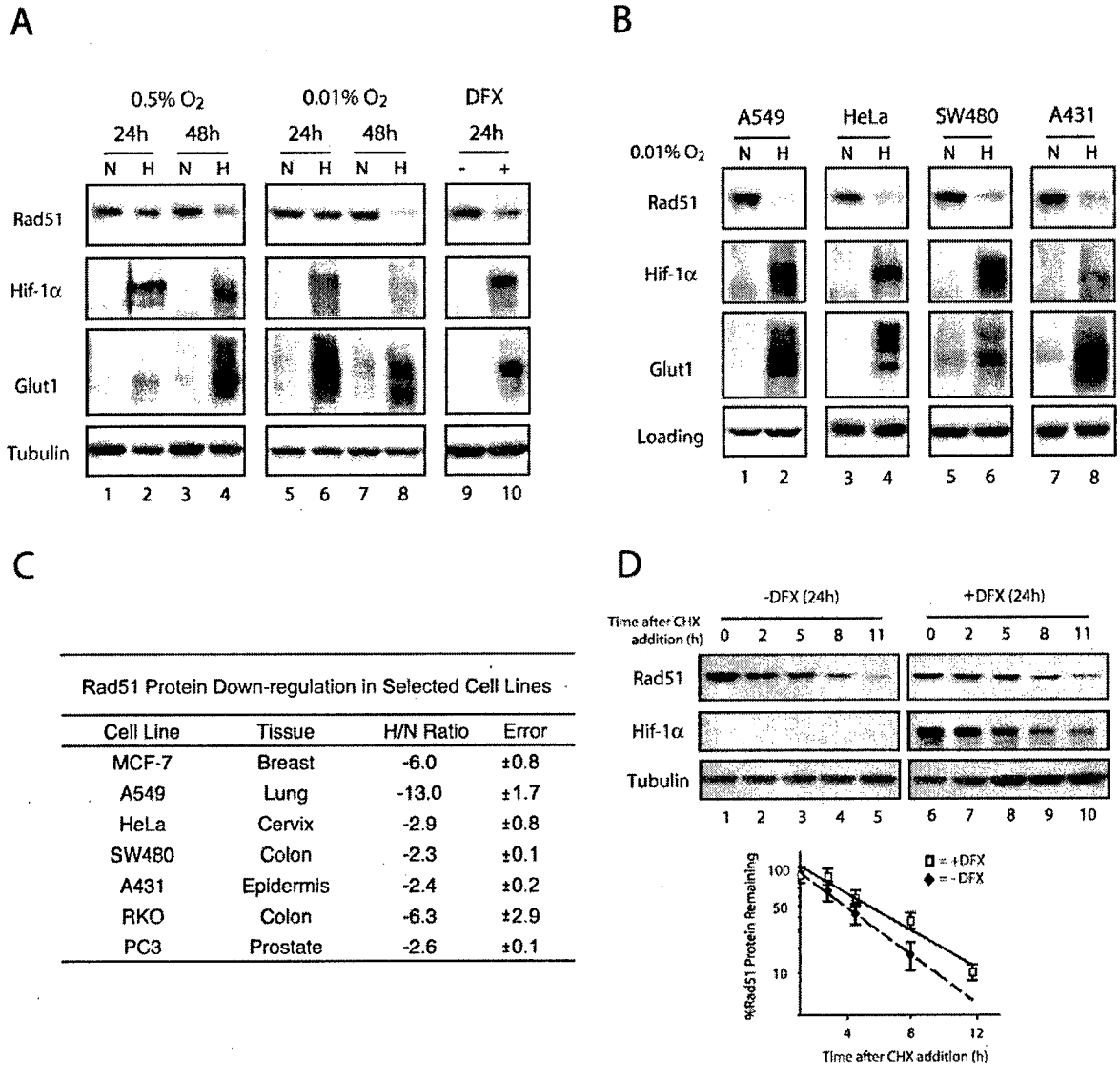

Rad51 Protein Down-regulation in Selected Cell Lines

Cell Line	Tissue	H/N Ratio	Error
MCF-7	Breast	-6.0	±0.8
A549	Lung	-13.0	±1.7
HeLa	Cervix	-2.9	±0.8
SW480	Colon	-2.3	±0.1
A431	Epidermis	-2.4	±0.2
RKO	Colon	-6.3	±2.9
PC3	Prostate	-2.6	±0.1

FIG. 2. Decreased levels of Rad51 protein in cell lines in response to hypoxia or the Fe^{2+} chelator DFX, and determination of Rad51 protein stability in the presence of DFX. (A) Western blot analyses were performed to determine the expression of the HR-associated protein Rad51 in MCF-7 cells after exposure to normoxia (lanes N), hypoxia (0.5 or 0.01% O_2) (lanes H), or DFX (250 μM). The time for which the cells were maintained under each condition (24 or 48 h) is shown. Expression of HIF-1α and Glut1 is shown for comparison, to verify that physiologically relevant levels of hypoxia were present in the treated cells. Note that Glut1 appears as several isoforms which are detected by our antibody. Tubulin expression is also presented to confirm equal sample loading. (B) Western blot analyses of Rad51 protein expression in A549, HeLa, SW480, and A431 cells after a 48-h exposure to normoxia or hypoxia (0.01% O_2). Tubulin expression is presented to confirm equal loading of samples for HeLa and SW480 cells, while β-actin was used as a loading control for A549 and A431 cells. (C) Average reduction in Rad51 protein levels after a 48-h exposure to hypoxia (0.01% O_2), as determined by densitometry analysis of Western blots generated from duplicate (RKO, A431, SW480, and PC3 cells) or triplicate (MCF-7, A549, and HeLa cells) hypoxia experiments. The tissue of origin for each cell line is shown. Reductions are expressed as H/N ratios normalized to the expression of β-actin and tubulin, and standard errors for each ratio are given. (D) To assess Rad51 protein stability, MCF-7 cells were either exposed to DFX (250 μM) or left untreated for 24 h, followed by coincubation with CHX (10 μg/ml) to block new protein synthesis. (Upper panels) Cells were harvested at the indicated times after addition of CHX, and Rad51 protein expression was determined by Western blotting. Expression of HIF-1α is shown to confirm both the induction of chemical hypoxia and successful abolition of new protein synthesis. In addition, tubulin protein levels were unchanged and served as standards to confirm equal loading of cellular protein samples. (Lower panel) Analysis of Rad51 protein expression at each time point after addition of CHX in cells exposed to DFX or left untreated, quantified as described in the legend to panel C. Each data point is the percentage of Rad51 protein remaining (after normalization to tubulin levels) in either DFX-treated or untreated cells at the indicated time.

pression after hypoxic stress could have broad implications for genetic instability in the tumor microenvironment, we sought to determine whether this phenomenon could also be detected in tumor cell lines derived from other tissues. A selection of tumor cell lines from various tissues were cultured under hypoxic and normoxic conditions, followed by Western blot analysis to assess Rad51 protein levels. As shown in Fig. 2B, significant decreases in Rad51 protein expression were observed

after 48 h of hypoxia in a wide range of human cell lines, including the A549 epithelial lung carcinoma cell line and the HeLa cervical cancer cell line. Densitometry analysis was used to approximate H/N protein expression ratios for several cell lines evaluated in this study, based on triplicate hypoxia experiments and normalization to either β-actin or tubulin expression. As shown in Fig. 2C, A549 and MCF-7 cells displayed the highest levels of down-regulation, with H/N ratios of −13 and −6, respectively. Taken together, significant hypoxia-mediated down-regulation of Rad51 protein is observed in numerous human cell lines derived from a wide range of tissues.

To determine whether the observed decreases in Rad51 protein expression could be accounted for by an increase in protein degradation, MCF-7 cells were either left untreated or exposed to DFX, followed by coincubation with CHX to block new protein synthesis. Cells were then harvested at various times after the addition of CHX, and Rad51 protein expression was determined by Western blotting. As shown in Fig. 2D, while a 24-h DFX exposure resulted in a threefold decrease in Rad51 protein expression (compare lanes 1 and 6), no significant differences in Rad51 protein stability between untreated cells and cells exposed to DFX were observed after the addition of CHX. In contrast, HIF-1α expression was substantially increased in the presence of DFX, and HIF-1α degraded rapidly after CHX addition, confirming both the induction of chemical hypoxia and successful abolition of new protein synthesis. In addition, levels of tubulin protein were unchanged and served as standards to confirm equal loading of cellular protein samples. These findings suggest that the hypoxia-mediated down-regulation of the *RAD51* gene does not occur at the posttranslational level.

Prolonged hypoxia leads to the down-regulation of *RAD51* mRNA expression. To determine if the decreases in Rad51 protein expression observed after severe hypoxia are also associated with decreased mRNA levels, Northern blot analyses were performed on total RNAs extracted from MCF-7 and A549 cells after 24- and 48-h exposures to 0.01% O_2. *RAD51* mRNA levels were substantially decreased at the 48-h time point, with H/N ratios of approximately −8 and −9 in MCF-7 and A549 cells, respectively (Fig. 3A and B, respectively). Ratios were averaged from multiple experiments and normalized to either 28S rRNA or β-*actin* mRNA levels. Significant decreases were also observed at the 24-h time point in both cell lines. The expression of *VEGF* is shown, to verify the induction of physiological levels of hypoxia, and β-*actin* and 28S rRNA are presented as loading controls. Consistent with the protein expression levels, a 24-h exposure of MCF-7 cells to DFX also resulted in decreased expression of *RAD51* mRNA (Fig. 3A, lane 6), and this finding was also verified by qPCR analysis (data not shown). Additionally, hypoxia-induced decreases in *RAD51* mRNA expression were observed in a number of other human cell lines, including SiHa, RKO, and DU145 (Fig. 3B; also data not shown). These findings provide consistent evidence that hypoxia regulates the expression of the *RAD51* gene at the mRNA level.

Transcriptional repression of the *RAD51* gene by hypoxia. We next sought to determine the mechanism by which hypoxia down-regulates steady-state levels of *RAD51* mRNA. To test a possible effect on *RAD51* mRNA stability, MCF-7 cells were exposed to DFX, followed by coincubation with ActD to block transcription. Cells were then harvested at various times after the addition of ActD, and *RAD51* mRNA expression was determined by Northern blotting. As shown in Fig. 3C, while a 24-h DFX exposure resulted in a twofold decrease in *RAD51* mRNA expression (compare lanes 1 and 6), no significant differences in mRNA stability after ActD addition were observed between cells exposed to DFX and cells left untreated (Fig. 3D). *RAD51* mRNA half-lives were determined to be approximately 20 and 15 h in DFX-exposed and untreated cells, respectively, and these values were based on duplicate ActD experiments. In contrast, *VEGF* expression is substantially increased in the presence of DFX, and *VEGF* mRNA degrades rapidly after ActD addition, confirming both the induction of chemical hypoxia and the successful inhibition of transcription. In addition, 28S rRNA levels were unchanged and served as standards to confirm equal sample loading. These data indicate that the hypoxia-induced down-regulation of *RAD51* mRNA expression cannot be accounted for by decreases in the stability of the mRNA; thus, they suggest that regulation occurs at the level of transcription.

To test whether the reduction in steady-state levels of *RAD51* mRNA under hypoxia is dependent on *RAD51* promoter regulation, the effect of hypoxia on *RAD51* promoter activity was examined by using a promoter-luciferase reporter system. As shown in Fig. 3E, a 1.8-kb fragment from the 5′-flanking region of the *RAD51* gene, containing the core promoter region(s) described in the Eukaryotic Promoter Database (30) and that identified by in silico analysis using the Genomatix promoter identification algorithm PromoterInspector (44), was isolated. A firefly luciferase reporter plasmid containing this fragment (pGL3-Rad51p) was transiently transfected into RKO cells 4 h prior to normoxic or hypoxic exposure (48 h), immediately followed by measurement of luciferase activity. *Renilla* luciferase activity from a cotransfected pRL-SV40 control vector was used for normalization. The luciferase reporter plasmid 5X-HRE, which contains five hypoxia response elements (HREs) tandemly ligated to a human cytomegalovirus minimal promoter, was used as a control to confirm physiologically relevant levels of hypoxia. As shown in Fig. 3F, exposure to hypoxia resulted in a fivefold repression of pGL3-Rad51p reporter activity. In contrast, 5X-HRE reporter activity increased approximately 50-fold, and no change in activity was observed in the promoterless control plasmid pGL3-Basic, in hypoxic cells. RKO cells were used in these studies due to the ease with which they are transfected and because of their ability to support high levels of *RAD51* promoter activities. *RAD51* promoter activity was also repressed by hypoxia in MCF-7 and A549 cells, with H/N ratios of −1.8- and −1.5-fold, respectively (data not shown). Taken together, these findings suggest that hypoxia down-regulates the expression of the *RAD51* gene via a mechanism involving transcriptional repression.

Persistent down-regulation of Rad51 expression posthypoxia. Given the dramatic decreases that we observed in *RAD51* mRNA and protein levels after 48 h of hypoxia, we sought to determine the extent to which these alterations persisted after reoxygenation. MCF-7 cells were exposed to 48 h of hypoxia, followed by a return to normoxic conditions for several days thereafter. Cell lysates were prepared at 24-h intervals throughout the time course, and Western blot analyses

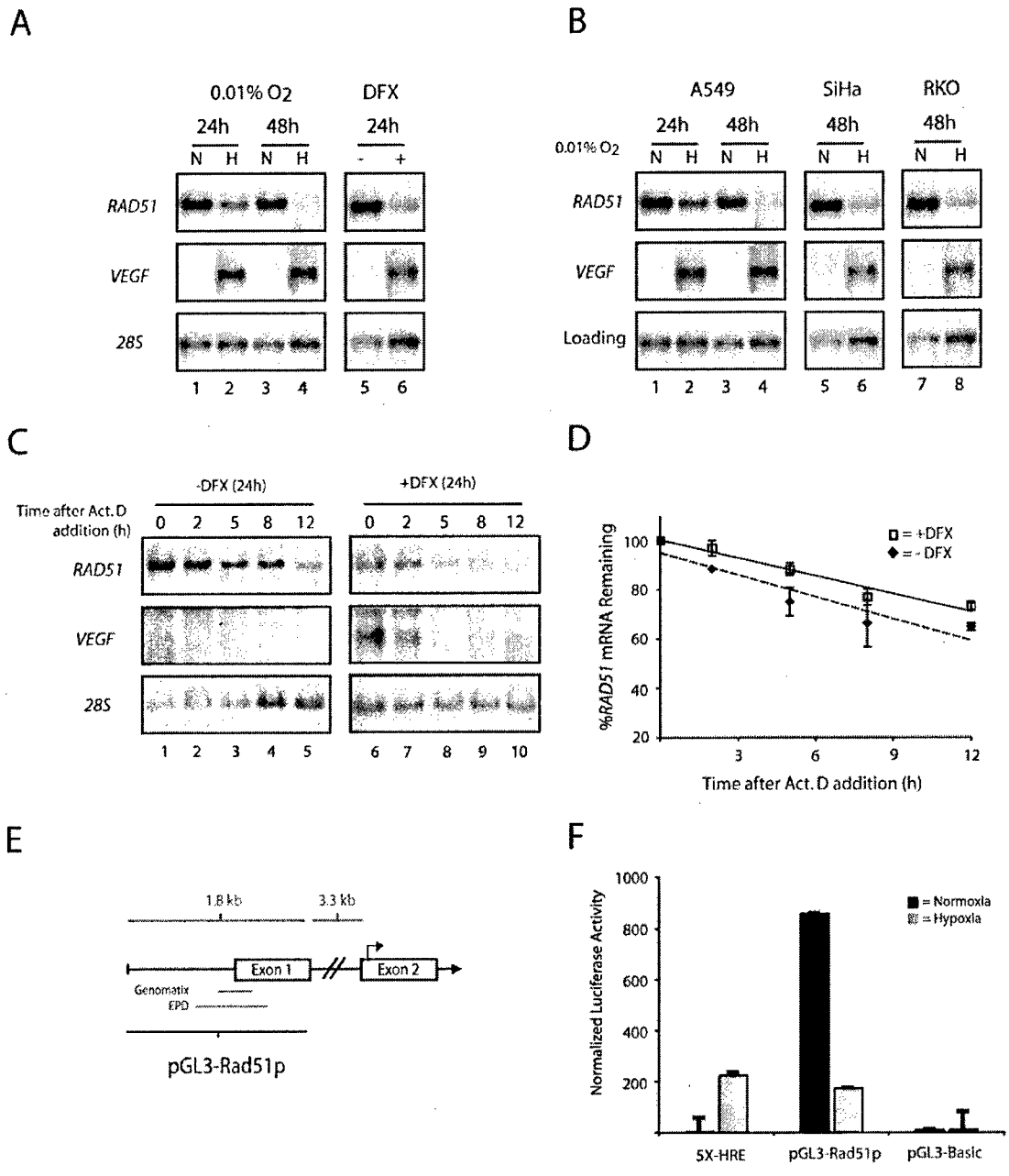

FIG. 3. Transcriptional repression of the *RAD51* gene by hypoxia. (A) Northern blot analyses were performed on total RNA extracted from MCF-7 cells after exposure to normoxia (lanes N), hypoxia (0.01% O_2) (lanes H), or DFX (250 μM). The time for which cells were maintained under each condition (24 or 48 h) is given. *VEGF* expression is shown for comparison, to verify that physiologically relevant levels of hypoxia were present in the treated cells, and expression of 28S rRNA is presented to confirm equal sample loading. (B) Northern blot analysis of *RAD51* mRNA expression in A549, SiHa, and RKO cells after a 24- or 48-h exposure to hypoxia (0.01% O_2). *VEGF* expression is shown for comparison, to verify that physiologically relevant levels of hypoxia were present in the treated cells. Expression of 28S rRNA (MCF-7, SiHa, and RKO cells) and β-*actin* mRNA (A549 cells) is presented to confirm equal sample loading. (C) To assess the stability of *RAD51* mRNA, MCF-7 cells were either left untreated or exposed to DFX (250 μM) for 24 h, followed by coincubation with ActD (5 μg/ml) to block transcription. Cells were harvested at the indicated times after the addition of ActD, and *RAD51* mRNA expression was determined by Northern blotting. Expression of *VEGF* is shown to confirm both the induction of chemical hypoxia and successful abolition of transcription. In addition, 28S rRNA levels were unchanged and served as standards to confirm equal sample loading. (D) Analysis of *RAD51* mRNA expression at each time point after ActD addition in cells exposed to DFX or left untreated, as determined by phosphorimager analysis of Northern blots. Values are the percentage of *RAD51* mRNA remaining in either DFX-treated or untreated cells at each time point, and error bars are based on standard errors calculated from duplicate experiments. (E) Schematic of the 5′-flanking region of the *RAD51* gene, with delineation of the promoter fragment used for luciferase reporter gene assays (pGL3-Rad51p). Approximate locations of the core promoter regions, as described in the Eukaryotic Promoter Database (EPD) and as identified by in silico analysis using the Genomatix promoter identification algorithm PromoterInspector, are shown for reference. Bent arrow above exon 2 indicates the ATG translation start codon. (F) To determine the effect of hypoxia on *RAD51* gene promoter activity, the pGL3-Rad51p luciferase (firefly) reporter plasmid was transiently transfected into RKO cells 4 h prior to normoxic or hypoxic exposure (for 48 h), immediately followed by measurement of luciferase activity. Firefly luciferase values were normalized to *Renilla* luciferase activity from a cotransfected pRL-SV40 control vector, and error bars are based on standard errors calculated from duplicate experiments. The activity of the luciferase reporter plasmid 5X-HRE, which contains five HREs tandemly ligated to a human cytomegalovirus minimal promoter, is shown as a control to confirm physiologically relevant levels of hypoxia. The activity of the promoterless luciferase reporter gene construct pGL3-Basic is also shown as a control.

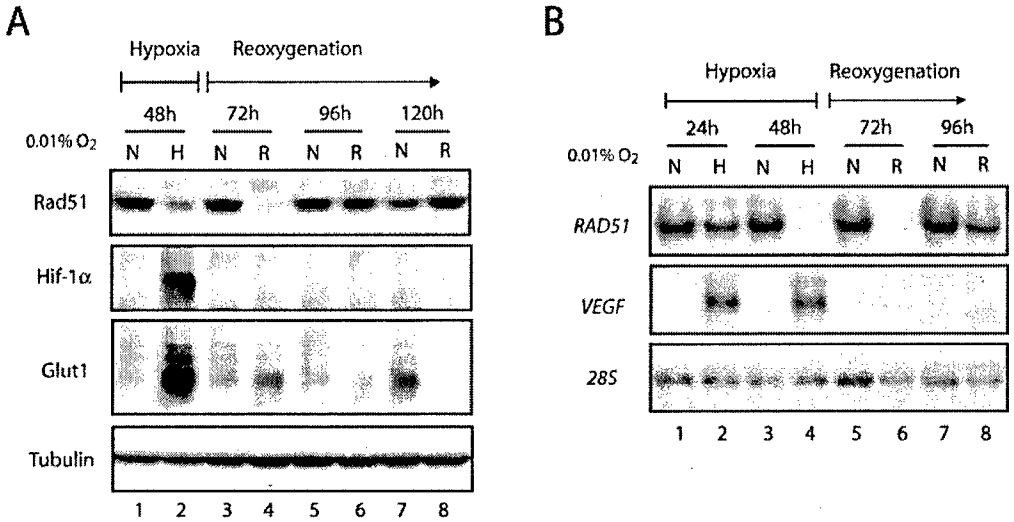

FIG. 4. Persistent down-regulation of Rad51 expression after hypoxia. (A) Western blot analyses were performed to determine the expression pattern of Rad51 protein in MCF-7 cells cultured under hypoxia for 48 h (0.01% O_2) (lane H) and then following reoxygenation (R), as indicated by the timeline shown. Samples were obtained at 24-h intervals posthypoxia (lanes R), with the 72-, 96-, and 120-h time points representing 24, 48, and 72 h following reoxygenation, respectively. As a control to show that Rad51 levels do not change over the same period under normoxia, Rad51 protein expression in cells grown in parallel under consistently normoxic conditions is shown for each time point (lanes N). Expression of HIF-1α and Glut1 is shown for comparison, to verify that physiologically relevant states of hypoxia and reoxygenation were observed in the treated cells. Tubulin expression is also presented to confirm equal sample loading. (B) Northern blot analysis was performed to determine the expression of *RAD51* mRNA in MCF-7 cells during the same time course and under the same conditions described for panel A. As indicated by the timeline shown, *RAD51* mRNA expression was assessed at 24 and 48 h of hypoxia (lanes H). RNA samples were also analyzed at 24-h intervals posthypoxia (lanes R), with the 72- and 96-h time points representing 24- and 48-h periods of reoxygenation, respectively. As a control to show that *RAD51* expression does not change over the same period under normoxia, *RAD51* mRNA expression in normoxic cells grown in parallel is shown for each time point (lanes N). *VEGF* expression is shown for comparison, to verify that physiologically relevant states of hypoxia and reoxygenation were obtained in the treated cells. Expression of 28S rRNA is also presented to confirm equal sample loading.

were performed to assess Rad51 expression levels during and after hypoxic exposure. Intriguingly, we detected the lowest levels of Rad51 protein in the period following hypoxia. As shown in Fig. 4A, Rad51 levels were lowest at 24 h after reoxygenation (referred to as the 72-h time point) (lane 4), and these levels did not return to normal, prehypoxia expression levels until after the 96-h time point (lane 6), which corresponds to 48 h posthypoxia. The HIF-1α protein is rapidly degraded under normoxic conditions, and thus it was not detected upon reoxygenation at any of the posthypoxia time points shown. Furthermore, we also observed a rapid decrease in Glut1 expression following reoxygenation, a response that is expected for this gene in the transition from hypoxia to normoxia. Rad51 protein expression levels at the 48- and 72-h time points were reduced approximately 6- and 12-fold, respectively, and these values were based on triplicate experiments. Reductions in Rad51 protein expression were also observed 20 h after a shorter, 24-h hypoxia exposure, although these decreases were not as pronounced (data not shown). In addition, similar trends were also observed at the protein level in A549 cells, with a slightly more rapid return of protein levels following reoxygenation (Fig. 5D).

Northern blot analysis revealed that *RAD51* mRNA levels were also maximally decreased at the 72-h time point, representing 24 h posthypoxia (Fig. 4B, lane 6). Furthermore, mRNA and protein expression data from three independent experiments revealed that the hypoxia-induced decrease in Rad51 protein levels was consistently preceded by decreased *RAD51* mRNA levels (data not shown). As expected, the expression of *VEGF* decreased rapidly to undetectable levels after reoxygenation and thus serves as a control for the physiological transition from hypoxia to normoxia. Taken together, these results indicate that hypoxia induces substantial decreases in *RAD51* mRNA levels, which are followed by corresponding reductions in Rad51 protein levels. Importantly, these reductions are most pronounced in the posthypoxia reoxygenation phase and persist for a significant period thereafter.

Hypoxia-mediated down-regulation of the *RAD51* gene is independent of the cell cycle profile. *RAD51* mRNA expression levels have been shown to be highest in the S and G_2 phases of the cell cycle, and lowest during G_0 and G_1, in mammalian cells (11). We thus sought to determine whether the observed decreases in Rad51 expression could be accounted for by specific changes in the cell cycle profile induced by hypoxia. To this end, we used flow cytometric analyses to determine the cell cycle profiles of several of the human cell lines listed in Fig. 2C upon exposure to hypoxia. As shown in Fig. 5A, a range of cell cycle profile changes were observed under hypoxia among the four cell lines studied. We reasoned that if Rad51 expression decreases could be accounted for by increases in the proportion of cells in the G_1 phase under hypoxia, for example, then there should be direct correlations between hypoxia-induced G_1 shifts and H/N ratios of Rad51 expression in the cell lines evaluated. As shown in Fig. 5B, no such correlations were observed; MCF7, A549, and HeLa cells all displayed small increases in the proportion of G_1-phase cells upon hypoxia exposure (1.3-, 1.2-, and 1.2-fold, respectively) yet exhibited

A

Cell Cycle Profile of Selected Cell Lines

Cell Line	Condition	Cell Cycle Phase (%) G1	S	G2/M
MCF-7	Normoxia	50	34	16
	Hypoxia	67	29	4
A549	Normoxia	58	31	11
	Hypoxia	72	27	1
HeLa	Normoxia	73	20	7
	Hypoxia	84	14	2
A431	Normoxia	55	38	7
	Hypoxia	52	35	13

B

G1-Shift and Rad51 Protein Levels

Cell Line	Fold Change (H/N) G1-Shift	Rad51
MCF-7	1.3	-6.0
A549	1.2	-13.0
HeLa	1.2	-2.9
A431	1.0	-2.4

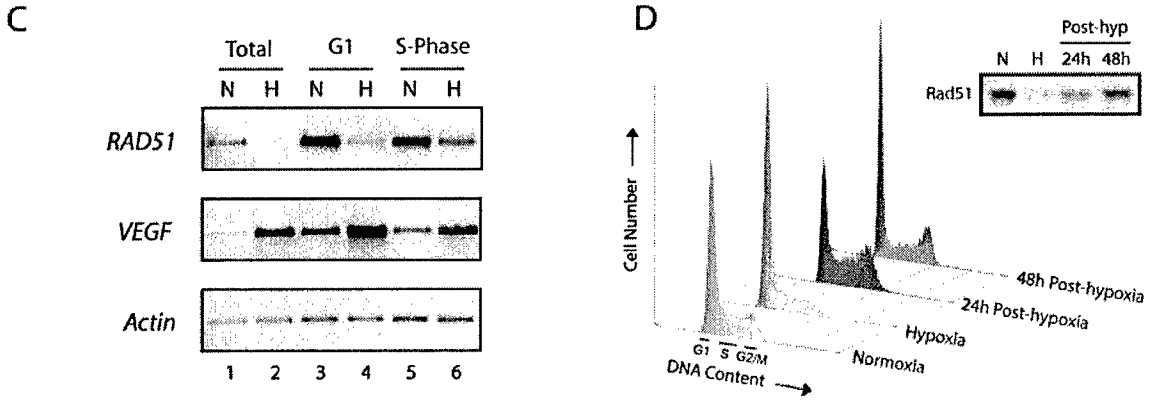

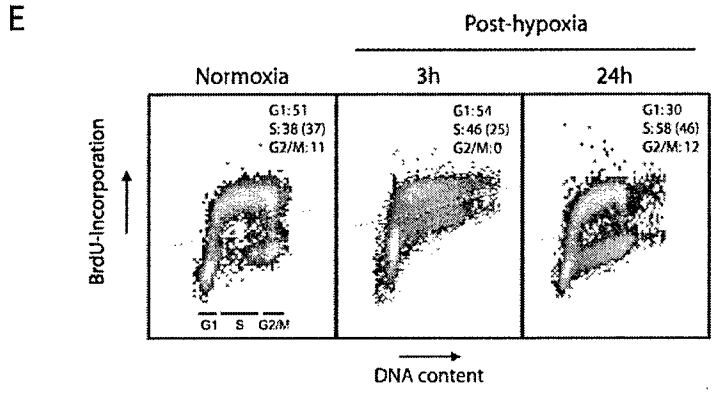

FIG. 5. Decreased Rad51 expression is not associated with the cell cycle profile. (A) Quantitative assessment of cell cycle profiles of four cell lines exposed to hypoxia (0.01% O_2) or normoxia for 48 h. Calculated proportions are expressed as percentages based on triplicate hypoxia experiments using flow cytometric analysis of PI-stained cells and histogram analysis software. (B) Fold changes in both the percentage of cells in the G_1 phase and the Rad51 protein level in hypoxia compared to normoxia, as calculated from panel A and Fig. 2C, respectively. (C) Semi-quantitative RT-PCR analysis of *RAD51* mRNA expression in isolated G_1- and S-phase populations of normoxic and hypoxic cells. Equal numbers of cell cycle-specific populations were obtained by DNA staining of cells with the vital fluorochrome Hoechst 33342, followed by flow cytometric analysis and cell sorting. Unsorted cells processed in parallel are also shown for reference (lanes 1 and 2). *VEGF* expression is shown for comparison, to verify physiologically relevant states of hypoxia in normoxic and hypoxic cell populations, and the expression of β-*actin* is presented to confirm equal sample loading. (D) Cell cycle profiles of A549 cells exposed to either normoxia or hypoxia for 48 h and of A549 cells reoxygenated immediately following hypoxia for the indicated times, shown as histograms based on PI staining for DNA content. Approximate ranges of G_1-, S-, and G_2/M-phase populations are shown for reference. (Inset) Rad51 protein expression in the A549 cells at the corresponding time points. (E) S-phase proliferation in normoxic A549 cells or in A549 cells reoxygenated for the indicated times, as assessed by BrdU incorporation. Dotted lines represent the threshold for positive BrdU incorporation, based on cells assayed in parallel without BrdU incubation at each time point. Quantitative assessments of cell cycle profiles at each time point are shown in each panel and were calculated as described in the legend to panel A. The percentage of total cells in each sample that incorporated BrdU is given in parentheses.

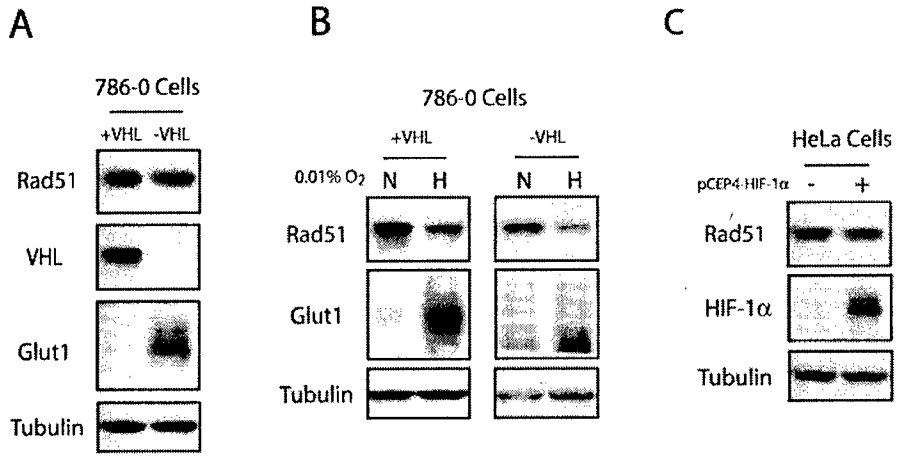

FIG. 6. Decreased Rad51 expression is not associated with HIF expression. (A) Western blot analyses were performed to determine the expression of Rad51 protein in log-phase 786-0 cells expressing a wild-type (+VHL) or mutant (−VHL) VHL gene. Expression of VHL and Glut1 is shown for comparison to verify the status of these cells. Tubulin expression is also presented to confirm equal sample loading. (B) Western blot analysis of Rad51 protein expression in 786-0 cells expressing either wild-type or mutant VHL following exposure to hypoxia (0.01% O_2) for 48 h. (C) Western blot analysis of Rad51 and HIF-1α expression levels in HeLa cells 48 h after transfection with the HIF-1α expression vector pCEP4-HIF-1α.

substantial (but variable) H/N ratios of Rad51 expression (−6.0, −13.0, and −2.9, respectively). A431 cells, by contrast, displayed no detectable G_1 shift under hypoxia yet displayed H/N expression ratios similar to those seen in HeLa cells (−2.4-fold).

In order to further confirm the cell cycle independence of the down-regulation of *RAD51* gene expression by hypoxia, specific populations of G_1- and S-phase cells were isolated from both normoxic and hypoxic A549 cells, followed by analysis of *RAD51* mRNA expression by semiquantitative RT-PCR. Cell cycle phase-specific cell populations were obtained by DNA staining of cells with the vital fluorochrome Hoechst 33342, followed by flow cytometric analysis and cell sorting. This technique has recently been reported to facilitate the recovery of intact mRNA from viable cells in distinct phases of the cell cycle (20). As shown in Fig. 5C, substantial decreases in *RAD51* mRNA expression were observed in both G_1- and S-phase cells after a 48-h exposure to hypoxia (lanes 4 and 6, respectively), with H/N ratios of −3.2 and −2.7, respectively. These H/N ratios were similar in magnitude to those observed in unsorted hypoxic cells processed in parallel (Fig. 5C, lanes 1 and 2), which displayed H/N ratios of approximately −3.4. *VEGF* expression is shown for comparison, to verify physiologically relevant states of hypoxia in the individual normoxic and hypoxic G_1- and S-phase cell populations, and the expression of β-*actin* is also presented to confirm equal sample loading. These data provide direct evidence that the down-regulation of *RAD51* gene expression by hypoxia occurs in both the G_1 and S phases of the cell cycle and thus cannot be attributed to changes in the cell cycle profile.

A lack of correlation between the cell cycle phase and decreased Rad51 expression was also observed during the post-hypoxia reoxygenation period, based on propidium iodide (PI) analyses of DNA content and on the technique of bromodeoxyuridine (BrdU) incorporation to assess rates of S-phase proliferation. As shown in Fig. 5D, marked increases in the proportions of A549 cells in the S and G_2/M phases were observed 24 h posthypoxia (58 and 12%, respectively), yet Rad51 levels in these cells were persistently decreased. In addition, cells were clearly entering S phase and undergoing DNA replication in the early posthypoxic period, when Rad51 expression remained at its lowest levels. For example, S-phase proliferation rates at 3 and 24 h posthypoxia were 25 and 46%, respectively (Fig. 5E). Collectively, these data demonstrate that posthypoxic A549 cells resume S-phase replication and enter the G_2/M phase of the cell cycle yet still show substantial decreases in Rad51 protein expression, indicating further that the down-regulation of Rad51 is not governed by the proportion of cells in G_1 or S phase and demonstrating an uncoupling between cell proliferation and DNA repair gene expression. Taken together, these findings provide strong evidence that decreased *RAD51* gene expression is more hypoxia specific than cell cycle phase dependent.

Reduced expression of Rad51 is not associated with HIF expression. The HIF family of proteins has been shown to regulate the expression of numerous genes that play roles in angiogenesis, glycolysis, invasion, and metastasis in response to hypoxia (17). It has also been demonstrated recently that HIF-1α can induce the expression of transcriptional repressors such as DEC1, a gene revealed by our microarray analysis to be induced by hypoxia (Fig. 1B). Hence, we tested whether the observed decreases in RAD51 expression induced by hypoxia might be mediated by HIF-1α or HIF-2α. HIF proteins are highly unstable under normal oxygen tensions, because both HIF-1α and HIF-2α are ubiquitinated through the interaction with the von Hippel-Lindau tumor suppressor protein (pVHL) and subsequently degraded by the 26S proteasome under normoxic conditions (19). The pVHL-deficient cell line 786-0 specifically overexpresses HIF-2α and consequently overexpresses HIF-2α downstream target genes, including *Glut1* and *VEGF* (24). Expression of the VHL cDNA in these cells restores the normoxic regulation of HIF-2α. We thus examined the expression of Rad51 protein in 786-0 cells complemented either with the VHL cDNA or with an empty vector. As shown in Fig. 6A,

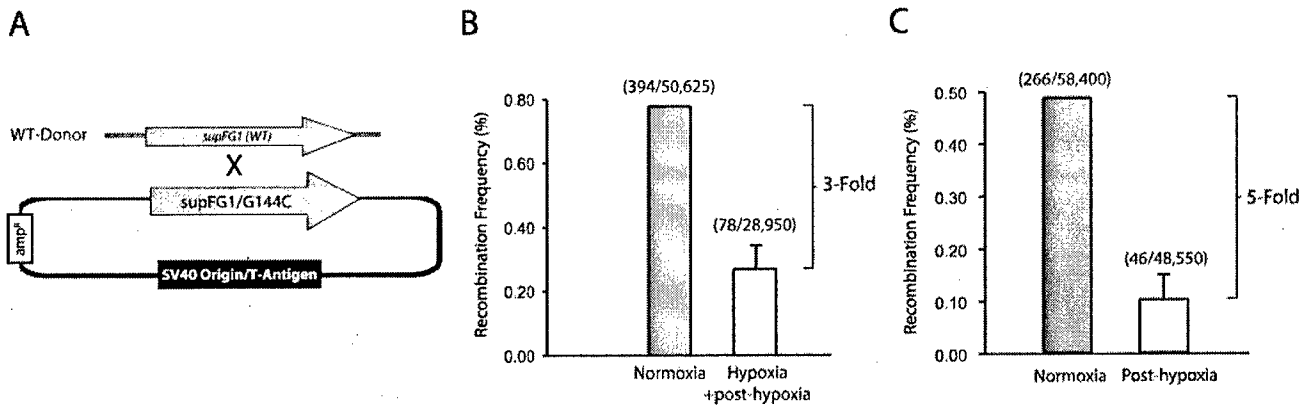

FIG. 7. Decreased HR in hypoxic and posthypoxic cells. (A) Schematic of the shuttle vector plasmid and donor DNA fragment used to assess HR. Plasmid pSupFG1/G144C contains a *supFG1* gene with an inactivating G:C-to-C:G point mutation at position 144. The donor is a homologous DNA fragment containing a portion of the wild-type *supFG1* gene. Abbreviations: amp^r, ampicillin resistance gene; WT, wild type. (B) Recombination frequencies in MCF-7 cells cotransfected with the shuttle vector and donor fragment, followed by culture either under normoxic conditions alone (72 h) or under hypoxia (0.01% O_2) for 48 h, immediately followed by reoxygenation and 24 h of normoxia (Hypoxia + post-hypoxia). The total number of blue colonies/ total number of colonies in each sample is given in parentheses. Error bars are based on standard errors calculated from duplicate experiments. (C) Recombination frequencies in MCF-7 cells cotransfected with the shuttle vector and donor fragment under normoxic conditions immediately following a 48-h exposure either to normoxia or to hypoxia (0.01% O_2) (Post-hypoxia).

the expression of Rad51 was not affected by VHL status or HIF-2α expression. The expression of VHL and Glut-1 proteins are shown to confirm VHL status and a constitutively hypoxic phenotype, respectively, in these two cell lines. Northern blotting also revealed no differences in steady-state *RAD51* mRNA levels between the VHL mutant and wild-type cells (data not shown). Interestingly, exposure of 786-0 cells expressing either wild-type or mutant VHL to hypoxia resulted in similar decreases in Rad51 expression (Fig. 6B). Taken together, these data suggest that the hypoxia-mediated down-regulation of Rad51 expression occurs independently of HIF-2α. It also suggests that the down-regulation does not require the expression of HIF-1α, since 786-0 cells lack HIF-1α expression (19). As an alternative approach to assessing the role of HIF-1α in the regulation of Rad51 expression by hypoxia, we transiently overexpressed a full-length HIF-1α cDNA in normoxic HeLa cells. Figure 6C demonstrates that exogenous overexpression of HIF-1α was not associated with decreased expression of Rad51. Collectively, these data suggest that hypoxia-induced decreases in *RAD51* gene expression are not mediated by HIF-dependent pathways.

Decreased HR in hypoxic and posthypoxic cells. We next sought to determine whether hypoxia-induced reductions in Rad51 protein expression were associated with functional decreases in HR. We utilized a shuttle vector recombination assay involving the transient transfection of a plasmid containing a mutated reporter gene along with a wild-type donor fragment into MCF-7 cells exposed to normoxia or hypoxia in order to assess frequencies of HR. Plasmid pSupFG1/G144C, containing a mutated version of the *supFG1* amber suppressor tRNA gene, *supFG1*-144, was used as the recombination substrate. A homologous fragment containing the wild-type *supFG1* gene was used as a donor for recombination. The function of the *supFG1* gene can be assayed by recovery of the episomal shuttle vector plasmid from the MCF-7 cells, with subsequent transformation into indicator bacteria carrying an amber stop codon in the *lacZ* gene. In this manner, *supFG1*-144 reports recombination events that cause the gene to revert to the functional sequence as detected in a blue/white colony screen (5). A schematic of this reporter system is presented in Fig. 7A for reference. Important features of this assay are the facts that vector replication and recombination are independent of the cell cycle and that previous studies in our lab have provided evidence that recombination events in this assay are dependent on Rad51 (8).

As shown in Fig. 7B, cotransfection of the shuttle vector and wild-type fragment into MCF-7 cells immediately prior to hypoxic exposure (for 48 h), followed by plasmid recovery 24 h posthypoxia, revealed a ~3-fold decrease in recombination frequency in hypoxic cells relative to that observed in MCF-7 cells incubated under normoxia for the same total time. Intriguingly, we observed the most substantial decreases in HR frequencies when the cells were transfected during the post-hypoxic period. Figure 7C shows that transfection of the shuttle vector and donor fragment into MCF-7 cells immediately following the hypoxic (48-h) period resulted in an almost five-fold decrease in HR, again relative to the frequency observed in cells maintained under normoxic conditions throughout. Thus, the observed decreases in HR parallel the changes in expression of Rad51 protein in hypoxia and posthypoxia. Taken together, these data provide evidence that the decreased expression of Rad51 caused by hypoxia is associated with a substantial and prolonged reduction in the capacity of cells to carry out HR both during and after hypoxia, for as long as 48 h following hypoxic exposure.

Inverse association between hypoxia and Rad51 expression in cervical and prostate cancer xenografts. We next sought to determine whether hypoxia-induced decreases in Rad51 expression could be detected in vivo in the tumor microenvironment. To this end, human prostate and cervical cancer xenografts in mice were generated from the PC3, Me180, and SiHa6 cell lines. These cell lines had all exhibited hypoxia-induced decreases in Rad51 expression in culture (Fig. 2C and 3B; also data not shown). Histological sections from the re-

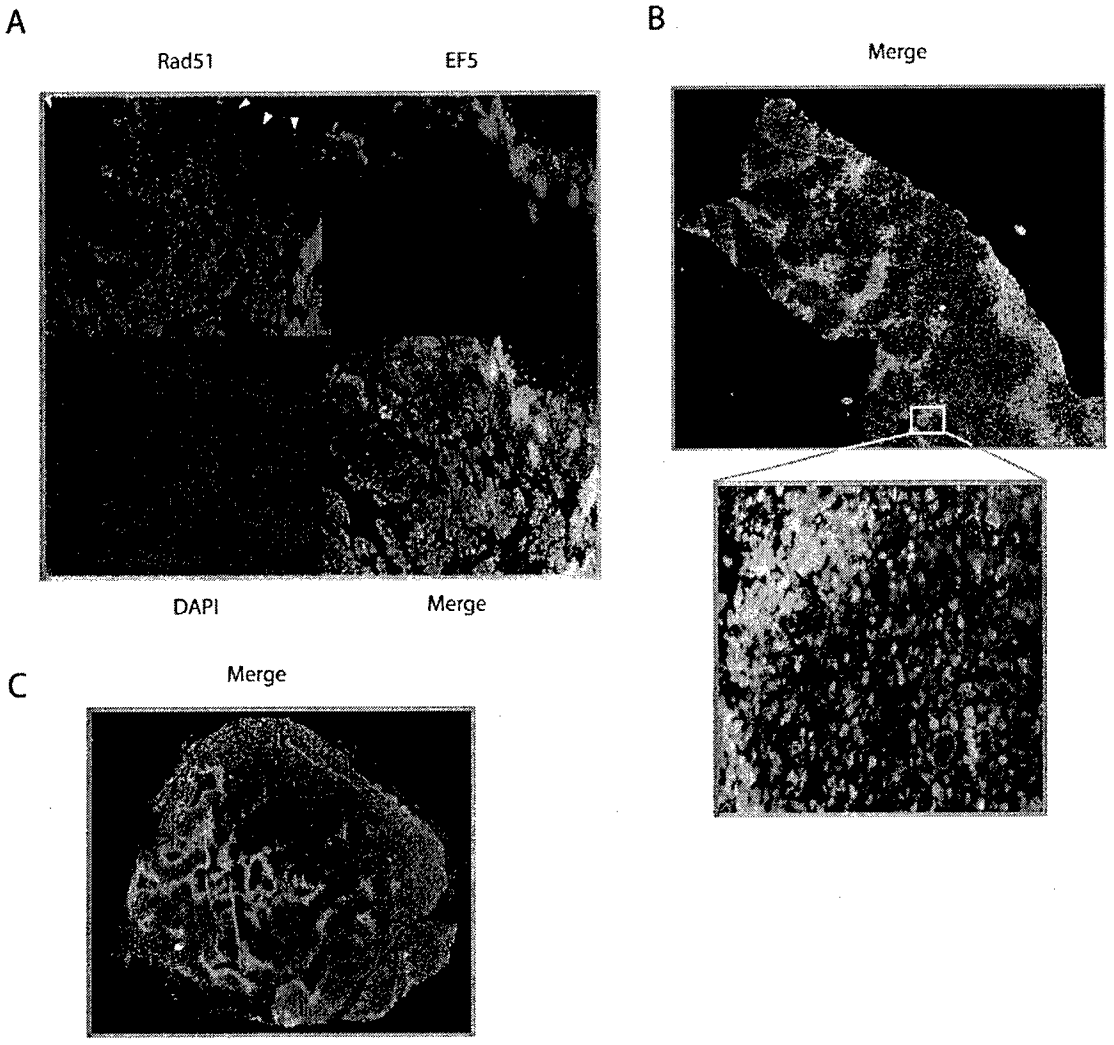

FIG. 8. Inverse association between hypoxia marker staining and Rad51 expression in cervical and prostate cancer xenografts. Shown are immunofluorescence analyses of staining with the hypoxia marker EF5 (red) and Rad51 expression (green) in tumor xenografts derived from Me180 cervical cancer cells (A), PC3 prostate cancer cells (B), and SiHa6 cervical cancer cells (C). Individual EF5, Rad51, and DAPI staining (blue), and Rad51-EF5 merged staining (yellow), are shown in panel A. Arrowheads in panel A indicate substantially decreased Rad51 expression within a region of strong EF5 staining.

sulting tumors were analyzed by immunofluorescence for Rad51 expression and staining with the hypoxia marker EF5. The binding of EF5 to cellular macromolecules occurs as a result of hypoxia-dependent bioreduction by cellular nitroreductases and thus can be used to detect hypoxia in solid tumors (10). As shown in Fig. 8, we detected an inverse association between Rad51 protein expression and EF5 staining in xenografts from all three cell lines. All tumors were found to contain hypoxic areas, as measured by an Eppendorf pO_2 probe prior to removal for immunostaining (data not shown) (9). This inverse association is particularly striking along the upper border of the section from a Me180 cervical xenograft shown in Fig. 8A, in which Rad51 expression is substantially decreased within a region of strong EF5 staining. In the merged image, the overlay of Rad51 expression and EF5 binding reveals minimal overlap in the majority of the section (Fig. 8A). Figure 8B and C also demonstrate consistent inverse associations between Rad51 expression and EF5 staining in PC3 and SiHa6 xenografts, respectively. Collectively, these findings demonstrate that hypoxia within the tumor microenvironment is associated with decreased Rad51 expression; thus, they extend our in vitro observations to the in vivo situation in tumors.

DISCUSSION

In the present study, we have demonstrated that hypoxia specifically down-regulates the expression of *RAD51*, a critical mediator of HR, both in vitro in cell culture and in vivo within the tumor microenvironment. Substantial decreases in Rad51 expression both during and after hypoxic exposure were observed in a wide range of cell types, and the mechanism of regulation appears to be independent of cell cycle profile and HIF expression. Analyses of protein stability, mRNA stability, and promoter activity indicate that hypoxia regulates *RAD51*

gene expression via a mechanism involving transcriptional repression. We detected decreased HR in cells both during and after hypoxic stress, demonstrating that the down-regulation of Rad51 expression by hypoxia has functional consequences for DNA repair. These findings were extended to the tumor microenvironment; we detected decreased expression of Rad51 in hypoxic regions of cervical and prostate tumor xenografts. Taken together, we propose a novel mechanism of genetic instability in the tumor microenvironment mediated by hypoxia-induced suppression of the HR pathway.

In a recent review regarding genetic instability and tumorigenesis, Loeb and colleagues proposed a paradigm shift in the way in which DNA repair pathways are thought to be regulated in mammalian cells (23). In the traditional view, it was thought that DNA repair genes were expressed constitutively in cells, such that they may be readily available as new DNA damage lesions arise from exogenous insults or endogenous processes such as replication errors or oxidative metabolism. Inactivation of these pathways in cancer was thought to occur primarily through genetic mutation or silencing by promoter methylation, thus resulting in an irreversible mutator phenotype. Recent studies, however, have supported the concept that genetic instability can arise from dysregulation, rather than complete inactivation, of DNA repair pathways (13). Our results are in accord with such a paradigm shift, as we detected substantial but reversible hypoxia-induced decreases in Rad51 expression that were associated with significant functional consequences with respect to recombinational repair.

The HR pathway in the maintenance of genetic stability. Despite extensive studies, there have been few reports describing mutations in the *RAD51* gene in human tumors (18). However, it was recently shown that overexpression of a dominant-negative form of the *RAD51* gene (*dnRAD51*), but not a wild-type form, was associated with increased tumorigenicity in Chinese hamster ovary (CHO) cells (1), suggesting that *RAD51* indeed acts as a tumor suppressor. Furthermore, recent studies have suggested that *BRCA1*, a well-documented tumor suppressor (41), may function specifically to promote high-fidelity HR while simultaneously suppressing the error-prone, nonhomologous end-joining (NHEJ) pathway (49). Along these lines, several reports have demonstrated up-regulated NHEJ repair activity in the context of impaired HR, and vice versa (39). Thus, the *BRCA1-RAD51* pathway likely represents an axis of tumor suppression, in which genome integrity is maintained by high-fidelity HR-mediated repair. As proposed for the case of inherited *BRCA1* deficency, hypoxia-induced acquired decreases in *RAD51* expression, and consequently diminished HR frequencies, thus may lead to genetic instability by shifting the balance between HR and NHEJ. We are currently investigating this possibility in further detail.

Hypoxia, DNA damage, and genetic instability. As discussed earlier, hypoxia is associated with a diverse spectrum of DNA damage and genetic aberrations. In particular, hypoxia-reoxygenation cycles are associated with oxidative stress and the production of reactive oxygen species, which are thought to induce high levels of both single-strand breaks and double-strand breaks. Studies have demonstrated that reoxygenation after a brief period of hypoxia can induce a high level of DNA damage (in the form of double-strand breaks) comparable to that observed after exposure to 4 to 5 Gy of ionizing radiation (IR) (15). In spite of this potentially large number of DNA strand breaks following hypoxic exposure, it is striking that we observed such profound decreases in Rad51 expression in the same time period, as Rad51 is a central protein in the pathway responsible for the error-free repair of such DNA lesions. In addition, studies have demonstrated that Rad51 is required for normal S-phase progression in mammalian cells, because of the role of Rad51 in resolving stalled and collapsed replication forks (36). Thus, the finding that posthypoxic cells resume DNA replication in the setting of decreased Rad51 expression suggests that hypoxia-induced down-regulation of Rad51 may have a major impact on genome integrity in the tumor microenvironment. This uncoupling of proliferation and Rad51 expression may be particularly important in regions of tumors undergoing fluctuating perfusion and consequently repeated cycles of hypoxia followed by reoxygenation. Hypoxia itself has been shown to induce an S-phase arrest which is reversible upon reoxygenation and may be associated with stalled replication forks (14, 16). In this situation, hypoxia-induced reductions in Rad51 expression would again have a major impact on the ability of tumor cells to maintain genomic integrity.

Regulation of DNA repair gene expression. Microarray data from this study have provided further evidence that the down-regulation of specific genes by hypoxia is as important as up-regulation in accurately characterizing gene expression profiles associated with hypoxia. The data presented here demonstrate that the hypoxia-induced decreases in Rad51 expression occur through a HIF-independent pathway involving transcriptional repression of the *RAD51* promoter. Initial analyses of promoters from genes involved in the HR pathway have revealed a complex picture of regulatory elements, and many of these elements appear to be conserved in mice and humans (18). Interestingly, the *RAD51* transcript contains an untranslated first exon (Fig. 3E), suggestive of gene regulation at the mRNA level. While the 5′ regulatory region of the *RAD51* gene contains a CpG-rich region and lacks a TATA box (a typical arrangement found in many housekeeping genes), recent analyses have demonstrated numerous potential regulatory elements in the core promoter region of this gene (18). In one study by Levy-Lahad et al., a single-nucleotide polymorphism at nucleotide 135 of the untranslated first exon of the *RAD51* gene was associated with increased breast cancer risk in *BRCA2* mutation carriers (21). These analyses strongly suggest that the expression of *RAD51* may be regulated by specific promoter elements in response to various stimuli, and they represent potential sites of dysregulation in the context of tumorigenesis and the tumor microenvironment.

Implications for cancer therapy. It has been established that hypoxic cells are more resistant to IR than their well-oxygenated counterparts due to decreased potentiation of free radical damage mediated by oxygen, and numerous studies have quantitatively associated tumor oxygenation with response to radiotherapy (32). Interestingly, however, it has also been reported that cells irradiated under normoxic conditions in the period immediately following hypoxia are actually more radiosensitive than cells irradiated without such hypoxic pretreatment (50). At the time, the underlying mechanism for this sensitivity was not clear. This phenomenon was observed in numerous cell lines, including two used in the present study, HeLa and A431 cells. Interestingly, cells with inactivated HR components ex-

hibit hypersensitivity to DNA-damaging agents, including IR (38). Specifically, several studies have demonstrated an association between down-regulation of Rad51 expression and increased radiosensitivity in a number of cell types (28). We propose that the persistent posthypoxic decreases in Rad51 expression reported here may partially account for the phenomenon of posthypoxia-associated radiosensitivity. These findings suggest that gene expression changes that persist in the posthypoxic period may significantly impact the response of cancer cells to therapy. Daily fractionated radiotherapy is thought to preferentially kill oxygenated cells and promote the reoxygenation of previously hypoxic cells. Hence, the extra sensitivity of immediately posthypoxic, reoxygenated cells (perhaps due to the dynamics of *RAD51* expression and dysregulation of other DNA repair genes) may provide insight into the basis for the efficacy of fractionated radiotherapy.

Substantial evidence now exists implicating tumor hypoxia in the development of aggressive tumor phenotypes. Recent studies have further clarified this association, leading to the finding that hypoxia up-regulates numerous genes involved in invasion and metastasis (37). We and others have demonstrated that the tumor microenvironment contributes to genetic instability and tumor progression, and the data presented in this study provide a mechanistic basis for this phenomenon. Furthermore, Rad51 dysregulation may also create heterogeneity in the DNA damage response among cells within tumors, with implications for the response to cancer therapies.

ACKNOWLEDGMENTS

We thank Tom Taylor for technical expertise in the FACS analyses, Geoffrey Lyon for assistance with tools for flow cytometry analysis, the Department of Microbial Pathogenesis for use of its BD FACscan flow cytometer, Anthony Valerio for assistance with real-time PCR assays, B. Kuba for excellent technical assistance, Greg Semenza for the pCEP-HIF-1α expression vector, William Kaelin for the 786-0 VHL cell lines, and Melissa Knauert for technical expertise in the HR shuttle assays. Finally, we thank Jianling Yuan, Shannon Gibson, Ryan Jensen, Denise Hegan, other members of the Glazer laboratory, and Jasjit, Ranjna, and Kavitha Bindra for insightful discussions regarding the manuscript.

This work was supported by a grant from the NIH (ES05775) to P.M.G. and by NCIC Project Program and U.S. Army DOD Prostate Program grants to D.W.H. and R.G.B. R.S.B. was supported by NIH/National Institute of General Medical Sciences Medical Scientist Training Grant GM07205.

REFERENCES

1. **Bertrand, P., S. Lambert, C. Joubert, and B. S. Lopez.** 2003. Overexpression of mammalian Rad51 does not stimulate tumorigenesis while a dominant-negative Rad51 affects centrosome fragmentation, ploidy and stimulates tumorigenesis, in p53-defective CHO cells. Oncogene **22**:7587–7592.
2. **Bindra, R. S., J. R. Vasselli, R. Stearman, W. M. Linehan, and R. D. Klausner.** 2002. VHL-mediated hypoxia regulation of cyclin D1 in renal carcinoma cells. Cancer Res. **62**:3014–3019.
3. **Brizel, D. M., S. P. Scully, J. M. Harrelson, L. J. Layfield, R. K. Dodge, H. C. Charles, T. V. Samulski, L. R. Prosnitz, and M. W. Dewhirst.** 1996. Radiation therapy and hyperthermia improve the oxygenation of human soft tissue sarcomas. Cancer Res. **56**:5347–5350.
4. **Bromfield, G. P., A. Meng, P. Warde, and R. G. Bristow.** 2003. Cell death in irradiated prostate epithelial cells: role of apoptotic and clonogenic cell kill. Prostate Cancer Prostatic Dis. **6**:73–85.
5. **Chan, P. P., M. Lin, A. F. Faruqi, J. Powell, M. M. Seidman, and P. M. Glazer.** 1999. Targeted correction of an episomal gene in mammalian cells by a short DNA fragment tethered to a triplex-forming oligonucleotide. J. Biol. Chem. **274**:11541–11548.
6. **Chiarotto, J. A., and R. P. Hill.** 1999. A quantitative analysis of the reduction in oxygen levels required to induce up-regulation of vascular endothelial growth factor (VEGF) mRNA in cervical cancer cell lines. Br. J. Cancer **80**:1518–1524.
7. **Coquelle, A., F. Toledo, S. Stern, A. Bieth, and M. Debatisse.** 1998. A new role for hypoxia in tumor progression: induction of fragile site triggering genomic rearrangements and formation of complex DMs and HSRs. Mol. Cell **2**:259–265.
8. **Datta, H. J., P. P. Chan, K. M. Vasquez, R. C. Gupta, and P. M. Glazer.** 2001. Triplex-induced recombination in human cell-free extracts. Dependence on XPA and HsRad51. J. Biol. Chem. **276**:18018–18023.
9. **De Jaeger, K., M. C. Kavanagh, and R. P. Hill.** 2001. Relationship of hypoxia to metastatic ability in rodent tumours. Br. J. Cancer **84**:1280–1285.
10. **Evans, S. M., B. Joiner, W. T. Jenkins, K. M. Laughlin, E. M. Lord, and C. J. Koch.** 1995. Identification of hypoxia in cells and tissues of epigastric 9L rat glioma using EF5 [2-(2-nitro-1H-imidazol-1-yl)-*N*-(2,2,3,3,3-pentafluoropropyl) acetamide]. Br. J. Cancer **72**:875–882.
11. **Flygare, J., F. Benson, and D. Hellgren.** 1996. Expression of the human *RAD51* gene during the cell cycle in primary human peripheral blood lymphocytes. Biochim. Biophys. Acta **1312**:231–236.
12. **Forsythe, J. A., B. H. Jiang, N. V. Iyer, F. Agani, S. W. Leung, R. D. Koos, and G. L. Semenza.** 1996. Activation of vascular endothelial growth factor gene transcription by hypoxia-inducible factor 1. Mol. Cell. Biol. **16**:4604–4613.
13. **Guo, H. H., and L. A. Loeb.** 2003. Tumbling down a different pathway to genetic instability. J. Clin. Investig. **112**:1793–1795.
14. **Hammond, E. M., N. C. Denko, M. J. Dorie, R. T. Abraham, and A. J. Giaccia.** 2002. Hypoxia links ATR and p53 through replication arrest. Mol. Cell. Biol. **22**:1834–1843.
15. **Hammond, E. M., M. J. Dorie, and A. J. Giaccia.** 2003. ATR/ATM targets are phosphorylated by ATR in response to hypoxia and ATM in response to reoxygenation. J. Biol. Chem. **278**:12207–12213.
16. **Hammond, E. M., S. L. Green, and A. J. Giaccia.** 2003. Comparison of hypoxia-induced replication arrest with hydroxyurea and aphidicolin-induced arrest. Mutat. Res. **532**:205–213.
17. **Harris, A. L.** 2002. Hypoxia—a key regulatory factor in tumour growth. Nat. Rev. Cancer **2**:38–47.
18. **Henning, W., and H. W. Sturzbecher.** 2003. Homologous recombination and cell cycle checkpoints: Rad51 in tumour progression and therapy resistance. Toxicology **193**:91–109.
19. **Ivan, M., K. Kondo, H. Yang, W. Kim, J. Valiando, M. Ohh, A. Salic, J. M. Asara, W. S. Lane, and W. G. Kaelin, Jr.** 2001. HIFα targeted for VHL-mediated destruction by proline hydroxylation: implications for O_2 sensing. Science **292**:464–468.
20. **Juan, G., E. Hernando, and C. Cordon-Cardo.** 2002. Separation of live cells in different phases of the cell cycle for gene expression analysis. Cytometry **49**:170–175.
21. **Levy-Lahad, E., A. Lahad, S. Eisenberg, E. Dagan, T. Paperna, L. Kasinetz, R. Catane, B. Kaufman, U. Beller, P. Renbaum, and R. Gershoni-Baruch.** 2001. A single nucleotide polymorphism in the *RAD51* gene modifies cancer risk in BRCA2 but not BRCA1 carriers. Proc. Natl. Acad. Sci. USA **98**:3232–3236.
22. **Li, C. Y., J. B. Little, K. Hu, W. Zhang, L. Zhang, M. W. Dewhirst, and Q. Huang.** 2001. Persistent genetic instability in cancer cells induced by non-DNA-damaging stress exposures. Cancer Res. **61**:428–432.
23. **Loeb, L. A., K. R. Loeb, and J. P. Anderson.** 2003. Multiple mutations and cancer. Proc. Natl. Acad. Sci. USA **100**:776–781.
24. **Lonergan, K. M., O. Iliopoulos, M. Ohh, T. Kamura, R. C. Conaway, J. W. Conaway, and W. G. Kaelin, Jr.** 1998. Regulation of hypoxia-inducible mRNAs by the von Hippel-Lindau tumor suppressor protein requires binding to complexes containing elongins B/C and Cul2. Mol. Cell. Biol. **18**:732–741.
25. **Mihaylova, V. T., R. S. Bindra, J. Yuan, D. Campisi, L. Narayanan, R. Jensen, F. Giordano, R. S. Johnson, S. Rockwell, and P. M. Glazer.** 2003. Decreased expression of the DNA mismatch repair gene *Mlh1* under hypoxic stress in mammalian cells. Mol. Cell. Biol. **23**:3265–3273.
26. **Nordsmark, M., M. Overgaard, and J. Overgaard.** 1996. Pretreatment oxygenation predicts radiation response in advanced squamous cell carcinoma of the head and neck. Radiother. Oncol. **41**:31–39.
27. **Nowell, P. C.** 1976. The clonal evolution of tumor cell populations. Science **194**:23–28.
28. **Ohnishi, T., T. Taki, S. Hiraga, N. Arita, and T. Morita.** 1998. In vitro and in vivo potentiation of radiosensitivity of malignant gliomas by antisense inhibition of the *RAD51* gene. Biochem. Biophys. Res. Commun. **245**:319–324.
29. **Paquette, B., and J. B. Little.** 1994. In vivo enhancement of genomic instability in minisatellite sequences of mouse C3H/10T1/2 cells transformed in vitro by X-rays. Cancer Res. **54**:3173–3178.
30. **Perier, R. C., V. Praz, T. Junier, C. Bonnard, and P. Bucher.** 2000. The eukaryotic promoter database (EPD). Nucleic Acids Res. **28**:302–303.
31. **Reynolds, T. Y., S. Rockwell, and P. M. Glazer.** 1996. Genetic instability induced by the tumor microenvironment. Cancer Res. **56**:5754–5757.
32. **Rockwell, S.** 1997. Oxygen delivery: implications for the biology and therapy of solid tumors. Oncol. Res. **9**:383–390.
33. **Roth, M. E., L. Feng, K. J. McConnell, P. J. Schaffer, C. E. Guerra, J. P. Affourtit, K. R. Piper, L. Guccione, J. Hariharan, M. J. Ford, S. W. Powell, H. Krishnaswamy, J. Lane, G. Intrieri, J. S. Merkel, C. Perbost, A. Valerio,**

B. Zolla, C. D. Graham, J. Hnath, C. Michaelson, R. Wang, B. Ying, C. Halling, C. E. Parman, D. Raha, B. Orr, B. Jedrzkiewicz, J. Liao, A. Tevelev, M. J. Mattessich, D. M. Kranz, M. Lacey, J. C. Kaufman, J. Kim, D. R. Latimer, and P. M. Lizardi. 2004. Expression profiling using a hexamer-based universal microarray. Nat. Biotechnol. **22**:418–426.

34. **Seagroves, T. N., H. E. Ryan, H. Lu, B. G. Wouters, M. Knapp, P. Thibault, K. Laderoute, and R. S. Johnson.** 2001. Transcription factor HIF-1 is a necessary mediator of the Pasteur effect in mammalian cells. Mol. Cell. Biol. **21**:3436–3444.
35. **Shibata, T., A. J. Giaccia, and J. M. Brown.** 2000. Development of a hypoxia-responsive vector for tumor-specific gene therapy. Gene Ther. **7**:493–498.
36. **Sonoda, E., M. S. Sasaki, J. M. Buerstedde, O. Bezzubova, A. Shinohara, H. Ogawa, M. Takata, Y. Yamaguchi-Iwai, and S. Takeda.** 1998. Rad51-deficient vertebrate cells accumulate chromosomal breaks prior to cell death. EMBO J. **17**:598–608.
37. **Subarsky, P., and R. P. Hill.** 2003. The hypoxic tumour microenvironment and metastatic progression. Clin. Exp. Metastasis **20**:237–250.
38. **Thompson, L. H., and D. Schild.** 2002. Recombinational DNA repair and human disease. Mutat. Res. **509**:49–78.
39. **Valerie, K., and L. F. Povirk.** 2003. Regulation and mechanisms of mammalian double-strand break repair. Oncogene **22**:5792–5812.
40. **Vaupel, P., K. Schlenger, C. Knoop, and M. Hockel.** 1991. Oxygenation of human tumors: evaluation of tissue oxygen distribution in breast cancers by computerized O_2 tension measurements. Cancer Res. **51**:3316–3322.
41. **Venkitaraman, A. R.** 2002. Cancer susceptibility and the functions of BRCA1 and BRCA2. Cell **108**:171–182.
42. **Vukovic, V., H. K. Haugland, T. Nicklee, A. J. Morrison, and D. W. Hedley.** 2001. Hypoxia-inducible factor-1α is an intrinsic marker for hypoxia in cervical cancer xenografts. Cancer Res. **61**:7394–7398.
43. **Wang, G. L., and G. L. Semenza.** 1993. Desferrioxamine induces erythropoietin gene expression and hypoxia-inducible factor 1 DNA-binding activity: implications for models of hypoxia signal transduction. Blood **82**:3610–3615.
44. **Werner, T.** 2003. The state of the art of mammalian promoter recognition. Brief Bioinform. **4**:22–30.
45. **Williams, K. J., R. L. Cowen, and I. J. Stratford.** 2001. Hypoxia and oxidative stress. Tumour hypoxia—therapeutic considerations. Breast Cancer Res. **3**:328–331.
46. **Young, S. D., R. S. Marshall, and R. P. Hill.** 1988. Hypoxia induces DNA overreplication and enhances metastatic potential of murine tumor cells. Proc. Natl. Acad. Sci. USA **85**:9533–9537.
47. **Yuan, J., and P. M. Glazer.** 1998. Mutagenesis induced by the tumor microenvironment. Mutat. Res. **400**:439–446.
48. **Yuan, J., L. Narayanan, S. Rockwell, and P. M. Glazer.** 2000. Diminished DNA repair and elevated mutagenesis in mammalian cells exposed to hypoxia and low pH. Cancer Res. **60**:4372–4376.
49. **Zhang, J., H. Willers, Z. Feng, J. C. Ghosh, S. Kim, D. T. Weaver, J. H. Chung, S. N. Powell, and F. Xia.** 2004. Chk2 phosphorylation of BRCA1 regulates DNA double-strand break repair. Mol. Cell. Biol. **24**:708–718.
50. **Zolzer, F., and C. Streffer.** 2002. Increased radiosensitivity with chronic hypoxia in four human tumor cell lines. Int. J. Radiat. Oncol. Biol. Phys. **54**:910–920.